

Microwave Imaging for Soil Characterization

A THESIS

submitted by

RAJESH MOHAN R

*for the award of the degree
of*

DOCTOR OF PHILOSOPHY



DIVISION OF ELECTRONICS ENGINEERING

SCHOOL OF ENGINEERING

COCHIN UNIVERSITY OF SCIENCE AND TECHNOLOGY

KOCHI

November 2018

Microwave Imaging for Soil Characterization

A THESIS

submitted by

RAJESH MOHAN R

*for the award of the degree
of*

DOCTOR OF PHILOSOPHY



DIVISION OF ELECTRONICS ENGINEERING

SCHOOL OF ENGINEERING

COCHIN UNIVERSITY OF SCIENCE AND TECHNOLOGY

KOCHI

November 2018

THESIS CERTIFICATE

This is to certify that the thesis entitled **MICROWAVE IMAGING FOR SOIL CHARACTERIZATION** submitted by Rajesh Mohan R to the Cochin University of Science and Technology, Kochi for the award of the degree of Doctor of Philosophy is a bonafide record of research work carried out by him under my supervision and guidance at the Division of Electronics Engineering, School of Engineering, Cochin University of Science and Technology. The contents of the thesis, in full or in parts, have not been submitted to any other University or Institute for the award of any degree or diploma.

I further certify that the corrections and modifications suggested by the audience during the pre-synopsis seminar and recommended by the Doctoral Committee of Rajesh Mohan R are incorporated in the thesis.

Kochi - 682 022

15/11/2018

Prof. (Dr.) S. Mridula

Research Guide

Professor

Division of Electronics Engineering

School of Engineering

CUSAT, Kochi 682 022.

DECLARATION

I hereby declare that the work presented in the thesis entitled **MICROWAVE IMAGING FOR SOIL CHARACTERIZATION** is based on the original research work carried out by me under the supervision and guidance of Dr. S. Mridula, Professor, Division of Electronics Engineering, School of Engineering, Cochin University of Science and Technology for the award of the degree of Doctor of Philosophy with Cochin University of Science and Technology. I further declare that the contents of the thesis, in full or in parts, have not been submitted to any other University or Institute for the award of any degree or diploma.

Kochi - 682 022

Rajesh Mohan R

15/11/2018

ACKNOWLEDGEMENT

Carrying out this research work has been a truly exciting experience for me and it would not have been possible to reach this far without the support and guidance that I received from many people.

First and foremost, I would like to express my gratitude to my guide Prof. S. Mridula for all the help she has given me during the period I spent undertaking this work on soil characterization using microwaves. Her role in my life has been of a macro-characterized nature - a friend, philosopher, mentor and teacher - roles which she has been playing with exemplary poise. I sincerely thank her for offering valuable advice, continuous supervision & timely encouragement and for sparing her time in seeing to it that this work is presented in the best possible way.

It is not often that one gets to acknowledge someone with the same sentiments as one does for the supervising guide. I do have this rare privilege. Let me place on record my whole-hearted appreciation for the selfless efforts made by Prof. Anju Pradeep, Division of Electronics Engineering, School of Engineering, CUSAT, in the completion of this work. Throughout the tenure of my research, her presence has been a meticulously-perfect blessing.

I am also immensely thankful to Prof. P. Mohanan, UGC BSR Professor, Department of Electronics, CUSAT, for his assistance and directive comments throughout my work and for his amazing ways of teaching electromagnetics. His offer of extending to me the excellent facilities at the Centre for Research in Electromagnetics & Antennas (CREMA), CUSAT, and timely interventions for corrective measures in work and publication are gratefully acknowledged.

I am grateful to Prof. K. Vasudevan, CSIR Emeritus Scientist, Department of Electronics, CUSAT, for his encouragement and support during the course of my research. I thank Prof. Binu Paul, Division of Electronics Engineering, School of Engineering, CUSAT, and also

member of the Doctoral Committee for the support and also for permitting me to utilize the facilities of the Advanced Communication Lab of the Division.

I am thankful to Prof. M. R. Radhakrishna Panicker, Principal, School of Engineering, CUSAT, for providing all the necessary facilities in the various laboratories of the Department.

My earnest gratitude to Prof. P. S. Sreejith, Dean, Faculty of Engineering, CUSAT for extending quality facilities at the University and for his creative suggestions during my pre-synopsis presentation and thesis submission. My sincere thanks to Prof. G. Madhu, former Principal, School of Engineering, CUSAT & Dean, Faculty of Engineering, for his constant motivation and support.

I gratefully acknowledge the help & encouragement from all teaching & non-teaching staff members of the Division of Electronics Engineering, CUSAT. Special thanks to the present Head, Prof. P. Abdulla and former Heads for their support and timely conduct of research progress-evaluation.

My sincere thanks to Sri. P. Y. Anil, Maintenance Engineer at the Department of Electronics, CUSAT, for lending me his time & expertise in the fabrication of antenna structures. Technical support offered by Sri. Narayanan, CTech Ltd. Thiruvankulam, Kochi, is also gratefully remembered. Thanks to my research-friends at the CREMA Lab - Dr. C. M. Nijas, Sri. Deepak & Smt. Roshna Deepak, Sri. Lindo Ouseph & Sri. Dinesh for their support in the experimental work.

Thanks to all my co-researchers at the Division of Electronics Engineering - Dr. C. J. Bindu, Dr. M. Sumi, Dr. Saira Joseph, Dr. P. R. Mini, Sri. T. A. Anjit, Sri. C. V. Anilkumar, Sri. Basil J Paul, Sri. A. I. Harikrishnan, Ms. N. R. Rema, Ms. H. P. Thushara and Ms. Reshma Lakshmanan - for their support and encouragement. Creative suggestions offered by Dr. Deepu V Nair, Technical Manager, Cambium Networks, Bengaluru, and Dr. Manoj Joseph, Scientist, ISRO, Jodhpur,

are sincerely acknowledged.

I wish to acknowledge the support from my colleagues at my parent institution, the Institute of Human Resources Development (IHRD), Kerala. Thanks especially to all the Directors (past and present) of IHRD for permitting me to avail of three-years' leave on deputation. Thanks to all my superiors & colleagues at various associate institutions under IHRD, especially to Prof. V. P. Devassia, Principal, Model Engineering College, Ernakulam, for the support and help rendered to me. I also appreciate the friendly support received from the students (both UG & PG) and Project Assistants of the Division of Electronics Engineering, CUSAT.

Last, but by no means the least, I value and acknowledge the support offered by all my relatives & family members. No one has been more important to me in the pursuit of this work than the people that I have existed with.

Thanks to my brother & sister and their family members for being the ultimate model for my character materialization. Thanks to my parents in-law, brothers-/sisters- in-law and their family for the support. Thanks to my daughter Parvathi for her backing & unending inspiration. Finally, I thank my wife Jaya for the unstinting support and understanding throughout the term of my work, which I am sure, was more strenuous for her than during her own research days. 'Thanks' would be too formal; however, I thank my amma & achan, whose love and care during their days of physical presence on Earth still guide me in whatever I do.

And I thank God, who presented Himself in all the above human forms to help me through these tough, but joyous days.

Rajesh Mohan R

ABSTRACT

KEYWORDS: Artificial Neural Network; cavity perturbation method; free-space transmission method; microwave imaging; sensor antenna; soil.

Microwave Imaging is an area of research where material characterization is done by means of interrogating microwaves over a wide frequency band. This technique can provide excellent diagnostic capabilities in non-destructive testing & evaluation, biomedical engineering, geophysical prospecting etc.

Every material has a unique set of electrical characteristics that are dependent on its dielectric properties (Zhu and Guo, 2017). Accurate measurements of these properties can provide valuable information about the material (Nelson and Kraszewski, 1990).

This research focusses on the characterization of soil using microwaves. Soil is a natural body consisting of layers that are primarily composed of minerals which differ from their parent materials in their texture, structure, consistency, colour, chemical, biological and other characteristics (Engman, 1990). Soil testing as a tool for judicious recommendation of moisture and fertilizer contents has great relevance for proper crop-management in agriculture (Topp et al., 1980), (Vivek et al., 2009). Thus a systematic study of the microwave sensing of soil properties in the presence of moisture and fertilizers has evolved as a major need of the hour. How much is the soils pH value and what is required to be added to improve soils fertility based on pH are the only relevant suggestions given by the Soil Testing Laboratory to a farmer. This work is an attempt to assist the farmers even better through soil characterization methods. Estimation of soil moisture and fertilizer contents is done using electromagnetic principles, so that crop growth and productivity can be further

improved. Out of the fourteen districts in Kerala, it is officially known that alkaline soils with pH values above 7.0 are available mostly in Palakkad only, while the soils in the other thirteen districts are acidic in nature, with pH below 7.0 (Premachandran, 2007). Research work is carried out on different soil samples obtained from Ernakulam and Palakkad districts.

The thesis presents four measurement methods for soil characterization, namely Cavity Perturbation Method (Bethe and Schwinger, 1943), Superstrate Method (Jingchu and Geyi, 2013), Free-space Transmission Method (Paz et al., 2011) and Sensor Antenna Method (Anju, 2015), (Deshours et al., 2018). Two important analytical models based on Artificial Neural Network (ANN) and Regression are also described. Measurement and analytical methods which provide significant results about the soil samples under test are combined to develop a methodology for mapping microwave characteristics of soil, leading to the creation of an image. Using the mapped microwave parameters and corresponding constituents, characteristic signature of each soil sample can be drawn similar to satellite-based remote-sensing. Knowledge of spatial soil-variability is also helpful for site-specific management of agricultural inputs, such as fertilizer, agrochemicals and irrigation. This could be beneficial in the development of precision agriculture technology.

The main objectives of the work presented in this thesis are to:

- characterize soil using microwaves based on its dielectric properties
- employ analytical models for soil characterization and
- use microwave imaging as a tool for estimation of soil moisture and fertilizer contents

Contents

ACKNOWLEDGEMENT	i
ABSTRACT	v
LIST OF FIGURES	xi
LIST OF TABLES	xxi
ABBREVIATIONS	xxxii
NOTATION	xxxiii
1 INTRODUCTION	1
1.1 Material Characterization using Microwaves	3
1.2 Soil and its Microwave Characteristics	5
1.2.1 Moisture Content	8
1.2.2 Fertilizer Content	9
1.3 Literature Survey	11
1.3.1 Permittivity Measurement for Material Characterization	12
1.3.2 Microwave Imaging for Soil Characterization . .	27
1.4 Motivation for the Work	31
1.5 Objectives of the Work	32
1.6 Thesis Outline	32
1.7 Chapter Summary	35

2	METHODOLOGY	37
2.1	Introduction	37
2.2	Measurement Methods for Material Characterization . . .	38
2.2.1	Cavity Perturbation Method	39
2.2.2	Superstrate Method	47
2.2.3	Free-space Transmission Method	56
2.2.4	Sensor Antenna Method	58
2.3	Analytical Methods for Material Characterization	61
2.3.1	ANN Model	62
2.3.2	Regression Analysis	67
2.4	Imaging Technique for Colour Mapping	68
2.5	Chapter Summary	70
3	MICROWAVE PROPERTIES OF SOIL	73
3.1	Introduction	73
3.2	Cavity Perturbation Method	74
3.2.1	Soil samples used	75
3.2.2	Experimental Results	75
3.3	Superstrate Method	77
3.3.1	Soil samples used	77
3.3.2	Experimental setup and Results	77
3.4	Chapter Summary	83
4	SOIL CHARACTERIZATION USING FREE-SPACE TRANSMISSION METHOD	85
4.1	Introduction	85
4.2	Estimation of Moisture Content	87
4.2.1	Soil samples used	87
4.2.2	Simulation Results	87
4.2.3	Experimental Results	90
4.2.4	Validation of the experimental results using Topp's Equation	110
4.2.5	ANN Model for Volumetric Water Content Estimation	116

4.2.6	Moisture detection using Colour-mapping	125
4.3	Estimation of Fertilizer Concentration	128
4.3.1	Soil samples and Fertilizers used	129
4.3.2	Experimental Results	130
4.3.3	ANN Model for Fertilizer-concentration Estimation	140
4.4	Chapter Summary	147
5	SOIL CHARACTERIZATION USING SENSOR ANTENNA	149
5.1	Introduction	149
5.2	Sensor Antenna	151
5.2.1	Sensor Antenna Configurations in the L, S and C bands	151
5.3	Experimental Results	154
5.4	Analytical Models	185
5.4.1	ANN Model	185
5.4.2	Regression Model	193
5.5	Moisture detection using colour mapping	199
5.6	Chapter Summary	201
6	CONCLUSION	205
6.1	Thesis Highlights	205
6.2	Performance Comparison of the different methods for Soil Characterization	209
6.3	Suggestions for Future Work	210
	Appendices	211
A	SOIL MOISTURE CONTENT MEASUREMENT USING RESISTANCE-PROBES	213
A.1	Introduction	213
A.2	Experimental setup and Results	214
A.3	Inference	218

B	SPECKLE NOISE REDUCTION IN IMAGES USING A COMBINED SPACE-FREQUENCY DOMAIN APPROACH	219
B.1	Introduction	219
B.2	Wavelet based Image Denoising Technique	221
B.2.1	Speckle Noise Model	221
B.2.2	Wiener Filter	221
B.2.3	Wavelet Thresholding	222
B.2.4	Threshold Computation	223
B.2.5	Despeckling Algorithm	223
B.2.6	Quantitative Evaluation	224
B.3	Simulation Results	225
B.3.1	General Images	225
B.3.2	SAR Images	227
B.4	Inference	229
	REFERENCES	231
	LIST OF PAPERS SUBMITTED ON THE BASIS OF THIS THESIS	249
	CURRICULUM VITAE	251
	INDEX	253

List of Figures

1.1	pH scale of Soil	7
1.2	Schematic of Free-space Transmission Method for measuring reflection and transmission (Ports 1 and 2 are connected to the VNA)	24
1.3	Organization of the Thesis	34
2.1	Structure of a slotted rectangular cavity resonator	40
2.2	Slotted S-band rectangular cavity resonator	42
2.3	Slotted S-band rectangular cavity resonator with FR4 / Arlon AD1000 sample	43
2.4	S_{21} plot of the empty slotted S-band rectangular cavity resonator	43
2.5	S_{21} plot of the slotted S-band rectangular cavity resonator with (a) FR-4 (b) Arlon AD1000	44
2.6	Network analyzer and S-band rectangular cavity resonator	46
2.7	Rectangular Microstrip Patch Antenna	48
2.8	Rectangular patch antenna with coaxial probe feeding	48
2.9	Structure of CPW-fed monopole antenna	50
2.10	Variation of resonant frequency of antennas with dielectric constant of superstrate; L, S & C bands; Superstrate Method	52
2.11	Percentage shift in frequency of Microstrip Patch Antenna and CPW-fed Monopole Antenna; Superstrate Method	53

2.12	Experimental setup of free-space transmission method with acrylic sample as Material Under Test	57
2.13	Sensor antenna at 4.35 GHz	60
2.14	Setup for sensing acetone; C-band; Sensor Antenna Method	60
2.15	Reflection characteristics of the sensor antenna; C-band .	61
2.16	A fully connected ANN with one hidden layer and one output layer	62
2.17	MPA / Slab Geometry for ANN model; Superstrate Method	65
2.18	Structure of the ANN model; Superstrate Method	66
2.19	Setup for detection of metallic disc embedded in soil; Colour-mapping using Imaging	69
2.20	Simulation result of detection of metallic disc embedded in soil using Imaging Technique	70
3.1	Experimental setup of Superstrate Method with Red Soil as Superstrate	78
3.2	Geometry of antennas fabricated; Superstrate Method . .	79
3.3	Variation of (a) frequency (b) normalized resistance and (c) normalized reactance of MPA for Red, White and Black soil samples; L-band ; Superstrate Method	81
3.4	Variation of (a) frequency (b) normalized resistance and (c) normalized reactance of CMA for Red, White and Black soil samples; L-band ; Superstrate Method	81
3.5	Variation of (a) frequency (b) normalized resistance and (c) normalized reactance of MPA for Red, White and Black soil samples; S-band ; Superstrate Method	81
3.6	Variation of (a) frequency (b) normalized resistance and (c) normalized reactance of CMA for Red, White and Black soil samples; S-band ; Superstrate Method	82
3.7	Variation of (a) frequency (b) normalized resistance and (c) normalized reactance of MPA for Red, White and Black soil samples; C-band ; Superstrate Method	82

3.8	Variation of (a) frequency (b) normalized resistance and (c) normalized reactance of CMA for Red, White and Black soil samples; C-band ; Superstrate Method	82
4.1	Simulation setup of Free-space Transmission Method . .	88
4.2	Free-space S_{11} & S_{21} characteristics of MPA under different cases; C-band; Free-space Transmission Method	89
4.3	(a) Structure of Microstrip Patch Antenna; $f_r=5.52\text{GHz}$; $L_p=16.5$ mm, $W_p=12.4$ mm, $L_s=34.0$ mm, $W_s=28.0$ mm (b) reflection characteristics	90
4.4	Experimental setup of Free-space Transmission Method .	91
4.5	Transmission characteristics with soil samples (pH=6.4) in the C-band; Free-space Transmission Method	92
4.6	Phase vs. frequency of dry acidic soil samples [pH=4.7, 4.9, 5.0, 5.1, 5.2 & 5.3]; C-band; Free-space Transmission Method	93
4.7	Phase vs. frequency of dry acidic soil samples [pH=5.4, 5.7, 5.8, 5.9, 6.1 & 6.2]; C-band; Free-space Transmission Method	94
4.8	Phase vs. frequency of dry acidic soil samples [pH=6.3, 6.4,7.0, 7.1,7.2 & 7.3]; C-band; Free-space Transmission Method	95
4.9	Phase vs. frequency of dry alkaline soil samples [pH=7.4 & 7.5]; C-band; Free-space Transmission Method	96
4.10	Phase vs. frequency of different acidic soil samples with varying moisture content; [pH=4.7, 4.9 & 5.0 (sample a, b)]; C-band; Free-space Transmission Method	97
4.11	Phase vs. frequency of different acidic soil samples with varying moisture content; [pH=5.0 (sample c), 5.1, 5.2, 5.3 & 5.4]; C-band; Free-space Transmission Method . .	98
4.12	Phase vs. frequency of different acidic soil samples with varying moisture content; [pH=5.7, 5.8, 5.9, 6.1 & 6.2 (sample a)]; C-band; Free-space Transmission Method .	99

4.13	Phase vs. frequency of different acidic soil samples with varying moisture content; [pH=6.2 (sample b-f), & 6.3]; C-band; Free-space Transmission Method	100
4.14	Phase vs. frequency of different acidic soil samples with varying moisture content; [pH=6.4]; C-band; Free-space Transmission Method	101
4.15	Phase vs. frequency of different alkaline soil samples with varying moisture content; [pH=7.0 & 7.1(samples a-c)]; C-band; Free-space Transmission Method	102
4.16	Phase vs. frequency of different alkaline soil samples with varying moisture content; [pH=7.1(samples d-g) & 7.2(samples a, b)]; C-band; Free-space Transmission Method	103
4.17	Phase vs. frequency of different alkaline soil samples with varying moisture content; [pH=7.2(samples c-e) & 7.3(samples a-c)]; C-band; Free-space Transmission Method	104
4.18	Phase vs. frequency of different alkaline soil samples with varying moisture content; [pH=7.3(samples d-h) & 7.4(sample a)]; C-band; Free-space Transmission Method	105
4.19	Phase vs. frequency of different alkaline soil samples with varying moisture content; [pH=7.4(samples b, c) & 7.5(samples a-d)]; C-band; Free-space Transmission Method	106
4.20	Phase vs. frequency of different alkaline soil samples with varying moisture content; [pH=7.5 (sample e)]; C-band; Free-space Transmission Method	107
4.21	ANN structure for θ_v estimation; Free-space Transmission Method	116
4.22	Flowchart of ANN Model for estimation of Volumetric Water Content, θ_v ; Free-space Transmission Method . .	117
4.23	GUI used for θ_v estimation; ANN Model; Free-space Transmission Method	124

4.24	Screen-shot of evaluated θ_v %; C-band; ANN Model; Free-space Transmission Method	125
4.25	Experimental setup of free-space transmission method with MPA as transmit antenna and probe as receiver . . .	127
4.26	S_{21} mapping of 2 moist locations in soil with 16 scanning points; Free-space Transmission Method & Colour-mapping	127
4.27	S_{21} mapping of 1 moist location in soil with 25 scanning points; Free-space Transmission Method & Colour-mapping	128
4.28	Dielectric constant of plain soil samples in the L, S & C bands; Free-space Transmission Method	132
4.29	Variation of ϵ'_r with pH of the soil-fertilizer mixture-ratio of 4.8% at the three frequencies; Free-space Transmission Method	134
4.30	Variation of ϵ'_r with pH of the soil-fertilizer mixture-ratio of 9.1% at the three frequencies; Free-space Transmission Method	135
4.31	Variation of ϵ'_r with pH of the soil-fertilizer mixture-ratio of 20% at the three frequencies; Free-space Transmission Method	136
4.32	Variation of ϵ'_r with pH of the soil-fertilizer mixture-ratios; L-band ; Free-space Transmission Method	137
4.33	Variation of ϵ'_r with pH of the soil-fertilizer mixture-ratios; S-band ; Free-space Transmission Method	138
4.34	Variation of ϵ'_r with pH of the soil-fertilizer mixture-ratios; C-band ; Free-space Transmission Method	138
4.35	Dielectric constant vs. soil-fertilizer mixture-ratio in % for different soil samples; pH=4.7, 4.9, 5.0, 5.2, 5.8 & 6.1 ; Free-space Transmission Method	139
4.36	Dielectric constant vs. soil-fertilizer mixture-ratio in % for different soil samples; pH=6.3, 7.0 & 7.4 ; Free-space Transmission Method	140

4.37	GUI used for fertilizer-soil mixture ratio estimation; ANN Model; Free-space Transmission Method	142
4.38	Screen-shot of evaluated amount of PBA-soil mixture-ratio for soil (pH=4.7, sample a); ANN Model; Free-space Transmission Method	147
5.1	Geometry of sensor antenna at L, S & C bands; Sensor Antenna Method	152
5.2	Fabricated structure [(a), (c), (e)] and Reflection characteristics [(b), (d), (f)] of sensor antenna in the L, S & C bands ($f_r=1.88$ GHz, 2.45 GHz & 5.2 GHz); Sensor Antenna Method	156
5.3	Experimental setup for measuring percentage shift in frequency for soil characterization; Sensor Antenna Method	157
5.4	Reflection characteristics of L-band sensor antenna in soil (pH=4.7 sample a); Sensor Antenna Method	159
5.5	Reflection characteristics of L-band sensor antenna in soil (pH=6.3 sample a); Sensor Antenna Method	159
5.6	Reflection characteristics of L-band sensor antenna in soil (pH=7.4 sample a); Sensor Antenna Method	160
5.7	Reflection characteristics of S-band sensor antenna in soil (pH=4.7 sample a); Sensor Antenna Method	160
5.8	Reflection characteristics of S-band sensor antenna in soil (pH=6.3 sample a); Sensor Antenna Method	160
5.9	Reflection characteristics of S-band sensor antenna in soil (pH=7.4 sample a); Sensor Antenna Method	161
5.10	Reflection characteristics of C-band sensor antenna in soil (pH=4.7 sample a); Sensor Antenna Method	161
5.11	Reflection characteristics of C-band sensor antenna in soil (pH=6.3 sample a); Sensor Antenna Method	161
5.12	Reflection characteristics of C-band sensor antenna in soil (pH=7.4 sample a); Sensor Antenna Method	162

5.13 Comparison of percentage shift in frequency of sensor antenna under varying moisture content for three different soil samples in the L, S & C bands; Sensor Antenna Method	163
5.14 Shift in frequency vs. fertilizer concentration for soil (pH=4.7, sample a); all fertilizers; MC=0ml ; C-band; Sensor Antenna Method	165
5.15 Shift in frequency vs. fertilizer concentration for soil (pH=4.7, sample a); all fertilizers; MC=1ml ; C-band; Sensor Antenna Method	165
5.16 Shift in frequency vs. fertilizer concentration for soil (pH=4.7, sample a); all fertilizers; MC=2ml ; C-band; Sensor Antenna Method	165
5.17 Shift in frequency vs. fertilizer concentration for soil (pH=4.9, sample a) mixed with 0 ml, 1 ml & 2 ml MC; all fertilizers; C-band; Sensor Antenna Method	166
5.18 Shift in frequency vs. fertilizer concentration for soil (pH=5.0, sample a) mixed with 0 ml, 1 ml & 2 ml MC; all fertilizers; C-band; Sensor Antenna Method	167
5.19 Shift in frequency vs. fertilizer concentration for soil (pH=5.1) mixed with 0 ml, 1 ml & 2 ml MC; all fertilizers; C-band; Sensor Antenna Method	168
5.20 Shift in frequency vs. fertilizer concentration for soil (pH=5.2) mixed with 0 ml, 1 ml & 2 ml MC; all fertilizers; C-band; Sensor Antenna Method	169
5.21 Shift in frequency vs. fertilizer concentration for soil (pH=5.3, sample a) mixed with 0 ml, 1 ml & 2 ml MC; all fertilizers; C-band; Sensor Antenna Method	170
5.22 Shift in frequency vs. fertilizer concentration for soil (pH=5.4) mixed with 0 ml, 1 ml & 2 ml MC; all fertilizers; C-band; Sensor Antenna Method	171
5.23 Shift in frequency vs. fertilizer concentration for soil (pH=5.7) mixed with 0 ml, 1 ml & 2 ml MC; all fertilizers; C-band; Sensor Antenna Method	172

- 5.24 Shift in frequency vs. fertilizer concentration for soil (**pH=5.8, sample a**) mixed with 0 ml, 1 ml & 2 ml MC; all fertilizers; C-band; Sensor Antenna Method 173
- 5.25 Shift in frequency vs. fertilizer concentration for soil (**pH=5.9**) mixed with 0 ml, 1 ml & 2 ml MC; all fertilizers; C-band; Sensor Antenna Method 174
- 5.26 Shift in frequency vs. fertilizer concentration for soil (**pH=6.1**) mixed with 0 ml, 1 ml & 2 ml MC; all fertilizers; C-band; Sensor Antenna Method 175
- 5.27 Shift in frequency vs. fertilizer concentration for soil (**pH=6.2, sample a**) mixed with 0 ml, 1 ml & 2 ml MC; all fertilizers; C-band; Sensor Antenna Method 176
- 5.28 Shift in frequency vs. fertilizer concentration for soil (**pH=6.3, sample a**) mixed with 0 ml, 1 ml & 2 ml MC; all fertilizers; C-band; Sensor Antenna Method 177
- 5.29 Shift in frequency vs. fertilizer concentration for soil (**pH=6.4, sample a**) mixed with 0 ml, 1 ml & 2 ml MC; all fertilizers; C-band; Sensor Antenna Method 178
- 5.30 Shift in frequency vs. fertilizer concentration for soil (**pH=7.0, sample a**) mixed with 0 ml, 1 ml & 2 ml MC; all fertilizers; C-band; Sensor Antenna Method 179
- 5.31 Shift in frequency vs. fertilizer concentration for soil (**pH=7.1, sample a**) mixed with 0 ml, 1 ml & 2 ml MC; all fertilizers; C-band; Sensor Antenna Method 180
- 5.32 Shift in frequency vs. fertilizer concentration for soil (**pH=7.2, sample a**) mixed with 0 ml, 1 ml & 2 ml MC; all fertilizers; C-band; Sensor Antenna Method 181
- 5.33 Shift in frequency vs. fertilizer concentration for soil (**pH=7.3, sample a**) mixed with 0 ml, 1 ml & 2 ml MC; all fertilizers; C-band; Sensor Antenna Method 182
- 5.34 Shift in frequency vs. fertilizer concentration for soil (**pH=7.4, sample a**) mixed with 0 ml, 1 ml & 2 ml MC; all fertilizers; C-band; Sensor Antenna Method 183

5.35	Shift in frequency vs. fertilizer concentration for soil (pH=7.5, sample a) mixed with 0 ml, 1 ml & 2 ml MC; all fertilizers; C-band; Sensor Antenna Method	184
5.36	Structure of the feed-forward neural network	185
5.37	GUI used for Moisture Content estimation; ANN Model; Sensor Antenna Method	186
5.38	Screen-shot of MC for soil (pH=5.3, sample a) mixed with PBA ; C-band; ANN Model; Sensor Antenna Method	193
5.39	Experimental setup for moisture detection using colour-mapping; Sensor Antenna Method	200
5.40	Result for moisture detection using colour-mapping (a) Camera shot (b) Colour-map; Sensor Antenna Method .	200
5.41	e-Agriculture Cycle (Courtesy : NEC Technologies India Pvt. Ltd.)	201
A.1	YL-69 Soil Moisture Sensor	214
A.2	Soil Moisture Sensing Unit with Electronic Board	215
A.3	Experimental setup for Sensing Soil Moisture using YL-69 Sensor and Arduino Uno Board	215
B.1	Image, first and second level Wavelet Transform decomposition	222
B.2	(a) General images(<i>lena, cameraman, egypt, monarch, house</i>) (b) images mixed with speckle noise variance of 0.01 (c) despeckled images by (Liu et al., 2014) (d) despeckled images using proposed algorithm	226
B.3	Plots to compare (a) PSNR (b) SSIM values of reconstructed general images for the two methods	227
B.4	(a) Original RISAT-1 image(b) mixed with speckle noise of variance 0.01 (c) despeckled image by Liu (d) despeckled image using the proposed algorithm	228
B.5	Plots to compare (a) PSNR (b) SSIM values of despeckled RISAT images for different variances	229

List of Tables

1.1	A comparison of popular methods for the measurement of permittivity	26
1.2	Comparison of Remote Sensing Methods for Soil Moisture Estimation	30
2.1	Comparison of S_{21} peaks of rectangular cavity resonator with and without samples; Cavity Perturbation Method	45
2.2	Simulation results for FR-4 and Arlon AD1000; S-band; Cavity Perturbation Method	45
2.3	Experimental results for FR-4, Arlon AD1000 and Acetone; S-band; Cavity Perturbation Method	46
2.4	Dimensions of Patch Antenna [Substrate : FR-4; $\epsilon'_r=4.4$, $h=1.6$ mm]	49
2.5	Dimensions of CPW-fed monopole antenna	50
2.6	Dependence of Resonant Frequency of Microstrip Patch Antenna and CPW-fed Monopole Antenna on Dielectric Constant of Superstrate; $f_r=1.85$ GHz, 2.45 GHz and 5.25 GHz; Superstrate Method	51
2.7	Percentage shift in frequency of MPA and CMA for different dielectric superstrates; $f_r=1.85$ GHz, 2.45 GHz and 5.25 GHz; Superstrate Method	52
2.8	Dependence of normalized resistance of MPA on loss tangent for various superstrates; L, S & C bands; Superstrate Method	54

2.9	Dependence of normalized reactance of MPA on loss tangent for various superstrates; L, S & C bands; Superstrate Method	54
2.10	Dependence of normalized resistance of CMA on loss tangent for various superstrates; L, S & C bands; Superstrate Method	55
2.11	Dependence of normalized reactance of CMA on loss tangent for various superstrates; L, S & C bands; Superstrate Method	55
2.12	Dielectric Constant of FR-4, Acrylic and Water in L, S and C bands	58
2.13	Dimensions of 4.35 GHz sensor antenna	60
2.14	Results of ϵ'_r and $\tan\delta$ obtained for test data $\epsilon'_r=5.4$ & different values of $\tan\delta$; ANN model; Superstrate Method	67
3.1	Dielectric Constant vs. pH of soil samples at S-band; Cavity Perturbation Method	76
3.2	Dielectric Constant vs. varying salt-soil mixture-ratio (soil pH=5.1) at S-band; Cavity Perturbation Method	76
3.3	Frequency and normalized impedance for Red, White and Black soil samples; L-band ($f_r=1.85$ GHz); Superstrate Method	79
3.4	Frequency and normalized impedance for Red, White and Black soil samples; S-band ($f_r=2.45$ GHz); Superstrate Method	80
3.5	Frequency and normalized impedance for Red, White and Black soil samples; C-band ($f_r=5.25$ GHz); Superstrate Method	80
4.1	Details of soil samples used in Free-space Transmission Method	88
4.2	S_{21} values of MPA in free-space, empty soil and with moisture in soil; C-band; Free-space Transmission Method	89

4.3	Dielectric constant of dry soil samples at three different frequencies; Free-space Transmission Method	108
4.4	Dielectric constant of soil sample for varying moisture content; L-band ($f_r=1.85$ GHz); Free-space Transmission Method	109
4.5	Dielectric constant of soil sample for varying moisture content; S-band ($f_r=2.45$ GHz); Free-space Transmission Method	109
4.6	Dielectric constant of soil sample for varying moisture content; C-band ($f_r=5.52$ GHz); Free-space Transmission Method	110
4.7	Error percentage between actual and experimentally-evaluated values of θ_v for 20 % moisture content; L-band ; Free-space Transmission Method	111
4.8	Error percentage between actual and experimentally-evaluated values of θ_v for 23.1 % moisture content; L-band ; Free-space Transmission Method	112
4.9	Error percentage between actual and experimentally-evaluated values of θ_v for 28.6 % moisture content; L-band ; Free-space Transmission Method	112
4.10	Error percentage between actual and experimentally-evaluated values of θ_v for 20 % moisture content; S-band ; Free-space Transmission Method	113
4.11	Error percentage between actual and experimentally-evaluated values of θ_v for 23.1 % moisture content; S-band ; Free-space Transmission Method	113

4.12	Error percentage between actual and experimentally-evaluated values of θ_v for 28.6 % moisture content; S-band ; Free-space Transmission Method	114
4.13	Error percentage between actual and experimentally-evaluated values of θ_v for 20 % moisture content; C-band ; Free-space Transmission Method	114
4.14	Error percentage between actual and experimentally-evaluated values of θ_v for 23.1 % moisture content; C-band ; Free-space Transmission Method	115
4.15	Error percentage between actual and experimentally-evaluated values of θ_v for 28.6 % moisture content; C-band ; Free-space Transmission Method	115
4.16	Percentage error in the computed and evaluated values of θ_v for dry samples ; L-band ; Free-space Transmission Method & ANN Model	118
4.17	Percentage error in the computed and evaluated values of θ_v for 20 % moisture content; L-band ; Free-space Transmission Method & ANN Model	118
4.18	Percentage error in the computed and evaluated values of θ_v for 23.1 % moisture content; L-band ; Free-space Transmission Method & ANN Model	119
4.19	Percentage error in the computed and evaluated values of θ_v for 28.6 % moisture content; L-band ; Free-space Transmission Method & ANN Model	119
4.20	Percentage error in the computed and evaluated values of θ_v for dry samples ; S-band ; Free-space Transmission Method & ANN Model	120
4.21	Percentage error in the computed and evaluated values of θ_v for 20 % moisture content; S-band ; Free-space Transmission Method & ANN Model	120

4.22	Percentage error in the computed and evaluated values of θ_v for 23.1 % moisture content; S-band ; Free-space Transmission Method & ANN Model	121
4.23	Percentage error in the computed and evaluated values of θ_v for 28.6 % moisture content; S-band ; Free-space Transmission Method & ANN Model	121
4.24	Percentage error in the computed and evaluated values of θ_v for dry samples ; C-band ; Free-space Transmission Method & ANN Model	122
4.25	Percentage error in the computed and evaluated values of θ_v for 20 % moisture content; C-band ; Free-space Transmission Method & ANN Model	122
4.26	Percentage error in the computed and evaluated values of θ_v for 23.1 % moisture content; C-band ; Free-space Transmission Method & ANN Model	123
4.27	Percentage error in the computed and evaluated values of θ_v for 28.6 % moisture content; C-band ; Free-space Transmission Method & ANN Model	123
4.28	Constituents of soil samples under test; Results courtesy : Sophisticated Test and Instrumentation Centre (STIC), CUSAT	130
4.29	ϵ'_r of soil with varying fertilizer mixture ratio; L-band ; Free-space Transmission Method	131
4.30	ϵ'_r of soil with varying fertilizer mixture ratio; S-band ; Free-space Transmission Method	131
4.31	ϵ'_r of soil with varying fertilizer mixture ratio; C-band ; Free-space Transmission Method	132
4.32	Dielectric constant of common fertilizers	133
4.33	Percentage error in the actual and evaluated values of PBA-soil mixture-ratio for different soil samples based on ANN model; Free-space Transmission Method	143
4.34	Percentage error in the actual and evaluated values of NPK-soil mixture-ratio for different soil samples based on ANN model; Free-space Transmission Method	144

4.35	Percentage error in the actual and evaluated values of Potash-soil mixture-ratio for different soil samples based on ANN model; Free-space Transmission Method	145
4.36	Percentage error in the actual and evaluated values of Urea-soil mixture-ratio for different soil samples based on ANN model; Free-space Transmission Method	146
5.1	Dimensions of sensor antenna operating in the L, S & C bands; Sensor Antenna Method	152
5.2	Shifted frequency for different materials; L-band ($f_r=1.88$ GHz); S-band ($f_r=2.45$ GHz); C-band ($f_r=5.2$ GHz); Sensor Antenna Method	153
5.3	Percentage shift in frequency of sensor antenna in the L, S & C bands; Sensor Antenna Method	154
5.4	Percentage shift in frequency for three select soil samples under varying moisture content; L-band ($f_r=1.88$ GHz); Sensor Antenna Method	157
5.5	Percentage shift in frequency for three select soil samples under varying moisture content; S-band ($f_r=2.45$ GHz); Sensor Antenna Method	158
5.6	Percentage shift in frequency for three select soil samples under varying moisture content; C-band ($f_r=5.2$ GHz); Sensor Antenna Method	158
5.7	Shift in frequency for fertilizer mixed with soil (pH=4.7, sample a); C-band ($f_r=5.2$ GHz); Fertilizers : PBA, NPK ; Sensor Antenna Method	164
5.8	Shift in frequency for fertilizer mixed with soil (pH=4.7, sample a); C-band ($f_r=5.2$ GHz); Fertilizers : Potash, Urea ; Sensor Antenna Method	164
5.9	Error in the actual and evaluated values of MC for soil [pH=4.7 (sample a)] mixed with PBA & NPK ; C-band; Sensor Antenna Method	187

5.10	Error in the actual and evaluated values of MC for soil [pH=4.7 (sample a)] mixed with Potash & Urea ; C- band; Sensor Antenna Method	187
5.11	Error in the actual and evaluated values of MC for soil [pH=5.3 (sample a)] mixed with PBA & NPK ; C-band; Sensor Antenna Method	188
5.12	Error in the actual and evaluated values of MC for soil [pH=5.3 (sample a)] mixed with Potash & Urea ; C- band; Sensor Antenna Method	188
5.13	Error in the actual and evaluated values of MC for soil [pH=6.4 (sample a)] mixed with PBA & NPK ; C-band; Sensor Antenna Method	189
5.14	Error in the actual and evaluated values of MC for soil [pH=6.4 (sample a)] mixed with Potash & Urea ; C- band; Sensor Antenna Method	189
5.15	Error in the actual and evaluated values of MC for soil [pH=7.0 (sample a)] mixed with PBA & NPK ; C-band; Sensor Antenna Method	190
5.16	Error in the actual and evaluated values of MC for soil [pH=7.0 (sample a)] mixed with Potash & Urea ; C- band; Sensor Antenna Method	190
5.17	Error in the actual and evaluated values of MC for soil [pH=7.2 (sample a)] mixed with PBA & NPK ; C-band; Sensor Antenna Method	191
5.18	Error in the actual and evaluated values of MC for soil [pH=7.2 (sample a)] mixed with Potash & Urea ; C- band; Sensor Antenna Method	191
5.19	Error in the actual and evaluated values of MC for soil [pH=7.5 (sample a)] mixed with PBA & NPK ; C-band; Sensor Antenna Method	192
5.20	Error in the actual and evaluated values of MC for soil [pH=7.5 (sample a)] mixed with Potash & Urea ; C- band; Sensor Antenna Method	192

5.21	Error in the actual and empirically-obtained values of MC for soil [pH=5.1, 5.2, 5.4, 5.9 & 6.1] mixed with Potash & Urea ; C-band; Sensor Antenna Method	194
5.22	Comparison of θ_v values for PBA-mixed dry soil samples (MC=0 ml)	196
5.23	Comparison of θ_v values for NPK-mixed dry soil samples (MC=0 ml)	196
5.24	Comparison of θ_v values for Potash-mixed dry soil samples (MC=0 ml)	196
5.25	Comparison of θ_v values for Urea-mixed dry soil samples (MC=0ml)	197
5.26	Comparison of θ_v values for PBA-mixed moist soil samples (MC=2 ml)	197
5.27	Comparison of θ_v values for NPK-mixed moist soil samples (MC=2 ml)	198
5.28	Comparison of θ_v values for Potash-mixed moist soil samples (MC=2 ml)	198
5.29	Comparison of θ_v values for Urea-mixed moist soil samples (MC=2 ml)	198
6.1	Performance Comparison for Soil Characterization; Measurement Methods	209
6.2	Performance Comparison for Soil Characterization; Analytical Methods	209
A.1	Comparison of results obtained for soil samples pH=4.7 & 4.9 using Sensor Antenna and SMP for varying moisture content	216
A.2	Comparison of results obtained for soil samples pH=5.0 & 5.3 using Sensor Antenna and SMP for varying moisture content	216
A.3	Comparison of results obtained for soil samples pH=6.4 & 7.0 using Sensor Antenna and SMP for varying moisture content	217

A.4 Comparison of results obtained for soil samples **pH=7.1 & 7.2** using Sensor Antenna and SMP for varying moisture content 217

A.5 Comparison of results obtained for soil samples **pH=7.3 & 7.5** using Sensor Antenna and SMP for varying moisture content 218

B.1 Comparison of PSNR in dB, SSIM and computation time in seconds for various general images 227

B.2 Comparison of PSNR in dB and SSIM values of RISAT image for different variances 228

ABBREVIATIONS

ACS	Asymmetric Coplanar Strip
ANN	Artificial Neural Network
CMA	CPW-fed Monopole Antenna
CPW	Coplanar Waveguide
CST	Computer Simulation Technology
FC	Fertilizer Concentration
GPR	Ground Penetrating Radar
HFSS	High Frequency Structure Simulator
ISM	Industrial, Scientific and Medical
MC	Moisture Content
MPA	Microstrip Patch Antenna
MSE	Mean Squared Error
SAR	Synthetic Aperture Radar
SMP	Sensor Module Probe
TDR	Time-domain Reflectometry
TSS	Total Soluble Salt
VNA	Vector Network Analyzer
VWC	Volumetric Water Content

NOTATION

ϵ_r	complex relative permittivity
ϵ'_r	dielectric constant
ϵ''_r	loss-factor
$\tan \delta$	loss-tangent
μ_r	complex relative permeability
θ_g	gravimetric water content
θ_v	volumetric water content
f_0	free-space resonant frequency of the cavity
f_s	shifted frequency due to insertion of sample
f_r	resonant frequency of antenna
V_c	volume of the cavity in mm^3
V_s	volume of the sample in mm^3
Q_0	Q-factor of empty cavity
Q_s	Q-factor obtained with sample
S_{11}	reflection coefficient
S_{21}	transmission coefficient
A	attenuation
$\Delta\phi$	phase shift
Δf	frequency shift
vs.	versus

Chapter 1

INTRODUCTION

Contents

1.1	Material Characterization using Microwaves	3
1.2	Soil and its Microwave Characteristics	5
1.3	Literature Survey	11
1.4	Motivation for the Work	31
1.5	Objectives of the Work	32
1.6	Thesis Outline	32
1.7	Chapter Summary	35

Microwaves are electromagnetic radiation with frequencies between 300 MHz and 300 GHz, corresponding to wavelengths ranging from as long as one meter to as short as one millimeter. International agreements regulate the use of the different parts of the microwave spectrum. The frequencies 915 MHz and 2.45 GHz are the most common among those dedicated to power applications for Industrial, Scientific and Medical purposes.

In recent years, there has been a lot of interest to explore the use of microwaves for imaging, non-destructive testing, characterization and

remote sensing of materials, media and objects. Every material has a unique set of electrical characteristics which are dependent on its dielectric properties. Accurate measurements of these properties can provide valuable information to properly incorporate the material into its intended application for better designs; they can also help in monitoring a manufacturing process for improved quality control.

Microwaves find application in a number of areas spanning many branches of science and engineering (Blackham and Pollard, 1997; Agilent, 2000; Liao et al., 2001; Wang et al., 2003; Brodie, 2012; Al Ghamdi et al., 2016). Some of the applications, wherein a knowledge about the dielectric properties of the material under test in the RF/microwave frequency range is required, are:

- Biology
- Agriculture
- Pharmacy and medicine
- Forestry and mining
- Automobile industry
- Civil engineering
- Electronics engineering
- Food and aerospace

The advantage of microwaves is that they can provide information about the inner structure of objects by carrying out measurements at the surface. Determination of complex permittivity of the material or object under test is the basic objective in microwave material characterization.

1.1 Material Characterization using Microwaves

Material Characterization describes those features of composition and structure (including defects) of a material that are relevant for a particular preparation, study of properties, or use, and suffice for reproduction of the material.

Material Characterization has two main aspects.

- Accurately measuring the physical and chemical properties of materials
- Accurately determining the structure of a material, at both the atomic and microscopic levels

Mechanical, electrical and magnetic properties of a material are strongly dependent on its structural characteristics. Therefore, material characterization is a very important part of any structure-property correlation exercise.

When microwaves are directed towards a material, energy gets reflected or transmitted through the surface or absorbed by it. The electromagnetic properties of the material depend on the proportions of energy. Permittivity (ϵ) and permeability (μ) are the key parameters describing the interaction of materials with electromagnetic fields. Dielectric profiles of materials are investigated in different parts of the frequency spectrum. Recent research applications are concentrated at microwave frequencies (Costanzo, 2012; Oliveira et al., 2017). At these frequencies, various non-resonant and resonant methods such as transmission line method, free-space method, coaxial probe method, cavity method and sensor antenna method are available for the measurement of dielectric parameters of materials (Venkatesh and Raghavan, 2005; Schueler et al., 2012; Then et al., 2014).

Application of an electric field changes the electric charge distribution of a material. Dielectric permittivity is a measure of this

change. It is commonly expressed in relation to that of free-space and is termed as complex relative permittivity, ϵ_r , consisting of a real part ϵ_r' and an imaginary part ϵ_r'' . It is expressed as

$$\epsilon_r = \epsilon_r' \pm j\epsilon_r'' \quad (1.1)$$

The real part of permittivity, called dielectric constant ϵ_r' , is a measure of how much energy from an external electric field is stored in the material. The imaginary part, ϵ_r'' , called the loss-factor, is a measure of how dissipative or lossy the material is to an external electric field. It is always greater than zero and is usually much smaller than ϵ_r' . The loss-factor includes the effects of both dielectric and conductive losses. Therefore, a material with a high loss-factor is easily heated by microwaves. On the other hand, a material with a very low loss-factor is transparent to microwaves. Another parameter frequently employed is the loss-tangent, defined as the ratio of loss-factor to dielectric constant, and expressed as

$$\tan\delta = \frac{\epsilon_r''}{\epsilon_r'} \quad (1.2)$$

Microwave Imaging is an area of research, where the idea is to make use of low-power microwaves to determine the electrical and physical properties of the object or medium under test. It can be defined as a technique used in sensing a given scene by means of interrogating microwaves. It can provide excellent diagnostic capabilities in several areas including non-destructive testing and evaluation, biomedical engineering, geophysical prospecting etc. (Pastorino, 2010; Persson et al., 2011). As any direct or in-situ method is usually destructive in nature, properties of objects that cannot be measured using in-situ procedures are good candidates for Microwave Imaging. Measurement of dielectric properties of a variety of materials over a wide frequency band is the first and crucial step to pursue the research field of

microwave imaging. This thesis focusses on the characterization of soil using microwaves.

1.2 Soil and its Microwave Characteristics

According to the glossary of science terms (Soil Science Society of America, 1970), soil is defined as the unconsolidated mineral material on the immediate surface of the earth that:

- serves as a natural medium for the growth of land plants
- has been subjected to and influenced by environmental factors of parent material, climate (including moisture and temperature effects), macro and micro organisms and topography, all acting over a period of time and producing a product that differs from the material from which it has derived all the properties and characteristics

Soil is made up of solid, liquid and gaseous components. The solid components are minerals derived originally from weathering rock and organic materials derived from plants and micro-organisms. The liquid component of the soil is made up of water, with varying amounts of nutrients and other soluble substances dissolved in it. Water and nutrients are used by plants to grow. Water may be lost by evaporation to the atmosphere, or by deep drainage through the soil. Soil is generally porous, containing many air spaces. Oxygen is required in soil for the growth of most plants. When soil becomes saturated with water, with no air left in the pores, it is said to be waterlogged.

Soil absorbs a great amount of water during rainfall; water that is not absorbed by soil drains away unless measures are taken to conserve. Amount of moisture and air in soil varies depending on climatic conditions and water drainage. As soil absorbs water, less air becomes available in soil; as soil dries, air replaces the water. Plants receiving excessive water for a long period of time usually suffer or die because

of oxygen deficiency. Soil in good physical condition drains better and holds more air than does soil in poor physical condition (Charman and Murphy, 1991). Characteristics of soil will allow one to determine what type of soil is contained in an area. Soil scientists and agronomers use characteristics of soil to learn more about a region's geographical suitability for agriculture and cultivation. Soils tend to vary greatly in chemical and physical properties even within fields that appear uniform. This variability is the source of interest in intensive soil sampling and variable rate technology for precision agriculture. Important soil properties that affect crop production are colour, structure, texture, porosity, permeability, slope, depth of rooting zone, drainage etc.

Microwaves are capable of penetrating more deeply into soil and vegetation as compared to optical waves (Calla, 1990). This is due to the variability of soil's microwave properties such as permittivity, permeability, conductivity etc. Permittivity of a material is not only frequency dependent but also dependent on density, water content, profile, sampling depth, mineral composition, granular size distribution, porosity, boundary conditions, vegetation canopies and geographic conditions. Some of these parameters, especially the last few, are typical in the case of soil. Hence study of characterization of soil is often carried out with the measurement of permittivity. Depth of penetration of microwaves is more for dry vegetation and dry soil, as compared to wet cases (Owe and de Gried, 1998). Penetration decreases with increase in the moisture content in vegetation and soil. Variability of dielectric constant of soil in the presence of water is the prime reason for the change in depth of penetration. Dielectric constant of dry soil is between 3 and 5 depending upon the texture, whereas dielectric constant of pure water is around 80 at room-temperature and at 1 GHz. Thus dielectric constant of moist soil will vary between dielectric constant of dry soil and saturated soil which is around 30 (Kraszewski, 1996; Hanson and Peters, 2000).

Soil is classified by the acidity and alkalinity of the matter contained in it. From a farmer's perspective, pH of soil is the most important

quantifiable parameter (Brady, 1972). It refers to how acidic or alkaline the soil is. A simple numerical scale is used to express pH and is shown in Fig. 1.1.

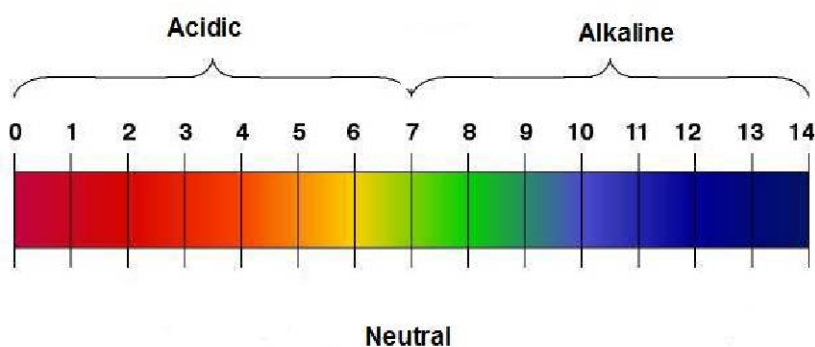


Figure 1.1: pH scale of Soil

The scale goes from 0 to 14, with 0 being most acidic, and 14 being most alkaline. The value 7 is neutral - neither acidic nor alkaline. Soil pH is important because it influences several soil factors affecting plant growth, such as soil bacteria, nutrient leaching, nutrient availability, toxic elements and soil structure. A soil test for pH determination informs the farmer whether his soil will produce good plant growth or whether he needs to treat his soil to adjust the pH level. For most plants, the optimum pH range is from 5.5 to 7.0, but some plants will grow in more acidic soil or may require a more alkaline level. Normally, lime or dolomite is used to increase the pH, or sweeten the soil and ammonium sulphate or sulphur coated urea is used to lower the pH or sour the soil. Growth and yield of most plants are unaffected until the pH reaches about 5. As the pH level drops below 5 and soil acidity increases, plant growth and yield decline. Yields can be affected directly by acidity, or indirectly by a change in the availability of some important nutrients. For example, as the pH decreases below 6, availability of phosphorus and sulphur may decrease. At the same time,

aluminium and manganese become more available and may cause yield reductions through toxicity. At pH levels above 7, other elements such as zinc may become deficient. Many soils are naturally acidic, but agricultural practices have contributed to the increasing acidification of many neutral to slightly acid soils. These practices include:

- use of some ammonium fertilizers, particularly ammonium sulphate
- production of legumes that fix nitrogen
- removal of nutrients in the form of crop-produce

Thus it is important for the agronomist to monitor the amount of water and fertilizer content in soil. Herein lies the significance of this research.

1.2.1 Moisture Content

Water has a strong influence on the dielectric properties of soil at microwave frequencies. Moisture Content (MC) of soil (also referred to as water content) is an indicator of the amount of water present in soil. Various soil-moisture mixture equations have been reported. There are two categories of such equations. The first category is a set of empirical equations for determining water content and/or soil density (Wobschall, 1977; Friedman, 2011). The second category is classified as volumetric mixing models, which are derived from discrete capacitor network theories or continuum mean field theories (Topp et al., 1980).

Soil water content is expressed on gravimetric basis or volumetric basis. Gravimetric Water Content, θ_g is the mass of water per mass of dry soil. It is expressed as:

$$\theta_g = \frac{m_{water}}{m_{soil}} = \frac{(m_{wet} - m_{dry})}{m_{dry}} \quad (1.3)$$

Volumetric Water Content, θ_v , is the ratio of volume of water to the total volume. It is expressed as:

$$\theta_v = \frac{\text{volume of water}}{\text{total volume}} \quad (1.4)$$

Topp stated that the apparent dielectric permittivity could directly be related to volumetric water content θ_v through a polynomial calibration curve, called Topp's Equation. This empirical approach simply fits mathematical expressions to measured data, unique to the physical characteristics of soil. Topp fitted a third-order polynomial to the observed relationship between ϵ_r' and θ_v for multiple soils. Topp's equation is given as:

$$\theta_v = 4.3 \times 10^{-6} \times \epsilon_r'^3 - 5.5 \times 10^{-4} \times \epsilon_r'^2 + 2.92 \times 10^{-2} \times \epsilon_r' - 5.3 \times 10^{-2} \quad (1.5)$$

This empirical relationship for mineral soils provides an adequate description for $\theta_v < 0.5$, which covers the entire range of interest in most mineral soils, with a θ_v estimation error of about 0.013. It is valid for all soils wetted with deionized water for frequencies below 17 GHz, the relaxation frequency of free water (Kelleners et al., 2005). Topp's equation has been used extensively in this research to validate the relation between ϵ_r' and θ_v for a variety of soil samples available in Kerala.

1.2.2 Fertilizer Content

Nutrients are essential for plant growth. They are classified as macro- and micro-nutrients, based on the quantity required. As they grow, plants extract nutrients they need from the soil. Unless these nutrients are replenished, plants will eventually cease to grow. In nature, nutrients are returned to the soil when plants die and decay. When

cultivated plants are harvested, nutrients that the plants extracted from soil are taken away. Loss of organic matter is a serious problem and can even lead to soil erosion. If the soil loses this organic matter, which has been built up over many years, plants may not grow well. To keep the soil productive, it is necessary to replace these nutrients artificially. This is done by applying to the soil substances that contain these nutrients. Nitrogen, phosphorus and potassium (NPK) are the three major macro-nutrients. Iron, boron and zinc are the main micro-nutrients. Many commercial fertilizers supply these essential elements. For agricultural purposes, variation in the concentration of fertilizers is considered as important as moisture content. Different levels of fertilizers give rise to a large variation in the dielectric constant. Thus, knowledge of the variation of the dielectric constant of soil with fertilizers is necessary for the accurate characterization of soil. Systematic study of microwave sensing of soil properties in the presence of moisture and fertilizers has thus evolved as a major need of the hour. Moreover, soil testing as a tool for judicious recommendation of moisture and fertilizer contents, has assumed great relevance for proper crop-management in agriculture.

NPK fertilizer is a complex fertilizer comprised primarily of the three major macro-nutrients required for healthy plant growth. The agriculture industry relies heavily on the use of NPK fertilizer to meet global food supply and ensure healthy crops. According to International Fertilizer Development Centre's (IFDC) Strategic Plan 2012-15, about half of the global population is alive as a result of the increased food production provided by the use of mineral fertilizers. Details of NPK mixture, usually quoted as NPK 20:20:20, are enumerated below.

- The first number is the percentage of nitrogen in the fertilizer. It is used by plants for producing leaf growth and greener leaves
- The second number is the amount of phosphorus which is used by plants to increase fruit development and to produce a strong root system

- The third number is the amount of potassium, often referred to as potash. It is used by plants for flower colour and size. It also supports the overall health of the plant by helping build strong cells

The remaining 40 percent of mixture is inert chemically, but will help the active chemicals in the fertilizer spread and get taken up by the plants.

1.3 Literature Survey

A detailed literature survey is conducted on the work reported in the area of material characterization and microwave sensing. As discussed, materials possess electrical characteristics which are related to their dielectric properties. A measurement of these properties provides valuable information to properly incorporate the material into its intended application. Moreover, measurement of dielectric properties can be used for non-destructive monitoring of materials undergoing physical or chemical changes. Several measurement methods for material characterization have been reported in literature. The particular method used depends on the frequency range of interest and the type of target material. Choice of measurement equipment and design of sample holder depend upon the dielectric materials to be measured, the extent of the research, available equipment and resources for studies.

Relevant literature on permittivity measurement for material characterization and microwave imaging for soil characterization is reviewed in the following sections. Significance of soil characterization using microwaves for estimation of moisture and fertilizer contents is emphasized.

1.3.1 Permittivity Measurement for Material Characterization

Measurement methods relevant for any desired application depend on the nature of the dielectric material to be measured (both physical and electrical), degree of accuracy required and the frequency of interest. Measuring instruments that provide reliable determination of the required electrical properties involving the unknown material in the frequency range of interest have been reported (Nelson, 1991).

The challenge in making accurate permittivity measurements lies in the designing of the material sample holder (both radio and microwave frequency ranges) and adequately modelling the circuit for reliable calculation of the permittivity from the electrical measurements. Appropriate estimation of the RF circuit parameters (impedance or admittance for example) will lead to the determination of the frequency-dependent dielectric properties of any material.

The methods for permittivity measurements in the low, medium and high frequency ranges, including the use of several bridges and resonant circuits have been reviewed in (Field, 1954). Dielectric properties of grain samples are reported from measurements with a precision bridge for audio frequencies from 250 Hz to 20 kHz with sample holders confined in a coaxial sample holder (Corcoran et al., 1970). Dielectric sample holder designs for the particular materials of interest are documented in (Nelson and Kraszewski, 1990). Results of grain and seed samples tested using a Q-meter based on resonant circuit are reported in the 1 MHz to 50 MHz range (Nelson, 1991).

For the higher frequency ranges, coaxial sample holders modelled as transmission-line sections with lumped parameters (measured with an RX-meter for 50 MHz to 250 MHz range and admittance meter for 200 MHz to 500 MHz range) are available. (Lawrence et al., 1998) gives the design and model of a coaxial sample holder to accommodate flowing grain and characterized by full two-port parameter measurements. Use of several organic solvents such as alcohols of known permittivities, and

signal flow analysis, provides measurement of dielectric properties of grain over a range of 25 MHz to 350 MHz.

At microwave frequencies, generally about 1 GHz and higher, transmission-line, resonant cavity and free-space methods are commonly used. Principles and methods of permittivity measurements are illustrated in several reviews (Altschuller, 1963). Dielectric property measurement methods can be categorized as reflection or transmission types using resonant or non-resonant systems, with open or closed structures for sensing of the properties of material samples. Waveguide and coaxial line transmission measurements represent closed structures while the free-space transmission measurements and open-ended coaxial-line systems represent open-structure methods. Resonant structures can include either closed resonant cavities or open resonant structures operated as two-port devices for transmission measurements or as one-port devices for reflection measurements. Attenuation and phase shift are the two main components of the complex transmission coefficient, which permit the calculation of the dielectric constant (ϵ'_r) and dielectric loss-factor (ϵ''_r) of the material under test (MUT). For free-space measurements, the lateral sample size must be sufficiently large to avoid problems caused by diffraction at the edges of the sample (Nelson, 1998).

In earlier measurements referred to in (Roberts and Hippel, 1946), standing wave ratios (SWRs) are required to measure in-line with and without the sample inserted. Based on the shift of the standing-wave node and changes in the widths of nodes, related to SWRs, sample length and waveguide dimensions, etc., ϵ'_r and ϵ''_r are computed with suitable computer programs. Similarly, the complex reflection coefficient of the empty and loaded sample holder can be measured using a network analyzer or other instrumentation, where similar determinations are made as discussed above. Microwave dielectric properties of wheat and corn are reported at several frequencies by free-space measurements with a Vector Network Analyzer (VNA). Dielectric sample holders with rectangular cross-sections are placed between horn antennas (Trabelsi et al., 1997).

Several methods, such as microwave measuring sensors, are used to measure the dielectric properties of agri-food materials in the microwave region (De Loor and Meijboom, 1966; Bengtsson and Risman, 1971). For liquid and semi-solid materials, including biological and food materials, open-ended coaxial-line probes are used for broadband permittivity measurements (Grant et al., 1989). A similar method is used for permittivity measurements on fresh fruits and vegetables (O'Toole et al., 2015). Due to density variations in material, such methods are not free of errors. If there are air bubbles or gaps between the end of the coaxial probe and the sample, the method is not suitable for determining permittivities of granular and pulverized samples.

Metamaterial-inspired microwave sensors have been proposed as an alternative to conventional methods, which are well-suited for the measurement of complex permittivity of materials (Eleftheriades and Selvanayagam, 2012; Raj et al., 2016).

Major permittivity measurement methods found in literature are listed below.

1. The Cavity Perturbation Method :

This method is frequently used for measuring dielectric properties of homogeneous food materials due to its simplicity, accuracy and high temperature capability (Bethe and Schwinger, 1943; Altschuller, 1963; De Loor and Meijboom, 1966; Bengtsson and Risman, 1971; Metaxas and Meredith, 1983). The method is also well-suited to low dielectric loss materials (Kent and Kress-Rogers, 1986), (HP 1992). Resonant cavities are designed in the standard TE (transverse electric) or TM (transverse magnetic) mode of propagation of the electro-magnetic fields. It is based on the shift in resonant frequency and the change in absorption characteristics of a tuned resonant cavity, due to insertion of a sample of target material. Measurement is made by placing a sample completely through the centre of a waveguide (rectangular or circular) that has been

made into a cavity. Changes in the centre frequency and width due to insertion of the sample provide information to calculate the dielectric constant. Changes in the Q-factor (ratio of energy stored to energy dissipated) are used to estimate the dielectric loss.

Size of the cavity must be designed for the frequency of interest, the relationship being inverse (higher frequency, smaller cavity). Each cavity needs calibration, but once the calibration curves have been obtained, calculations are rapid. Sample preparation is relatively easy, and permittivities of a large number of samples can be determined in a short time. This method is also easily adaptable to high (up to +140°C) or low (-35°C) temperatures (Bengtsson and Risman, 1971) and has been used to determine the dielectric properties of many agri-food products over a wide range of frequencies, temperatures and composition.

For ease of measurement, VNA can be used to automatically display changes in frequency and width (Engelder and Buffler, 1991). The American Society for Testing and Materials (ASTM 2001) recommends a standard procedure for waveguide cavity design. Research reported in (Venkatesh et al., 1998) has focussed on the development of such a measuring system to operate at certain Industrial, Scientific and Medical (ISM) approved frequencies (915 MHz - 2.45 GHz) and wide temperature ranges.

Solid sample preparation :

For solid materials, samples in the form of rods can be formed, moulded or machined directly from their material into microwave transparent test tubes. While quartz is the best available material for this purpose, borosilicate glass is considered acceptable, but ordinary glass should not be used. Wall thickness should be as thin as possible while having the required mechanical rigidity. Paper or plastic straws also be used instead of glass. For a semi-solid material such as TyloseTM, sample preparation is quite

difficult; however a special micropipeting equipment for such gel-type materials has been successfully designed and built (Meda, 1996).

Liquid sample preparation :

Liquids are filled into test-tube sample holders with a pipette. Small diameter pipettes themselves also make excellent sample holders. For low-loss dielectric materials, 200 μl pipettes are suitable; 10 μl pipettes are suitable for high-loss materials. Materials that can be melted are poured into sample holders and allowed to solidify. This method is appropriate if the material does not change its properties following melting and resolidification. An accurate method of measuring the complex permittivity of highloss liquids like water is presented in (Mathew and Raveendranath, 1993). Measurement of complex permittivity of liquids using open-ended coaxial cavity resonators, based on the cavity perturbation method is presented in (Raveendranath et al., 1996). The dielectric parameters of water and nitrobenzene are measured using cavity perturbation method (Raveendranath et al., 2000). For this, a capillary tube filled with the sample liquid is introduced into the coaxial resonator. This causes shifts in the resonance frequency and loaded Q-factor of the resonator. These parameters are used to determine the real and imaginary parts of the complex permittivity of the sample liquid, respectively.

Dielectric properties (both dielectric constant and dielectric loss-factor) and penetration depth of supersaturated glucose aqueous solutions (45 % w/w to 56 % w/w) at 2.45 GHz are investigated at temperatures ranging from 25°C to 80°C, using cavity perturbation method (Mathew and Raveendranath, 2000; Liao et al., 2001).

Measurement details and the perturbation equations adapted for calculation of dielectric constant and loss-factor along with accuracy information are reported in (Venkatesh, 2002). Cavity

perturbation method has also been used to measure the dielectric properties of garlic at selected levels of moisture content and at 35°C to 75°C, wherein the transmission characteristics are measured using Hewlett-Packard 5410B Network Analyzer and S-parameter test set combination (Sharma and Prasad, 2002).

Semi-solid samples preparation :

Sample preparation involves either filling the sample in its molten state and then solidifying or applying a vacuum at one end while forcing the sample into a thin cylindrical shaped holder. It is important to develop suitable fixtures to contain samples at different threshold conditions, because temperature measurements may be difficult for materials such as cheese, butter etc. (Horsfield et al., 1996).

2. Transmission/Reflection Method :

Massachusetts Institute of Technology made early efforts to characterize the dielectric properties of materials (Von Hippel, 1954). Values of ϵ'_r and ϵ''_r are derived from transmission line theory, which indicated that these properties could be determined by power-measuring the phase and amplitude of a reflected microwave signal from a sample of material placed against the end of a short-circuited transmission line, such as a waveguide or a coaxial line. For a waveguide structure, rectangular samples that fit into the dimensions of the waveguide at the frequency being measured, are required. For coaxial lines, an annular sample needs to be fabricated. Thickness of the sample should be approximately one-quarter of the wavelength of the energy that has penetrated the sample. Since the shift in wavelength is related to dielectric constant, a guess must first be made as to the magnitude of the constant. Typical thickness at 2.45 GHz ranges from 5 mm for woods to 19 mm for fats and oils. In (Kim et al., 1998), the authors have measured and predicted the dielectric properties of biscuit dough at 27 MHz and their results are found to be significantly useful for the baking industry operating at both

radio frequency and microwave spectrums. Coaxial-line and rectangular wave-guide sample holders are used with various microwave measurement systems assembled for dielectric properties determination on grain, seed and fruit/vegetable tissue samples at frequencies from 1 GHz to 22 GHz. The same sample holders are also found to be useful for measurements on pulverized coal and mineral samples (Nelson, 1983).

In the transmission/reflection line method, measurement involves placing a sample in a section of waveguide or coaxial line and measuring the complex scattering parameters - reflection coefficient S_{11} and transmission coefficient S_{21} - with a VNA. Calibration is carried out before making the measurement. The method requires sample preparation such as machining so that the sample fits tightly into the waveguide or coaxial line. Calibrations in transmission line measurements use various terminations that produce different resonant behaviour in the transmission line. For good dielectric measurement, maximum electric field is required; this is achieved by open-circuited or other capacitive termination. Calibration in coaxial line measurements is made using either short-circuited, open-circuited or matched-load termination (James, 1990).

The VNA is first calibrated and the MUT is placed in a sample holder. The MUT must fit tightly in the sample holder in order to reduce measurement uncertainty caused by air gaps. Calibration plane can be extended to the sample surface by two methods. The first method is to manually feed the phase-factor which is equivalent to the distance between the sample surface and the connector calibration plane. Phase-factor can be easily included into the measurement with the features in the VNA. VNA will shift the calibration plane from the connector to the MUT surface. The second method involves the de-embedding function of the VNA. This requires measuring the S-parameter of an empty sample holder after calibration is done. The measured

S-parameter of the empty holder is then input into the VNA. Using the de-embedding function in the VNA, the influence of the sample holder on actual material measurement can be cancelled out. Both methods produce similar results. The measured S-parameters are then post-processed to determine the complex dielectric properties. In (HakimBoughrie et al., 1997), a non-iterative transmission/ reflection method applicable to permittivity measurements using arbitrary sample lengths in wide-band frequencies is discussed. The method is based on a simplified version of the Nicolson-Ross-Weir (NRW) method. For low-loss materials, this method is stable over the entire frequency range. Accuracy on dielectric permittivity is similar to that obtained with iterative methods.

One of the variants of the transmission/reflection method is the Time-domain Spectroscopy method, also called the Time-domain Reflectometry (TDR) method. The TDR method, developed in the 1980's, has been used for the study of the dielectric properties of food. Essentially, this method also utilizes the reflection characteristic of the MUT to compute the dielectric properties. Measurement is very rapid and accuracy is high, within a few percent error (Afsar et al., 1986). Sample size is very small and the substance measured must be homogeneous. Although these methods are expensive, they are excellent tools for advanced research on the interaction of the electromagnetic energy and materials over a wide frequency range. Dielectric properties of honey-water mixture have been investigated and tabulated using the TDR method in the frequency range of 10 MHz to 10 GHz at 25°C (Puranik et al., 1991).

Topp, in (Topp et al., 1980) found that TDR signal electric loss is a function of the bulk electrical conductivity σ , regardless of whether this conductivity arises from soil-water solution conductivity or from clay type and content. This means that the effects of soil-water conductivity and clay content can be lumped

together and taken into account by including the bulk electrical conductivity in the TDR calibration.

The Open-ended Probe Technique, pioneered by (Stuchly and Stuchly, 1980), circumvents many disadvantages of the transmission line measurement method. It calculates the dielectric properties from the phase and amplitude of the reflected signal at the end of an open-ended coaxial line inserted into a sample to be measured. Care must be exercised with this method because errors are introduced at extreme frequencies, as well as for low values of dielectric constant and loss-factor. This method is valid for 915 MHz and 2450 MHz, for materials with loss-factors greater than 1 (Sheen and Woodhead, 1999). Interpretation for lower-loss materials such as fats and oils must be treated with caution. Typical open-ended probes utilize 3.5 mm diameter coaxial line.

For measurement of solid samples, probes with flat flanges are utilized (HP 1992). The open-ended probe method is successfully commercialized and software & hardware are available. It is highly desirable to measure dielectric properties of biomaterials over the temperature range commonly experienced in insect controls, as thermal treatment for controlling insects in fruits is done between 20°C and 60°C. An open-ended coaxial probe method is used to measure the dielectric properties of insects over a frequency range from 1 MHz to 1800 MHz (Wang et al., 2003).

The coaxial probe method is basically a modification of the transmission line method. It uses a coaxial line, which has a tip that senses the signal reflected from the material. The tip is brought into contact with the substance by touching the probe to a flat face of a solid or by immersing it in a liquid. The method is quite easy to use and it is possible to measure the dielectric properties over a wide range of frequencies (500 MHz - 110 GHz); however, it is of limited accuracy particularly with materials with low values of ϵ'_r and ϵ''_r . Variations of the basic

coaxial-line probe are the elliptical-ended and conical-tipped ones. Dielectric properties of six fruit commodities along with four associated insect pests have been measured between 1 MHz and 1800 MHz using an open-ended coaxial probe method and at temperatures between 20°C and 60°C (Wang et al., 2003).

Microstrips have long been used as microwave components. They show many properties making them suitable for use in dielectric permittivity measurement. Effective permittivity (a combination of the substrate permittivity and the permittivity of the material above the line) of a microstrip transmission line is dependent on the permittivity of the region above the line. This effect has been utilized in implementing microwave circuits for the investigation of dielectric permittivity. Measurement of effective permittivity is well-suited to implementation in industrial equipment. Such a system determines the effective permittivity of a microstrip line covered by an unknown dielectric substance (Kear and Holmes, 1995). Use of printed circuit boards and adding substrate materials to characterize materials and measuring permittivity using algorithmic models, have been reported. (Ghannouchi and Bosisio, 1989) report on non-destructive broadband permittivity measurements using open-ended coaxial lines as impedance sensors, which are of great interest in a wide variety of biomedical applications. They also report an attempt to replace Automatic Network Analyzer such as the HP8510B by combining the capabilities of personal computers with customized software. The reported measuring system consists of a microwave junction designed to operate from 2 GHz to 8 GHz and a number of standard microwave laboratory instruments (power meters, counters, sweepers, etc.) controlled by an IEEE 488 bus interface by a microcomputer (HP9816) to provide a precision low-cost automatic reflectometer suitable for permittivity measurements.

The device under test is an open-ended coaxial test probe immersed in the test liquid kept at a constant temperature. Data acquisition and reduction are fully automatic. Complex reflection coefficient is calculated from the four power readings and the calibration parameters of the six-port reflectometer (SPR). SPR can provide non-destructive broadband permittivity measurements with an accuracy comparable to commercial ANA accuracy but at a considerable reduction in equipment costs. This effective transmission line method, used to represent the fringing fields in the test medium, provides a good model to interpret microwave permittivity measurements in dielectric liquids. Using such a model, the precision on relatively high-loss dielectric liquid measurements is good. However, this method involves a more complex mathematical procedure in order to translate the signal characteristics into useful permittivity data. HP developed the first radio-frequency dielectric probe for evaluating colloidal liquids such as milk. The unit can accurately measure dielectric properties of materials such as food, pharmaceutical and bio-chemical products. The HP E5050A Colloid Dielectric Probe is designed for permittivity evaluation of colloidal liquid materials in the food, chemical, pharmaceutical and biochemical industries. It operates from 200 kHz to 20 MHz with the HP4285A precision LCR meter and HP vectra personal computer. The advanced sensing method provides permittivity versus frequency characteristics. Its electromagnetic method eliminates the electrode polarization effect, which may cause measurement errors when ionic materials are measured with metal electrodes.

In (Joshi et al., 1994), variational method for the analysis of microstrip antenna with dielectric overlay is investigated with special reference to the strip thickness dependence. Effective permittivity is calculated for different overlay thicknesses and permittivities. A study of thickness-dependent variation in

microwave properties of $\text{Mg}_x\text{Mn}_{(0.9x)}\text{Al}_{0.1}\text{Zn}_{0.8}\text{Fe}_{1.2}\text{O}_4$ thick films and enhancement of power efficiency of Ag thick film patch antenna is carried out in (Kashid et al., 2013). Xband microwave properties of the thick film are measured by superstrate method using Ag thick film patch antenna as the resonant element. Complex permittivity and permeability of these thick films are also measured by this method. Measurement of permittivity of dielectric materials and how it affects and gets affected by an electric field is presented in (Jingchu and Geyi, 2013). Here the authors have proposed a new method for determining the properties of dielectric materials. A dielectric sample in free-space illuminated by an incident field from a nearby antenna produces a scattered field, which will affect the input impedance of the antenna. The change of the input impedance of the antenna is then used to determine the permittivity and the loss of the dielectric sample.

3. Free-space Transmission Method :

Of the measurement methods available, free-space method is grouped under non-destructive and contact-less measuring methods. It does not require special sample preparation. Hence the method is particularly suitable for materials at high temperature and for inhomogeneous dielectrics. In addition, it may be easily implemented in industrial applications for continuous monitoring and control. e.g, moisture content determination and density measurement.

In the free-space transmission method, a sample is placed between a transmitting antenna and a receiving antenna; attenuation and phase shift of the signal are measured, the results of which can be used to characterize the material dielectric properties. Accurate measurement of permittivity over a wide range of frequencies can be achieved by free-space methods. In most systems, the accuracy of ϵ_r' and ϵ_r'' determined depends mainly on the performance of the measuring system and the

validity of the equations used for the calculation. The usual assumption made in this method is that a uniform plane wave is normally incident on the flat surface of a homogenous material, and that the planar sample has infinite extent laterally, so that diffraction effects at the edges of the sample can be neglected.

Fig. 1.2 represents a free-space measuring method with the transmitting and receiving antenna elements and the sample holder in between. (Trabelsi et al., 1997) accounts for multiple reflections, mismatches and diffraction effects at the edges of the sample as they are generally considered the main sources of errors. To enhance the measurement accuracy, special attention is given to the choice of the radiating elements, design of the sample holder/geometry and location between the two radiating elements.

Free-space method is used to determine transmission coefficients of materials in the aviation industry (Skocik and Neumann, 2015). Measurements are conducted at high frequencies from 220 GHz to 325 GHz on a teflon sample because of the ease of verifying the results.

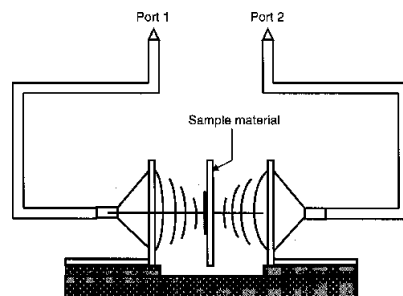


Figure 1.2: Schematic of Free-space Transmission Method for measuring reflection and transmission (Ports 1 and 2 are connected to the VNA)

4. Sensor Antenna Method :

Microwave sensor interacts with matter to measure properties. It

can be used for material characterization to sense parameters such as moisture content, density, structure and shape of materials, and even chemical reaction. Advantages of microwave sensor over traditional sensor is its speed of measurement, non-destructive nature and precision. Sensors have shown the potential to be ubiquitous and shape the upcoming industrial facilities and medical diagnostic systems (Schueler et al., 2012). Choice of sensors depends on the measured or sensed parameters, functional principles or on applications. Microwave sensors include electromagnetic-sensing types as well as wireless sensors. Although microwave sensors are generally more expensive than low frequency sensors, they possess special features. A prominent example is a radar sensor used for air traffic control or for body scanning. Wireless (or contactless) sensing has the added advantage in harsh or moveable environments. Effectiveness of a microwave sensor strongly depends on the technique of coupling microwave to test materials. Eight categories of coupling mechanisms for microwave sensor are reported (Kraszewski, 1991).

Microwave sensors based on metamaterials have been proposed as alternative to conventional methods. These are reported to be well-suited for the measurement of complex permittivity of materials. (Anju, 2015) reports that metamaterial-based sensors offer a very convenient and accurate method for characterisation of any type-solid or liquid, thereby making them effective for agricultural purpose. (Raj et al., 2016) discusses the design and development of a metamaterial-inspired planar microwave sensor for the measurement of complex permittivity of solid and liquid samples under test. An empirical relation between sensor resonance characteristics and complex permittivity of the sample is derived. The designed sensor is fabricated on an FR4 substrate and is experimentally validated for various standard solid samples and hazardous chemical liquids. The proposed sensor

works in the frequency range of 5.3 GHz to 8.2 GHz and is capable of measuring dielectric properties of a variety of samples.

Table 1.1 summarizes the features of four popular methods discussed thus far in terms of relevant technical performance parameters.

For the transmission/reflection method, the capability for loss measurement is limited. Also, sample preparation for this system is relatively difficult. Since this research focusses on the characterization of soil, pre-processing steps such as drying, pulverization etc. will be more crucial for the transmission/reflection method when compared with the other three schemes. However, one of the simple methods in which an antenna is loaded with a material whose dielectric properties are to be studied, is reported in (Jingchu and Geyi, 2013). As the MUT forms a superstrate on the antenna beneath, the method is called Superstrate Method for material characterization. Therefore, cavity perturbation method, superstrate method, free-space transmission method and sensor antenna method are considered in detail for the study of soil characterization. Material characterization using these methods is described in Chapter 2 as a prelude to soil characterization.

Table 1.1: A comparison of popular methods for the measurement of permittivity

Parameter	Cavity Perturbation Method	Transmission / Reflection Method	Free-space Transmission Method	Sensor Antenna Method
Frequency	Narrowband	Narrowband	Broadband	Broadband
Sample size	Very small	Moderate	Large	Small
Temperature monitoring/control	Difficult	Difficult	Very easy	Easy
Accuracy for :				
Low-loss material	Moderate	Low	Low	Moderate
High-loss material	Low	Low	Moderate	High
Sample preparation	Difficult	Difficult	Easy	Easy
Most suitable test material	Solids, liquids, semi-solids	Solids	Large flat sheets	Solids, liquids, semi-solids
Measured parameter (Permittivity and/or Permeability)	Permittivity and Permeability	Permittivity and Permeability	Permittivity or Permeability	Permittivity and Permeability

1.3.2 Microwave Imaging for Soil Characterization

This section reviews the literature on microwave imaging as a tool for soil characterization. The role played by microwave remote sensing, one of the key methods of imaging, is also reviewed. Since the thesis focusses on soil, significant findings of the literature survey, utilizing all the major in-situ and remote sensing methods carried out on soil, are discussed.

Microwave imaging is a science which has evolved from traditional detecting/locating methods in order to evaluate hidden or embedded objects in a structure using electromagnetic waves in the microwave regime (Fallahpour, 2013). Microwave imaging methods can be classified as either quantitative or qualitative (Lianlin et al., 2010). Quantitative imaging (or inverse scattering) methods give the electrical and geometrical parameters (i.e., shape, size and location) of an imaged object by solving a non-linear inverse problem (Fallahpour et al., 2014). It is converted into a linear inverse problem by using suitable approximations. Direct matrix inversion methods can be invoked to solve the inversion problem. To overcome this issue, direct inversion is replaced with iterative solvers. Techniques in this class are called forward iterative methods and are usually time consuming (Zaeytijd et al., 2007). On the other hand, qualitative microwave imaging methods calculate a qualitative profile (known as reflectivity function or qualitative image) to represent the hidden object. These methods use approximations to simplify the imaging problem and use back-propagation to reconstruct the unknown image profile. Synthetic Aperture Radar (SAR), Ground Penetrating Radar (GPR) etc. are some of the most popular qualitative microwave imaging methods (Fallahpour, 2013).

Progress achieved in the active microwave remote sensing of soil moisture during the four years of the AgRISTARS program is summarized in (Dobson and Ulaby, 1986). The AgRISTARS is a Joint Program for Agriculture and Resources Inventory Surveys through Aerospace Remote Sensing. The study highlights the following four

main points: (i) Dielectric constant of dry soil is dependent on soil bulk density & frequency over the microwave region (ii) Addition of water to a dry soil medium results in an increase in the dielectric constant that is smaller in magnitude for initial increments of bound water than for subsequent additions of bulk water (iii) Quantity of bound water is controlled by soil texture and mineralogy, which results in profound differences among soil types with respect to the dielectric constant at a given moisture content (iv) As the dielectric constant of moist soils is proportional to the number of water dipoles per unit volume, the preferred measure for soil moisture is volumetric.

Changes in the characteristics of the pore fluid in soils, such as concentration, valence and permittivity, affect the electrical properties of the bulk fluid as stated in (Santamaria and Fam, 1997). Also the formation of double layers causes volumetric changes and alters the fabric of the soil. The authors, in (Soontornpipit et al., 2006), present a method and dual-use designs for simultaneous sensing of soil moisture and communication from the buried antenna to an external receiver. Using Genetic Algorithm and FDTD method, the sensing band is designed to have maximum sensitivity to the moisture of the surrounding soil, while the communication band is designed to have minimal detuning due to changes in soil moisture. Dielectric permittivity in terms of a frequency-dependent part and a frequency-independent part is studied in (Chen et al., 2008). These two parts correspond to polarizations at different frequency range. (Lu et al., 2009) present a new soil moisture retrieval algorithm, based on a modified radiative transfer model, in which the volume scattering inside soil layers is calculated through Dense Media Radiative Transfer (DMRT) theory.

Experimental results of studies carried out for understanding the behaviour of solid dielectrics in the form of soil at microwave frequency and the dielectric and electric response of some fertilizers in soil in the presence of microwave energy are presented in the article (Vivek et al., 2009). Different fertilizers such as Urea, Shree Ram-33, Shree Ram-50P, D.A.P and Mosaic are used along with soil samples. A

compact and low-cost rectangular patch antenna that is used as a sensor for real-time agriculture measurements is presented in (You et al., 2010). An in-situ method for measuring both electric and magnetic properties of Hawaiian volcanic soil for GPR applications in a broad frequency range from 50 MHz to 1 GHz is presented in paper (Youn et al., 2010). The frequency and temperature dependent complex permittivity or conductivity of a silty clay loam is examined in a broad saturation and porosity range with network analyzer method in (Wagner et al., 2011). Novel miniature metamaterial-based soil moisture sensors are presented in the paper (Kitic et al., 2012). The sensors are based on resonant-type metamaterials and employ split-ring resonators (SRR), spiral resonators and fractal SRRs to achieve small dimensions, high sensitivity and compatibility with standard planar fabrication technologies.

(Pooja and Dharmendra, 2013) deal with the task of estimating soil moisture under vegetation cover by using the two-layer model based on transmission-line theory. The two-layer model measures the impedance of both the layers namely, soil and vegetation. This impedance is a function of dielectric constant & thickness of both the layers. Soil moisture value is retrieved from the real part of complex dielectric constant of soil by using well-known polynomial relation proposed in (Topp et al., 1980). Some papers which throw light on the use of microwave remote sensing for surface soil moisture estimation are (Engman, 1990; Wang and Qu, 2009; Manab, 2010; Mironov et al., 2013). Relevant pieces of information collected from a review of these papers are: Researches in soil-moisture remote sensing began in the mid-1970's shortly after the surge in satellite development. No direct measurement of volumetric water content is possible in any of the approaches to remote sensing of soil moisture; only indirect methods are applicable. Technological advances in satellite remote sensing have offered a variety of methods for measuring soil moisture across a wide area continuously over time. Subsequent research effort has occurred along many diverse paths, from optical to microwave region of the electromagnetic spectrum. Near-surface soil moisture content can be

measured by Optical means, Thermal-infrared means and Microwave Remote Sensing means. Microwave remote sensing can be classified into passive microwave remote sensing and active microwave remote sensing. The relative merits of the different remote sensing methods for surface soil moisture estimation are summarized in Table 1.2.

Table 1.2: Comparison of Remote Sensing Methods for Soil Moisture Estimation

Description	Optical	Thermal infrared	Microwave (passive)	Microwave (active)
Properties observed	Soil reflection	Surface temperature	Brightness temperature, Dielectric properties, Soil temperature	Backscatter coefficient, Dielectric properties
Advantages	Fine spatial resolution, Broad coverage	Broad coverage, Physically well understood	Low atmospheric noise, Moderate surface penetration, Physically well understood	Low atmospheric noise, Moderate surface penetration, High spatial resolution, Physically well understood
Limitations	Limited surface penetration, Cloud contamination, Many other noise sources	Limited surface penetration, Cloud contamination, Perturbed by meteorological conditions & vegetation	Low spatial resolution, Perturbed by surface roughness & vegetation	Limited swath width, Perturbed by surface roughness & vegetation

The primary differences among these methods are: (a) wavelength region of the electromagnetic spectrum used (b) source of the electromagnetic energy (c) response measured by the sensor and (d) the physical relation between the response and soil moisture content. Radars measure the energy scattered back from the surface, while radiometers measure the self-emission from the surface of the Earth. As remote sensors do not measure soil moisture content directly, mathematical models that describe the connection between the measured signal and soil moisture content must be derived. Usually, the forward model simulates the response of the instrument on the basis of relevant land surface parameters. A method is then developed for inverting the model by minimizing the residual error between the model-simulated and sensor-measured values. Microwave remote sensing provides a unique capability for the estimation of soil moisture by measuring the electromagnetic radiation in the region between 0.5 cm and 100 cm. The fundamental basis of microwave remote sensing for soil moisture is the large contrast between the dielectric constant

(ϵ_r') of water (about 80) and soil particles (< 4). As the moisture-content increases, ϵ_r' of the soil-water mixture increases and this change is detectable by microwave sensors.

Both passive and active microwave remote sensing methods have demonstrated the most promising ability for globally monitoring soil moisture variations. Passive remote sensors, such as Space Imaging's IKONOS, detect naturally reflected or radiated energy (Satellite Imaging Corporation, 2014). Active sensors (such as radars), on the other hand, send out their own electromagnetic energy and then record what comes back to them. The most common active imaging microwave configuration is the Synthetic Aperture Radar (SAR), which transmits a series of pulses as the radar antenna traverses the scene. These SAR systems can provide resolutions of the order of tens of metres over a swath width of 50 km to 500 km. SAR satellite systems such as ENVISAT C-band Advanced SAR (Spazio, 2011), Canadian C-band RADARSAT (Canadian Space Agency, 2015), Japanese L-band ALOS-PALSAR (Rosenqvist et al., 2004) and German X-band Terra-SAT (Mittermayer et al., 2002), with frequencies suitable for soil moisture retrieval, are in use now. The Soil Moisture and Ocean Salinity (SMOS) and Soil Moisture Active Passive (SMAP) missions offer a combined passive/active microwave approach of retrieving soil moisture to increase the accuracy of the retrievals for high-resolution soil moisture products (Bindlish et al., 2009; Jin et al., 2017).

1.4 Motivation for the Work

As discussed in the previous sections, one can characterize soil and estimate the moisture and fertilizer contents in it through a variety of microwave means. Surface soil moisture is the water in the upper 10 cm of soil. In the two-way interaction between land and atmosphere, soil moisture is the second most important forcing function - the first being sea-surface temperature - and it becomes a significant factor in the summer months. Therefore a systematic study about the microwave

sensing of soil properties has evolved as a major need of the hour. How much is the soil's pH value and what is required to be added to improve soil's fertility based on pH are the only relevant suggestions given by the Soil Testing Laboratory to a farmer. This work is an attempt to assist the farmers even better by estimating the soil moisture and fertilizer contents, using electromagnetic principles, so that crop growth and productivity can be further improved.

1.5 Objectives of the Work

The main objectives of the work presented in this thesis are to:

- characterize soil using microwaves based on its dielectric properties
- employ analytical models for soil characterization and
- use Microwave Imaging as a tool for estimation of soil moisture and fertilizer contents

1.6 Thesis Outline

The thesis is organized into six chapters and two appendices. Pictorial representation of the organization of the thesis is given in Fig. 1.3.

Chapter 1 gives an introduction to material characterization using microwaves. Microwave properties of materials and soil are presented. The chapter also presents a literature review on relevant topics connected with material characterization and microwave imaging for soil characterization. The chapter ends by explaining the motivation and objectives of the work and presents the organization of the thesis.

Chapter 2 focusses on the methodologies adopted in this work. Different measurement and analytical methods for material characterization are explained in this chapter. Imaging method for colour-mapping is also explained.

Different methods for the determination of microwave properties of soil are explained in **Chapters 3 to 6**. **Chapter 3** discusses the characterization of soil using the two traditional methods, namely the Cavity Perturbation Method and the Superstrate Method. Simulation as well as experimental results are also presented and discussed in detail.

Chapter 4 discusses the characterization of soil using the Free-space Transmission Method. Computation of dielectric constant of soil samples is also carried out. Simulation as well as experimental results for the characterization of soil in the presence of moisture and fertilizers are presented. Colour-mapping as a tool to detect the presence of moisture in soil is presented. The chapter discusses an analytical method using an Artificial Neural Network (ANN) model for moisture content estimation and the results are validated.

Chapter 5 discusses the characterization of soil using the Sensor Antenna Method. Dielectric constant of soil samples with varying soil-fertilizer mixture-ratios and moisture content is computed. Simulation as well as experimental results for soil-characterization in the presence of moisture and fertilizers are explained. This chapter also discusses moisture detection in soil using sensor antenna and colour-mapping. ANN and Regression models for added moisture and fertilizer contents are presented.

Chapter 6 summarizes the highlights of the research work. Performance comparison of the various methods and suggestions for future studies are also presented.

Appendix A explains the soil moisture content measurement using commercially available resistance probes. The efficacy of the sensor antenna method in comparison with a sensor module is tested and the result is included here. **Appendix B** describes a combined space-frequency domain approach for speckle noise reduction. Integration of soil moisture sensors with communication modules will lead to remote characterization of soil as done in satellite-based sensing. An algorithm to reduce contamination of the colour-mapped image with speckle noise is presented; the result as applied to general and Synthetic Aperture Radar images is included here.

The thesis includes bibliography and a list of publications by the author in the related field.

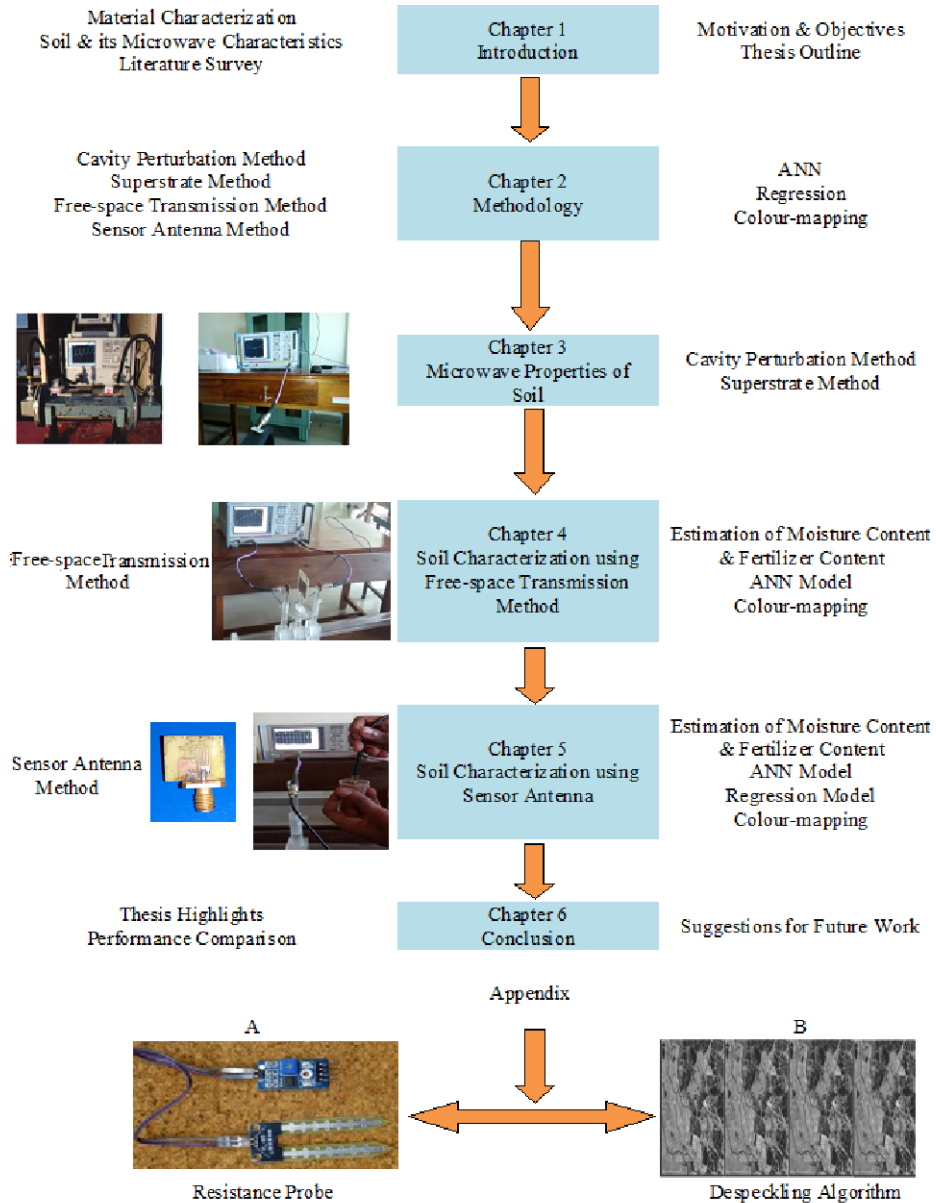


Figure 1.3: Organization of the Thesis

1.7 Chapter Summary

This chapter introduces the concept of microwave imaging for material characterization. Microwave properties of materials, especially soil, are presented. The chapter also contains a literature review on material characterization and microwave imaging for soil characterization. The chapter concludes by explaining the motivation and objectives of the present work. It also presents the overall organization of the thesis.

Chapter 2

METHODOLOGY

Contents

2.1	Introduction	37
2.2	Measurement Methods for Material Characterization	38
2.3	Analytical Methods for Material Characterization	61
2.4	Imaging Technique for Colour Mapping	68
2.5	Chapter Summary	70

2.1 Introduction

This thesis presents microwave imaging for soil characterization, in the L, S and C bands of the frequency spectrum. The dependence of complex permittivity and permeability of soil on frequency is an important measure for its characterization. However, prior to soil characterization using conventional methods, they are validated through simulation and experiment using standard dielectric materials. This chapter discusses four major measurement methods for material

characterization used in this research, namely cavity perturbation method, superstrate method, free-space transmission method and sensor antenna method. It also describes two important analytical methods, based on Artificial Neural Network (ANN) and Regression. An imaging technique for colour-mapping of materials for detecting embedded objects is also described. Simulation as well as experimental setups and corresponding results of material characterization using standard dielectric materials are presented. These methodologies - both measurement and analytical - are followed for the development of similar schemes for the characterization of soil, which are discussed in the ensuing chapters.

2.2 Measurement Methods for Material Characterization

Depending upon the nature of the materials being characterized, measurement schemes are either bounded or free-field. If the materials are solid with a proper shape, samples are placed in a transmission system (such as waveguide) and the terminal scattering parameters are measured. Non-rigid materials are characterized by free-field measurements in which the back and forward scattering of an incident wave are measured using an appropriate antenna system. Oblique wave incidence can be accommodated in such a system.

In both measurement schemes, the scattering parameters are measured over various frequency bands using a network analyzer. The sample-region scattering parameters are related to the complex permittivity and permeability of the material under test. By substituting experimental values in analytical expressions, the desired material parameters can be extracted numerically at a given frequency (Bernard and Gautray, 1991; Nelson and Bartley, 2002).

The principal measurement methods used for material characterization are

1. Cavity Perturbation Method
2. Superstrate Method
3. Free-space Transmission Method
4. Sensor Antenna Method

2.2.1 Cavity Perturbation Method

To provide a resonant circuit at UHF and higher frequencies, an enclosure completely surrounded by conducting walls is required. A shielded enclosure, such as a waveguide, confines electromagnetic fields inside, avoids radiation effects and furnishes large areas for current flow. These enclosures have natural resonant frequencies and a very high quality-factor (Q-factor). A waveguide with iris-coupled end plates constitutes a cavity resonator. The cavity perturbation method has its simplicity showcased by the minimum number of microwave components. Dielectric permittivity can be computed using just two microwave devices; i.e., a cavity resonator & a network analyzer (Bengtsson and Risman, 1971).

Method based on the perturbation of cavity resonators is commonly used to measure the permittivity and permeability of samples of dielectric and ferrite materials at microwave frequencies. It is also used to measure the local electric- and magnetic-field strengths in microwave structures. Volume of the sample inserted should be very small in comparison to the volume of the empty cavity. This method is applicable for low-loss samples. A piece of sample material affects the centre frequency (f) and Q-factor of the cavity. From these parameters, the complex permittivity or permeability of the material can be calculated at a single frequency.

The cavity can be either rectangular or cylindrical. The sample is inserted along the symmetric axis of the cavity in the position of maximum electric field strength for easy measurement and calculation

(Jha and Akhtar, 2015). Fig. 2.1 shows a rectangular cavity resonator inserted with a sample.

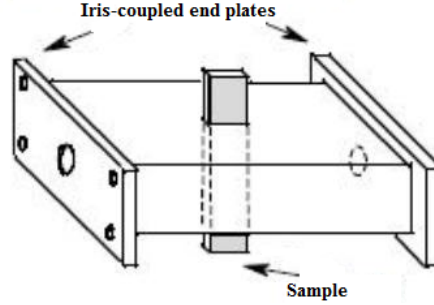


Figure 2.1: Structure of a slotted rectangular cavity resonator

For rectangular cavity, TE_{10N} (N is integer) modes are widely used for dielectric properties measurements. The geometrical centre is always one of the maximum electric field positions in the odd modes (N is odd). When a small object is introduced into a microwave cavity resonator, the electric field is perturbed, causing a change in resonant frequency. This change in resonant frequency can be used to determine the permittivity of samples. Since it is possible to measure the change in frequency with high accuracy, this provides a valuable method for measuring the electric and magnetic properties of the object if the properties of the cavity are known, or for characterizing the cavity if the properties of the perturber are known. The dielectric constant and loss-tangent of the specimen are calculated from the changes of resonant frequency and Q -factor of the metal cavity. Equations for computation of dielectric constant, ϵ'_r , loss-factor, ϵ''_r and loss-tangent, $\tan\delta$ are given in 2.1, 2.2 and 2.3 (Bethe and Schwinger, 1943).

$$\epsilon'_r = 1 + \frac{V_c(f_0 - f_s)}{2V_s f_s} \quad (2.1)$$

$$\epsilon''_r = \frac{(\epsilon'_r - 1)}{2\epsilon'_r} \frac{f_s}{(f_0 - f_s)} \left[\frac{1}{Q_s} - \frac{1}{Q_0} \right] \quad (2.2)$$

$$\tan\delta = \frac{\epsilon_r''}{\epsilon_r'} \quad (2.3)$$

where

f_0 = free-space resonant frequency of the cavity in GHz,

f_s = shifted frequency due to insertion of the sample in GHz,

V_c = volume of the cavity in mm^3 ,

V_s = volume of the sample in mm^3 ,

Q_0 = Q-factor of empty cavity and

Q_s = Q-factor obtained with the sample.

Simulation of the Cavity Perturbation Method using standard dielectric materials:

An S-band rectangular cavity resonator is used to compute the dielectric constant of a known sample. The resonator is simulated using AnsoftTM High Frequency Structure Simulator (HFSS), a tool used for antenna design. The dimension of the resonator is $304 \text{ mm} \times 72 \text{ mm} \times 35 \text{ mm}$ ($V_c=766080 \text{ mm}^3$). A lumped-port excitation is applied to both ends of the waveguide structure. The resonator has a slot on the broader side with a dimension of $100 \text{ mm} \times 5 \text{ mm}$.

Samples used:

HFSS simulations are carried out on two materials FR-4 and Arlon AD1000. FR-4 is a grade designation assigned to glass-reinforced epoxy laminate sheets, tubes, rods and printed circuit boards (PCB). It is a composite material composed of woven fibre-glass cloth with an epoxy resin binder that is flame resistant. With near-zero water absorption, it possesses considerable mechanical strength, good fabrication characteristics and electrical insulating qualities in both dry and humid conditions. Dielectric constant of FR-4 is reported to be between 4.2 and 4.8 and is frequency-dependent (Sears and Zemansky, 1955). Arlon AD1000, a woven-glass reinforced laminate, is a high dielectric constant substrate that permits circuit miniaturization. It is

reported to have a dielectric constant of 10.2 or greater (RogersCorp, 2008).

Fig. 2.2 shows a slotted rectangular cavity resonator simulated using HFSS. Appropriate size of the samples are inserted separately into the slot of the resonator as shown in Fig 2.3.

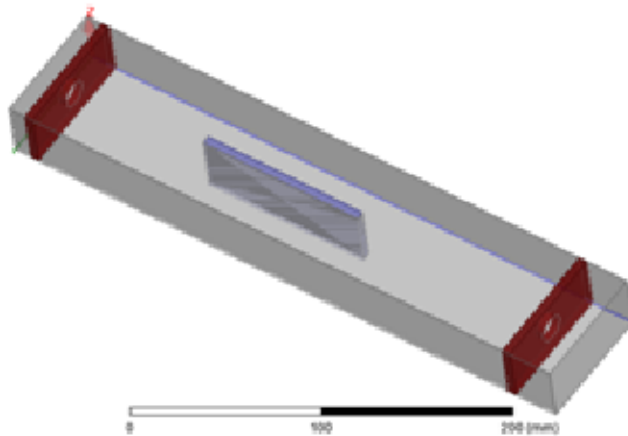


Figure 2.2: Slotted S-band rectangular cavity resonator

The S_{21} parameter is plotted for the empty structure for a frequency sweep from 1 GHz to 5 GHz. The plot obtained in HFSS is shown in Fig 2.4. This plot helps to analyse the structure and find out the frequency points at mode-peaks. Markers indicate those dominant peaks that should be considered for the further studies in the S-band.

S_{21} is plotted for the two insertions and is shown in Fig. 2.5. Frequency at which the peak values of S_{21} for the rectangular cavity resonator with and without samples occur is shown in Table 2.1.

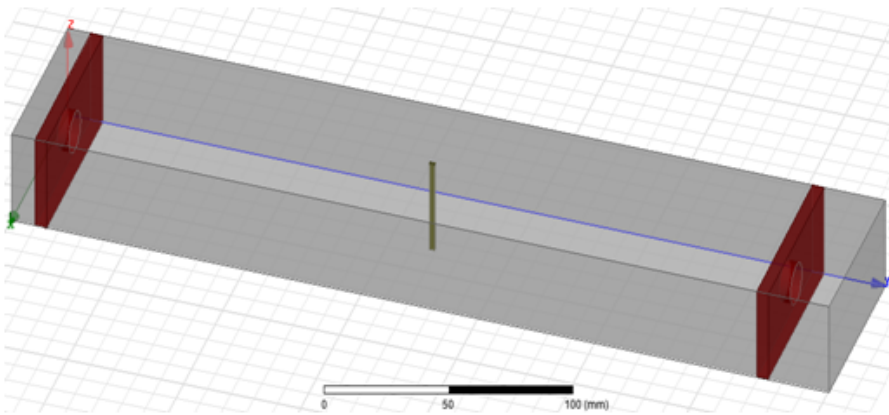


Figure 2.3: Slotted S-band rectangular cavity resonator with FR4 / Arlon AD1000 sample

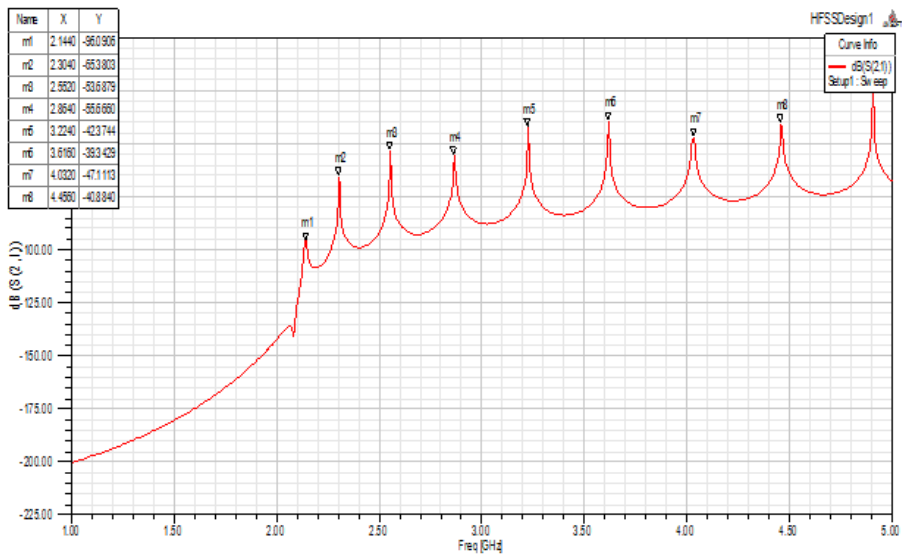
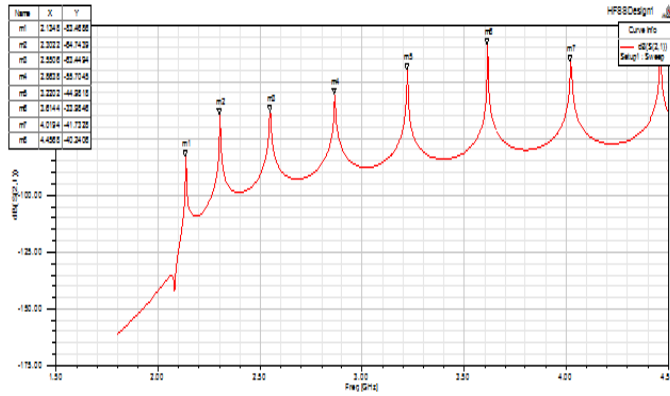
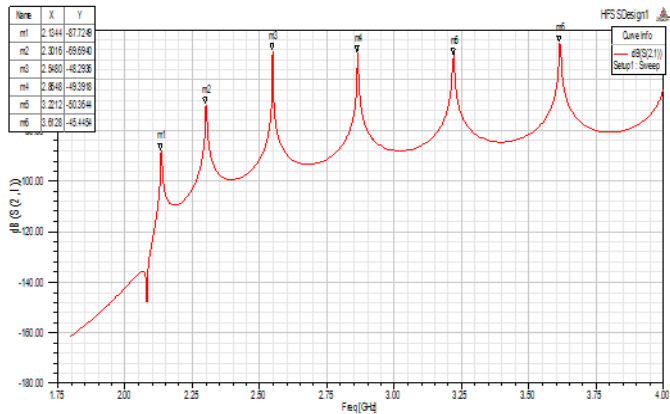


Figure 2.4: S_{21} plot of the empty slotted S-band rectangular cavity resonator



(a)



(b)

Figure 2.5: S_{21} plot of the slotted S-band rectangular cavity resonator with (a) FR-4 (b) Arlon AD1000

A left shift in the peaks is seen to have occurred. A shift in the frequency response indicates the presence of an external object in the cavity of the resonator and the extent of the shift is an indication of the loss incurred by the system due to the introduction of the sample. Diameter and height of the materials inserted into the slot of the cavity resonator are 2.674 mm and 35 mm respectively ($V_s=196.55 \text{ mm}^3$). ϵ'_r of FR-4 and Arlon AD1000 is computed using Eqn. 2.1. Results are shown in Table 2.2.

Table 2.1: Comparison of S_{21} peaks of rectangular cavity resonator with and without samples; Cavity Perturbation Method

Peak No.	Frequency in GHz at which S_{21} peaks occur for		
	Empty Cavity	Cavity with	
		FR-4	Arlon AD1000
1	2.144	2.1402	2.1334
2	2.304	2.3022	2.2914
3	2.553	2.5506	2.5320
4	2.864	2.8638	2.8521
5	3.224	3.2202	3.2122
6	3.616	3.6144	3.5987

Table 2.2: Simulation results for FR-4 and Arlon AD1000; S-band; Cavity Perturbation Method

Parameters	FR-4		Arlon AD1000	
	Empty	with sample	Empty	with sample
Frequency (GHz)	2.144	2.1402	2.144	2.1334
ϵ'_r	-	4.4602	-	10.6829

Experimental Validation of Cavity Perturbation Method:

The setup of cavity perturbation method using S-band cavity resonator and Agilent's Network Analyzer PNA E8362B is shown in Fig. 2.6.

In the experimental validation, FR-4, Arlon AD1000 and Acetone are used. Acetone (chemical name : propanone) is an organic compound with the formula $(CH_3)_2CO$. It is a colourless, mobile, flammable liquid, and is the simplest ketone. Dielectric constant, ϵ'_r , of acetone is 20.7 at 77°F (Maryott and Smith, 1951) and it varies with temperature (Onimisi et al., 2016). FR-4 and Arlon AD1000 are cut into a size of 3.60 mm \times 1.56 mm \times 35 mm ($V_s=196.56$ mm³). Acetone is taken in a thin glass

tube of diameter 2.68 mm ($V_s=197.44 \text{ mm}^3$). The two samples are then inserted into the slot of the cavity resonator.

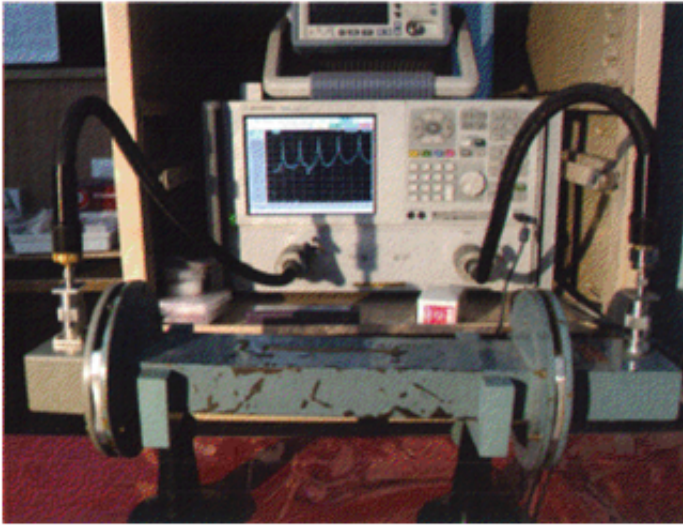


Figure 2.6: Network analyzer and S-band rectangular cavity resonator

At the centre, the electric field is maximum for odd modes and minimum for even modes. Hence result is observed for the odd modes. The shift in frequency and the computed value of ϵ'_r are shown in Table 2.3.

Table 2.3: Experimental results for FR-4, Arlon AD1000 and Acetone; S-band; Cavity Perturbation Method

Parameter	Without sample	With sample		
		FR-4	Arlon AD1000	Acetone
Frequency (GHz)	2.531703	2.527565	2.519347	2.507087
ϵ'_r	-	4.1903	10.5574	20.0483

The value of ϵ'_r is in agreement with the simulated result. The variation is due to the slight change in V_s taken for simulation and experiment.

Results of simulation and experiment discussed above indicate that cavity perturbation method can be used for material characterization. The method is hence extended for soil characterization, as described in Chapter 3.

2.2.2 Superstrate Method

In the superstrate method, the setup consists of an antenna, loaded with the material whose dielectric properties are to be studied. The material under test (MUT) forms a superstrate on the antenna beneath. It is a simple & non-destructive method that overcomes the shortcomings of the Cavity Perturbation Method. A shift in resonant frequency is observed and the dielectric constant of the MUT is a measure of the shift (Jingchu and Geyi, 2013). Ansoft HFSS is used for simulation and Rohde & Schwarz ZVB8 VNA is used for measurement.

Antennas Used:

Two types of antenna are used for carrying out the simulation and experiment in the study.

1. Microstrip Patch Antenna
2. Coplanar Waveguide (CPW)-fed Monopole Antenna

Microstrip Patch Antenna (MPA):

The MPA, or simply patch antenna, is a metallic strip or patch mounted on a dielectric layer, called the substrate, which is supported by a ground plane. Depending on the shape of the patch, MPAs can be rectangular, square, circular, disc-sector etc. They are versatile in terms of resonant frequency, polarization, pattern and impedance. ϵ_r' of the substrate is typically between 2.2 and 12. A rectangular microstrip patch antenna is shown in Fig. 2.7.

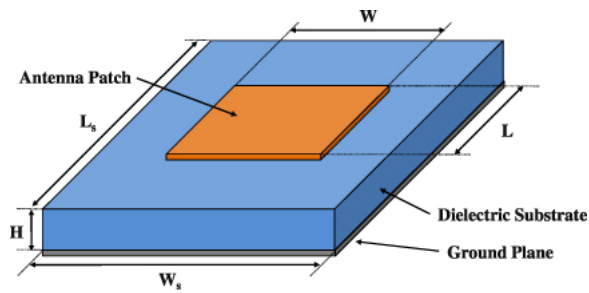


Figure 2.7: Rectangular Microstrip Patch Antenna

Of the many configurations that are used to feed the MPA, coaxial-probe feed is considered in this work. A rectangular MPA with coaxial-probe feeding is shown in Fig. 2.8

Since some of the waves travel in the substrate and some in air, an effective dielectric constant ϵ'_{reff} is introduced to account for fringing.

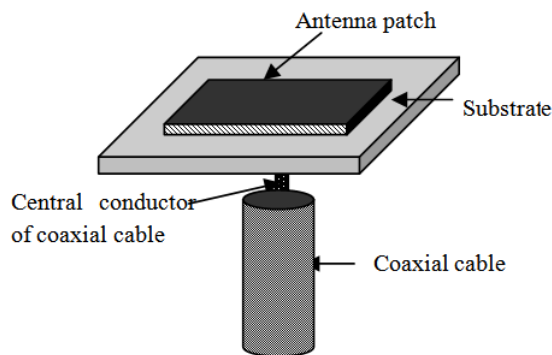


Figure 2.8: Rectangular patch antenna with coaxial probe feeding

Given the resonant frequency, f_r , ϵ'_r and height h of the substrate, the design equations to get the width, W and length, L of the patch are as follows (Balanis, 2005).

$$W = \frac{1}{2f_r \sqrt{\mu_0 \epsilon_0}} \sqrt{\frac{2}{\epsilon'_r + 1}} = \frac{v_0}{2f_r} \sqrt{\frac{2}{\epsilon'_r + 1}} \quad (2.4)$$

where ϵ_0 & μ_0 are the absolute permittivity & absolute permeability and v_0 is the velocity of electromagnetic waves in free space.

$$\epsilon'_{eff} = \frac{\epsilon'_r + 1}{2} + \frac{\epsilon'_r - 1}{2} \left[1 + 12 \frac{h}{W} \right]^{-1/2} \quad (2.5)$$

A popular & practical approximate relation for the normalized extension of the length is

$$\frac{\Delta L}{h} = 0.412 \frac{(\epsilon'_{eff} + 0.3) \left(\frac{W}{h} + 0.264 \right)}{(\epsilon'_{eff} - 0.258) \left(\frac{W}{h} + 0.8 \right)} \quad (2.6)$$

Since the length of the patch has been extended by ΔL on each side, the effective length of the patch is

$$L_{eff} = L + 2\Delta L \quad (2.7)$$

Antenna structures are created to resonate at 1.85 GHz, 2.45 GHz and 5.25 GHz (in the L, S and C bands respectively) using HFSS. Dimensions of the structure are given in Table 2.4.

Table 2.4: Dimensions of Patch Antenna [Substrate : FR-4; $\epsilon'_r=4.4$, $h=1.6$ mm]

Dimensions (in mm)		Frequency, f_r (GHz)		
		1.85	2.45	5.25
Patch	L	47.1	28.0	16.4
	W	37.3	24.0	12.0
Substrate	L_s	84.0	60.0	40.0
	W_s	67.0	50.0	36.0

CPW-fed Monopole Antenna (CMA):

Printed monopoles are conformal for modular design and can be fabricated along with the printed circuit board of the system, making fabrication easier. A CMA is an ideal example of a uniplanar monopole antenna. Fig. 2.9 shows the geometry of the CMA. The antenna is designed on an FR-4 substrate of dielectric constant 4.4 and height 1.6 mm. Dimensions of the structure are given in Table 2.5. The ground plane dimensions and the gap are optimized for good impedance matching.

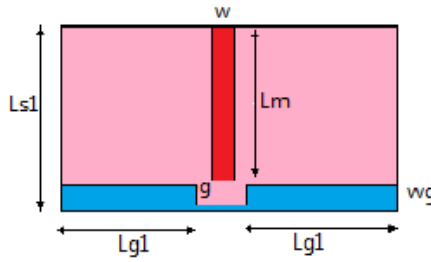


Figure 2.9: Structure of CPW-fed monopole antenna

Table 2.5: Dimensions of CPW-fed monopole antenna

Dimensions (in mm)	Frequency, f_r (GHz)		
	1.85	2.45	5.25
L_{s1}	46.0	33.5	15.2
L_m	36.0	24.5	9.2
w	3.0	3.0	3.0
w_g	10.0	9.0	6.0
L_{g1}	20.0	21.0	12.2
g	0.45	0.45	0.40

Simulation setup and Results:

The setup comprises a resonant antenna loaded with a dielectric material (MUT as superstrate), whose parameters ϵ_r' and $\tan\delta$ are varied to study their effect on the frequency and impedance characteristics of

the antenna. Two different antennas, namely Coaxial Probe-fed Rectangular MPA and CPW-fed Monopole, are used. As mentioned in Section 1.2, this research focusses on the characterization of soil using microwaves by evaluating the ϵ'_r of various soil samples. It also aims at the estimation of moisture and fertilizer contents in soil by computing the ϵ'_r of soil-moisture and soil-fertilizer mixtures. Literature gives the value of ϵ'_r of water as around 80 and that of most commercial fertilizers as ranging between 4 and 12 (Madelung, 1996; Honeywell, 2011; rfcafe, 2015). Hence in this simulation, seven discrete values of ϵ'_r between 4 and 80 are considered for the MUT; they are 4, 8, 10, 20, 40, 60 and 80. Also, $\tan\delta$ of materials considered in this work falls below 0.1. Hence, for each ϵ'_r , four values of $\tan\delta$ - 0.1, 0.01, 0.001 and 0.0001 - are used.

Superstrate method is validated at the three frequencies in the L, S and C bands. Frequency variation of the antenna with respect to ϵ'_r of the superstrate at the three frequencies is listed in Table 2.6.

Table 2.6: Dependence of Resonant Frequency of Microstrip Patch Antenna and CPW-fed Monopole Antenna on Dielectric Constant of Superstrate; $f_r=1.85$ GHz, 2.45 GHz and 5.25 GHz; Superstrate Method

ϵ'_r of MUT	Frequency, f_r (GHz)					
	MPA			CMA		
	1.85	2.45	5.25	1.85	2.45	5.25
4	1.741	2.340	4.840	1.750	2.280	4.905
8	1.672	2.276	4.535	1.680	2.190	4.680
10	1.655	2.205	4.430	1.660	2.160	4.600
20	1.570	2.165	4.100	1.580	2.040	4.240
40	1.470	2.091	3.845	1.480	1.810	3.600
60	1.393	2.063	3.660	1.400	1.650	3.160
80	1.325	2.044	3.460	1.330	1.520	2.800

Fig. 2.10 shows this variation. It is observed that there is a shift in resonant frequency (f_r) of the antenna for change in dielectric constant. As the dielectric constant of the superstrate material increases, f_r of the antenna decreases at all the three frequency-bands.

Percentage shift in f_r of the two antennas as a function of ϵ_r' of the superstrate at the three frequencies is listed in Table 2.7.

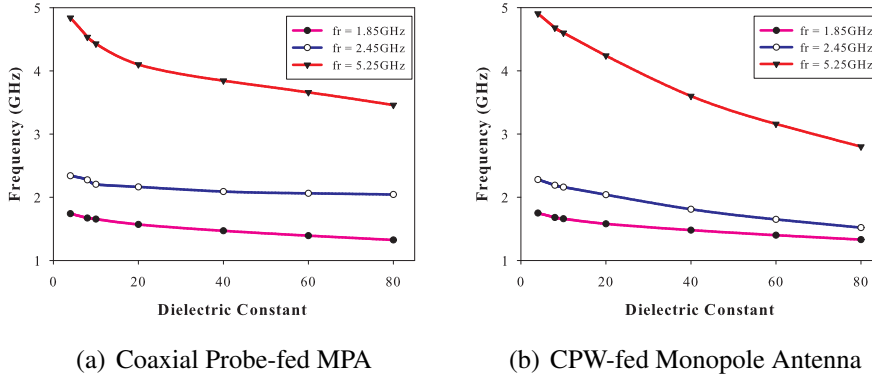


Figure 2.10: Variation of resonant frequency of antennas with dielectric constant of superstrate; L, S & C bands; Superstrate Method

Table 2.7: Percentage shift in frequency of MPA and CMA for different dielectric superstrates; $f_r=1.85$ GHz, 2.45 GHz and 5.25 GHz; Superstrate Method

ϵ_r' of MUT	Percentage frequency shift					
	L-band		S-band		C-band	
	MPA	CMA	MPA	CMA	MPA	CMA
4	5.9	5.4	4.5	6.8	7.8	6.6
8	9.6	9.2	7.1	10.6	13.6	10.9
10	10.5	10.3	10.0	11.8	15.6	12.4
20	15.1	14.6	11.7	16.7	21.9	19.2
40	20.5	20.0	14.7	26.1	26.8	31.4
60	24.7	24.3	15.8	32.7	30.3	39.8
80	28.7	28.1	16.6	38.0	34.1	46.7

Figs. 2.11(a) to (c) show the variation of percentage shift in frequency with respect to dielectric constant for the two antennas. It is observed that there is an increase in percentage shift in f_r of the antenna for increase in dielectric constant.

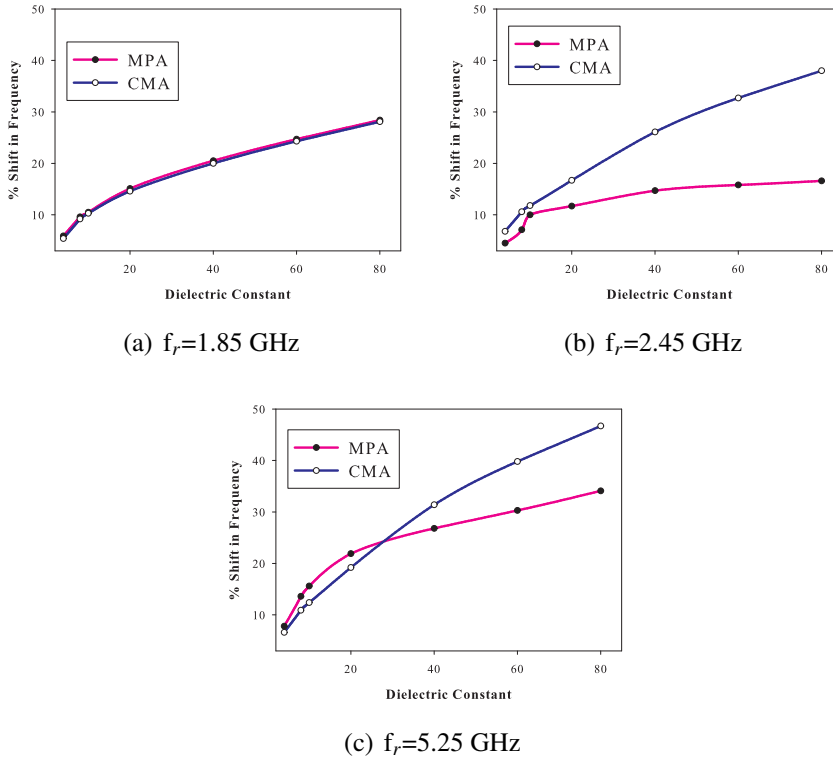


Figure 2.11: Percentage shift in frequency of Microstrip Patch Antenna and CPW-fed Monopole Antenna; Superstrate Method

The variation in the impedance characteristics of the antenna with ϵ_r' and $\tan\delta$ of the superstrate material is also noted. Normalized impedance of each antenna is obtained for different superstrates using Smith Chart. Tables 2.8 to 2.11 show the variation of normalized resistance and reactance versus $\tan\delta$ for both structures and frequencies.

Table 2.8: Dependence of **normalized resistance** of **MPA** on loss tangent for various superstrates; L, S & C bands; Superstrate Method

f_r in GHz	$\tan\delta$	Normalized Resistance						
		$\epsilon'_r=4$	$\epsilon'_r=8$	$\epsilon'_r=10$	$\epsilon'_r=20$	$\epsilon'_r=40$	$\epsilon'_r=60$	$\epsilon'_r=80$
1.85	0.0001	1.2251	1.2075	1.4242	1.2884	1.4915	1.2928	1.3766
	0.001	1.2251	1.2000	1.3078	1.2605	1.5005	1.2946	1.3676
	0.01	1.2374	1.1781	1.3095	1.3897	1.5425	1.3228	1.4535
	0.1	1.0866	1.1666	1.3184	1.6524	1.7436	1.7087	1.7973
2.45	0.0001	1.1082	1.0447	0.8038	1.0902	1.1105	1.0937	1.1319
	0.001	1.0270	0.9828	1.1215	1.0628	1.1777	1.0898	1.1187
	0.01	1.0371	1.2362	1.2362	1.1171	1.0556	1.1578	1.1943
	0.1	1.0647	1.0068	1.1807	1.1967	1.3617	1.2751	1.3150
5.25	0.0001	1.1669	1.0331	0.9290	0.8193	0.8076	0.8699	1.0460
	0.001	1.1781	0.9269	0.9112	0.8306	0.8175	0.8640	1.0223
	0.01	1.1968	0.9906	0.9628	0.8270	0.7543	0.8320	0.8937
	0.1	1.2485	0.9116	0.7977	0.7977	0.5417	0.5314	0.5314

Table 2.9: Dependence of **normalized reactance** of **MPA** on loss tangent for various superstrates; L, S & C bands; Superstrate Method

f_r in GHz	$\tan\delta$	Normalized Reactance						
		$\epsilon'_r=4$	$\epsilon'_r=8$	$\epsilon'_r=10$	$\epsilon'_r=20$	$\epsilon'_r=40$	$\epsilon'_r=60$	$\epsilon'_r=80$
1.85	0.0001	-0.1155	-0.2603	-0.5518	-0.1658	-0.1478	-0.2716	-0.1315
	0.001	-0.2320	-0.2116	-0.1232	-0.3017	-0.1412	-0.2773	-0.1573
	0.01	-0.2526	-0.3029	-0.1270	-0.1794	-0.1573	-0.3010	-0.0534
	0.1	-0.6325	-0.3551	-0.1832	-0.4706	-0.4495	-0.4220	-0.1105
2.45	0.0001	-0.0345	-0.0621	-0.2967	-0.0387	0.0680	-0.0661	0.0051
	0.001	-0.0753	-0.1081	-0.0010	-0.0612	0.0630	-0.0579	-0.0058
	0.01	-0.0929	-0.3060	-0.3060	-0.0507	-0.1984	-0.0010	0.0713
	0.1	-0.2947	-0.1230	-0.3409	-0.3899	-0.2357	-0.2861	-0.2147
5.25	0.0001	0.2127	0.2700	0.2276	0.1585	0.0610	0.0479	0.0158
	0.001	0.2241	0.2614	0.2334	0.1771	0.0700	0.0252	0.0093
	0.01	0.2352	0.2923	0.2938	0.2107	0.0164	0.0681	0.0144
	0.1	0.4960	0.5557	0.5040	0.5040	0.1962	0.0673	0.0773

Table 2.10: Dependence of **normalized resistance** of CMA on loss tangent for various superstrates; L, S & C bands; Superstrate Method

f_r in GHz	$\tan\delta$	Normalized Resistance						
		$\epsilon'_r=4$	$\epsilon'_r=8$	$\epsilon'_r=10$	$\epsilon'_r=20$	$\epsilon'_r=40$	$\epsilon'_r=60$	$\epsilon'_r=80$
1.85	0.0001	1.1759	1.9500	1.2336	1.1760	0.9511	0.8022	0.7267
	0.001	1.1754	1.1942	1.2325	1.1742	0.9486	0.7826	0.7217
	0.01	1.1763	1.1925	1.2291	1.1667	0.9372	0.7696	0.6733
	0.1	1.0743	1.5627	1.1499	1.0834	0.7826	0.5846	0.4588
2.45	0.0001	1.1870	1.2784	1.3523	1.4194	0.8486	0.9610	1.0754
	0.001	1.1357	1.2776	1.3513	1.4173	1.2174	1.0058	1.0999
	0.01	1.1423	1.2824	1.3461	1.3913	0.8250	0.9409	1.0248
	0.1	1.1407	1.2584	1.3001	1.1501	0.8956	0.7171	0.6042
5.25	0.0001	1.1107	1.5278	1.5102	1.3323	1.3014	1.5081	1.6508
	0.001	1.2370	1.5219	1.4875	1.3391	1.2486	1.5205	1.5510
	0.01	1.5212	1.4988	1.4748	1.3222	1.2470	1.1591	1.8283
	0.1	1.4098	1.4109	1.3706	1.1531	0.9134	0.7253	0.5895

Table 2.11: Dependence of **normalized reactance** of CMA on loss tangent for various superstrates; L, S & C bands; Superstrate Method

f_r in GHz	$\tan\delta$	Normalized Reactance						
		$\epsilon'_r=4$	$\epsilon'_r=8$	$\epsilon'_r=10$	$\epsilon'_r=20$	$\epsilon'_r=40$	$\epsilon'_r=60$	$\epsilon'_r=80$
1.85	0.0001	0.4001	0.3666	0.3228	0.1591	-0.0156	-0.0443	0.0924
	0.001	0.3993	0.3657	0.3220	0.1589	-0.0145	-0.0216	0.0119
	0.01	0.3951	0.3616	0.3189	0.1616	0.0044	0.0412	0.0847
	0.1	0.3304	-0.1525	0.2471	0.0776	-0.0443	0.0910	-0.1525
2.45	0.0001	0.4345	0.4189	0.3899	0.1145	0.0224	-0.0383	0.0314
	0.001	0.4424	0.4183	0.3894	0.1149	-0.0350	-0.0488	-0.0083
	0.01	0.4567	0.4284	0.3982	0.1156	0.0283	-0.0131	0.0331
	0.1	0.3714	0.3533	0.3219	0.0315	0.0343	0.0709	0.1316
5.25	0.0001	0.1335	0.0277	-0.0172	-0.1971	-0.2333	-0.1715	-0.2545
	0.001	0.1727	0.0074	-0.0839	-0.1606	-0.2610	-0.0791	-0.2848
	0.01	0.1380	0.0567	-0.0019	-0.1227	-0.1024	-0.2177	0.0906
	0.1	0.2049	0.0401	-0.0633	-0.1154	0.0997	0.1997	0.2764

It can be inferred from Tables 2.8 to 2.11 that the characteristics of the antenna depend on the superstrate parameters. This method is thus extended to soil characterization, as described in Chapter 3.

2.2.3 Free-space Transmission Method

The Transmission/Reflection (T/R) method is a popular method for material characterization (Hippel, 1954; Chen et al., 2004). In the T/R method, a dielectric sample is placed in a section of coaxial line, waveguide or planar structures and permittivity of the dielectric material is computed from the measured scattering parameters. These methods are best suited for the measurement of dielectric properties of medium-loss to high-loss samples. The main drawbacks of these methods are that the sample size must be big enough and the measurement accuracy is relatively low for low-loss materials. The free-space transmission method is a typical T/R method for material characterization (Paz et al., 2011).

Experimental Setup

In the free-space transmission method, a material sample is placed between a transmitting antenna and a receiving antenna. For this, a pair of identical coaxial probe-fed MPA, fabricated on a substrate (with $\epsilon'_r=4.4$, $\tan\delta=0.02$ and thickness=1.6 mm), are used as transmit/receive antennas. A sample-holder containing the material whose dielectric properties are to be determined, is placed in between the antennas. The study is conducted at three frequencies, viz. 1.88 GHz, 2.45 GHz and 5.52 GHz, in the L, S and C bands. Rohde & Schwarz ZVB8 VNA is used for measurement. The antennas are connected to the ports of the VNA. The VNA is calibrated in transmission mode (response-type calibration), with the empty sample holder between the two antennas. The sample holder is a box of rectangular cross-section made of acrylic having dimension 10 cm \times 10 cm \times 0.3 cm. After calibrating the VNA, the material is inserted into the sample holder. The experimental setup, with a piece of acrylic sample as the material under test (MUT), is shown in Fig. 2.12.

The transmission coefficient, S_{21} is observed with and without the sample in between the MPAs. The presence of the material is detected

by interpreting the transmission parameters of the receiving antenna. Sample materials taken up for testing are acrylic ($\epsilon'_r=4.2$ at 2.45 GHz) and water ($\epsilon'_r=80$ at 2.45 GHz). Measurement of magnitude and phase of transmission coefficient ($|S_{21}|$ and ϕ) gives the attenuation A and phase shift $\Delta\phi$ according to Eqns. 2.8 and 2.9.

$$A \text{ in dB} = 20\log|S_{21}| \quad (2.8)$$

$$\Delta\phi \text{ in degrees} = \phi_{\text{sample}} - \phi_{\text{empty}} - 2\pi n \quad (2.9)$$

where n is an integer.

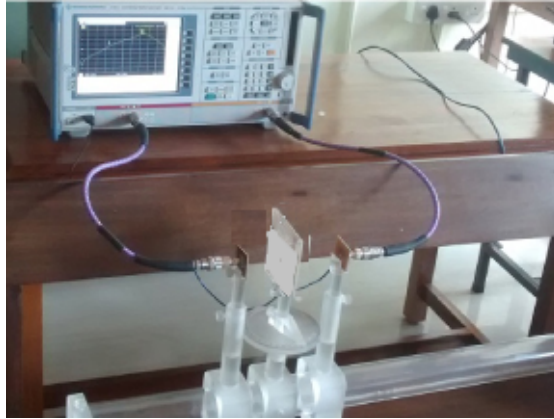


Figure 2.12: Experimental setup of free-space transmission method with acrylic sample as Material Under Test

From these, the dielectric constant (ϵ'_r) of the material under test is calculated using the expression

$$\epsilon'_r = \left[\frac{\Delta\phi c}{2\pi d f} + 1 \right]^2 \quad (2.10)$$

where f (GHz) is the frequency of the incident electromagnetic wave, c (m/s) is its velocity in free-space and d (mm) is the sample-thickness in the holder (Paz et al., 2011).

ϵ'_r values of the materials under test in the L, S and C bands obtained using the method are given in Table 2.12.

Table 2.12: Dielectric Constant of FR-4, Acrylic and Water in L, S and C bands

Material	ϵ'_r at		
	$f_r=1.88$ GHz	$f_r=2.45$ GHz	$f_r=5.52$ GHz
Acrylic	4.38	4.17	3.94
Water	79.82	79.45	78.43

The values obtained are in good agreement with those available in literature. Also, in the microwave frequency range, ϵ'_r is inversely proportional to frequency (Zivkovic and Murk, 2012); this inverse relationship is evident from the table. The free-space transmission method thus forms a basis for characterization of soil. This is discussed in detail in Chapter 4.

2.2.4 Sensor Antenna Method

In many microwave sensing devices, resonant structures are essential elements because they allow localization of high field areas. They are very efficient in the frequency band for which they are designed. Shift in resonant frequency of the sensors decides their sensitivity in different environments.

Sensor antennas are simple alternatives to bulky sensor systems. They allow measurements with minimal environmental disturbances and non-ionising power levels. In a broad sense, any antenna whose inherent characteristics get altered based on environmental stimuli or external material presence is called a sensor antenna. Microwave sensors measure properties of materials based on microwave interaction with matter. They can be used to provide information about the material such as its dielectric property, moisture content and chemical composition (Kitic et al., 2012; Then et al., 2014). Microwave sensors

offer many advantages over traditional sensors such as rapid, non-destructive, precise and fully automated measurement.

This section presents a methodology using a sensor antenna for material characterization at microwave frequencies. Simulation using Ansoft HFSS and experimental validation are discussed in the following section.

Sensor Antenna

The sensor antenna used consists of a nine-arm spiral resonator embedded onto the signal strip of a 50Ω Asymmetric Coplanar Strip (ACS) transmission line fabricated on a substrate with $\epsilon_r=4.4$, thickness=1.6 mm and loss-tangent=0.02 (Anju, 2015). The antenna operates in the C-band and has an overall size of $10 \text{ mm} \times 10 \text{ mm} \times 1.6 \text{ mm}$. Since the structure is coplanar, any material beneath the spiral affects the resonant frequency. Also a sharp resonance gives high sensitivity to the antenna, making it suitable for sensor applications.

Sensors used in real environment fluid characterization and agriculture applications demand small dimensions to allow measurements with minimal disturbance to the surroundings, varying penetration depth and non-ionizing power levels. The antenna satisfies the above conditions. Structure and reflection characteristics of the antenna are shown in Figs. 2.13(a) and (b). Its dimensions are given in Table 2.13.

Simulation Result

Antenna is tested in acetone ($\epsilon'_r \approx 20$) using the arrangement shown in Fig. 2.14. The material should be kept directly beneath the signal arm of the antenna and must be in close contact with it (Anju, 2015). Minimum size of the material is $3 \text{ mm} \times 3 \text{ mm} \times 1 \text{ mm}$. Result obtained when the antenna is placed in acetone is shown in Fig. 2.15.

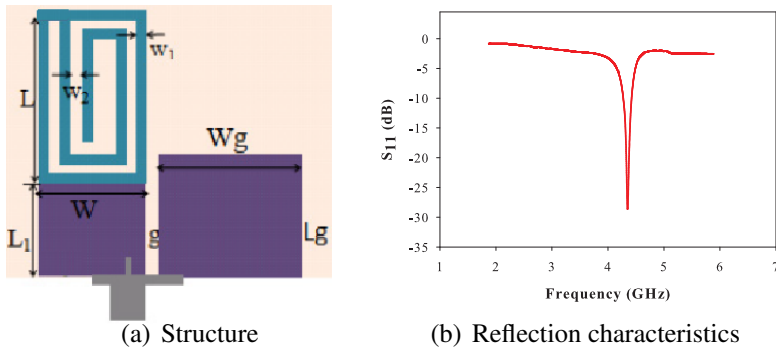


Figure 2.13: Sensor antenna at 4.35 GHz

Table 2.13: Dimensions of 4.35 GHz sensor antenna

Symbol	Parameter	Dimension in mm
L	Length of the spiral arm	4.70
L_1	Length of the transmission line segment	2.60
W	Width of the spiral resonator	3.00
L_g	Length of ground	3.50
W_g	Width of ground	4.00
w_1	Width of the spiral arm	0.30
w_2	Gap between the spiral	0.30
g	Gap between the transmission line and ground	0.30

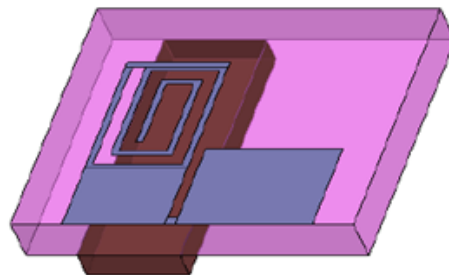


Figure 2.14: Setup for sensing acetone; C-band; Sensor Antenna Method

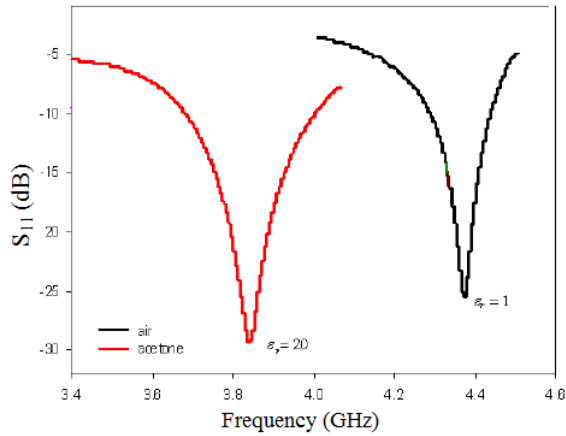


Figure 2.15: Reflection characteristics of the sensor antenna; C-band

It can be seen that there is a shift in frequency of the antenna, from 4.35 GHz to 3.84 GHz, when it is placed in acetone. The simulation results clearly suggest that the antenna characteristics vary with the material parameters. Hence the sensor antenna method can be extended to soil characterization, as described in Chapter 5.

2.3 Analytical Methods for Material Characterization

Methods for material characterization were explained in the previous section. To make better decisions of the concepts presented, analytical models based on simulation or statistics are usually used. This approach results in gaining an understanding of the characterization method by using simple structure-models and/or mathematical equations. This section describes two important analytical models based on Artificial Neural Network (ANN) and Regression.

2.3.1 ANN Model

An Artificial Neural Network (ANN) is a biologically-inspired computational model composed of various processing elements called artificial neurons. The model emulates the behaviour of biological neural systems in digital software or hardware. The neurons are connected with coefficients or weights which construct the neural network's structure (Haykin, 2005). The processing elements have weighted inputs, transfer function and outputs for processing information. There are many types of neural networks with different structures, but all are described by the transfer functions used in neurons, the way of training given or learning rule and by the connection formula. A typical ANN model consists of an input layer, one or more hidden layers and one output layer, as shown in Fig. 2.16.

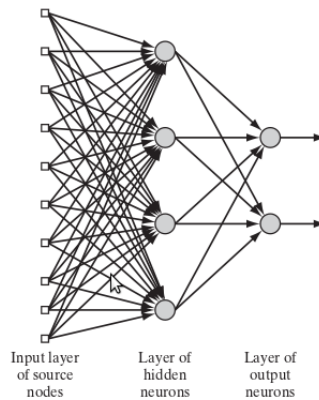


Figure 2.16: A fully connected ANN with one hidden layer and one output layer

For complex problems, multilayer perceptron (MLP) is the best model, as it overcomes the drawbacks of the single-layer perceptron by adding more hidden layers. In a feed-forward multilayer perceptron network, the inputs signals multiplied by the connection weights are first summed and then directed to a transfer function to give output for

that neuron. The transfer function executes on the weighted sum of the neuron's inputs.

A neural network is trained with input and target pair patterns with the ability of learning. In MLP network, back-propagation (BP) learning algorithm is used (Roja, 1996). Input data is fed forward through the network to optimize the weights between neurons. Adjustment of weights is done by backward propagation of the error during training phase. The network takes the input and target values in the training data set and changes the value of the weighted links to reduce the difference between the output and target values. The error is minimized across many training cycles called epoch. During each cycle, the network reaches a specified level of accuracy. The number of processing elements per layer, as well as the number of layers, greatly affect the abilities of the MLP. Too few of them can slow down the learning process, and too many of them can alter the generalizing abilities of the MLP due to overfitting or memorization of the training data set (Alsmadi et al., 2009).

The Levenberg-Marquardt algorithm (LMA) is a popular algorithm used in mathematics and computing to solve non-linear least squares problems. These minimization problems arise especially in least squares curve fitting. However, as with many fitting algorithms, the LMA finds only a local minimum, which is not necessarily the global minimum. It locates the minimum of a multivariate function that can be expressed as the sum of squares of non-linear real-valued functions. It is an iterative method that works in such a way that performance function will always be reduced in each iteration of the algorithm. This feature makes LMA the fastest training algorithm for networks of moderate size. Any network training function that adjusts the weight and bias values according to Levenberg-Marquardt optimization, minimizes a combination of squared errors and weights, and then determines the correct combination so as to produce a network that generalizes well.

Model Creation

As mentioned, a multilayer perceptron network trained by LMA is the most common neural network used for typical image processing applications. In this work, ANN models are created using the Neural Network Toolbox in MATLAB[®]. Each model comprises the input layer, hidden layer and the output layer, whose numbers depend on the application. The number of neurons in the input and output layers of the ANNs are identical to the number of input and output parameters respectively, while the number of neurons in the hidden layer of the neural network is calibrated during the training and validation process.

Training and Validation

The ANNs are trained by introducing a set of examples of proper network behaviour to the ANNs. During training, the learning rule is used to iteratively adjust the weights and biases of the network in order to move the network outputs closer to the target values by minimizing the network performance indicator. The LMA, which has a higher rate of convergence, is used for the training. Data sets used for training and validation of each ANN model depend on the application. Also, out of the N input data, majority of the data are randomly assigned as training data while the remaining are used for validation purpose. One of the most important parameters used as the network performance indicator is the mean squared error (MSE). It is defined as shown in Eqn. 2.11.

$$\text{MSE} = \frac{\sum_{i=1}^N (y_i - o_i)^2}{N} \quad (2.11)$$

where y_i is the target, o_i is the observed output and N is the number of data set.

ANN Model for Material Characterization using Superstrate Method

This section presents a simple ANN model for material characterization applications using Superstrate Method. As discussed in Section 2.2.2, setup of the superstrate method consists of an antenna, loaded with the material under test (MUT) whose dielectric properties are to be studied. The MUT forms a superstrate on the antenna beneath. The simulation model consists of the probe-fed Microstrip Patch Antenna (MPA) resonating in the L-band, fabricated on a substrate (with $\epsilon_r'=4.4$, $\tan\delta=0.02$ and thickness=1.6 mm). The dimensions of the patch and MUT are 47.1 mm x 37.3 mm and 47.1 mm x 37.3 mm x 0.5 mm respectively. 182 varieties of the material-slab, comprising 26 distinct ϵ_r' values each with 7 distinct $\tan\delta$ values are considered for the studies. The ϵ_r' values taken are 2.0, 2.6, 3.2, 3.8, 4.4, 5.0, 5.2, 5.4, 5.6, 5.8, 6.0, 6.2, 6.4, 6.6, 6.8, 7.0, 7.2, 7.4, 7.6, 7.8, 8.0, 8.6, 9.2, 9.8, 10.4 and 11.0, each with 7 distinct $\tan\delta$ values 0.0001, 0.001, 0.004, 0.007, 0.01, 0.04 and 0.07.

Structure of MPA with MUT loaded on it is shown in Fig.2.17.

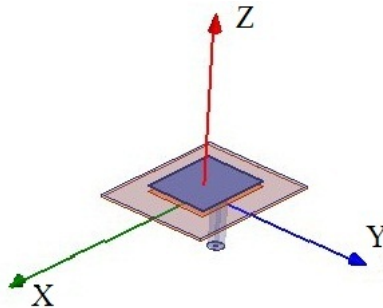


Figure 2.17: MPA / Slab Geometry for ANN model; Superstrate Method

A single feed-forward ANN model, with 2 hidden layers having 20 and 10 neurons respectively, is used for modelling, as shown in Fig.2.18. The input data for training the model consists of the complex reflection

coefficients in polar representation, impedance values at the resonant frequency and 200 points of the return loss in dB over the operating band of the L-band MPA. The model accepts each input data corresponding to a particular ϵ'_r and $\tan\delta$ as a column vector F of the training data-matrix as given in Eqn. 2.12.

$$F = \begin{bmatrix} |\Gamma| \\ \angle\Gamma \\ R_X \\ X_L \text{ or } X_C \\ 200 S_{11} \text{ points} \end{bmatrix} \quad (2.12)$$

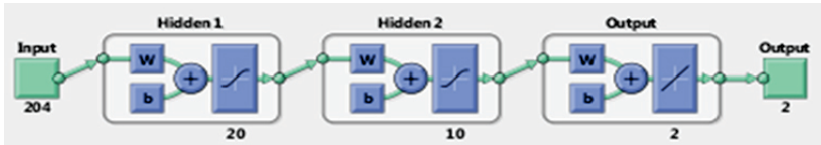


Figure 2.18: Structure of the ANN model; Superstrate Method

For training the ANN model, ϵ'_r is swept through 25 distinct values, ranging from 2.0 to 11.0 (with an increment of 0.6 between 2 & 5 and between 8 & 11 and an increment of 0.2 between 5 & 8), while $\tan\delta$ is swept through 7 distinct values, excluding the whole range for $\epsilon'_r=5.4$, which is used for testing purpose. Thus the full model resulted in a training matrix F of dimension 204×175 and a testing matrix of dimension 204×7 . The model gives superior performance with zero-error for both ϵ'_r and $\tan\delta$ for a member of the trained data-set. Result obtained for test data with $\epsilon'_r=5.4$ and values of $\tan\delta$ ranging from 0.0001 to 0.07 for MUT on the patch is shown in Table 2.14.

Table 2.14: Results of ϵ'_r and $\tan\delta$ obtained for test data $\epsilon'_r=5.4$ & different values of $\tan\delta$; ANN model; Superstrate Method

$\tan\delta$ (actual)	Values obtained	
	ϵ'_r	$\tan\delta$
0.0001	5.1656	0.0005
0.001	5.1753	0.0011
0.004	5.2004	0.0033
0.007	5.2566	0.0059
0.010	5.2758	0.0083
0.040	6.2706	0.0377
0.070	5.1610	0.0720

This model can be extended to soil characterization for the evaluation of ϵ'_r , as discussed in Chapters 4 and 5.

2.3.2 Regression Analysis

Regression Analysis is a statistical tool for relating multiple independent variables to a dependent variable. Once the relationship is established, information about the independent variables can be used to make powerful estimations about why things are the way they are. A typical example is the conventional Cartesian coordinate system in which the x and y coordinates find a linear function that predicts the dependent variable values as a function of the independent variable. In its simplest form, regression shows the relationship between independent variable (X) and dependent variable (Y), as in the formula below.

$$Y = \beta_0 + \beta_1 X + u \quad (2.13)$$

The magnitude and direction of this relation are given by the slope parameter (β_1), and the status of the dependent variable when the

independent variable is absent is given by the intercept parameter (β_0). An error term (u) captures the amount of variation not predicted by the slope and intercept terms.

Regression thus shows how variation in one variable co-occurs with variation in another. The model is designed to study the relationship between variables that appear in a data set. Accuracy of the method depends on the fitness of the data set chosen. A prior knowledge of the variables to be identified as independent variables in the model is required. The sample is taken randomly from some population. The two variables X and Y are the two measured outcomes for each observation in data set. The statistical measures for goodness-of-fit such as coefficient of determination (R^2) and significance (P-value) between the variables X and Y serve to show how well the values fit the data.

Chapter 5 discusses the characterization of soil using sensor antenna. Regression analysis is carried out there, using the regression tool in Microsoft Excel (Remenyi et al., 2009), to establish a relationship between shift in frequency of the sensor and moisture content in soil.

2.4 Imaging Technique for Colour Mapping

Imaging can be defined as seeing the internal structure of an object. In Microwave Imaging, a transmitting sensor (typically an antenna) transmits an electromagnetic signal which illuminates the object and is then detected with a receiving antenna or a suitable probe at the other side of the object (Nikolova, 2017).

Different ranges of electromagnetic spectra have various applications. Microwaves, infrared rays, ultraviolet rays, X-rays and gamma rays are commonly used for many applications such as biomedical, food, agriculture etc. Low-power electromagnetic fields at microwave frequencies are used for imaging. The microwave frequency causes dielectric heating through energy absorption in water. So this

technique helps to identify the homogeneity and heterogeneity due to presence of water and can therefore be used to assess moisture content.

This thesis explores the possibility of using microwave imaging for characterization of materials, especially soil. In this research, images are created from the results of material under test (MUT) using different measurement methods. A characteristic signature of the material can be drawn with the mapped microwave parameters and corresponding constituents. Colour-mapping for moisture detection in soil is described in Chapters 4 and 5.

As a prelude to moisture detection in soil, simulation is carried out for imaging the presence of a metal disc in a sample of soil. Setup involves a microstrip patch antenna radiating onto a sample of soil taken in a container in which the disc is embedded. On the other side, a sensor-probe is used for scanning the transmission coefficient (S_{21}) at 25 locations, which are distinct and equally-spaced. The locations are spatially arranged along 5×5 points as in a grid. The setup is shown in Fig. 2.19.

The disc to be detected is placed at different positions and imaged by positioning the probe at the 25 points. Fig. 2.20 shows the different positioning of the disc and the corresponding mapping.

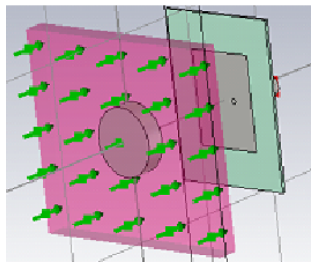
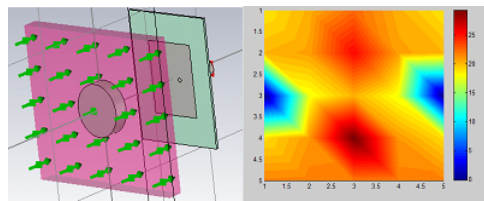
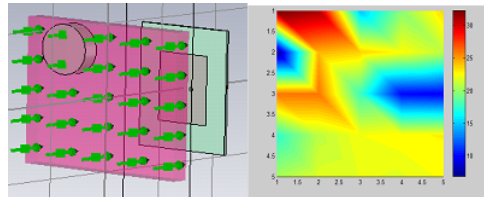


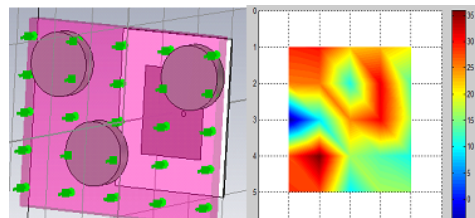
Figure 2.19: Setup for detection of metallic disc embedded in soil;
Colour-mapping using Imaging



(a) At the centre



(b) At one corner



(c) At three corners

Figure 2.20: Simulation result of detection of metallic disc embedded in soil using Imaging Technique

Probe sensing has the advantage of imaging the presence of impurity in the spatial domain. Improved image resolution can be obtained by taking more number of observation points.

2.5 Chapter Summary

The thesis presents microwave imaging methods for soil characterization. As a prelude to measurements using different soil samples, four major measurement methods - cavity perturbation method, superstrate method, free-space transmission method and sensor antenna method - used for material characterization are discussed in

this chapter, using standard dielectric materials available. The outcome of experimental results using soil samples from different districts of Kerala is presented in the ensuing chapters.

The cavity perturbation method uses a cavity resonator and a network analyzer for the characterization. Both simulation and experimental studies using the method provide good results for dielectric constant (ϵ'_r) of FR-4, Arlon AD1000 and acetone. However one difficulty of the method is that it requires a thin holder as the volume of the material under test (MUT) is to be very small. The superstrate method, where the MUT loads the antenna beneath, is presented next. It overcomes the shortcomings of the cavity perturbation method. The work uses a coaxial probe-fed rectangular microstrip patch antenna (MPA) and a CPW-fed monopole antenna (CMA) as test-antennas. Variation in dielectric constant, ϵ'_r (from 4 to 80) and loss-tangent, $\tan\delta$ (from 0.0001 to 0.1) of the MUT changes the frequency and impedance characteristics of the antenna. The values chosen are in lieu of the corresponding parameters of soil and moisture. Results of work conducted in the L, S & C bands show that there is a decrease in frequency of the antenna for increasing values of ϵ'_r . It is also observed that there is a variation of normalized resistance and normalized reactance of the antenna with respect to $\tan\delta$, reinstating the dependence of the antenna characteristics on the parameters of the MUT. The procedure mentioned here is extended to the characterization of soil in the next chapter. An experimental setup of the free-space transmission method, where ϵ'_r of the MUT is computed from the phase-shift of the transmission parameter, provides characterization of materials such as acrylic and water. This methodology is extended to soil characterization, as discussed in Chapter 4. The sensor antenna method suggests that material characterization based on change in the resonant frequency of a suitable sensor is possible. Variation in reflection characteristics of a sensor antenna consisting of a nine-arm spiral resonator embedded onto the signal strip of a 50Ω ACS transmission line fabricated on a substrate with $\epsilon'_r=4.4$, thickness=1.6 mm and loss-tangent=0.02 resonating at

4.35 GHz reveals the method's suitability for material characterization. Chapter 5 presents soil characterization using sensor antennas.

A methodology to model the superstrate method based on ANN is discussed. A training matrix of size 204×175 and a testing matrix of size 204×7 is used, in lieu of the 7 different $\tan\delta$ values of 25 different ϵ'_r values of the MUT used for training the model. Result obtained for test-data with $\epsilon'_r=5.4$ and $\tan\delta$ ranging from 0.0001 to 0.07 shows low error. ANN models for soil characterization are presented in Chapters 4 and 5. With a view to establishing a relationship between variables of the structure utilized in the methodology and different MUT using suitable statistical means, the concept of regression is discussed. Regression Analysis is presented in Chapter 5 to relate the Moisture Content (MC) in soil to the frequency-shift (Δf) of a sensor antenna.

The chapter ends by presenting an imaging technique for colour-mapping of materials for detecting embedded objects. This methodology is adopted in Chapters 4 and 5 for detecting the presence of moisture in soil.

To conclude, the highlight of this chapter is that it provides a prelude for carrying out research on characterization of soil.

Chapter 3

MICROWAVE PROPERTIES OF SOIL

Contents

3.1	Introduction	73
3.2	Cavity Perturbation Method	74
3.3	Superstrate Method	77
3.4	Chapter Summary	83

3.1 Introduction

As discussed in Chapter 1, microwave imaging has emerged as a new area of research, where low-power microwaves are used to characterize a material by means of interrogating microwaves. It is also seen that characterization can be done if dielectric properties of the material can be measured. Section 1.4 discussed the need for a thorough and systematic understanding of the microwave characterization of soil and why this has evolved as a major area of significance, motivating us to

take this further for investigative study. As seen, one can characterize soil and estimate its relevant constituents such as moisture and fertilizer contents through a variety of microwave means. Variability of soils properties - mainly permittivity and permeability - can be studied using microwave methods. Dependence of permittivity of soil on parameters such as frequency, water content, sampling depth, mineral composition, granular size, porosity and geographic conditions is also understood as mentioned in Section 1.3. Therefore a detailed characterization of soil is to be carried out either with the direct measurement of its dielectric properties, mainly ϵ'_r , or by resorting to methods where the variation in the parameters of microwave structures such as antennas are determined to compute these. This chapter describes the characterization of soil using the conventional methods of material characterization such as Cavity Perturbation Method and Superstrate Method. The objective is to ascertain the microwave properties of soil prior to its detailed characterization.

3.2 Cavity Perturbation Method

Cavity perturbation method (Section 2.2.1) is one of the most commonly used methods to characterize the microwave property of a material. Preliminary studies, involving both simulation and experiment with FR-4 sample and acetone, validated the utility of the method for material characterization. This chapter presents the results of experiments conducted on soil samples taken in thin glass tubes, using the slotted cavity resonator operating in the S-band. Soil characterization is done based on standard equations prescribed for the method from a knowledge of the shifts in frequency and Q-factor (Bethe and Schwinger, 1943).

3.2.1 Soil samples used

Six acidic soil samples, with pH values of 3.4, 3.6, 3.7, 4.3, 4.6 and 5.1, belonging to the Udayamperoor series of Ernakulam district, Kerala are used. Reported amount of Total Suspended Solids (TSS) in these samples ranges between 0.07 and 0.21 mg/kg of soil. TSS - also called Total Soluble Salt - is a popular term for expressing soil salinity. Since the TSS values are low, the soil samples are considered as non-contaminated (Hazelton and Murphy, 2007).

3.2.2 Experimental Results

Good quality glass tube of radius 1 mm which can pass through the slot of the S-band cavity resonator is fabricated. Dielectric characterization of soil can be carried out from the changes of resonant frequency and Q-factor of the cavity when it is perturbed by the introduction of soil sample, as discussed in Section 2.2.1. As the more relevant dielectric parameter of soil is ϵ'_r , it is computed for the six samples using Eqn. 3.1 (referred to in Section 2.2.1).

$$\epsilon'_r = 1 + \frac{V_c(f_0 - f_s)}{2V_s f_s} \quad (3.1)$$

For this, the volume of the empty cavity (V_c), volume of the sample taken in the tube (V_s), resonant frequency of the empty cavity (f_0) and shifted frequency due to the insertion of the sample (f_s) are to be known. Agilent's Network Analyzer PNAE8362B is used for measurement. The cavity resonator is of dimension 304 mm × 72 mm × 35 mm; hence $V_c = 766080 \text{ mm}^3$. Also, f_0 is obtained as 2.531703 GHz from the network analyzer. 1.5 ml of soil is taken in the tube. $V_s = \pi \times 1 \text{ mm} \times 1 \text{ mm} \times 35 \text{ mm} = 109.96 \text{ mm}^3$. f_s corresponding to the different soil samples is found out. ϵ'_r values are taken at the first odd mode. Table 3.1 shows the variation of the ϵ'_r values with pH of soil for this mode.

Table 3.1: Dielectric Constant vs. pH of soil samples at S-band; Cavity Perturbation Method

Soil sample		f_s (GHz)	ϵ'_r
pH	TSS (mg/kg)		
3.4	0.07	2.530235	3.0210
3.6	0.08	2.529524	4.0007
3.7	0.12	2.529697	3.7623
4.3	0.08	2.530213	3.0513
4.6	0.09	2.529895	3.4895
5.1	0.21	2.530208	3.0582

Results obtained thus far give the value of ϵ'_r of different soil samples in the region using the cavity perturbation method operating in the S-band. ϵ'_r varies for different soil samples.

To study the effect of contaminants in soil, known quantity of finely-powdered common salt is added, mixed well and taken in the glass tube. 1.5 ml of soil (pH=5.1) is taken up for study. The salt-soil ratios considered are 0 %, 11 %, 14 % and 20 %. ϵ'_r of common salt (NaCl) is reported in literature as 6.1 (Robinson and Hallet, 1966). Hence the addition of common salt will raise the ϵ'_r of all soil samples. Value of ϵ'_r for different salt-soil mixture-ratios in the S-band for the first odd mode is given in Table 3.2.

Table 3.2: Dielectric Constant vs. varying salt-soil mixture-ratio (soil pH=5.1) at S-band; Cavity Perturbation Method

Salt-soil ratio (%)	f_s (GHz)	ϵ'_r
0	2.530208	3.0582
11	2.529636	3.8464
14	2.529537	3.9828
20	2.529453	4.0986

From the results it is evident that addition of salt increases the dielectric constant of soil. The more the content of salt, greater is the ϵ'_r of the salt-soil mixture. The effect of other contaminants such as fertilizers which are purposely added to soil to improve the fertility, is investigated in detail in Chapters 4 and 5.

3.3 Superstrate Method

The superstrate method (Section 2.2.2) is a widely used method to characterize a material. The setup consists of a suitable antenna, loaded with a material whose dielectric properties are to be studied. The material forms a superstrate on the antenna beneath. Dielectric constant of the material under test is computed from the shift in resonant frequency and impedance of the antenna. The antennas, their geometry and materials used along with their dielectric parameters are discussed in Section 2.2.2. Simulation setup using Ansoft HFSS validated the utility of the method for material characterization. In this section, results of experiments are conducted on soil samples spread on top of the antenna are presented.

3.3.1 Soil samples used

Three different soil samples - Red, White & Black - are used for the study. Red Soil and White Soil are obtained from the Geotechnical Lab, Division of Civil Engineering, CUSAT, and Black Soil is obtained from the District Soil Conservation Office, Ernakulam.

3.3.2 Experimental setup and Results

The experimental arrangement consists of an antenna on which soil, whose dielectric properties are to be studied, is loaded. Two types of antenna - probe-fed microstrip patch antenna (MPA) and CPW-fed monopole antenna (CMA) - are used, as discussed in Section 2.2.2. The

setup is shown in Fig. 3.1. Measurements are carried out using Rohde and Schwarz ZVB8 VNA. Antenna structures are fabricated to resonate in the L, S and C bands. Typical antenna geometry is shown in Figs. 3.2(a) and 3.2(b). Dimensions of the fabricated antennas at different frequencies are detailed in Section 2.2.2, Tables 2.4 and 2.5.

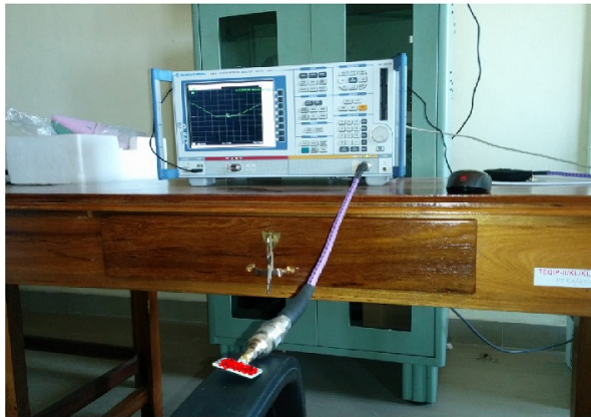


Figure 3.1: Experimental setup of Superstrate Method with Red Soil as Superstrate

As the ϵ_r' and $\tan\delta$ of the soil samples used are unknown, variation of frequency and impedance of the antenna with the soil sample is measured. Results obtained for the two antennas in the three frequency bands are given in Tables 3.3 to 3.5. Corresponding plots are shown in Figs. 3.3 to 3.8.

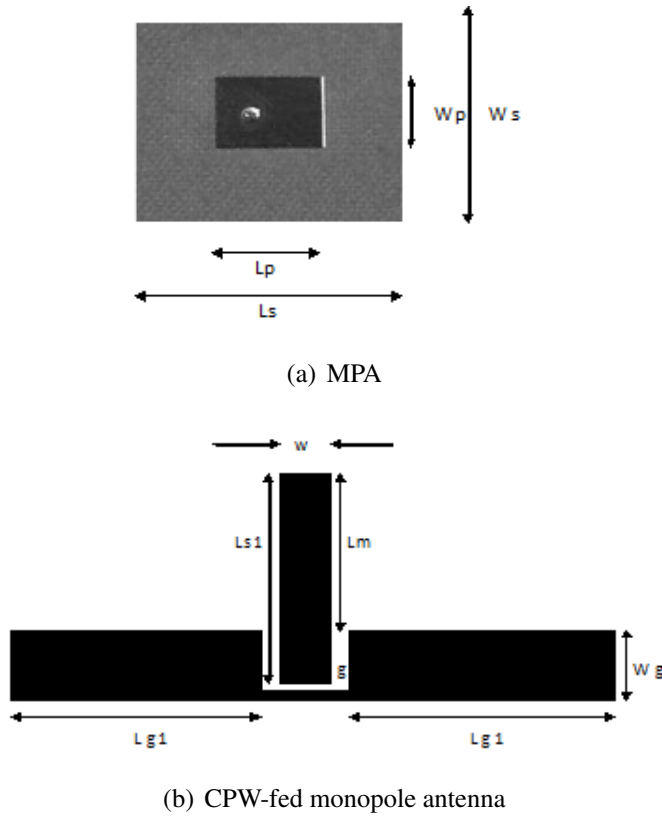


Figure 3.2: Geometry of antennas fabricated; Superstrate Method

Table 3.3: Frequency and normalized impedance for Red, White and Black soil samples; **L-band** ($f_r=1.85$ GHz); Superstrate Method

Soil type	Frequency (GHz)		Normalized Resistance		Normalized Reactance	
	MPA	CMA	MPA	CMA	MPA	CMA
Red	1.7956	1.8002	1.0261	1.0288	-0.0922	-0.0927
White	1.7865	1.8187	1.0031	1.0037	-0.2410	-0.1480
Black	1.7801	1.7714	0.9212	0.9318	-0.0105	-0.0135

Table 3.4: Frequency and normalized impedance for Red, White and Black soil samples; **S-band** ($f_r=2.45$ GHz); Superstrate Method

Soil type	Frequency (GHz)		Normalized Resistance		Normalized Reactance	
	MPA	CMA	MPA	CMA	MPA	CMA
Red	2.4144	2.4232	1.0319	1.0348	-0.0935	-0.0949
White	2.3887	2.3992	1.0087	1.0068	-0.2240	-0.1690
Black	2.3112	2.3011	0.9289	0.9427	-0.0118	-0.0139

Table 3.5: Frequency and normalized impedance for Red, White and Black soil samples; **C-band** ($f_r=5.25$ GHz); Superstrate Method

Soil type	Frequency (GHz)		Normalized Resistance		Normalized Reactance	
	MPA	CMA	MPA	CMA	MPA	CMA
Red	5.1433	5.1462	1.0355	1.0371	-0.0904	-0.0929
White	5.1018	5.1846	1.0061	1.0054	-0.2370	-0.1230
Black	5.0960	5.0030	0.9388	0.9409	-0.0129	-0.0131

Loading of the soil sample varies the frequency and impedance of the antenna. Simulation results, as discussed in Chapter 2, also showed similar variation of frequency and impedance with respect to the ϵ'_r of the MUT. The Superstrate Method thus shows how the antenna exhibits different characteristics for different soil samples. Hence the work presented in this chapter proves that soil has microwave properties. Further characterization of soil is performed using other microwave methods in the ensuing chapters.

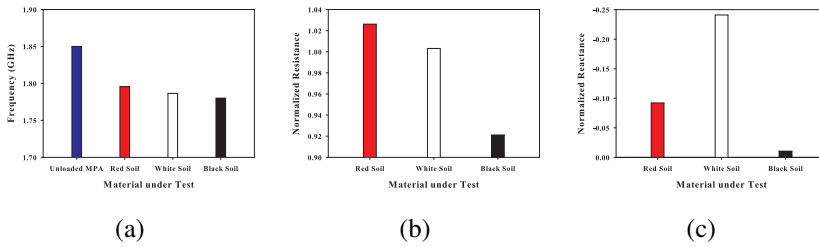


Figure 3.3: Variation of (a) frequency (b) normalized resistance and (c) normalized reactance of **MPA** for Red, White and Black soil samples; **L-band**; Superstrate Method

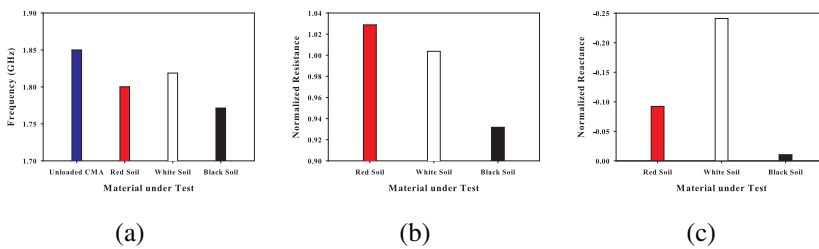


Figure 3.4: Variation of (a) frequency (b) normalized resistance and (c) normalized reactance of **CMA** for Red, White and Black soil samples; **L-band**; Superstrate Method

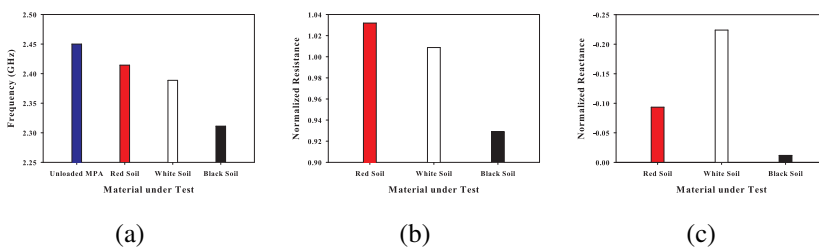


Figure 3.5: Variation of (a) frequency (b) normalized resistance and (c) normalized reactance of **MPA** for Red, White and Black soil samples; **S-band**; Superstrate Method

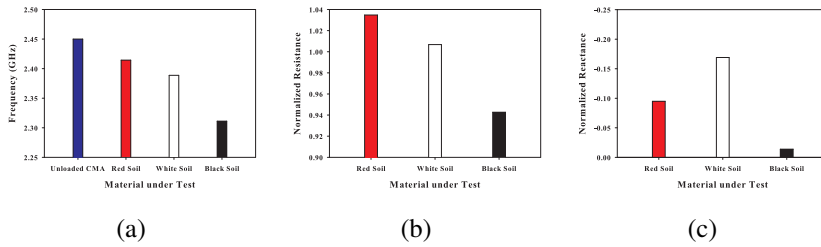


Figure 3.6: Variation of (a) frequency (b) normalized resistance and (c) normalized reactance of **CMA** for Red, White and Black soil samples; **S-band**; Superstrate Method

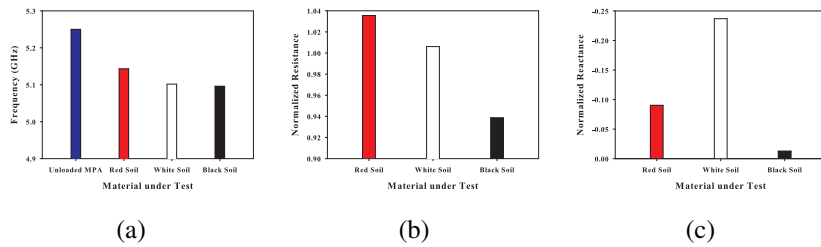


Figure 3.7: Variation of (a) frequency (b) normalized resistance and (c) normalized reactance of **MPA** for Red, White and Black soil samples; **C-band**; Superstrate Method

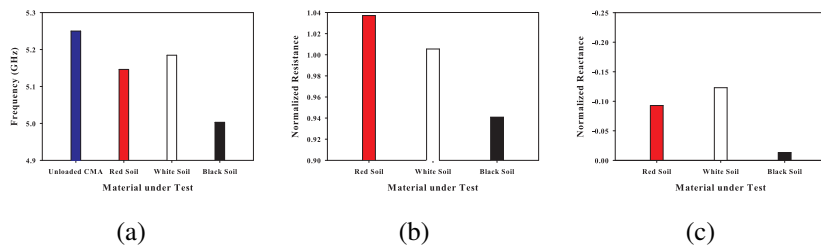


Figure 3.8: Variation of (a) frequency (b) normalized resistance and (c) normalized reactance of **CMA** for Red, White and Black soil samples; **C-band**; Superstrate Method

3.4 Chapter Summary

In this chapter, soil characterization using conventional methods such as cavity perturbation method and superstrate method is presented. In the cavity perturbation method, simulation as well as experimental studies are conducted on different soil samples taken in glass tubes inserted into the cavity resonator operating in the S band. Results reveal that there is a variation in ϵ_r' with soil pH. Thus microwave properties of soil are confirmed; hence soil can be subjected to any method for material characterization using microwaves. The superstrate method, which used probe-fed MPA and CPW-fed monopole antenna on which soil, whose dielectric properties are to be studied is loaded, emphasized the relevance of usage of microwave frequencies for material-property study, especially soil. The three soil samples used are seen to affect antenna parameters such as its frequency and impedance. This is in agreement with the findings of the simulation study. Thus the two methods offer simple and convenient scheme for sensing of soil properties. However these two methods suffer from the following shortcomings. (i) In the cavity perturbation method, soil has to be taken in thin glass tubes as the volume of the sample needs to be very small. This requires pulverization of the soil samples into fine powder. (ii) In the superstrate method, soil has to be spread uniformly over the antenna structure beneath; any soil leakage into the structure can cause damage to it. To overcome these drawbacks, soil characterization using Free-space Transmission Method and Sensor Antenna Method is presented in Chapters 4 and 5.

The highlight of this chapter is that it provides a motivational basis for carrying out more research to correlate dielectric properties of soil with parameters such as pH, moisture content, fertilizer content etc.

Chapter 4

SOIL CHARACTERIZATION USING FREE-SPACE TRANSMISSION METHOD

Contents

4.1	Introduction	85
4.2	Estimation of Moisture Content	87
4.3	Estimation of Fertilizer Concentration	128
4.4	Chapter Summary	147

4.1 Introduction

Chapter 2 discussed four methods for material characterization. An analytical method to analyze the result using the superstrate method based on ANN model was also presented. The chapter ended by discussing an imaging technique for colour-mapping of materials for

detecting objects embedded in soil. In Chapter 3, soil characterization using Cavity Perturbation Method and Superstrate Method were discussed. Microwave properties of soil were confirmed using these two methods. It was concluded that soil can be subjected to any method for material characterization using microwaves. The shortcomings of the methods were also mentioned, which provided a necessity to carry out soil characterization using other methods. Moreover, a need for carrying out more research to correlate dielectric properties of soil with pH, moisture content, fertilizer concentration etc. was felt. This chapter presents the Free-space Transmission Method used for the characterization of soil, where the shortcomings are overcome. Simulation using CST Microwave Studio® (CST MWS®), a specialist tool for 3D electromagnetic simulation of high frequency components, and validation using an experimental setup are discussed. The free-space transmission method in which a material sample is placed between a transmitting antenna and a receiving antenna was described in Section 2.2.3. The suitability of the method for material characterization was validated using standard dielectric materials, such as acrylic and water, with known ϵ'_r . Since the ϵ'_r values obtained were in good agreement with those available in literature, it was decided to use the free-space transmission method for characterization of soil.

This chapter discusses the following points.

1. Computation of ϵ'_r of dry soil samples
2. Computation of ϵ'_r of soil samples mixed with varying moisture content
3. Estimation of Moisture Content (MC) and Fertilizer Concentration (FC) in different soil samples at the L, S and C bands. MC, estimated in terms of Volumetric Water Content (VWC), is expressed as a percentage and noted as θ_v
4. Development of a model based on Artificial Neural Network to evaluate soil parameters

5. Colour-mapping of samples to indicate the presence of moisture

4.2 Estimation of Moisture Content

4.2.1 Soil samples used

Out of the fourteen districts in Kerala, it is officially known (Premachandran, 2007) that alkaline soils with pH values above 7.0 are available mostly in Palakkad only, while the soils in the other thirteen districts are acidic in nature, with pH below 7.0. Experiments based on soils are carried out on 62 samples (31 acidic and 31 alkaline) obtained from Ernakulam (acidic) and Palakkad (alkaline). Soil Testing Laboratories at Ernakulam and Palakkad, which supplied the samples, provided information of soil-pH. In some cases, the Total Soluble Salt content is reported. To distinguish between soil samples with the same pH (but with other constituents), they are noted using letters a, b, c, etc. Details of soil samples tested are as enumerated in Table 4.1.

4.2.2 Simulation Results

Free-space Transmission Method was explained in Chapter 2 with reference to material characterization. Here a similar setup is used for soil. A sample-holder containing the soil sample, whose dielectric properties are to be determined, is placed between two Microstrip Patch Antennas (MPA) resonating in the C band. Microwaves are incident on the sample. Since soil in the C band has a dielectric constant between 2 & 5, (Ghosh et al., 1998), a material with a dielectric constant of 3.5 is chosen from the library of the simulation software CST MWS®. Transmission coefficient (S_{21}) is observed without and with the sample in between the MPAs. Setup without and with soil sample in between the antennas are shown in Fig. 4.1. This research focusses on the characterization of soil in the presence of moisture and other added matter. Hence, drops of water are added to the soil sample to

understand whether presence of moisture in soil can influence antenna parameters. This is done by changing dielectric constant from 3.5 (soil) to 80 (water) at one location. Presence of soil and any moisture contained within it is found by interpreting the transmission parameter.

Table 4.1: Details of soil samples used in Free-space Transmission Method

Type & Region	Serial No.	pH	No. of Samples	Type & Region	Serial No.	pH	No. of Samples
Acidic soil (31 samples) Udayamperur Series, Ernakulam	1	4.7	2(a, b)	Alkaline soil (31 samples) Anuppur/Agali Series, Palakkad	1	7.0	3(a to c)
	2	4.9	2(a, b)		2	7.1	7(a to g)
	3	5.0	3(a to c)		3	7.2	5(a to e)
	4	5.1	1		4	7.3	8(a to h)
	5	5.2	1		5	7.4	3(a to c)
	6	5.3	2(a, b)		6	7.5	5(a to e)
	7	5.4	1				
	8	5.7	1				
	9	5.8	2(a, b)				
	10	5.9	1				
	11	6.1	1				
	12	6.2	6(a to f)				
	13	6.3	2(a, b)				
	14	6.4	6(a to f)				

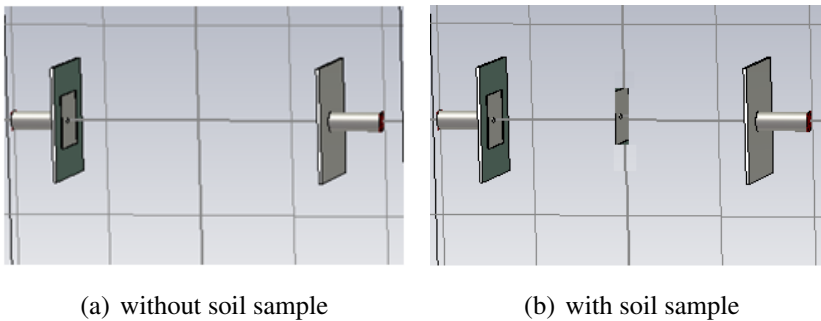


Figure 4.1: Simulation setup of Free-space Transmission Method

Fig. 4.2 shows the free-space S_{11} and S_{21} characteristics of the MPA resonating at $f_r=5.52$ GHz in the C-band for the free-space, with soil-sample and moist soil-sample cases. Shift in S_{21} characteristics of the antenna is seen when the soil-sample is placed in between the two MPAs; also the shift is more appreciable, when the soil is wetted. This suggests that the free-space transmission method can be used for monitoring moisture in soil. The results are shown in Table 4.2.

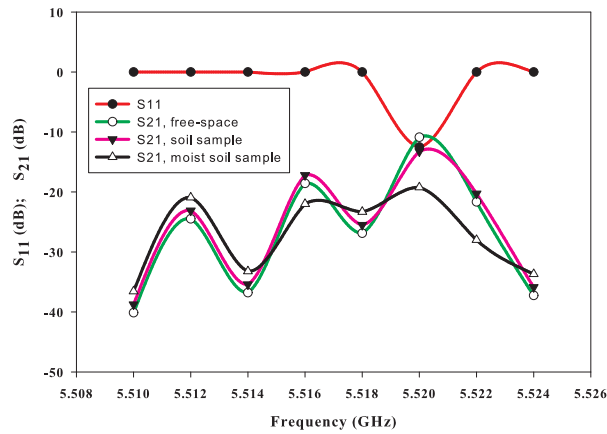


Figure 4.2: Free-space S_{11} & S_{21} characteristics of MPA under different cases; C-band; Free-space Transmission Method

Table 4.2: S_{21} values of MPA in free-space, empty soil and with moisture in soil; C-band; Free-space Transmission Method

Setup	S_{21} (dB)
MPA in free-space	-10.876
Soil sample in between MPAs	-11.245
Moisture in soil sample	-19.238

4.2.3 Experimental Results

The setup consists of a pair of MPAs working as transmit/receive antennas. Sample-holder filled with soil samples is placed between the antennas connected to the VNA. Measurements are carried out in the L, S and C bands, with the MPAs resonating at $f_r=1.85$ GHz, 2.45 GHz and 5.52 GHz. The coaxial probe-fed MPAs are fabricated on a substrate ($\epsilon'_r=4.4$, $\tan\delta=0.02$ and thickness=1.6 mm). Figs. 4.3 (a) & (b) show the MPA structure, resonating at 5.52 GHz and its reflection characteristics. Similar antennas are designed for the L and S bands. The experimental setup is shown in Fig. 4.4.

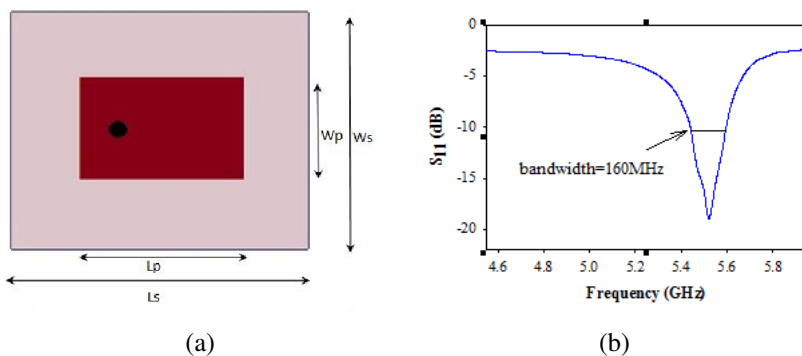


Figure 4.3: (a) Structure of Microstrip Patch Antenna; $f_r=5.52$ GHz; $L_p=16.5$ mm, $W_p=12.4$ mm, $L_s=34.0$ mm, $W_s=28.0$ mm (b) reflection characteristics

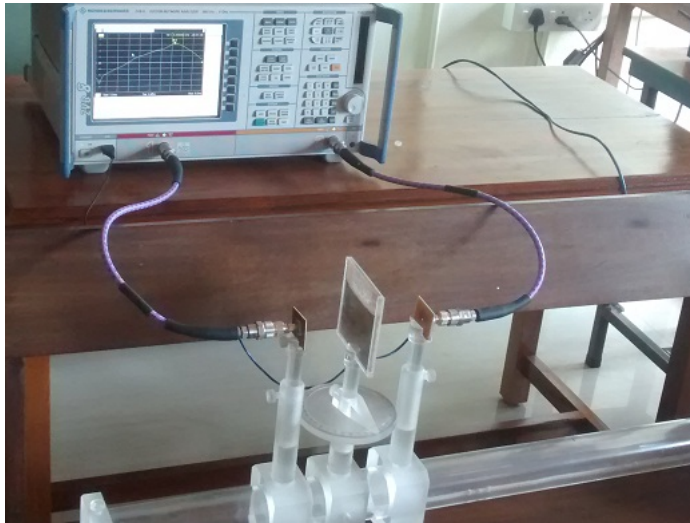
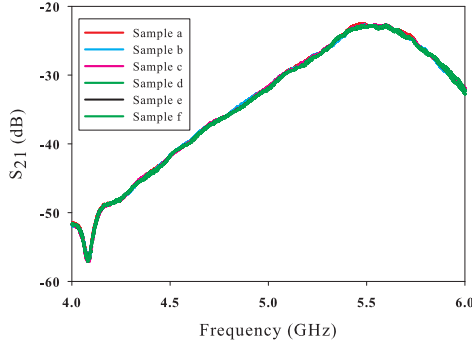


Figure 4.4: Experimental setup of Free-space Transmission Method

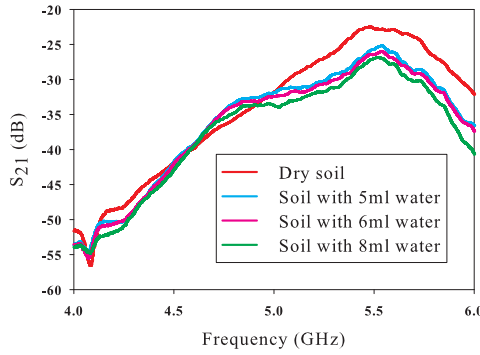
Two different cases are considered.

1. 62 different samples of 20 ml of dry soil, with varying pH value
2. All samples, individually mixed with 5 ml, 6 ml and 8 ml of water (moisture-content values of 20%, 23.1% and 28.6% respectively) to understand the effect of moisture in soil

The transmission characteristics curve (S_{21}) is plotted for both the cases. A shift in S_{21} is noted when samples are mixed with water because the power received by the receiving antenna decreases in the presence of soil-water mixture in between the transmitting and receiving MPAs. S_{21} variations for all the cases are obtained; an illustration for the six dry soil samples of pH=6.4 and one sample of pH=6.4 (sample a) mixed with varying moisture content (MC) in the C-band is shown in Fig. 4.5. Fig. 4.5(a) shows minute variations in S_{21} for soil samples with the same pH. This may be due to the presence of small amount of contaminants in the soil. Fig. 4.5(b) shows changes in S_{21} for same soil sample with varying MC, justifying losses caused by the addition of water.



(a) 6 dry soil samples of pH=6.4



(b) Soil (pH=6.4, sample a) with varying MC

Figure 4.5: Transmission characteristics with soil samples (pH=6.4) in the C-band; Free-space Transmission Method

As discussed in Section 2.2.3, variation in phase is relevant in the context of the experiment to compute ϵ_r' . The relationship is reproduced here for reference.

$$\epsilon_r' = \left[\frac{\Delta\phi c}{2\pi d f} + 1 \right]^2 \quad (4.1)$$

Hence, phase values versus frequency in the operating band of the antenna are noted for cases (1) and (2). Corresponding plots for acidic samples are shown in Figs. 4.6, 4.7 & 4.8 and alkaline samples in Fig. 4.9 for case (1). The phase variation for free-space transmission

without any soil sample is also shown for comparison.

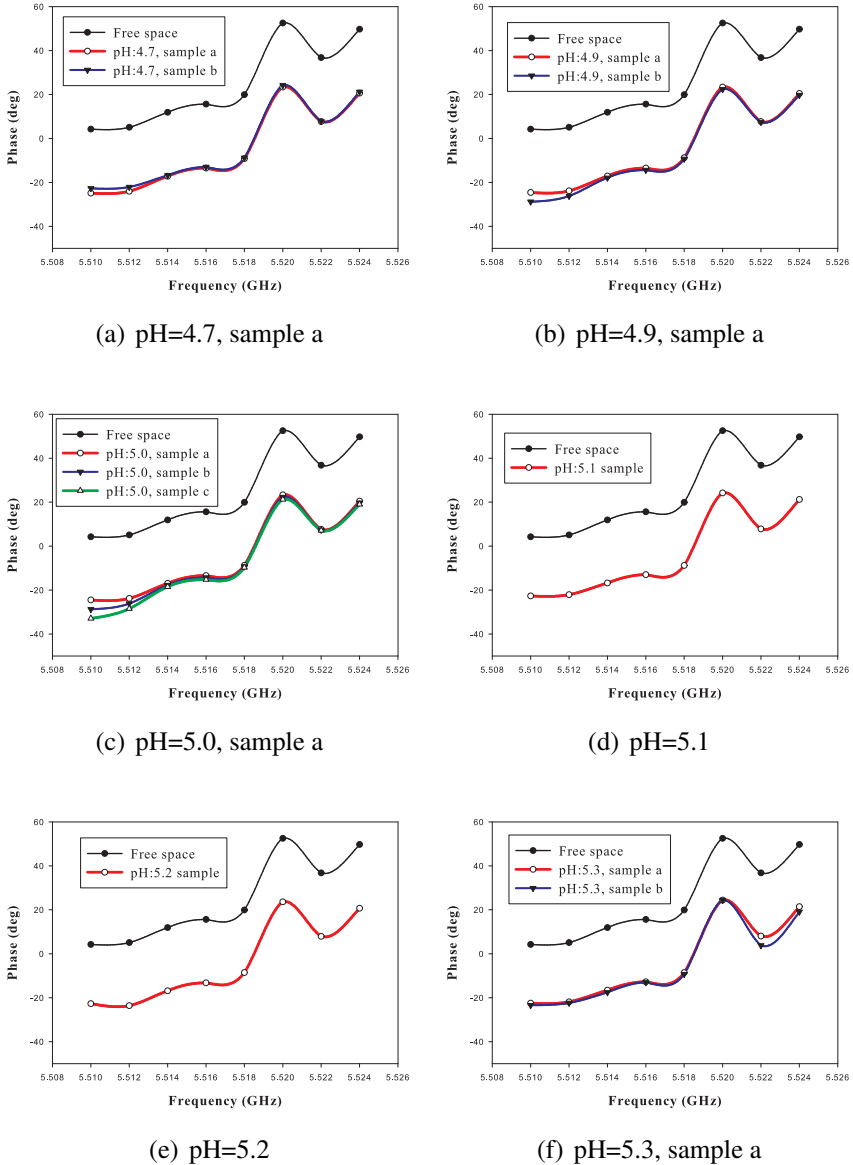
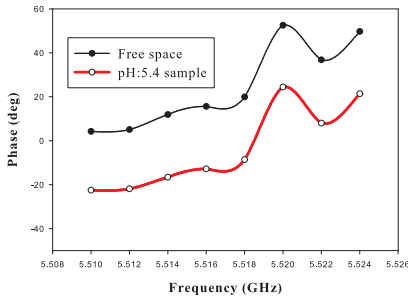
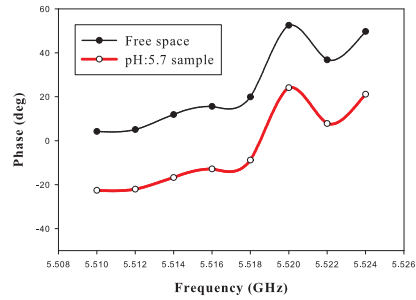


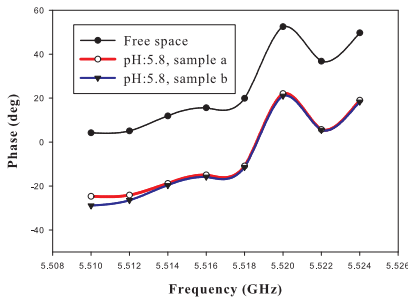
Figure 4.6: Phase vs. frequency of dry acidic soil samples [pH=4.7, 4.9, 5.0, 5.1, 5.2 & 5.3]; C-band; Free-space Transmission Method



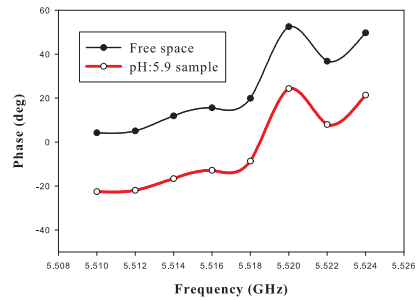
(a) pH=5.4



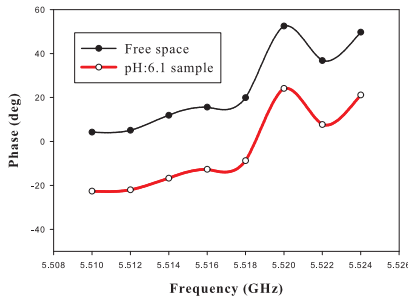
(b) pH=5.7



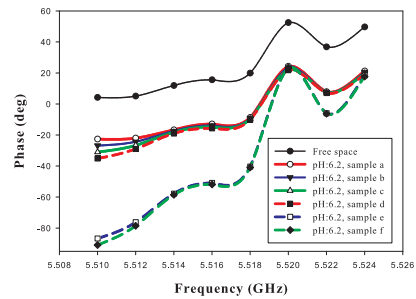
(c) pH=5.8, sample a



(d) pH=5.9

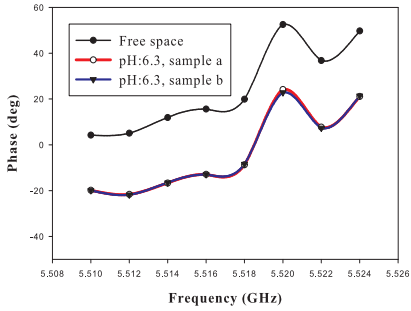


(e) pH=6.1

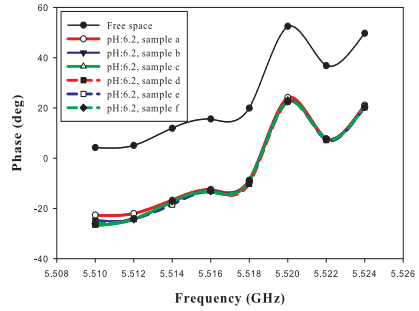


(f) pH=6.2, sample a

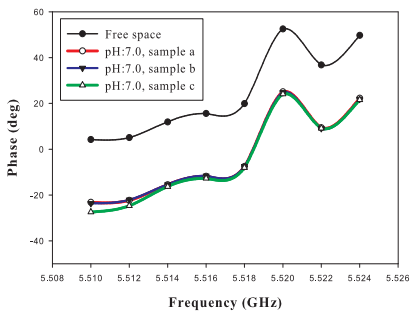
Figure 4.7: Phase vs. frequency of dry acidic soil samples [pH=5.4, 5.7, 5.8, 5.9, 6.1 & 6.2]; C-band; Free-space Transmission Method



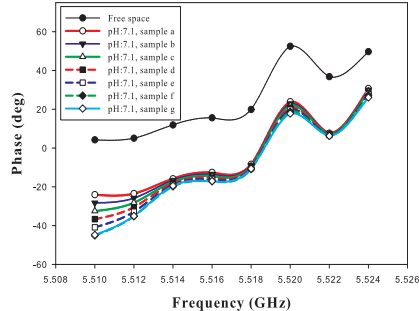
(a) pH=6.3, sample a



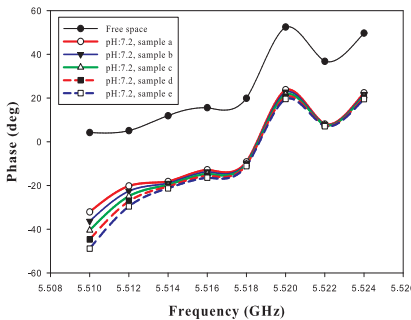
(b) 6.4, sample a



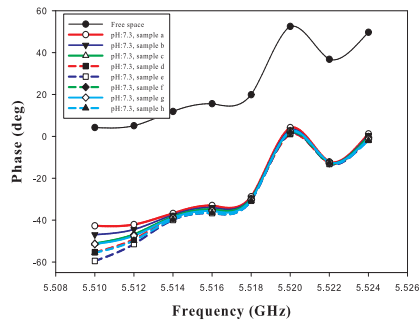
(c) pH=7.0, sample a



(d) pH=7.1, sample a



(e) pH=7.2, sample a



(f) pH=7.3, sample a

Figure 4.8: Phase vs. frequency of dry acidic soil samples [pH=6.3, 6.4,7.0, 7.1,7.2 & 7.3]; C-band; Free-space Transmission Method

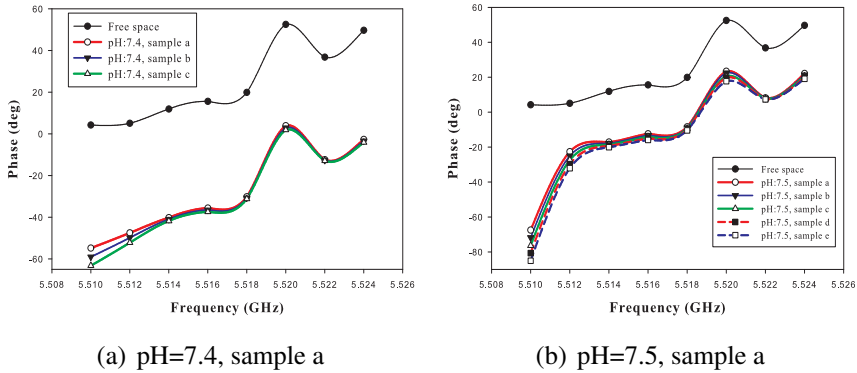
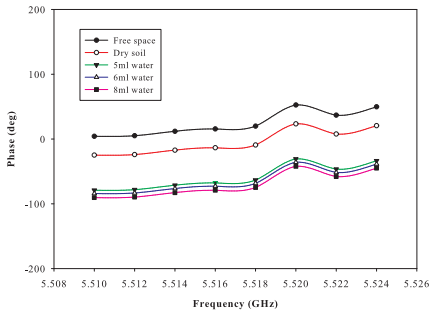


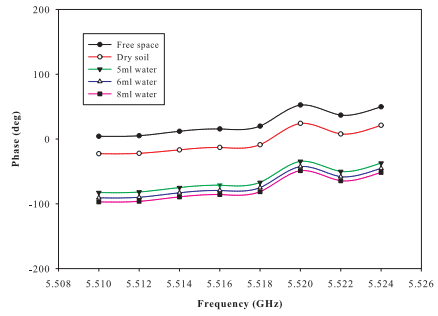
Figure 4.9: Phase vs. frequency of dry alkaline soil samples [pH=7.4 & 7.5]; C-band; Free-space Transmission Method

Figs. 4.6 to 4.9 show the phase versus frequency plots of all the dry soil samples. Difference in phase-characteristics of different soil samples indicates response-variation due to change in pH. Also, variation in phase-characteristics for soil samples with the same pH may be due to contaminants.

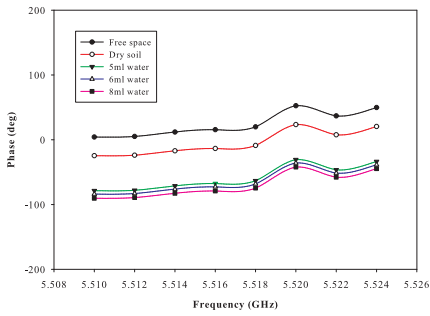
Water is added to soil to improve its plant-growth capability. To know the variation of phase-characteristics of the soil samples in the presence of moisture, the experimental procedure is extended by adding water to dry soil. As mentioned in case (2), 5 ml, 6 ml and 8 ml of water are added to 20 ml of dry soil samples, giving percentage moisture-content values of 20%, 23.1% and 28.6% respectively. Figs. 4.10 to 4.14 show phase-plots for acidic samples for varying moisture-content; corresponding plots for alkaline samples are shown in Figs. 4.15 to 4.20.



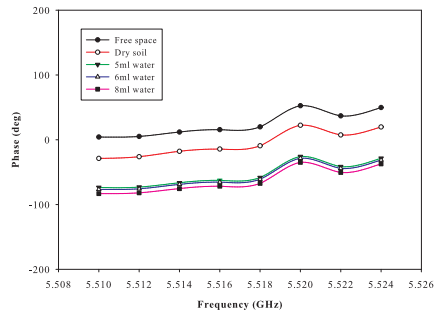
(a) pH=4.7, sample a



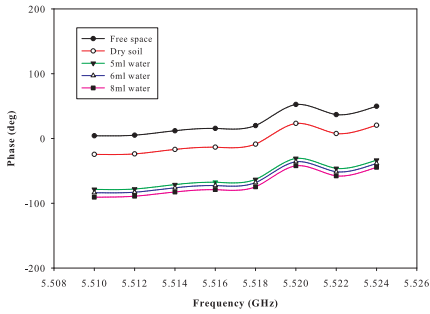
(b) pH=4.7, sample b



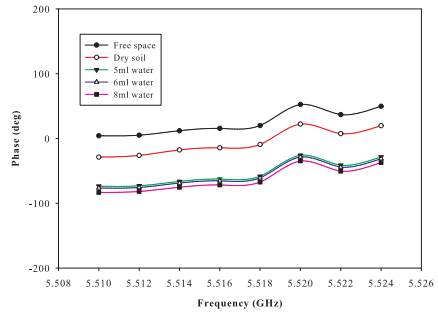
(c) pH=4.9, sample a



(d) pH=4.9, sample b

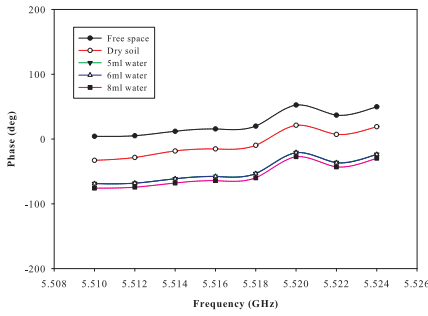


(e) pH=5.0, sample a

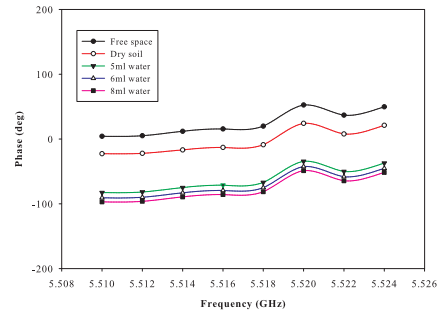


(f) pH=5.0, sample b

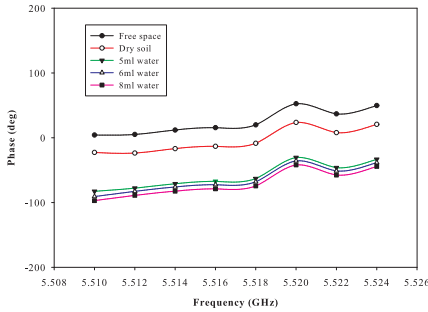
Figure 4.10: Phase vs. frequency of different acidic soil samples with varying moisture content; [pH=4.7, 4.9 & 5.0 (sample a, b)]; C-band; Free-space Transmission Method



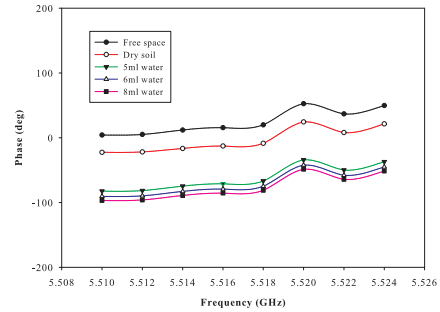
(a) pH=5.0, sample c



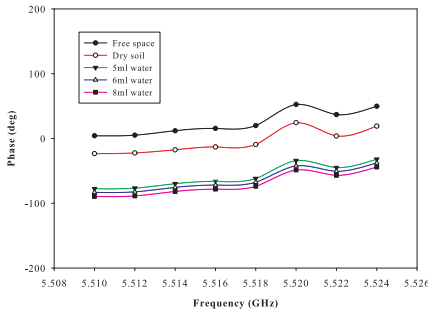
(b) pH=5.1



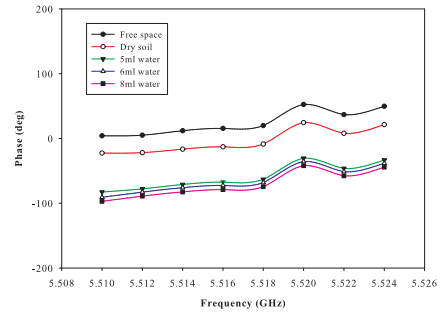
(c) pH=5.2



(d) pH=5.3, sample a

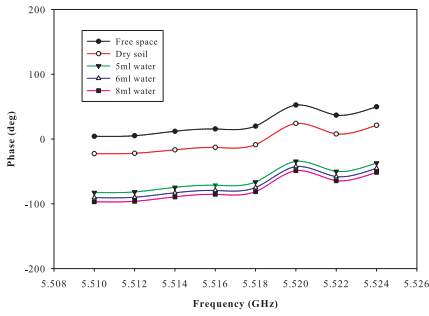


(e) pH=5.3, sample b

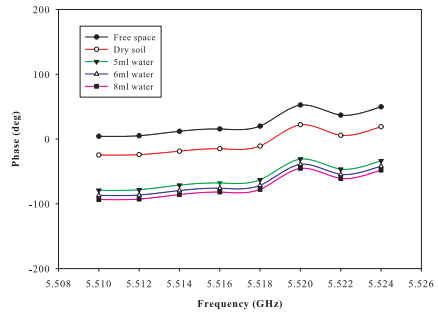


(f) pH=5.4

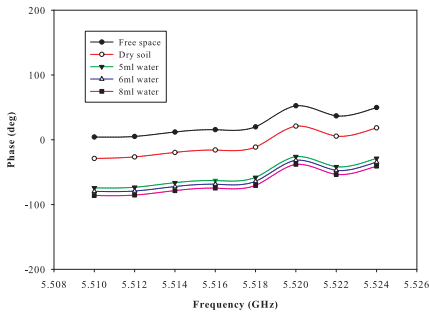
Figure 4.11: Phase vs. frequency of different acidic soil samples with varying moisture content; [pH=5.0 (sample c), 5.1, 5.2, 5.3 & 5.4]; C-band; Free-space Transmission Method



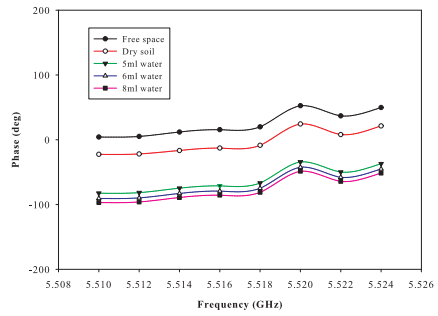
(a) pH=5.7



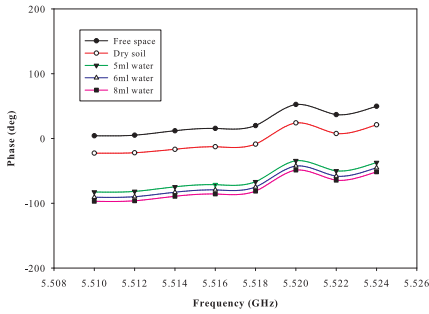
(b) pH=5.8, sample a



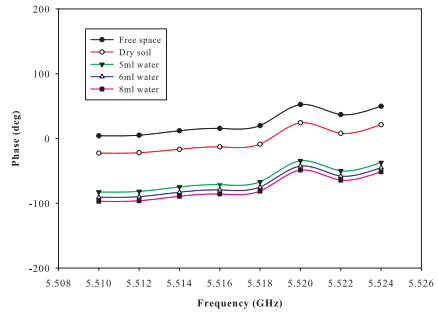
(c) pH=5.8, sample b



(d) pH=5.9

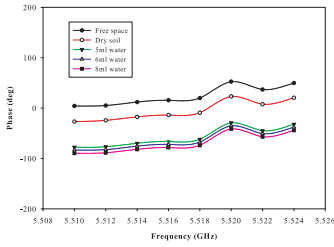


(e) pH=6.1

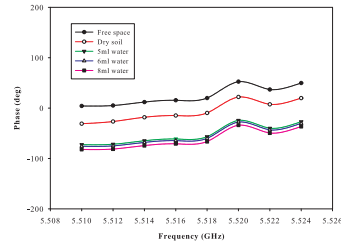


(f) pH=6.2, sample a

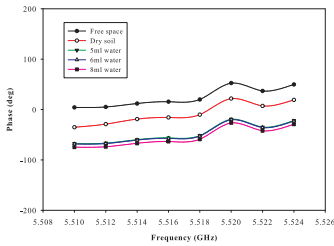
Figure 4.12: Phase vs. frequency of different acidic soil samples with varying moisture content; [pH=5.7, 5.8, 5.9, 6.1 & 6.2 (sample a)]; C-band; Free-space Transmission Method



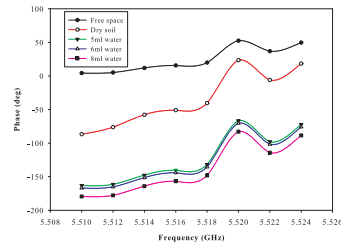
(a) pH=6.2, sample b



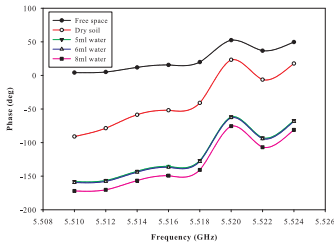
(b) pH=6.2, sample c



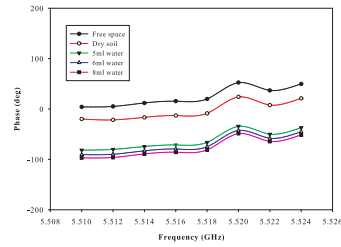
(c) pH=6.2, sample d



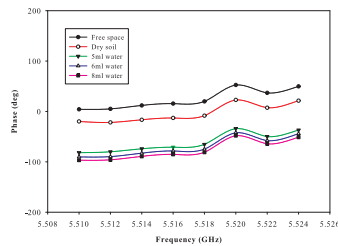
(d) pH=6.2, sample e



(e) pH=6.2, sample f

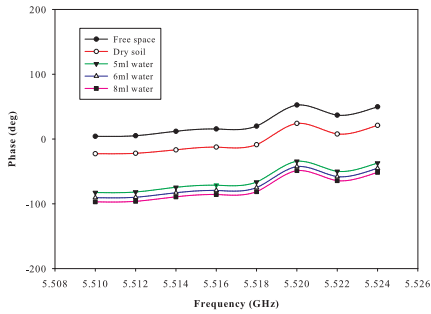


(f) pH=6.3, sample a

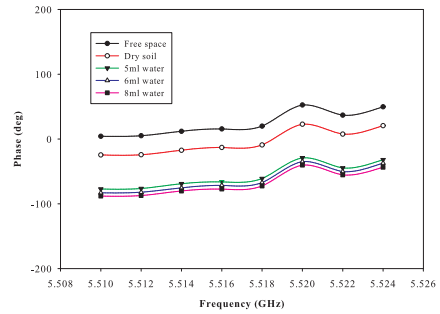


(g) pH=6.3, sample b

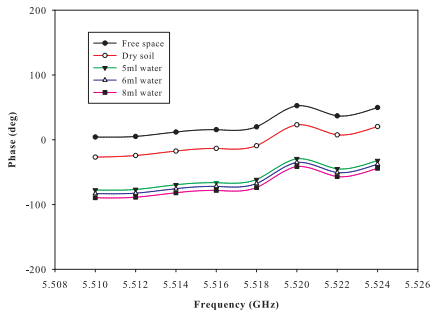
Figure 4.13: Phase vs. frequency of different acidic soil samples with varying moisture content; [pH=6.2 (sample b-f), & 6.3]; C-band; Free-space Transmission Method



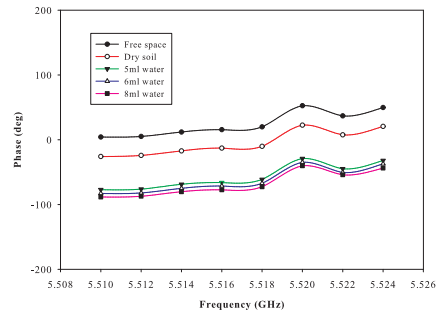
(a) pH=6.4, sample a



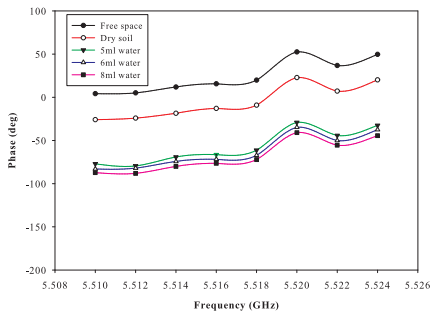
(b) pH=6.4, sample b



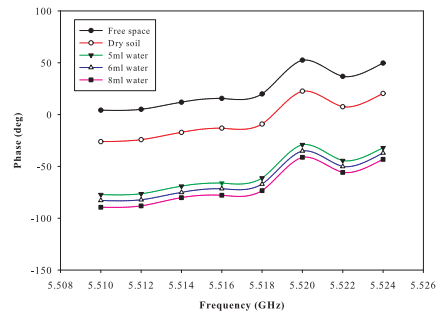
(c) pH=6.4, sample c



(d) pH=6.4, sample d

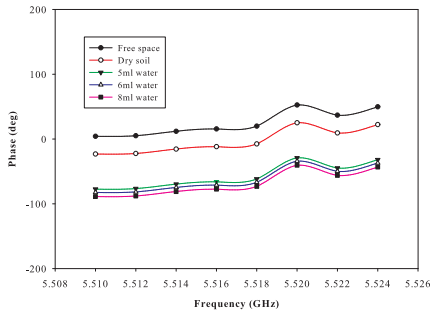


(e) pH=6.4, sample e

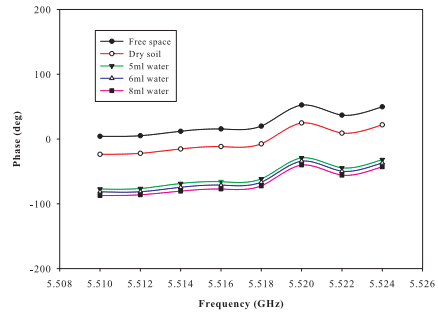


(f) pH=6.4, sample f

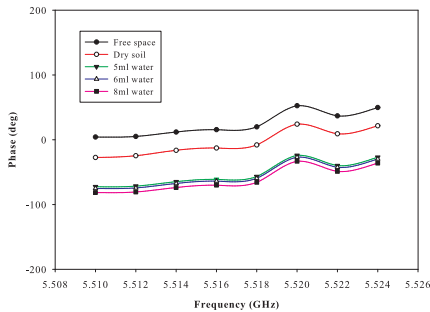
Figure 4.14: Phase vs. frequency of different acidic soil samples with varying moisture content; [pH=6.4]; C-band; Free-space Transmission Method



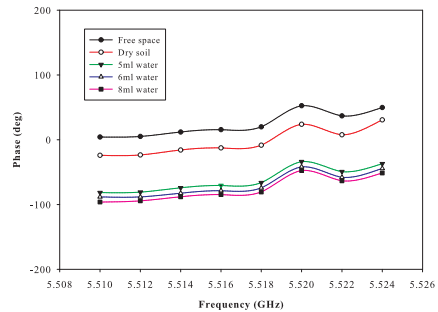
(a) pH=7.0, sample a



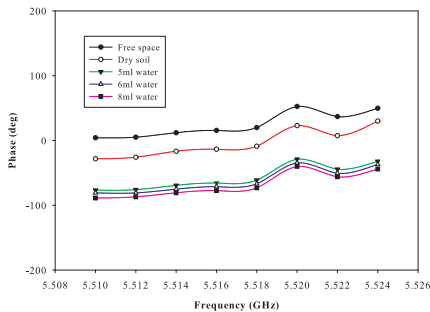
(b) pH=7.0, sample b



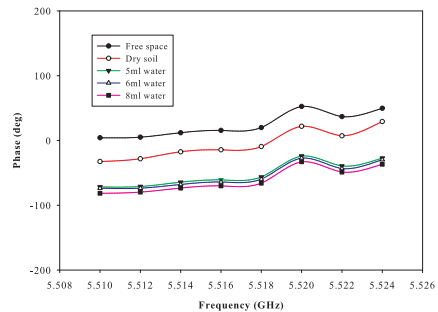
(c) pH=7.0, sample c



(d) pH=7.1, sample a

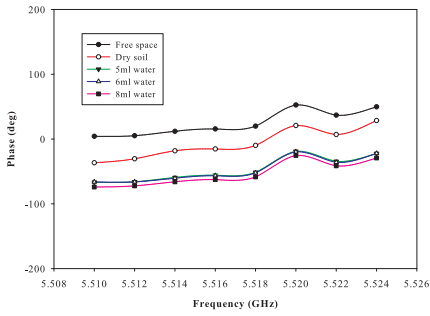


(e) pH=7.1, sample b

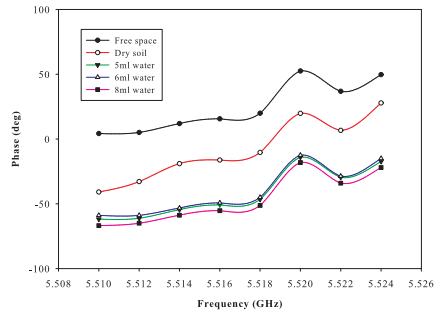


(f) pH=7.1, sample c

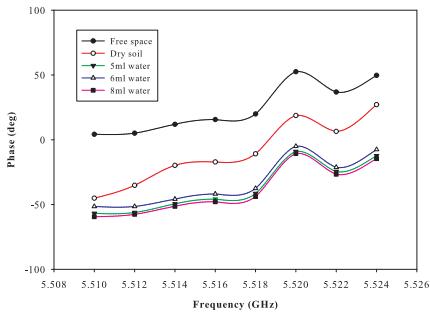
Figure 4.15: Phase vs. frequency of different alkaline soil samples with varying moisture content; [pH=7.0 & 7.1(samples a-c)]; C-band; Free-space Transmission Method



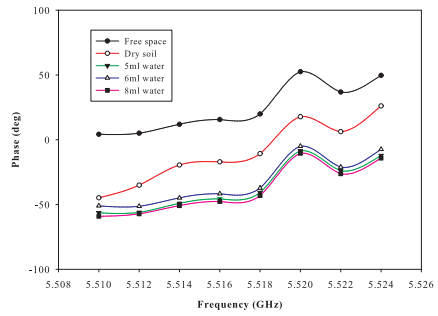
(a) pH=7.1, sample d



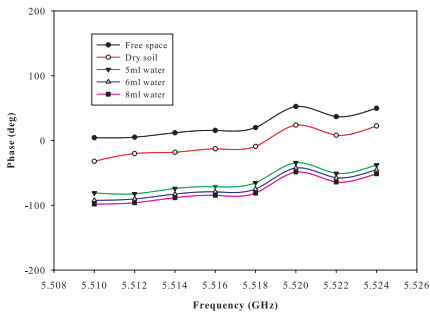
(b) pH=7.1, sample e



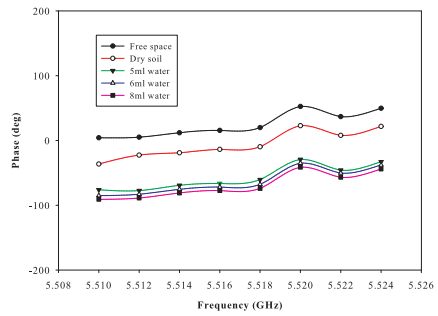
(c) pH=7.1, sample f



(d) pH=7.1, sample g

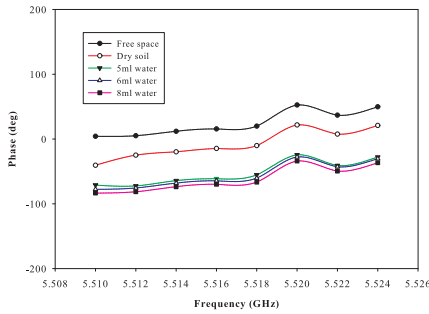


(e) pH=7.2, sample a

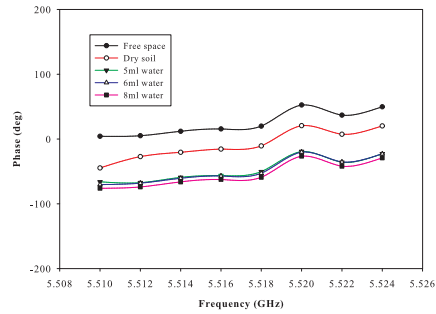


(f) pH=7.2, sample b

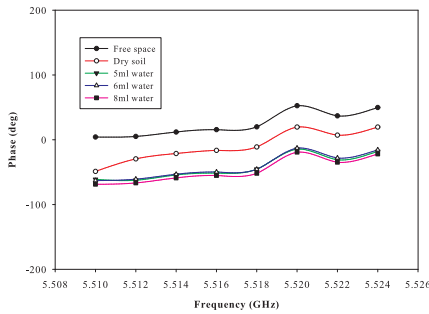
Figure 4.16: Phase vs. frequency of different alkaline soil samples with varying moisture content; [pH=7.1(samples d-g) & 7.2(samples a, b)]; C-band; Free-space Transmission Method



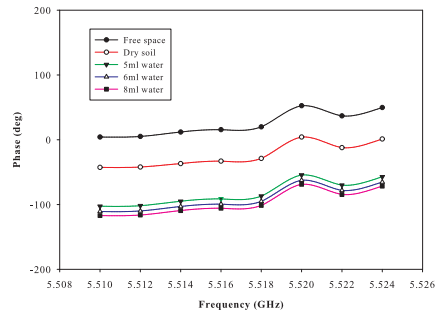
(a) pH=7.2, sample c



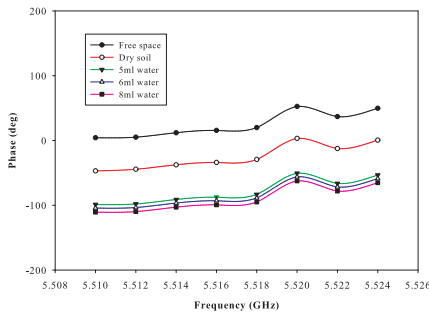
(b) pH=7.2, sample d



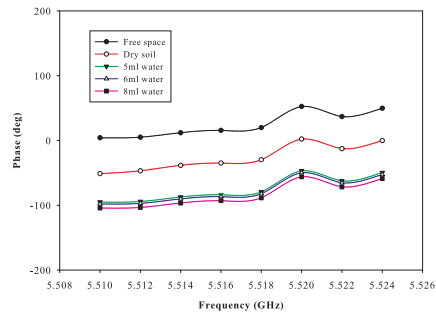
(c) pH=7.2, sample e



(d) pH=7.3, sample a

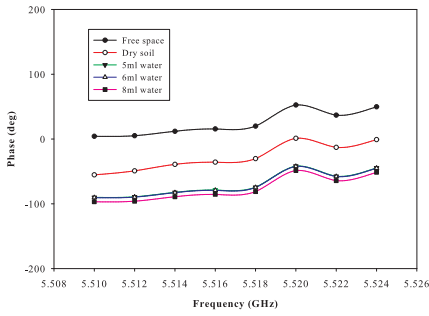


(e) pH=7.3, sample b

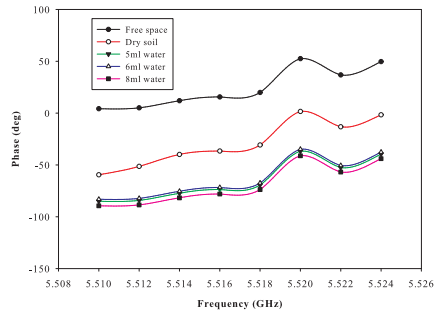


(f) pH=7.3, sample c

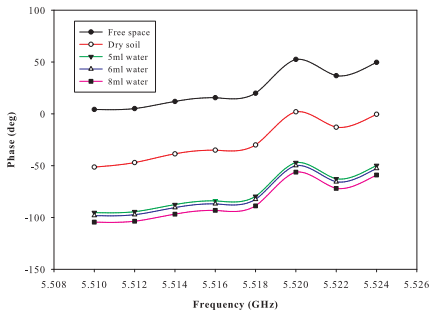
Figure 4.17: Phase vs. frequency of different alkaline soil samples with varying moisture content; [pH=7.2(samples c-e) & 7.3(samples a-c)]; C-band; Free-space Transmission Method



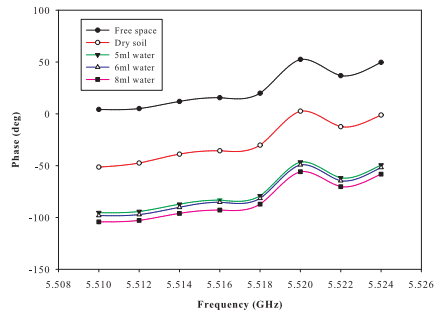
(a) pH=7.3, sample d



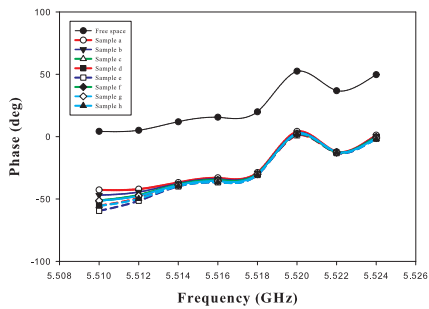
(b) pH=7.3, sample e



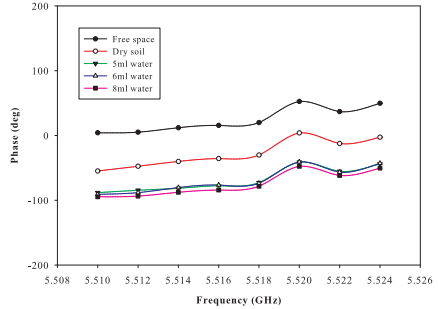
(c) pH=7.3, sample f



(d) pH=7.3, sample g

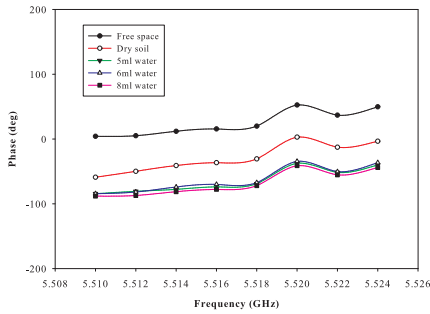


(e) pH=7.3, sample h

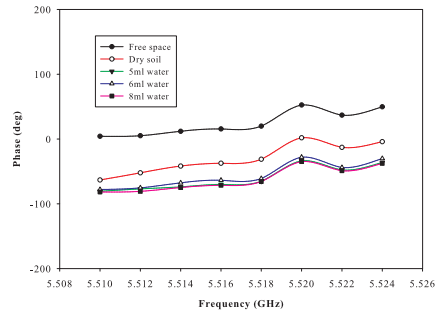


(f) pH=7.4, sample a

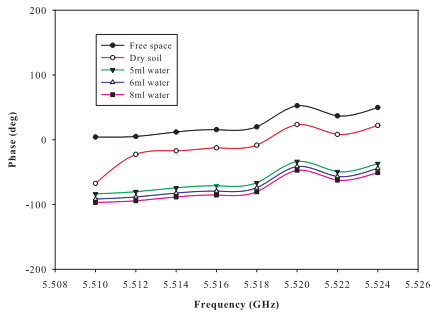
Figure 4.18: Phase vs. frequency of different alkaline soil samples with varying moisture content; [pH=7.3(samples d-h) & 7.4(sample a)]; C-band; Free-space Transmission Method



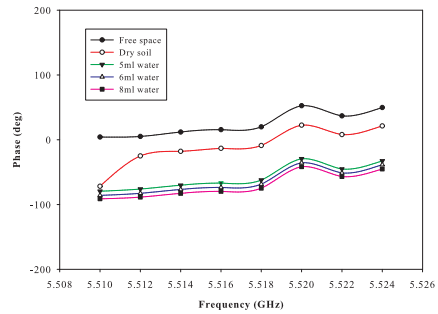
(a) pH=7.4, sample b



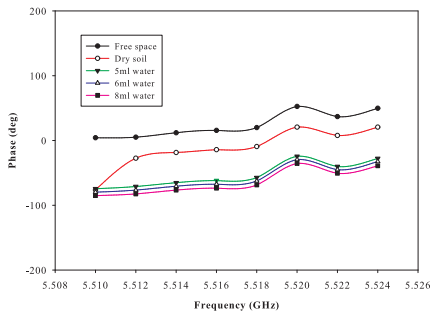
(b) pH=7.4, sample c



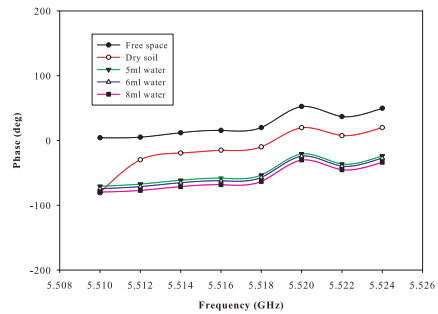
(c) pH=7.5, sample a



(d) pH=7.5, sample b

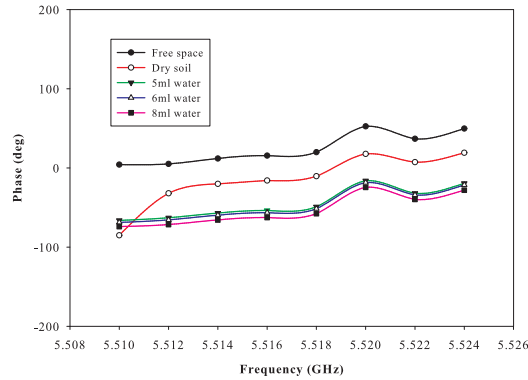


(e) pH=7.5, sample c



(f) pH=7.5, sample d

Figure 4.19: Phase vs. frequency of different alkaline soil samples with varying moisture content; [pH=7.4(samples b, c) & 7.5(samples a-d)]; C-band; Free-space Transmission Method



(a) pH=7.5, sample e

Figure 4.20: Phase vs. frequency of different alkaline soil samples with varying moisture content; [pH=7.5 (sample e)]; C-band; Free-space Transmission Method

Figs. 4.10 to 4.20 show the phase versus frequency plots (C-band) of all the soil samples with varying moisture content. These plots indicate larger phase-variations with increasing moisture content. Consequently, ϵ_r' of the soil samples too will increase with moisture content, as proposed in Eqn. 4.1. Table 4.3 shows the values of ϵ_r' for nine select dry soil samples computed using the above equation, in the L, S and C bands.

It is seen that there is a variation in the value of ϵ_r' with frequency for all samples; the variation is between 3.12 and 3.98. As frequency increases, ϵ_r' decreases for most of the soil samples. This relationship between ϵ_r' and frequency is in agreement with the literature (Alex and Behari, 1996). However, no fixed pattern for the variation is noted. This is because ϵ_r' could also depend on other agronomic and organic properties of soil.

Table 4.3: Dielectric constant of dry soil samples at three different frequencies; Free-space Transmission Method

Soil		ϵ'_r		
pH	Sample	$f_r=1.85$ GHz	$f_r=2.45$ GHz	$f_r=5.52$ GHz
4.7	a	3.98	3.90	3.82
4.9	a	3.62	3.43	3.30
5.0	a	3.79	3.53	3.25
5.2	-	3.83	3.75	3.50
5.8	a	3.45	3.76	3.66
6.1	-	3.64	3.47	3.12
6.3	a	3.48	3.55	3.19
7.0	a	3.32	3.72	3.54
7.4	a	3.78	3.80	3.28

To monitor the change in ϵ'_r of moist soil samples, the following procedure is adopted. 5 ml of water is added to 20 ml of soil (volumetric water content, $\theta_v=20\%$). The experiment is repeated for all nine samples using free-space transmission method and the corresponding phase-variation is observed. The values of ϵ'_r of the moist samples are computed using Equation 4.1.

The procedure is repeated with 6 ml and 8 ml of water ($\theta_v=23.1\%$ and 28.6% respectively). For both the additions, the corresponding values of ϵ'_r are computed in a similar manner. The measurements are carried out in all the three frequency bands (L, S & C) and ϵ'_r is computed. Tables 4.4, 4.5 and 4.6 show the computed values of ϵ'_r for the nine select samples at the three frequencies.

Table 4.4: Dielectric constant of soil sample for varying moisture content; **L-band** ($f_r=1.85$ GHz); Free-space Transmission Method

Soil		ϵ'_r (dry soil)	ϵ'_r (moist soil)		
pH	Sample		$\theta_v=20\%$	$\theta_v=23.1\%$	$\theta_v=28.6\%$
4.7	a	3.98	13.61	15.63	19.61
4.9	a	3.62	13.06	15.04	18.90
5.0	a	3.79	13.32	15.31	19.23
5.2	-	3.83	13.38	15.38	19.31
5.8	a	3.45	12.81	14.75	18.57
6.1	-	3.64	13.09	15.07	18.94
6.3	a	3.48	12.86	14.81	18.62
7.0	a	3.32	12.62	14.55	18.31
7.4	a	3.78	13.31	15.30	19.21

Table 4.5: Dielectric constant of soil sample for varying moisture content; **S-band** ($f_r=2.45$ GHz); Free-space Transmission Method

Soil		ϵ'_r (dry soil)	ϵ'_r (moist soil)		
pH	Sample		$\theta_v=20\%$	$\theta_v=23.1\%$	$\theta_v=28.6\%$
4.7	a	3.90	13.49	15.50	19.45
4.9	a	3.43	12.78	14.73	18.53
5.0	a	3.53	12.93	14.89	18.73
5.2	-	3.75	13.26	15.25	19.15
5.8	a	3.76	13.27	15.27	19.17
6.1	-	3.47	12.84	14.79	18.61
6.3	a	3.55	12.97	14.92	18.76
7.0	a	3.72	13.22	15.20	19.10
7.4	a	3.80	13.34	15.33	19.25

Table 4.6: Dielectric constant of soil sample for varying moisture content; **C-band** ($f_r=5.52$ GHz); Free-space Transmission Method

Soil		ϵ'_r (dry soil)	ϵ'_r (moist soil)		
pH	Sample		$\theta_v=20$ %	$\theta_v=23.1$ %	$\theta_v=28.6$ %
4.7	a	3.82	13.37	15.38	19.32
4.9	a	3.31	12.60	14.53	18.31
5.0	a	3.25	12.52	14.44	18.20
5.2	-	3.51	12.89	14.85	18.70
5.8	a	3.43	13.13	15.11	18.99
6.1	-	3.12	12.33	14.25	17.95
6.3	a	3.20	12.45	14.36	18.09
7.0	a	3.31	12.96	14.92	18.77
7.4	a	3.28	12.57	14.51	18.27

From Tables 4.4 to 4.6, it is evident that as MC increases, ϵ'_r of the soil-moisture mixture also increases. There is also an appreciable decrease in ϵ'_r as frequency changes from the L to the C band, as reported by (Zivkovic and Murk, 2012).

4.2.4 Validation of the experimental results using Topp's Equation

Volumetric Water Content, θ_v of all nine soil samples in the dry and added moisture states for the three frequency bands is computed using Topp's Equation (given in Section 1.5 reproduced here for reference).

$$\theta_v = 4.3 \times 10^{-6} \times \epsilon_r'^3 - 5.5 \times 10^{-4} \times \epsilon_r'^2 + 2.92 \times 10^{-2} \times \epsilon_r' - 5.3 \times 10^{-2} \quad (4.2)$$

To validate the methodology adopted and the results obtained thus far, the Volumetric Water Content, θ_v 's corresponding to the computed ϵ_r' are determined for the three moisture content levels (20 %, 23.1 % and 28.6

%) for the nine samples at the three frequencies. The error, expressed as a percentage, between actual and experimentally-evaluated values of moisture content levels is calculated. Tables 4.7 to 4.15 show the error percentage for all the moisture content levels and the three frequency bands, where;

ϵ'_{r1} - Dielectric constant of dry soil sample, computed using eqn. 4.1

θ_{v1} - Volumetric water content of dry soil sample (inherent), computed using eqn. 4.2

ϵ'_{r2} - Dielectric constant of soil sample, computed using eqn. 4.1, for added moisture

θ_{v2} - Volumetric water content of soil sample, computed using eqn. 4.2, for added moisture

θ_{v3} - Volumetric water content of soil sample for added moisture + θ_{v1}

$$\text{error \%} = \frac{(\theta_{v3} - \theta_{v2})}{\theta_{v3}} \times 100$$

For example, the error percentage is calculated for the 20 % moisture case for pH=4.7a, as $\frac{(20+5.477)-25.337}{(20+5.477)} = 0.55\%$.

Table 4.7: Error percentage between actual and experimentally-evaluated values of θ_v for **20 %** moisture content; **L-band**; Free-space Transmission Method

Soil		ϵ'_{r1}	θ_{v1}	ϵ'_{r2}	θ_{v2}	θ_{v3}	error %
pH	Sample						
4.7	a	3.98	5.477	13.61	25.337	25.477	0.55
4.9	a	3.62	4.570	13.06	24.412	24.570	0.64
5.0	a	3.79	5.000	13.32	24.852	25.000	0.59
5.2	-	3.83	5.101	13.38	24.953	25.101	0.59
5.8	a	3.45	4.137	12.81	23.984	24.137	0.63
6.1	-	3.64	4.621	13.09	24.463	24.621	0.64
6.3	a	3.48	4.214	12.86	24.070	24.214	0.59
7.0	a	3.32	3.804	12.62	23.655	23.804	0.63
7.4	a	3.78	4.975	13.31	24.836	24.975	0.56

Table 4.8: Error percentage between actual and experimentally-evaluated values of θ_v for **23.1 %** moisture content; **L-band**; Free-space Transmission Method

Soil		ϵ'_{r1}	θ_{v1}	ϵ'_{r2}	θ_{v2}	θ_{v3}	error %
pH	Sample						
4.7	a	3.98	5.477	15.63	28.545	28.577	0.11
4.9	a	3.62	4.570	15.04	27.639	27.670	0.11
5.0	a	3.79	5.000	15.31	28.057	28.100	0.15
5.2	-	3.83	5.101	15.38	28.164	28.201	0.13
5.8	a	3.45	4.137	14.75	27.186	27.237	0.19
6.1	-	3.64	4.621	15.07	27.685	27.721	0.13
6.3	a	3.48	4.214	14.81	27.279	27.314	0.13
7.0	a	3.32	3.804	14.55	26.867	26.904	0.14
7.4	a	3.78	4.975	15.30	28.041	28.075	0.12

Table 4.9: Error percentage between actual and experimentally-evaluated values of θ_v for **28.6 %** moisture content; **L-band**; Free-space Transmission Method

Soil		ϵ'_{r1}	θ_{v1}	ϵ'_{r2}	θ_{v2}	θ_{v3}	error %
pH	Sample						
4.7	a	3.98	5.477	19.61	34.053	34.079	0.08
4.9	a	3.62	4.570	18.90	33.144	33.170	0.08
5.0	a	3.79	5.000	19.23	33.571	33.600	0.09
5.2	-	3.83	5.101	19.31	33.673	33.701	0.08
5.8	a	3.45	4.137	18.57	32.712	32.737	0.08
6.1	-	3.64	4.621	18.94	33.197	33.221	0.07
6.3	a	3.48	4.214	18.62	32.778	32.814	0.11
7.0	a	3.32	3.804	18.31	32.366	32.404	0.12
7.4	a	3.78	4.975	19.21	33.545	33.575	0.09

Table 4.10: Error percentage between actual and experimentally-evaluated values of θ_v for **20 %** moisture content; **S-band**; Free-space Transmission Method

Soil		ϵ'_{r1}	θ_{v1}	ϵ'_{r2}	θ_{v2}	θ_{v3}	error %
pH	Sample						
4.7	a	3.90	5.277	13.49	25.138	25.277	0.55
4.9	a	3.43	4.086	12.78	23.932	24.086	0.64
5.0	a	3.53	4.341	12.93	24.190	24.341	0.62
5.2	-	3.75	4.899	13.26	24.751	24.899	0.59
5.8	a	3.76	4.924	13.27	24.768	24.924	0.63
6.1	-	3.47	4.188	12.84	24.035	24.188	0.63
6.3	a	3.55	4.392	12.97	24.258	24.392	0.55
7.0	a	3.72	4.823	13.22	24.684	24.823	0.56
7.4	a	3.80	5.025	13.34	24.886	25.025	0.56

Table 4.11: Error percentage between actual and experimentally-evaluated values of θ_v for **23.1 %** moisture content; **S-band**; Free-space Transmission Method

Soil		ϵ'_{r1}	θ_{v1}	ϵ'_{r2}	θ_{v2}	θ_{v3}	error %
pH	Sample						
4.7	a	3.90	5.277	15.50	28.348	28.377	0.10
4.9	a	3.43	4.086	14.73	27.152	27.186	0.13
5.0	a	3.53	4.341	14.89	27.404	27.441	0.13
5.2	-	3.75	4.899	15.25	27.964	27.999	0.13
5.8	a	3.76	4.924	15.27	27.995	28.024	0.10
6.1	-	3.47	4.188	14.79	27.247	27.288	0.15
6.3	a	3.55	4.392	14.92	27.451	27.492	0.15
7.0	a	3.72	4.823	15.20	27.887	27.923	0.13
7.4	a	3.80	5.025	15.33	28.087	28.125	0.14

Table 4.12: Error percentage between actual and experimentally-evaluated values of θ_v for **28.6 %** moisture content; **S-band**; Free-space Transmission Method

Soil		ϵ'_{r1}	θ_{v1}	ϵ'_{r2}	θ_{v2}	θ_{v3}	error %
pH	Sample						
4.7	a	3.90	5.277	19.45	33.851	33.877	0.08
4.9	a	3.43	4.086	18.53	32.659	32.686	0.08
5.0	a	3.53	4.341	18.73	32.922	32.941	0.06
5.2	-	3.75	4.899	19.15	33.468	33.499	0.09
5.8	a	3.76	4.924	19.17	33.494	33.524	0.09
6.1	-	3.47	4.188	18.61	32.764	32.788	0.07
6.3	a	3.55	4.392	18.76	32.962	32.992	0.09
7.0	a	3.72	4.823	19.10	33.404	33.423	0.06
7.4	a	3.80	5.025	19.25	33.596	33.625	0.09

Table 4.13: Error percentage between actual and experimentally-evaluated values of θ_v for **20 %** moisture content; **C-band**; Free-space Transmission Method

Soil		ϵ'_{r1}	θ_{v1}	ϵ'_{r2}	θ_{v2}	θ_{v3}	error %
pH	Sample						
4.7	a	3.82	5.076	13.37	24.936	25.076	0.56
4.9	a	3.31	3.778	12.60	23.620	23.778	0.66
5.0	a	3.25	3.624	12.52	23.481	23.624	0.61
5.2	-	3.51	4.290	12.89	24.121	24.290	0.70
5.8	a	3.43	4.086	13.13	24.531	24.086	1.85
6.1	-	3.12	3.288	12.33	23.148	23.288	0.60
6.3	a	3.20	3.495	12.45	23.359	23.495	0.54
7.0	a	3.31	3.778	12.96	24.241	23.778	1.95
7.4	a	3.28	3.701	12.57	23.568	23.701	0.56

Table 4.14: Error percentage between actual and experimentally-evaluated values of θ_v for **23.1 %** moisture content; **C-band**; Free-space Transmission Method

Soil		ϵ'_{r1}	θ_{v1}	ϵ'_{r2}	θ_{v2}	θ_{v3}	error %
pH	Sample						
4.7	a	3.82	5.076	15.38	28.164	28.176	0.04
4.9	a	3.31	3.778	14.53	26.835	26.878	0.16
5.0	a	3.25	3.624	14.44	26.691	26.724	0.12
5.2	-	3.51	4.290	14.85	27.341	27.390	0.18
5.8	a	3.43	4.086	15.11	27.747	27.186	2.06
6.1	-	3.12	3.288	14.25	26.386	26.388	0.01
6.3	a	3.20	3.495	14.36	26.563	26.595	0.12
7.0	a	3.31	3.778	14.92	27.451	26.878	2.13
7.4	a	3.28	3.701	14.51	26.803	26.801	0.01

Table 4.15: Error percentage between actual and experimentally-evaluated values of θ_v for **28.6 %** moisture content; **C-band**; Free-space Transmission Method

Soil		ϵ'_{r1}	θ_{v1}	ϵ'_{r2}	θ_{v2}	θ_{v3}	error %
pH	Sample						
4.7	a	3.82	5.076	19.32	33.686	33.676	0.03
4.9	a	3.31	3.778	18.31	32.366	32.378	0.04
5.0	a	3.25	3.624	18.20	32.218	32.224	0.02
5.2	-	3.51	4.290	18.70	32.883	32.890	0.02
5.8	a	3.43	4.086	18.99	33.261	32.686	1.76
6.1	-	3.12	3.288	17.95	31.880	31.888	0.03
6.3	a	3.20	3.495	18.09	32.070	32.095	0.08
7.0	a	3.31	3.778	18.77	32.978	32.378	1.85
7.4	a	3.28	3.701	18.27	32.312	32.301	0.03

Validation results show that the error in the computed volumetric water content, θ_{v1} , in comparison with the actual θ_{v1} is very less. The maximum error percentage is found to be 2.13 % (Table 4.14). Thus the free-space transmission method is valid for moisture-content monitoring in soil characterization. Therefore, the method can be extended for the computation of ϵ'_r of soil samples mixed with various types and concentration of fertilizers, as described in Section 4.3.

4.2.5 ANN Model for Volumetric Water Content Estimation

The previous section discussed the estimation of Moisture Content in different soil samples at the L, S and C bands using the free-space transmission method. Moisture Content is evaluated in terms of Volumetric Water Content, expressed as a percentage and denoted as θ_v . The experimental results are validated using Topp's Equation. This section presents a neural network-based methodology to estimate θ_v in soil at the three bands.

A multilayered artificial neural network, using the Levenberg-Marquardt algorithm, is used as the model. In the proposed model, a single feed-forward ANN structure, whose architecture is shown in Fig. 4.21 is used.

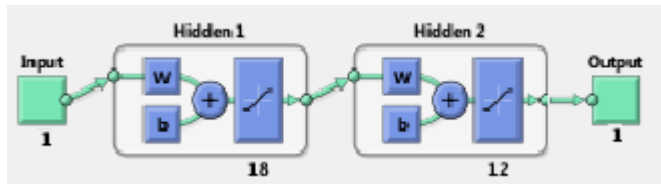


Figure 4.21: ANN structure for θ_v estimation; Free-space Transmission Method

It has 2 hidden layers having 18 and 12 neurons respectively. The input data for training the model consists of the experimentally computed values of ϵ'_r of each dry soil sample and at all θ_v 's. The target

consists of the corresponding θ_v , expressed in percentage, computed using Topp's Equation. To estimate the value of θ_v of the soil sample at hand, the computed value of ϵ_r' is given as input to the ANN model. Training and testing procedure is carried out using MATLAB[®]. Percentage of data-set used for training, validation & testing are respectively 84, 12 & 4 %. Fig. 4.22 illustrates the procedure using a flowchart.

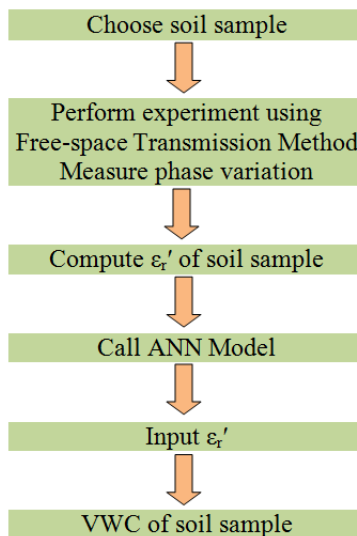


Figure 4.22: Flowchart of ANN Model for estimation of Volumetric Water Content, θ_v ; Free-space Transmission Method

Result pertaining to the select nine dry samples is shown in Table 4.16 for the L-band. It shows the error, expressed as a percentage, between the values of θ_v computed using Eqn. 4.2 and evaluated using the ANN model. Tables 4.17 to 4.19 show similar results for the three moisture contents. Similarly, Tables 4.20 to 4.27 show results for the S and C bands.

Table 4.16: Percentage error in the computed and evaluated values of θ_v for **dry samples; L-band**; Free-space Transmission Method & ANN Model

Soil		ϵ'_r	θ_v %		Error %
pH	Sample		Computed	Evaluated	
4.7	a	3.98	5.477	5.478	0.018
4.9	a	3.62	4.570	4.577	0.153
5.0	a	3.79	5.000	4.998	0.040
5.2	-	3.83	5.101	5.100	0.200
5.8	a	3.45	4.137	4.140	0.073
6.1	-	3.64	4.621	4.619	0.043
6.3	a	3.48	4.214	4.215	0.024
7.0	a	3.32	3.804	3.807	0.079
7.4	a	3.78	4.975	4.977	0.040

Table 4.17: Percentage error in the computed and evaluated values of θ_v for **20 %** moisture content; **L-band**; Free-space Transmission Method & ANN Model

Soil		ϵ'_r	θ_v %		Error %
pH	Sample		Computed	Evaluated	
4.7	a	13.61	25.337	25.336	0.004
4.9	a	13.06	24.412	24.413	0.004
5.0	a	13.32	24.852	24.853	0.004
5.2	-	13.38	24.953	24.955	0.008
5.8	a	12.81	23.984	23.986	0.008
6.1	-	13.09	24.463	24.462	0.004
6.3	a	12.86	24.070	24.100	0.125
7.0	a	12.62	23.655	23.559	0.406
7.4	a	13.31	24.836	24.890	0.217

Table 4.18: Percentage error in the computed and evaluated values of θ_v for **23.1 %** moisture content; **L-band**; Free-space Transmission Method & ANN Model

Soil		ϵ'_r	θ_v %		Error %
pH	Sample		Computed	Evaluated	
4.7	a	15.63	28.545	28.539	0.021
4.9	a	15.04	27.639	27.637	0.007
5.0	a	15.31	28.057	28.064	0.025
5.2	-	15.38	28.164	28.161	0.011
5.8	a	14.75	27.186	27.182	0.007
6.1	-	15.07	27.685	27.684	0.004
6.3	a	14.81	27.279	27.198	0.297
7.0	a	14.55	26.867	26.862	0.019
7.4	a	15.30	28.041	28.034	0.025

Table 4.19: Percentage error in the computed and evaluated values of θ_v for **28.6 %** moisture content; **L-band**; Free-space Transmission Method & ANN Model

Soil		ϵ'_r	θ_v %		Error %
pH	Sample		Computed	Evaluated	
4.7	a	19.61	34.053	34.062	0.026
4.9	a	18.90	33.144	33.129	0.045
5.0	a	19.23	33.571	33.564	0.021
5.2	-	19.31	33.673	33.569	0.309
5.8	a	18.57	32.712	32.682	0.092
6.1	-	18.94	33.197	33.189	0.024
6.3	a	18.62	32.778	32.798	0.061
7.0	a	18.31	32.366	32.354	0.037
7.4	a	19.21	33.545	33.525	0.060

Table 4.20: Percentage error in the computed and evaluated values of θ_v for **dry samples; S-band; Free-space Transmission Method & ANN Model**

Soil		ϵ'_r	θ_v %		Error %
pH	Sample		Computed	Evaluated	
4.7	a	3.90	5.277	5.268	0.171
4.9	a	3.43	4.086	4.081	0.122
5.0	a	3.53	4.341	4.344	0.069
5.2	-	3.75	4.899	4.897	0.041
5.8	a	3.76	4.924	4.927	0.061
6.1	-	3.47	4.188	4.184	0.096
6.3	a	3.55	4.392	4.391	0.023
7.0	a	3.72	4.823	4.829	0.124
7.4	a	3.80	5.025	5.020	0.100

Table 4.21: Percentage error in the computed and evaluated values of θ_v for **20 % moisture content; S-band; Free-space Transmission Method & ANN Model**

Soil		ϵ'_r	θ_v %		Error %
pH	Sample		Computed	Evaluated	
4.7	a	13.49	25.138	25.129	0.036
4.9	a	12.78	23.932	23.926	0.025
5.0	a	12.93	24.190	24.200	0.041
5.2	-	13.26	24.751	24.758	0.028
5.8	a	13.27	24.768	24.759	0.036
6.1	-	12.84	24.035	24.039	0.017
6.3	a	12.97	24.258	24.251	0.029
7.0	a	13.22	24.684	24.682	0.008
7.4	a	13.34	24.886	24.778	0.434

Table 4.22: Percentage error in the computed and evaluated values of θ_v for **23.1 %** moisture content; **S-band**; Free-space Transmission Method & ANN Model

Soil		ϵ'_r	θ_v %		Error %
pH	Sample		Computed	Evaluated	
4.7	a	15.50	28.348	28.347	0.004
4.9	a	14.73	27.152	27.151	0.004
5.0	a	14.89	27.404	27.409	0.018
5.2	-	15.25	27.964	27.960	0.014
5.8	a	15.27	27.995	27.992	0.011
6.1	-	14.79	27.247	27.246	0.004
6.3	a	14.92	27.451	27.453	0.007
7.0	a	15.20	27.887	27.882	0.018
7.4	a	15.33	28.087	28.079	0.028

Table 4.23: Percentage error in the computed and evaluated values of θ_v for **28.6 %** moisture content; **S-band**; Free-space Transmission Method & ANN Model

Soil		ϵ'_r	θ_v %		Error %
pH	Sample		Computed	Evaluated	
4.7	a	19.45	33.851	33.849	0.006
4.9	a	18.53	32.659	32.653	0.018
5.0	a	18.73	32.922	32.924	0.006
5.2	-	19.15	33.468	32.466	0.006
5.8	a	19.17	33.494	33.492	0.006
6.1	-	18.61	32.764	32.766	0.006
6.3	a	18.76	32.962	32.963	0.003
7.0	a	19.10	33.404	34.402	0.006
7.4	a	19.25	33.596	33.597	0.003

Table 4.24: Percentage error in the computed and evaluated values of θ_v for **dry samples; C-band**; Free-space Transmission Method & ANN Model

Soil		ϵ'_r	θ_v %		Error %
pH	Sample		Computed	Evaluated	
4.7	a	3.82	5.076	5.077	0.019
4.9	a	3.31	3.778	3.774	0.106
5.0	a	3.25	3.624	3.625	0.027
5.2	-	3.51	4.290	4.290	0.0
5.8	a	3.43	4.086	4.081	0.122
6.1	-	3.12	3.288	3.287	0.030
6.3	a	3.20	3.495	3.494	0.029
7.0	a	3.31	3.778	3.774	0.106
7.4	a	3.28	3.701	3.701	0.0

Table 4.25: Percentage error in the computed and evaluated values of θ_v for **20 % moisture content; C-band**; Free-space Transmission Method & ANN Model

Soil		ϵ'_r	θ_v %		Error %
pH	Sample		Computed	Evaluated	
4.7	a	13.37	24.936	24.937	0.004
4.9	a	12.60	23.620	23.623	0.013
5.0	a	12.52	23.481	23.57	0.379
5.2	-	12.89	24.121	24.13	0.037
5.8	a	13.13	24.531	24.532	0.004
6.1	-	12.33	24.148	24.147	0.004
6.3	a	12.45	23.359	23.358	0.004
7.0	a	12.96	24.241	24.243	0.008
7.4	a	12.57	23.568	23.482	0.365

Table 4.26: Percentage error in the computed and evaluated values of θ_v for **23.1 %** moisture content; **C-band**; Free-space Transmission Method & ANN Model

Soil		ϵ'_r	θ_v %		Error %
pH	Sample		Computed	Evaluated	
4.7	a	15.38	28.164	28.162	0.007
4.9	a	14.53	26.835	26.836	0.004
5.0	a	14.44	26.691	26.685	0.022
5.2	-	14.85	27.341	27.412	0.260
5.8	a	15.11	27.747	27.749	0.007
6.1	-	14.25	26.386	26.388	0.008
6.3	a	14.36	26.563	26.561	0.008
7.0	a	14.92	27.451	27.450	0.004
7.4	a	14.51	26.803	26.692	0.414

Table 4.27: Percentage error in the computed and evaluated values of θ_v for **28.6 %** moisture content; **C-band**; Free-space Transmission Method & ANN Model

Soil		ϵ'_r	θ_v %		Error %
pH	Sample		Computed	Evaluated	
4.7	a	19.32	33.686	33.688	0.006
4.9	a	18.31	32.366	32.367	0.003
5.0	a	18.20	32.218	32.220	0.006
5.2	-	18.70	32.883	32.841	0.128
5.8	a	18.99	33.261	33.264	0.009
6.1	-	17.95	31.880	31.881	0.003
6.3	a	18.09	32.070	32.080	0.031
7.0	a	18.77	32.978	32.975	0.009
7.4	a	18.27	32.312	32.219	0.288

Results in Tables 4.16 to 4.27 show that the error in the computed and evaluated values of θ_v for the nine select soil samples for varying moisture content in the three frequency bands is very less. The maximum error percentage is found to be 0.414 % (Table 4.26).

A Graphical User Interface (GUI), developed using MATLAB[®] to make the program user-friendly is shown in Fig. 4.23. A screen-shot of the evaluated θ_v % for the four moisture content cases of the seven acidic soil samples considered in the C-band (Tables 4.24 to 4.27, column 5) is shown in Fig. 4.24.

Thus the free-space transmission method is validated for moisture-content monitoring of soil using ANN model.

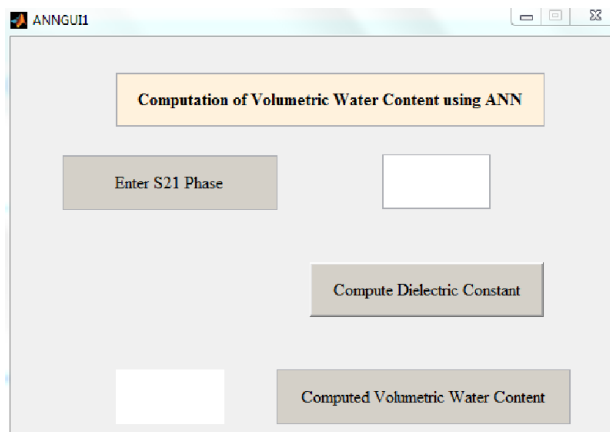


Figure 4.23: GUI used for θ_v estimation; ANN Model; Free-space Transmission Method

```

>> test1

outputs =

Columns 1 through 7

    5.0769    24.9373    28.1622    33.6877    3.7741    23.6229    26.8358

Columns 8 through 14

    32.3673    3.6247    23.5703    26.6848    32.2201    4.2904    24.1292

Columns 15 through 21

    27.4122    32.8413    4.0807    24.5324    27.7493    33.2638    3.2867

Columns 22 through 28

    23.1473    26.3884    31.8810    3.4941    23.3584    26.5612    32.0804

```

Figure 4.24: Screen-shot of evaluated θ_v , %; C-band; ANN Model; Free-space Transmission Method

4.2.6 Moisture detection using Colour-mapping

An imaging technique for colour-mapping of materials was discussed in Chapter 2 for detecting embedded objects. With this, a characteristic signature of the material can be drawn with the mapped microwave parameters and corresponding constituents. A method for imaging the presence of a metal disc in a sample of soil was also presented. The simulation setup involved a patch antenna radiating onto the disc-embedded soil sample taken in a container. A sensor-probe was used for scanning 25 locations, arranged along 5×5 equally-spaced points. The disc to be detected was placed at different positions and imaged by positioning the probe at the 25 observation points.

In Section 4.2.3, the setup of the free-space transmission method consisting of a pair of Microstrip Patch Antennas was presented. Sample-holder filled with soil samples was placed between the antennas connected to the VNA. Transmission coefficient (S_{21}) was found. A similar arrangement, with the receiving antenna replaced by a

sensor-probe, is now presented for water detection. Suitability of the arrangement in detecting the presence of water in soil is tested. Water is added at 2 locations using a syringe. Variation in S_{21} for added water at various distinct and equally-spaced locations is noted. Using the probe, S_{21} at 16 different points is measured using the VNA, by scanning 4 points each along rows and columns. The values of S_{21} are:

$$\begin{bmatrix} -42.35 & -51.32 & -42.35 & -42.35 \\ -48.65 & -56.76 & -50.25 & -50.36 \\ -43.45 & -51.45 & -50.36 & -56.76 \\ -42.35 & -42.35 & -48.12 & -47.30 \end{bmatrix}$$

An image is constructed with the 16 values of S_{21} using MATLAB[®]. From this image, a conclusion regarding the locations of moisture in the soil sample is drawn. The experimental setup is shown in Fig. 4.25. Illustrative result along with a camera-shot of the holder with moisture is shown in Fig. 4.26. Fig. 4.27 shows the result of a similar procedure with a 5×5 scanning with water injected at one location. The 25 values of S_{21} obtained in this case are:

$$\begin{bmatrix} -45.45 & -47.30 & -48.12 & -48.12 & -48.12 \\ -45.45 & -47.30 & -50.36 & -54.25 & -50.36 \\ -45.45 & -45.45 & -48.12 & -50.36 & -48.12 \\ -45.45 & -45.45 & -47.30 & -48.12 & -47.30 \\ -45.45 & -45.45 & -45.45 & -45.45 & -45.45 \end{bmatrix}$$

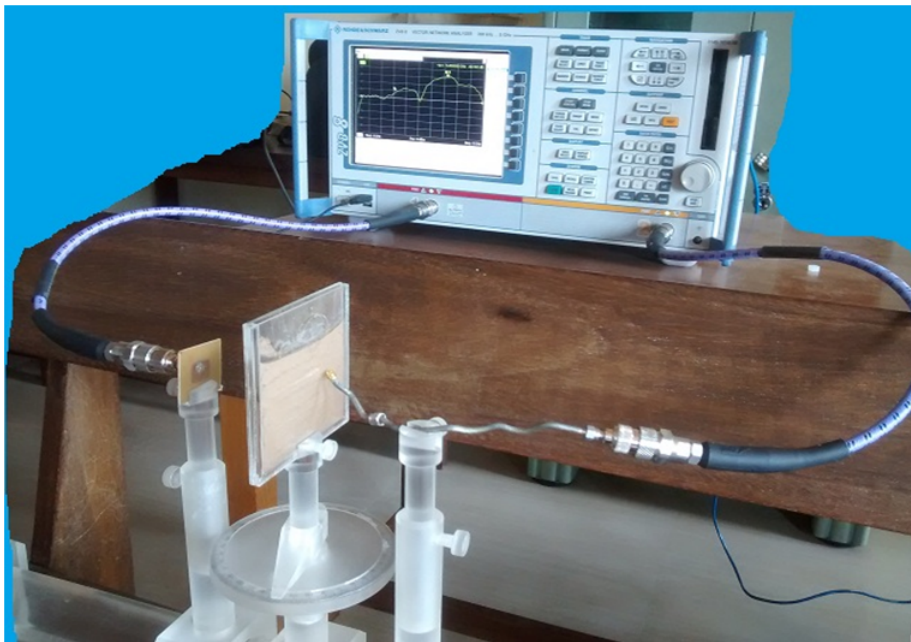
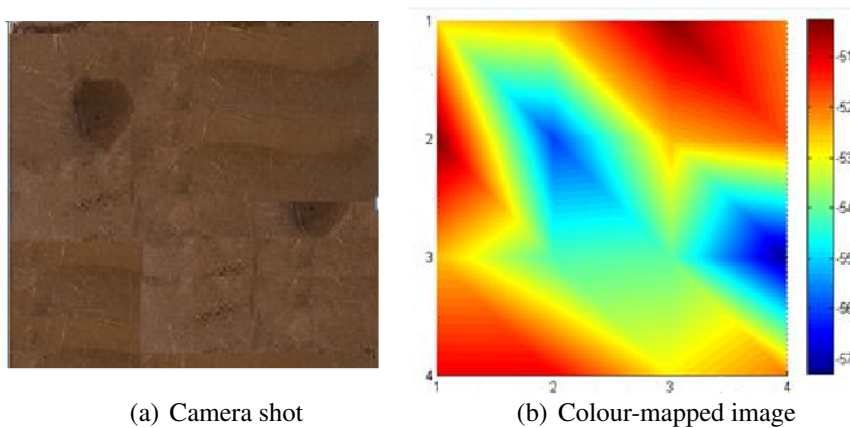


Figure 4.25: Experimental setup of free-space transmission method with MPA as transmit antenna and probe as receiver



(a) Camera shot

(b) Colour-mapped image

Figure 4.26: S_{21} mapping of 2 moist locations in soil with 16 scanning points; Free-space Transmission Method & Colour-mapping

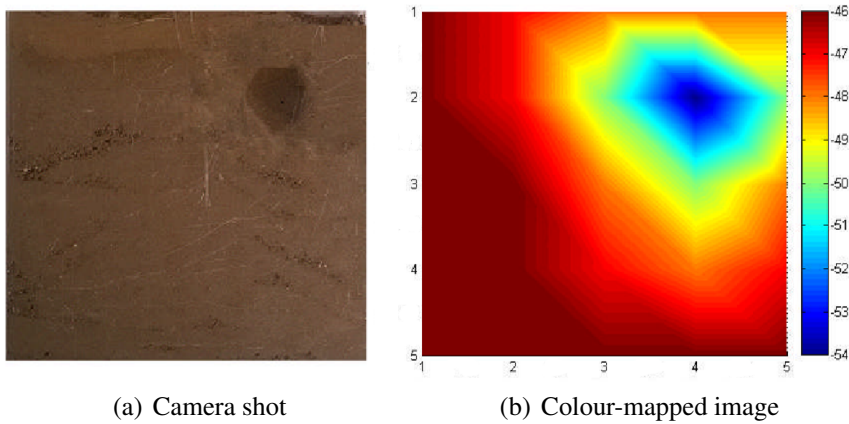


Figure 4.27: S_{21} mapping of 1 moist location in soil with 25 scanning points; Free-space Transmission Method & Colour-mapping

Results show that colour-mapping can be used as a tool for soil-moisture detection. Increase in the number of observation points improves the resolution of the colour-mapping, leading to better spotting of moist locations.

4.3 Estimation of Fertilizer Concentration

Water has a strong influence on the dielectric properties of soil at microwave frequencies. For agricultural purposes, variation in the concentration of fertilizers is considered as important as moisture content. Different levels of fertilizers give rise to a large variation in the dielectric constant of soil. Thus, knowledge of the variation of the dielectric constant of soil with fertilizers is necessary for their efficient use in soil. Microwave sensing of soil properties in the presence of moisture and fertilizers has thus evolved as a major need of the hour. Moreover, soil testing as a tool for judicious fertilizer recommendation has assumed great relevance. The following section discusses the experimental setup and methodology used for the measurement of dielectric constant of soil-fertilizer mixture and the ensuing results.

The objective of this work is to compute ϵ'_r of soil samples mixed with common fertilizers using microwave free-space transmission method. It is informed by the providers of the soil samples under test that proper extractants have been used to ensure that elements such as phosphorus, potassium, sodium, magnesium, calcium, sulphur, manganese, copper, zinc etc, which are the essential constituents of common fertilizers, are chemically removed from the soil samples. To confirm the absence of mineral constituents in the soil samples, quantitative analysis is conducted at the Sophisticated Analytical Instruments Facility attached to the Sophisticated Test and Instrumentation Centre (STIC) of Cochin University of Science and Technology. X-ray powder diffraction technique, one of the widely used methods (Moore and Reynolds Jr., 1999) for the identification of unknown crystalline materials and determination of amounts of minerals, is reportedly used by STIC. Result of the analysis detailing the constitution of soil samples is given in Table 4.28. It reveals that no traces of standard fertilizers or any of their compounds are present in the soil samples, as guaranteed by the providers. Thus additional mixing of these fertilizers is purposely done for experimentation to detect their presence in soil.

4.3.1 Soil samples and Fertilizers used

The soil samples under test are the same as mentioned in Section 4.2.1.

The fertilizers used are Powdered Boric Acid (PBA), a mixture of Nitrogen, Phosphorus and Potassium (NPK), Potash and Urea, which are commonly used in agriculture.

Table 4.28: Constituents of soil samples under test;
Results courtesy : Sophisticated Test and Instrumentation Centre
(STIC), CUSAT

Type of Soil	Andesine [(Na Ca)AlSiO ₈]	Feldspar [KAlSi ₃ O ₈]	Tschernichite [(Ca Na)(Si ₆ Al ₂) O ₁₆ 4(H ₂ O)]	Quartz [SiO ₂]	Kaolinite [Al ₂ Si ₂ O ₅ (OH) ₄]
Acidic pH=4.7(a,b), 4.9(a,b) 5(a,b,c), 5.1, 5.2	Present	Present	Absent	Absent	Absent
Acidic pH=5.3(a,b), 5.4, 5.7 5.8(a,b), 5.9, 6.1	Absent	Absent	Absent	Present	Present
Acidic pH=6.2(a-f), 6.3(a,b) 6.4(a-f)	Absent	Present	Absent	Absent	Present
Alkaline pH=7.0(a-c), 7.1(a-g) 7.2(a-e)	Present	Absent	Absent	Absent	Present
Alkaline pH=7.3(a-h), 7.4(a-c) 7.5(a-e)	Absent	Present	Absent	Present	Absent
White	Absent	Present	Present	Present	Absent
Red	Absent	Absent	Present	Present	Present
Black	Absent	Present	Present	Absent	Absent

4.3.2 Experimental Results

Two different cases are taken up for study:

1. Nine out of the 62 different soil samples as given in Table 4.1 are considered. pH of these samples are 4.7, 4.9, 5.0, 5.2, 5.8, 6.1, 6.3, 7.0 and 7.4. All the samples are dry, powdered and fertilizer-extracted
2. 20 ml of these samples are individually mixed with 1 ml, 2 ml and 5 ml of the four fertilizers. 1 ml of fertilizer in 20 ml of soil gives a mixture-ratio of $1/21=4.8\%$; similarly the other two ratios are $2/22=9.1\%$ and $5/25=20\%$. The sample-mixtures are based on

the statistics provided by the Department of Agriculture, Kerala (Online, 2016).

The experimental setup is identical to the one used in Section 4.2.3. Both the cases are studied in the L, S and C bands.

Using eqn. 4.1, values of ϵ'_r are computed for both the cases at all the three frequencies. Results obtained are shown in Tables 4.29 to 4.31 for the four fertilizers.

Table 4.29: ϵ'_r of soil with varying fertilizer mixture ratio; **L-band**; Free-space Transmission Method

Sample No.	Plain soil (20 ml)			Mixture-ratio											
				PBA			NPK			Potash			Urea		
	pH	sample	ϵ'_r	4.8 %	9.1 %	20 %	4.8 %	9.1 %	20 %	4.8 %	9.1 %	20 %	4.8 %	9.1 %	20 %
1	4.7	a	3.98	9.15	9.26	9.34	3.94	4.05	4.19	4.26	4.31	4.35	4.28	4.35	4.69
2	4.9	a	3.62	7.41	7.50	7.57	2.80	2.83	2.86	3.47	3.51	3.84	3.86	3.97	4.16
3	5.0	a	3.79	7.63	7.72	7.79	3.68	3.87	3.90	3.64	3.75	4.08	3.89	3.97	4.22
4	5.2	-	3.83	8.23	8.33	8.40	3.69	3.79	3.94	3.99	4.12	4.65	4.17	4.21	4.84
5	5.8	a	3.45	8.72	8.82	8.90	3.89	3.93	4.26	4.18	4.48	4.81	3.96	4.04	4.47
6	6.1	-	3.64	7.30	7.39	7.45	2.69	2.72	2.85	3.88	4.08	4.31	3.81	3.98	4.24
7	6.3	a	3.48	7.64	7.74	7.81	3.47	3.59	3.93	3.98	4.18	4.49	3.77	3.97	4.29
8	7.0	a	3.32	8.10	8.20	8.27	3.70	3.84	4.17	3.90	3.98	4.28	3.94	4.09	4.62
9	7.4	a	3.78	8.26	8.36	8.43	3.90	4.14	4.77	4.28	4.49	4.67	3.91	4.15	4.48

Table 4.30: ϵ'_r of soil with varying fertilizer mixture ratio; **S-band**; Free-space Transmission Method

Sample No.	Plain soil (20 ml)			Mixture-ratio											
				PBA			NPK			Potash			Urea		
	pH	sample	ϵ'_r	4.8 %	9.1 %	20 %	4.8 %	9.1 %	20 %	4.8 %	9.1 %	20 %	4.8 %	9.1 %	20 %
1	4.7	a	3.90	7.79	7.93	8.05	4.02	4.15	4.84	4.22	4.30	4.36	3.98	4.05	4.34
2	4.9	a	3.43	6.46	6.58	6.67	2.76	3.07	3.42	3.37	3.53	3.58	3.84	3.94	4.20
3	5.0	a	3.53	6.81	6.93	7.03	3.18	3.24	3.58	3.41	3.71	3.76	3.67	3.86	4.16
4	5.2	-	3.75	7.28	7.41	7.52	3.45	3.51	3.76	3.95	4.02	4.08	3.97	4.13	4.38
5	5.8	a	3.76	7.48	7.61	7.73	3.54	3.60	3.86	4.04	4.11	4.17	3.85	3.99	4.27
6	6.1	-	3.47	6.64	6.76	6.86	2.50	3.16	3.80	3.68	3.61	3.67	3.57	3.73	4.14
7	6.3	a	3.55	6.93	7.05	7.16	3.27	3.33	3.98	3.74	3.81	3.86	3.62	3.88	4.08
8	7.0	a	3.72	7.11	7.24	7.34	3.36	3.42	3.77	3.83	3.90	3.96	3.98	4.13	4.31
9	7.4	a	3.80	7.62	7.76	7.87	3.64	3.71	4.11	4.12	4.19	4.26	3.66	3.71	3.99

Table 4.31: ϵ'_r of soil with varying fertilizer mixture ratio; **C-band**;
Free-space Transmission Method

Sample No.	Plain soil (20 ml)			Mixture-ratio											
				PBA			NPK			Potash			Urea		
	pH	sample	ϵ'_r	4.8 %	9.1 %	20 %	4.8 %	9.1 %	20 %	4.8 %	9.1 %	20 %	4.8 %	9.1 %	20 %
				ϵ'_r	ϵ'_r	ϵ'_r	ϵ'_r	ϵ'_r	ϵ'_r	ϵ'_r	ϵ'_r	ϵ'_r	ϵ'_r	ϵ'_r	ϵ'_r
1	4.7	a	3.82	5.59	5.67	5.74	3.92	3.95	4.30	4.13	4.19	4.24	3.88	4.06	4.29
2	4.9	a	3.30	4.90	4.97	5.03	3.45	3.47	3.91	3.22	3.68	3.72	3.69	3.74	4.11
3	5.0	a	3.25	5.19	5.26	5.32	3.03	3.68	3.99	3.50	3.89	3.94	3.38	3.61	3.86
4	5.2	-	3.50	5.29	5.36	5.43	3.82	4.24	4.79	3.92	3.97	4.02	3.77	3.85	4.11
5	5.8	a	3.66	4.91	4.98	5.04	3.86	4.21	4.75	3.57	3.62	3.66	3.62	3.79	4.19
6	6.1	-	3.12	4.98	5.05	5.11	3.40	3.52	3.96	3.55	3.73	3.78	3.48	3.56	3.94
7	6.3	a	3.19	4.85	4.92	4.98	3.85	4.01	4.44	3.56	3.61	3.65	3.43	3.52	3.86
8	7.0	a	3.54	4.64	4.70	4.76	3.86	4.20	4.54	3.37	3.42	3.46	3.55	3.72	3.98
9	7.4	a	3.28	5.33	5.40	5.47	3.41	3.76	3.98	3.92	3.97	4.02	3.51	3.76	3.89

Variation of ϵ'_r of the nine plain soil samples with varying pH value at the three frequencies is plotted in Fig. 4.28. It is seen that ϵ'_r decreases with increase in frequency for most samples, as reported in literature (Alex and Behari, 1996).

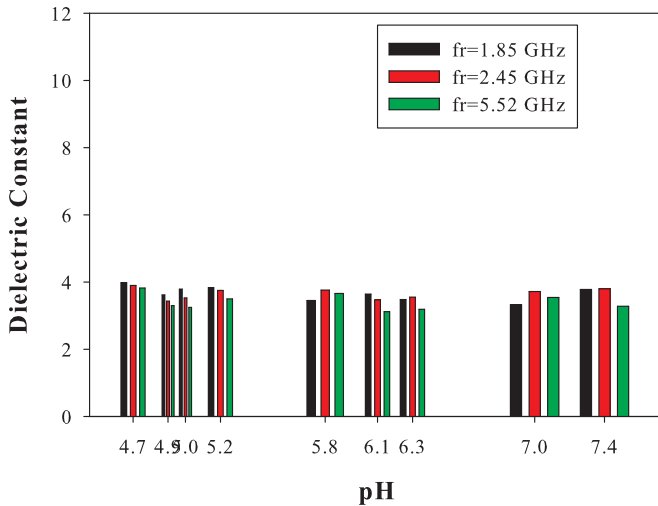


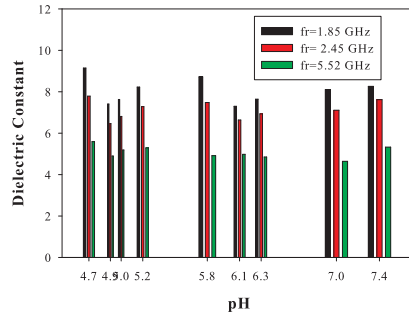
Figure 4.28: Dielectric constant of plain soil samples in the L, S & C bands; Free-space Transmission Method

Fig. 4.29 shows the variation of ϵ'_r of the nine soil samples (varying

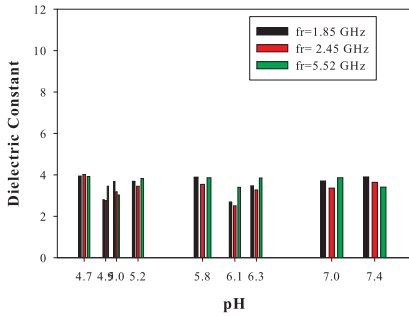
pH) with the four fertilizers added at a soil-fertilizer mixture-ratio of 4.8% at the three frequencies. Similar plots for soil-fertilizer mixture ratios of 9.1% and 20% are shown in Figs. 4.30 and 4.31 respectively. It is observed that as frequency increases from the L-band to the C-band, ϵ'_r of most soil samples decreases for any given soil-fertilizer mixture-ratio. For example, for soil with pH=4.7 (sample a), ϵ'_r decreases from 9.15 to 5.59 for the soil-PBA mixture, for a mixture-ratio of 4.8 %. It is also observed that ϵ'_r value is the largest for PBA-mixed soil samples for all mixture-ratios and at all the frequencies. This is to be expected as PBA has the highest ϵ'_r value and NPK, the lowest, as given in Table 4.32 (ClipperControls, 2015). It is further noted that variation of ϵ'_r with frequency is more for PBA-mixed soil than for other soil-fertilizer mixtures.

Table 4.32: Dielectric constant of common fertilizers

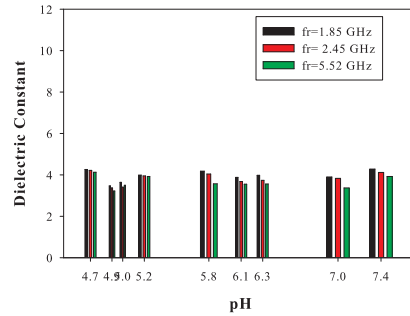
Fertilizer	Dielectric constant
Powdered Boric Acid, PBA	11.8
Nitrogen, N	1.5
Phosphorus, P	4.1
Potassium, K	5.0
Urea	3.5



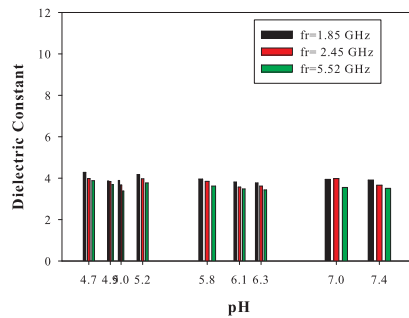
(a) PBA



(b) NPK

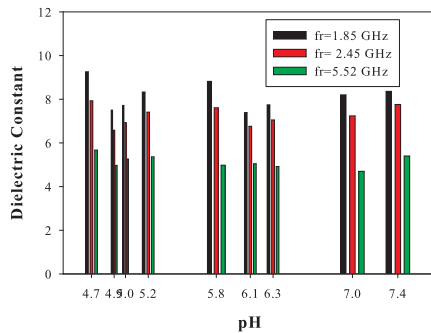


(c) Potash

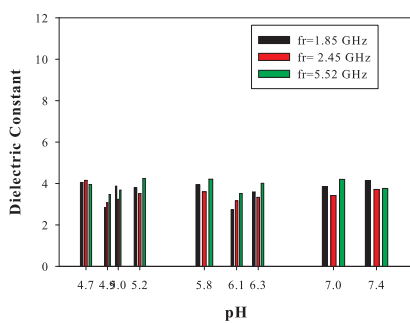


(d) Urea

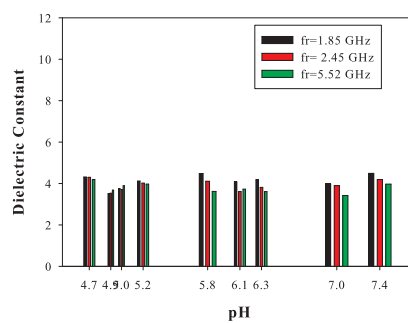
Figure 4.29: Variation of ϵ'_r with pH of the soil-fertilizer mixture-ratio of **4.8%** at the three frequencies; Free-space Transmission Method



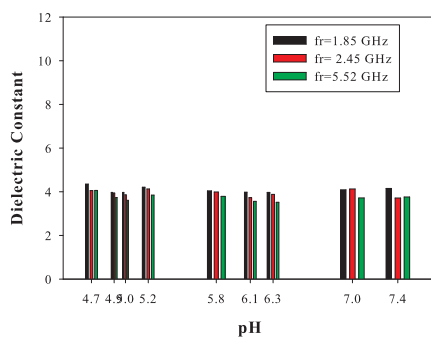
(a) PBA



(b) NPK

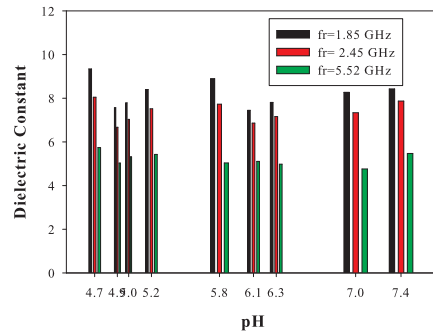


(c) Potash

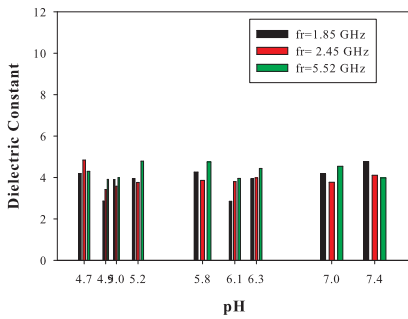


(d) Urea

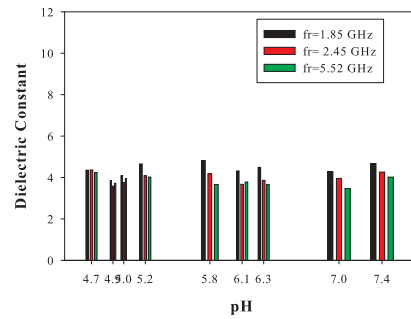
Figure 4.30: Variation of ϵ_r' with pH of the soil-fertilizer mixture-ratio of **9.1%** at the three frequencies; Free-space Transmission Method



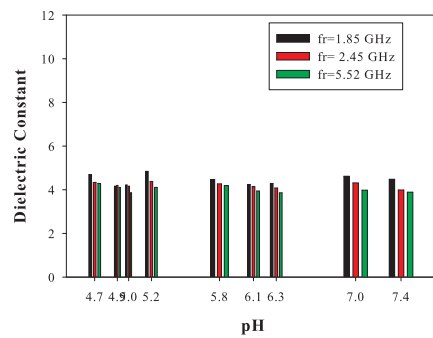
(a) PBA



(b) NPK



(c) Potash



(d) Urea

Figure 4.31: Variation of ϵ'_r with pH of the soil-fertilizer mixture-ratio of **20%** at the three frequencies; Free-space Transmission Method

Variation of ϵ'_r of the nine soil samples (varying pH) for different soil-fertilizer mixture-ratio of the four fertilizers (at all three frequencies) is plotted in Figs. 4.32 to 4.34. It is observed that for any given frequency, ϵ'_r value of all soil samples increases with increase in soil-fertilizer mixture-ratio. For example, for soil with pH=4.7 (sample a), ϵ'_r increases from 9.15 to 9.34 for the soil-PBA mixture, for an increase in mixture-ratio from 4.8 % to 20 % in the L-band (Table 4.29).

The dependence of ϵ'_r on the soil-fertilizer mixture-ratio for the nine select soil samples is illustrated in Figs. 4.35 and 4.36. It is noticed that as soil-fertilizer mixture-ratio increases from 4.8% to 20%, ϵ'_r also increases.

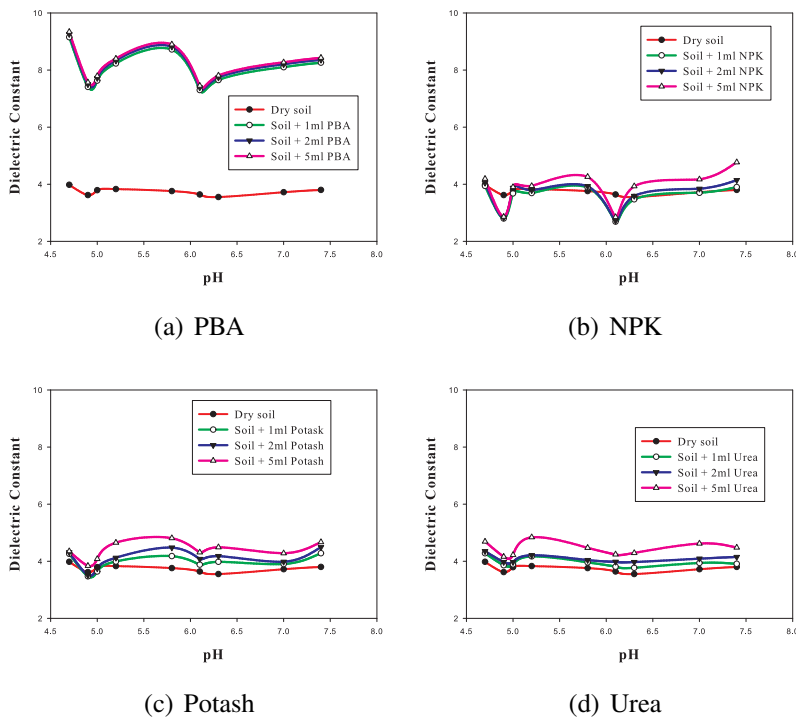


Figure 4.32: Variation of ϵ'_r with pH of the soil-fertilizer mixture-ratios; **L-band**; Free-space Transmission Method

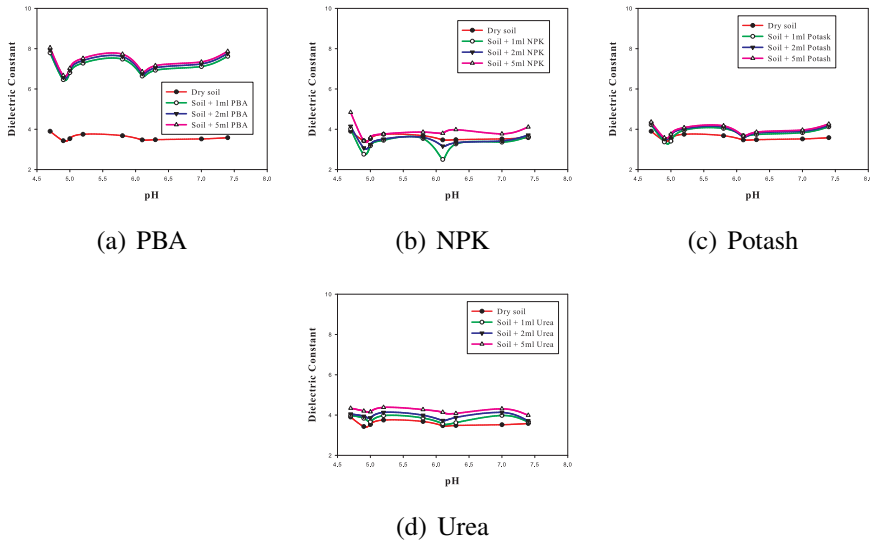


Figure 4.33: Variation of ϵ'_r with pH of the soil-fertilizer mixture-ratios; **S-band**; Free-space Transmission Method

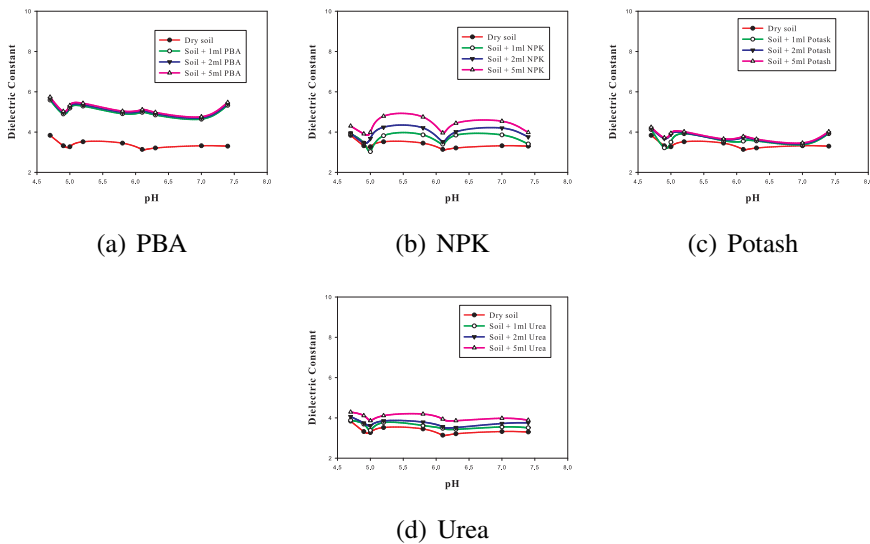
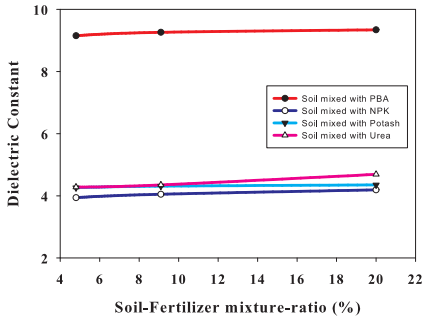
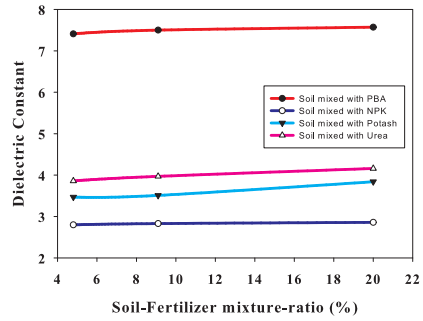


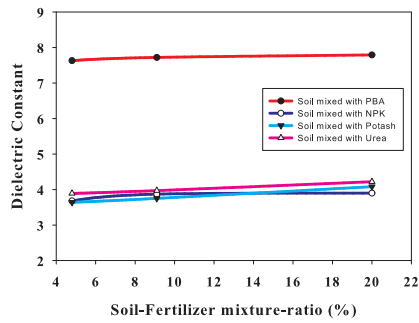
Figure 4.34: Variation of ϵ'_r with pH of the soil-fertilizer mixture-ratios; **C-band**; Free-space Transmission Method



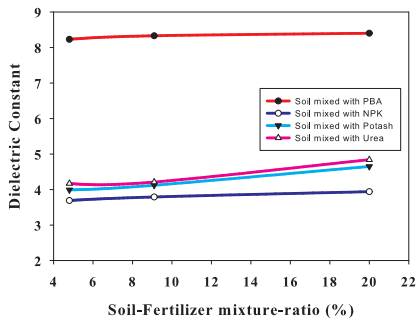
(a) pH=4.7, sample a



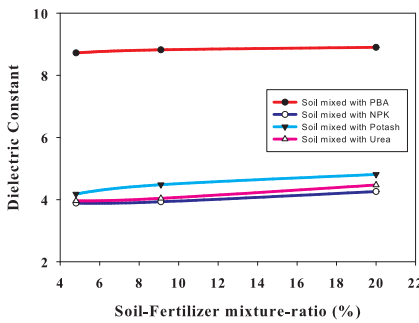
(b) pH=4.9, sample a



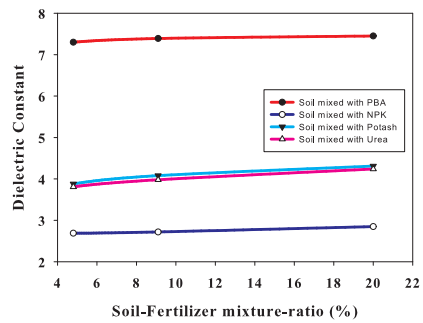
(c) pH=5.0, sample a



(d) pH=5.2

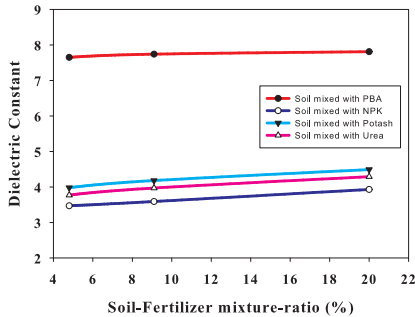


(e) pH=5.8, sample a

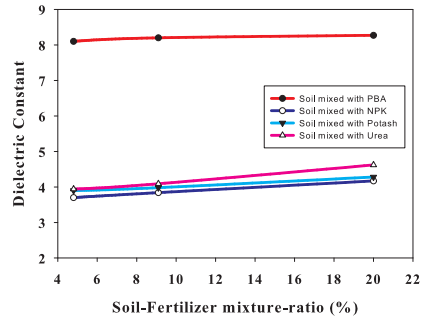


(f) pH=6.1

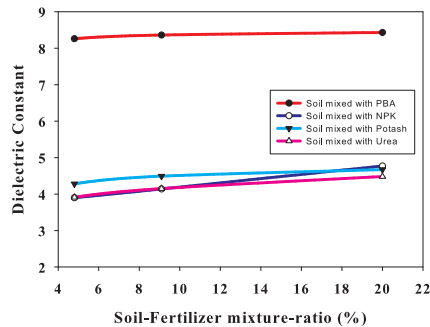
Figure 4.35: Dielectric constant vs. soil-fertilizer mixture-ratio in % for different soil samples; pH=4.7, 4.9, 5.0, 5.2, 5.8 & 6.1 ; Free-space Transmission Method



(a) pH=6.3, sample a



(b) pH=7.0, sample a



(c) pH=7.4, sample a

Figure 4.36: Dielectric constant vs. soil-fertilizer mixture-ratio in % for different soil samples; **pH=6.3, 7.0 & 7.4**; Free-space Transmission Method

4.3.3 ANN Model for Fertilizer-concentration Estimation

The characterization of soil with added fertilizers at the L, S and C bands using the Free-space Transmission Method was discussed in the previous section. Four different types of fertilizers and three soil-fertilizer mixtures ratios were considered. This section presents a neural network-based methodology to estimate fertilizer concentration in soil at the three bands.

A multilayered artificial neural network, using the Levenberg-Marquardt algorithm, is used as the model. It has 2 hidden layers having 20 and 15 neurons respectively. The input training data comprise the ϵ'_r of fertilizer-soil mixture-ratio computed using the free-space transmission method at the three bands. The three different mixture ratios (4.8 %, 9.1 % and 20%) and the nine soil samples (pH=4.7, 4.9, 5.0, 5.2, 5.8, 6.1, 6.3, 7.0 & 7.4) are used.

The target consists of the corresponding soil-fertilizer mixture-ratio, expressed in percentage. Percentage of data-set used for training, validation and testing are respectively 88, 8 and 4 %. Training and testing procedure is carried out using MATLAB[®]. ANN models corresponding to each of the fertilizer types are created. To estimate the value of soil-fertilizer mixture-ratio of the soil sample at hand, the measured value of ϵ'_r at the three bands is given as input to the appropriate ANN model. The model then returns the fertilizer-soil mixture ratio in %.

Table 4.33 lists the values of ϵ'_r of the PBA-soil samples at different mixture-ratios at the three bands. It also shows the value of the PBA-soil mixture-ratio returned by the ANN model and the percentage error in the actual and evaluated amounts. Similar results for the other three fertilizers are given in Tables 4.34 to 4.36.

A Graphical User Interface (GUI), developed using MATLAB[®] to make the program user-friendly is shown in Fig. 4.37.

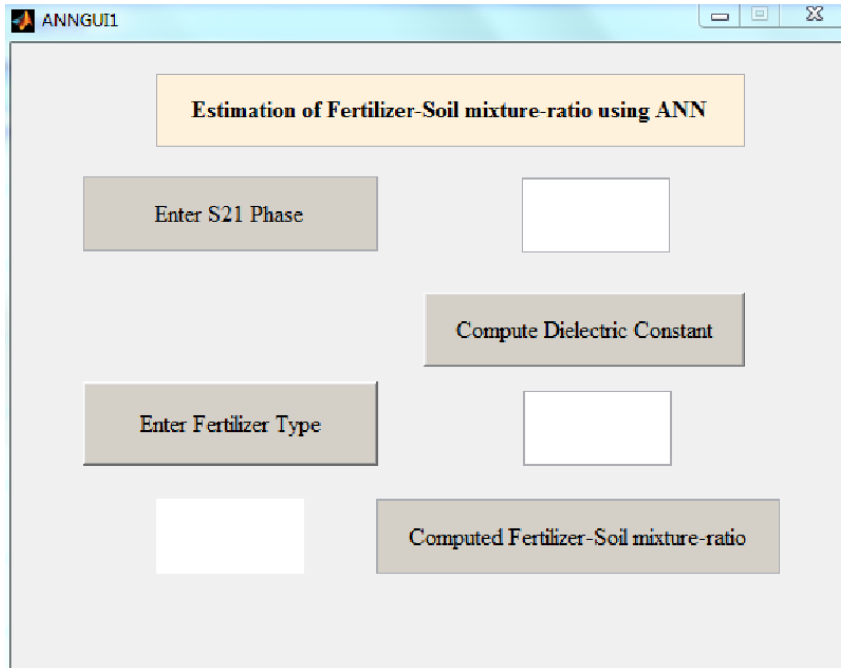


Figure 4.37: GUI used for fertilizer-soil mixture ratio estimation; ANN Model; Free-space Transmission Method

A screen-shot of the evaluated amount of PBA-soil mixture-ratio for soil (pH=4.7, sample a) [Table 4.33, row 1, column 6] is shown in Fig. 4.38.

The maximum error percentage in the fertilizer-mixture ratio is found to be 1.57% (Table 4.36). Thus, if the area from which the soil sample is obtained, type of crop-cultivation and the fertilizer predominantly added are known, the fertilizer-soil mixture ratio returned by the model can be used to advise the farmer to take corrective steps.

Table 4.33: Percentage error in the actual and evaluated values of **PBA-soil mixture-ratio** for different soil samples based on ANN model; Free-space Transmission Method

Sample No.	Actual Mixture-ratio %	ϵ'_r			Evaluated Mixture-ratio %	Error %
		1.85 GHz	2.45 GHz	5.52 GHz		
1 (4.7 a)	0	3.98	3.90	3.82	0.0015	0.15
	4.8	9.15	7.79	5.59	4.8006	0.01
	9.1	9.26	7.93	5.67	9.0986	0.02
	20	9.34	8.05	5.74	20.0005	0
2 (4.9 a)	0	3.62	3.43	3.30	0.0073	0.73
	4.8	7.41	6.46	4.90	4.8000	0
	9.1	7.50	6.58	4.97	9.0996	0
	20	7.57	6.67	5.03	20.0005	0
3 (5.0 a)	0	3.79	3.53	3.25	0.0157	1.57
	4.8	7.63	6.81	5.19	4.8015	0.03
	9.1	7.72	6.93	5.26	9.0998	0
	20	7.79	7.03	5.32	20.0012	0.01
4 (5.2)	0	3.83	3.75	3.50	0.0012	0.12
	4.8	8.23	7.28	5.29	4.7997	0.01
	9.1	8.33	7.41	5.36	9.1025	0.03
	20	8.40	7.52	5.43	20.0002	0
5 (5.8 a)	0	3.45	3.76	3.66	0.0027	0.27
	4.8	8.72	7.48	4.91	4.8004	0.01
	9.1	8.82	7.61	4.98	9.0999	0
	20	8.90	7.73	5.04	19.9992	0
6 (6.1)	0	3.64	3.47	3.12	0.0017	0.17
	4.8	7.30	6.64	4.98	4.8009	0.02
	9.1	7.39	6.76	5.05	9.1006	0.01
	20	7.45	6.86	5.11	20.0072	0.04
7 (6.3 a)	0	3.48	3.55	3.19	0.0022	0.22
	4.8	7.65	6.93	4.85	4.8004	0.01
	9.1	7.74	7.05	4.92	9.1007	0.01
	20	7.81	7.16	4.98	19.9996	0
8 (7.0 a)	0	3.32	3.72	3.54	0.0092	0.92
	4.8	8.10	7.11	4.64	4.8003	0.01
	9.1	8.20	7.24	4.70	9.1001	0
	20	8.27	7.34	4.76	19.9996	0
9 (7.4 a)	0	3.78	3.80	3.28	0.0006	0
	4.8	8.26	7.62	5.33	4.8013	0.03
	9.1	8.36	7.76	5.40	9.0996	0
	20	8.43	7.87	5.47	20.0086	0.04

Table 4.34: Percentage error in the actual and evaluated values of **NPK-soil mixture-ratio** for different soil samples based on ANN model; Free-space Transmission Method

Sample No.	Actual Mixture-ratio %	ϵ'_r			Evaluated Mixture-ratio %	Error %
		1.85 GHz	2.45 GHz	5.52 GHz		
1 (4.7 a)	0	3.98	3.90	3.82	0.0015	0.15
	4.8	3.94	4.02	3.92	4.7994	0.01
	9.1	4.05	4.15	3.95	9.0973	0.03
	20	4.19	4.84	4.30	19.9993	0
2 (4.9 a)	0	3.62	3.43	3.30	0.0073	0.73
	4.8	2.80	2.76	3.45	4.8005	0.01
	9.1	2.83	3.07	3.47	9.1018	0.02
	20	2.86	3.42	3.91	19.9965	0.02
3 (5.0 a)	0	3.79	3.53	3.25	0.0157	1.57
	4.8	3.68	3.18	3.03	4.7989	0.02
	9.1	3.87	3.24	3.68	9.1048	0.05
	20	3.90	3.58	3.99	19.9986	0.01
4 (5.2)	0	3.83	3.75	3.50	0.0012	0.12
	4.8	3.69	3.45	3.82	4.8000	0
	9.1	3.79	3.51	4.24	9.1012	0.01
	20	3.94	3.76	4.79	19.9992	0
5 (5.8 a)	0	3.45	3.76	3.66	0.0027	0.27
	4.8	3.89	3.54	3.86	4.7979	0.04
	9.1	3.93	3.60	4.21	9.1009	0.01
	20	4.26	3.86	4.75	19.9981	0.01
6 (6.1)	0	3.64	3.47	3.12	0.0017	0.17
	4.8	2.69	2.50	3.40	4.7982	0.04
	9.1	2.72	3.16	3.52	9.0988	0.01
	20	2.85	3.80	3.96	20.0008	0
7 (6.3 a)	0	3.48	3.55	3.19	0.0022	0.22
	4.8	3.47	3.27	3.85	4.8002	0
	9.1	3.59	3.33	4.01	9.1009	0.01
	20	3.93	3.98	4.44	20.0003	0
8 (7.0 a)	0	3.32	3.72	3.54	0.0092	0.92
	4.8	3.70	3.36	3.86	4.8042	0.09
	9.8	3.84	3.42	4.20	9.0988	0.01
	20	4.17	3.77	4.54	20.0015	0.01
9 (7.4 a)	0	3.78	3.80	3.28	0.0006	0
	4.8	3.90	3.64	3.41	4.7860	0.29
	9.1	4.14	3.71	3.76	9.0847	0.17
	20	4.77	4.11	3.98	19.9998	0

Table 4.35: Percentage error in the actual and evaluated values of **Potash-soil mixture-ratio** for different soil samples based on ANN model; Free-space Transmission Method

Sample No.	Actual Mixture-ratio %	ϵ'_r			Evaluated Mixture-ratio %	Error %
		1.85 GHz	2.45 GHz	5.52 GHz		
1 (4.7 a)	0	3.98	3.90	3.82	0.0015	0.15
	4.8	4.26	4.22	4.13	4.7886	0.24
	9.1	4.31	4.30	4.19	9.1003	0
	20	4.35	4.36	4.24	20.0000	0
2 (4.9 a)	0	3.62	3.43	3.30	0.0073	0.73
	4.8	3.47	3.37	3.22	4.7478	1.09
	9.1	3.51	3.53	3.68	9.0997	0
	20	3.84	3.58	3.72	19.9980	0.01
3 (5.0 a)	0	3.79	3.53	3.25	0.0157	1.57
	4.8	3.64	3.41	3.50	4.8030	0.06
	9.1	3.75	3.71	3.89	9.1005	0.01
	20	4.08	3.76	3.94	19.9996	0
4 (5.2)	0	3.83	3.75	3.50	0.0012	0.12
	4.8	3.99	3.95	3.92	4.8023	0.05
	9.1	4.12	4.02	3.97	9.0958	0.05
	20	4.65	4.08	4.03	19.9994	0
5 (5.8 a)	0	3.45	3.76	3.66	0.0027	0.27
	4.8	4.18	4.04	3.57	4.8026	0.05
	9.1	4.48	4.11	3.62	9.1045	0.05
	20	4.81	4.17	3.66	20.0007	0
6 (6.1)	0	3.64	3.47	3.12	0.0017	0.17
	4.8	3.88	3.68	3.55	4.7881	0.25
	9.1	4.08	3.61	3.73	9.1018	0.02
	20	4.31	3.67	3.78	19.9999	0
7 (6.3 a)	0	3.48	3.55	3.19	0.0022	0.22
	4.8	3.98	3.74	3.56	4.7969	0.06
	9.1	4.18	3.81	3.61	9.0998	0
	20	4.49	3.86	3.65	19.9926	0.04
8 (7.0 a)	0	3.32	3.72	3.54	0.0092	0.92
	4.8	3.90	3.83	3.37	4.7966	0.07
	9.1	3.98	3.90	3.42	9.1038	0.04
	20	4.28	3.96	3.46	19.9990	0.01
9 (7.4 a)	0	3.78	3.80	3.28	0.0006	0
	4.8	4.28	4.12	3.92	4.8041	0.09
	9.1	4.49	4.19	3.97	9.0867	0.15
	20	4.67	4.26	4.02	19.9917	0.04

Table 4.36: Percentage error in the actual and evaluated values of **Urea-soil mixture-ratio** for different soil samples based on ANN model; Free-space Transmission Method

Sample No.	Actual Mixture-ratio %	ϵ'_r			Evaluated Mixture-ratio %	Error %
		1.85 GHz	2.45 GHz	5.52 GHz		
1 (4.7 a)	0	3.98	3.90	3.82	0.0015	0.15
	4.8	4.28	3.98	3.88	4.8006	0.01
	9.1	4.35	4.05	4.06	9.1023	0.03
	20	4.69	4.34	4.29	20.0032	0.02
1 (4.9 a)	0	3.62	3.43	3.30	0.0073	0.73
	4.8	3.86	3.84	3.69	4.8106	0.22
	9.1	3.97	3.94	3.74	9.1614	0.67
	20	4.16	4.20	4.11	20.0102	0.05
3 (5.0 a)	0	3.79	3.53	3.25	0.0157	1.57
	4.8	3.89	3.67	3.38	4.7937	0.13
	9.1	3.97	3.86	3.61	9.1105	0.12
	20	4.22	4.16	3.86	20.0072	0.04
4 (5.2)	0	3.83	3.75	3.50	0.0012	0.12
	4.8	4.17	3.97	3.77	4.7986	0.03
	9.1	4.21	4.13	3.85	9.0934	0.07
	20	4.84	4.38	4.11	19.9957	0.02
5 (5.8 a)	0	3.45	3.76	3.66	0.0027	0.27
	4.8	3.96	3.85	3.62	4.7876	0.26
	9.1	4.04	3.99	3.79	9.1001	0
	20	4.47	4.27	4.19	19.9978	0.01
6 (6.1)	0	3.64	3.47	3.12	0.0017	0.17
	4.8	3.81	3.57	3.48	4.8139	0.29
	9.1	3.98	3.73	3.56	9.1228	0.25
	20	4.24	4.14	3.94	20.0051	0.03
7 (6.3 a)	0	3.48	3.55	3.19	0.0022	0.22
	4.8	3.77	3.62	3.43	4.7937	0.13
	9.1	3.97	3.88	3.52	9.0982	0.02
	20	4.29	4.08	3.86	19.9929	0.04
8 (7.0 a)	0	3.32	3.72	3.54	0.0092	0.92
	4.8	3.94	3.98	3.55	4.7926	0.15
	9.1	4.09	4.13	3.72	9.0339	0.73
	20	4.62	4.31	3.98	20.0082	0.04
9 (7.4 a)	0	3.78	3.80	3.28	0.0006	0
	4.8	3.91	3.66	3.51	4.8058	0.12
	9.1	4.15	3.71	3.76	9.1260	0.29
	20	4.48	3.99	3.89	20.0035	0.02


```

outputs =
Columns 1 through 4
    0.0015    4.8006    9.0986    20.0005

```

Figure 4.38: Screen-shot of evaluated amount of PBA-soil mixture-ratio for soil (pH=4.7, sample a); ANN Model; Free-space Transmission Method

4.4 Chapter Summary

This chapter presents the characterization of soil using free-space transmission method, at the L, S and C bands, where a sample-holder filled with soil samples is placed between a pair of Microstrip Patch Antennas (MPA) connected to two ports of a VNA. CST MWS[®]-based simulation is carried out to check the feasibility of the method. The parameters monitored are the moisture content (MC) and fertilizer concentration (FC) using various soil samples available in Ernakulam and Palakkad districts of Kerala. pH of soil samples under test varied from low-acidic (4.7) to moderate-alkaline (7.5). The effect of added moisture in varying quantity on the dielectric constant of soil samples is monitored. Using Topp's Equation, the methodology is validated by comparing the experimental and actual values of ϵ'_r of varying soil-moisture mixtures. Low error values obtained suggest that the method is valid for moisture-content monitoring in soil characterization. Experiment is carried out with a similar setup using an MPA as transmitter and a sensor-probe as receiver to detect the presence of moisture in soil through the variation in S_{21} values and consequent colour-mapping. An ANN model is also developed that returns the Volumetric Water Content, θ_v , of any soil sample, when the corresponding measured value of ϵ'_r is given as a test input. Similarly, the effect of adding fertilizers in different proportions on the dielectric constant of soil samples, is also monitored. Four types of commercially

used fertilizers (PBA, NPK, Potash & Urea) generally used to increase soil fertility, are considered. An analytical model based on ANN to estimate fertilizer concentration in soil at the three bands is also proposed. Shortcomings of conventional methods such as Cavity Perturbation Method and Superstrate Method used for soil characterization are mitigated in the Free-space Transmission Method.

The experiments detailed in this chapter led to the evaluation of the dielectric constant of a set of dry soil samples, soil-moisture mixtures and soil-fertilizer mixtures of the samples from Ernakulam and Palakkad districts of Kerala. Experimental results are validated using Topp's equation, relating the dielectric constant and volumetric water content. The free-space transmission method thus offers a very simple and convenient scheme for soil characterization. One major advantage with this method and the associated model developed is that there is no need to test the pH value of the soil sample. Hence all the associated pre-processing steps, such as drying, pulverizing etc. of soil samples under test, can be avoided. Microwave Imaging can hence be used as a potential tool for soil characterization. The work also revealed the following:

- Presence of moisture and its varying concentration increase the dielectric constant of soil
- Presence of fertilizers and their varying concentration increase/decrease the dielectric constant of soil

The highlight of the chapter is the experimental compilation of dielectric constant of various soil samples, under different moisture and fertilizer mixture-ratios.

Chapter 5

SOIL CHARACTERIZATION USING SENSOR ANTENNA

Contents

5.1	Introduction	149
5.2	Sensor Antenna	151
5.3	Experimental Results	154
5.4	Analytical Models	185
5.5	Moisture detection using colour mapping	199
5.6	Chapter Summary	201

5.1 Introduction

In Chapter 2, four methodologies for material characterization, namely Cavity Perturbation Method, Superstrate Method, Free-space Transmission Method and Sensor Antenna Method were discussed. Characterization of soil using Cavity Perturbation Method and

Superstrate Method were presented in Chapter 3, which confirmed the microwave properties of soil. The need for using other methodologies to overcome the shortcomings of the methods was also mentioned. Chapter 4 presented the Free-space Transmission Method for the characterization of soil, in which a sample of soil is placed between a pair of transmitting and receiving antennas. Monitoring the effect of added moisture and fertilizers on the dielectric constant of soil samples from Ernakulam and Palakkad districts of Kerala was done. Use of a sensor-probe to detect the presence of moisture in soil through variation in S_{21} and consequent colour-mapping was also presented. An analytical model based on Artificial Neural Network to monitor Volumetric Water Content and Fertilizer Concentration was discussed.

The use of Sensor Antenna for material characterization was presented in Section 2.2.4. This chapter presents a methodology using a Sensor Antenna to monitor soil moisture and fertilizer at microwave frequencies. Simulation based on Ansoft HFSS and validation using an experimental setup are discussed. Metamaterial-based sensor antennas ((Anju, 2015)), fabricated on a substrate with $\epsilon'_r = 4.4$ and loss-tangent=0.02 are used to conduct experiments on soil in the L, S and C bands.

Analytical tools such as ANN and Regression are used to validate the results obtained for soil characterization. An equation, establishing a relationship between moisture content and shift in frequency of the sensor antenna, is developed using regression analysis. Microwave colour-mapping, used as a tool to monitor soil moisture, is presented. Here, change in colour-map at moist spots arising due to the shift in resonant frequency of the sensor, is a measure of moisture content. These sensors can be used in a laboratory setup to find the dry or humid nature of soil. In a real field environment, an embedded array of such sensors may be deployed to adjust for too little or too much rain and fertilizers. Omnidirectional radiation pattern, small dimensions, varying penetration depth and non-ionizing power levels ensure that the sensors can be used in real-environment fluid-characterization and agriculture applications.

5.2 Sensor Antenna

In a broad sense, any antenna whose inherent characteristics get altered based on environmental stimuli or external material presence is called a sensor antenna. It can be used to provide information about the material dielectric property, moisture content, density, structure, shape of materials and even chemical composition. Microwave sensors offer many advantages over traditional sensors such as rapid, non-destructive, precise and fully automated measurement. Resonant microwave sensors have high sensitivity and need simple signal processing. Material measurement using microwaves utilize their interaction with the medium of propagation, which is completely determined by the relative permittivity and permeability of the medium.

In such sensors, the change in resonant frequency and/or loss due to detuning can be used for sensing (Ekmekci and Turhan-Sayan, 2011). Relative permeability (μ_r) of most practical materials that are the subject of measurement with microwave sensors is unity. Hence permittivity (ϵ_r) is preferred for characterization. Also, only the real part of complex permittivity, called dielectric constant ϵ_r' , is calculated from resonant frequency information.

5.2.1 Sensor Antenna Configurations in the L, S and C bands

Three different antenna configurations are employed in the L, S and C bands, as illustrated in Fig. 5.1. The sensor antenna designed to operate in the L-band consists of a nine-arm spiral resonator. It is embedded on to the signal strip of a 50 Ω Asymmetric Coplanar Strip (ACS) transmission line fabricated on a substrate with $\epsilon_r=4.4$, thickness=1.6 mm and loss-tangent=0.02. Structure of the sensor resonating in the S-band has an additional arm. Sensor used in the C-band has the same structure as that designed for the L-band, with a short at the top end of the spiral. This short changes the sensor's capacitance, thereby altering

its resonant frequency. All structures are coplanar; the resonant frequency of each is sensitive to the presence of any material beneath the spiral. Corresponding dimensions are given in Table 5.1.

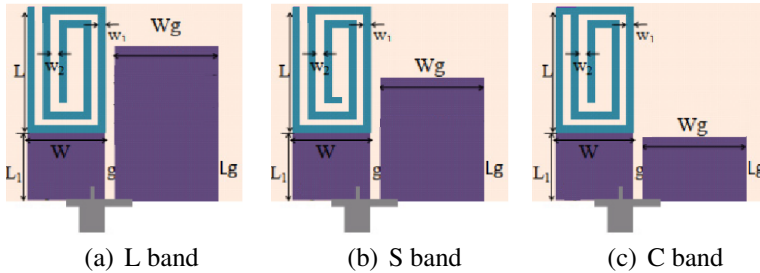


Figure 5.1: Geometry of sensor antenna at L, S & C bands; Sensor Antenna Method

Table 5.1: Dimensions of sensor antenna operating in the L, S & C bands; Sensor Antenna Method

Symbol	Parameter	Dimension in mm		
		L-band	S-band	C-band
L	Length of spiral arm	8.00	5.77	4.70
L_1	Length of transmission line segment	5.47	4.18	3.40
W	Width of spiral resonator	4.83	3.68	3.00
L_g	Length of ground	10.46	6.75	3.00
W_g	Width of ground	7.24	5.53	4.50
W_1	Width of spiral arm	0.50	0.37	0.30
W_2	Gap between spiral	0.48	0.37	0.30
g	Gap between transmission line and ground	0.50	0.37	0.30

Simulation Results

A box, suiting the dimensions of each sensor geometry, is created below the spiral to verify the functionality of the sensor. The material of the box is varied to see how the resonant frequency of the antenna varies

with the dielectric constant (ϵ_r') of the sample. Shift in frequency for different materials is shown in Table 5.2 for the three geometries.

Table 5.2: Shifted frequency for different materials; L-band ($f_r=1.88$ GHz); S-band ($f_r=2.45$ GHz); C-band ($f_r=5.2$ GHz); Sensor Antenna Method

Material	Dielectric constant	f_s (GHz)		
		L-band	S-band	C-band
Arlon AD 250 TM	2.5	1.8682	2.4368	5.1750
Soil	3.5	1.8621	2.4341	5.1802
Silicon dioxide	4.0	1.8561	2.4236	5.1475
Silicon nitrate	7.0	1.8443	2.4104	5.1329
Sapphire	10.0	1.8383	2.4053	5.1303
Gallium arsenide	12.9	1.8324	2.3972	5.0950
Diamond	16.5	1.8264	2.3873	5.0757

The percentage shift in frequency of each sensor-geometry in relation to dielectric constant of the material is obtained using Eq. 5.1.

$$\text{Percentage shift in frequency} = \frac{(f_r - f_s)}{f_r} \times 100 \quad (5.1)$$

where f_r is the resonant frequency of the antenna and f_s is the shifted frequency on placing the box. Table 5.3 shows a comparison of percentage shift in frequency of the sensor versus dielectric constant of the material in the L, S & C bands.

From the above tables, it is evident that as dielectric constant (ϵ_r') of the material increases, the shift in frequency of the sensor also increases. It is also observed that the percentage shift in frequency of the sensor decreases as the band of operation moves from L to C. This suggests that the sensor antenna is more sensitive at the L band. The greater sensitivity at the L band may be due to its larger size (Table 5.1) which makes it get in contact with more area of the material.

Shift in resonant frequency of the antenna is the parameter that helps to sense the presence of a dielectric material. Simulation results reveal that the sensor antenna can be used for material characterization at the L, S & C bands.

Table 5.3: Percentage shift in frequency of sensor antenna in the L, S & C bands; Sensor Antenna Method

Relative permittivity	Percentage shift at		
	L-band ($f_r=1.88$ GHz)	S-band ($f_r=2.45$ GHz)	C-band ($f_r=5.2$ GHz)
2.5	0.63	0.54	0.48
3.5	0.95	0.65	0.38
4.0	1.27	1.08	1.01
7.0	1.90	1.62	1.29
10.0	2.22	1.82	1.34
12.9	2.53	2.16	2.02
16.5	2.85	2.56	2.39

5.3 Experimental Results

In the previous section, efficacy of the sensor antenna in material characterization was discussed. This research focusses on the characterization of soil at microwave frequencies using different methods. So the simulated sensor antenna structure at the three frequencies are fabricated to carry out experiments for the characterization of soil. Two different cases are taken up for study.

- 1. Monitoring of Moisture Content (MC):** Shift in resonant frequency is noted using L, S & C band sensors for varying MC, for three soil samples with pH=4.7, 6.3 and 7.4. Quantity of soil taken is 5 ml; MC's considered are 0 ml (dry soil), 1 ml and 2 ml, giving a percentage Volumetric Water Content (θ_v) of 0%, 16.67 % and 28.57 % respectively.

2. Monitoring of a combination of Fertilizer and Moisture

Content: Shift in resonant frequency is noted using a C-band sensor for 20 samples of 5 ml of dry soil with varying pH values mixed with the four commercial fertilizers mentioned in the previous chapters, namely PBA, NPK, Potash and Urea at three soil-fertilizer mixture-ratios of 16.67%, 28.57% and 37.5%. (the quantities of fertilizer added are 1 ml, 2 ml and 3 ml, giving the three mixture-ratios). The three different soil-fertilizer mixture-ratios are also mixed with θ_v of 0%, 16.67 % and 28.57 %.

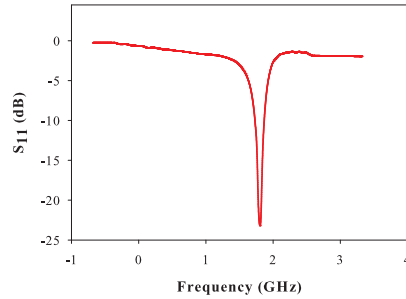
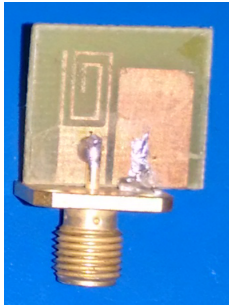
Figs. 5.2(a) to 5.2(f) show the fabricated sensors and their reflection characteristics designed respectively for the L, S & C bands.

The experimental setup is shown in Fig. 5.3. Here the sensor antenna, connected to Port 1 of Rohde and Schwarz ZVB8 VNA, is inserted into a plastic cup of capacity 10 ml. Reflection characteristics, S_{11} , of the sensor is measured and shifts in resonant frequency corresponding to the different cases mentioned above are noted.

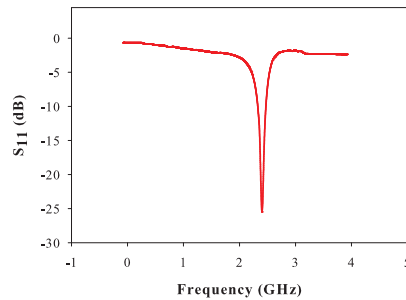
Two different cases for soil characterization using sensor antenna were mentioned in the previous section.

Case 1: Moisture Content

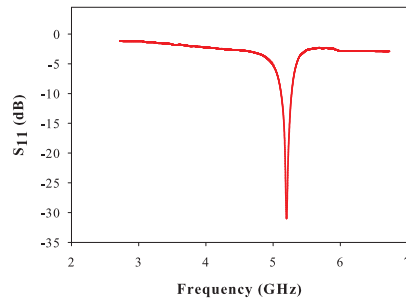
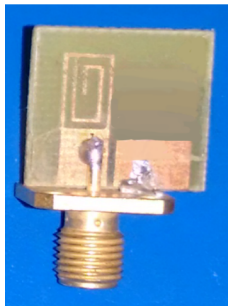
Results obtained for the percentage shift in resonant frequency at the three frequency bands are tabulated in Tables 5.4, 5.5 and 5.6. f_r is the resonant frequency of the sensor antenna and f_s is the shifted frequency when the sensor is inserted into soil.



(a) Structure at L band (b) Reflection characteristics at L band



(c) Structure at S band (d) Reflection characteristics at S band



(e) Structure at C band (f) Reflection characteristics at C band

Figure 5.2: Fabricated structure [(a), (c), (e)] and Reflection characteristics [(b), (d), (f)] of sensor antenna in the L, S & C bands ($f_r=1.88$ GHz, 2.45 GHz & 5.2 GHz); Sensor Antenna Method



Figure 5.3: Experimental setup for measuring percentage shift in frequency for soil characterization; Sensor Antenna Method

Table 5.4: Percentage shift in frequency for three select soil samples under varying moisture content; L-band ($f_r=1.88$ GHz); Sensor Antenna Method

pH	Soil	MC (in ml)	f_s (GHz)	S_{11} (dB)	shift (%)
	Sample				
4.7	a	0	1.683164	-17.03	10.47
		1	1.406240	-10.27	25.20
		2	0.998280	-7.97	46.90
6.3	a	0	1.698392	-15.41	9.66
		1	1.505128	-15.26	19.94
		2	1.022720	-11.13	45.60
7.4	a	0	1.694068	-17.93	9.89
		1	1.140972	-19.22	39.31
		2	1.010876	-27.05	46.23

Table 5.5: Percentage shift in frequency for three select soil samples under varying moisture content; S-band ($f_r=2.45$ GHz); Sensor Antenna Method

Soil		MC (in ml)	f_s (GHz)	S_{11} (dB)	shift (%)
pH	Sample				
4.7	a	0	2.224600	-31.80	9.20
		1	1.837990	-16.26	24.98
		2	1.308300	-11.24	46.60
6.3	a	0	2.221660	-26.11	9.32
		1	1.789235	-14.60	26.97
		2	1.318100	-12.59	46.20
7.4	a	0	2.194955	-23.06	10.41
		1	1.703730	-16.03	30.46
		2	1.324225	-10.24	45.95

Table 5.6: Percentage shift in frequency for three select soil samples under varying moisture content; C-band ($f_r=5.2$ GHz); Sensor Antenna Method

Soil		MC (in ml)	f_s (GHz)	S_{11} (dB)	shift (%)
pH	Sample				
4.7	a	0	4.819360	-10.12	7.32
		1	4.113720	- 8.39	20.89
		2	2.782000	-20.49	46.50
6.3	a	0	4.860440	-9.71	6.53
		1	4.427800	- 9.82	14.85
		2	2.781480	-23.96	46.51
7.4	a	0	5.031520	-10.26	3.24
		1	4.826692	- 8.12	7.179
		2	2.848040	-22.22	45.23

Fig. 5.4 shows the plot of reflection coefficient, S_{11} as a function of frequency when the L-band sensor is inserted in dry soil (pH=4.7, sample a) and the same mixed with 1 ml and 2 ml water. Similar plots for soils with pH=6.3 and 7.4 are shown in Figs. 5.5 and 5.6. Figs. 5.7 to 5.12 show plots for the three dry soil samples and those mixed with 1 ml and 2 ml water for the two sensor antennas operating in the S and C bands. It is clear from the figures that the resonant frequency decreases as more and more water is added to the soil; also the percentage shift in frequency increases as the moisture content increases.

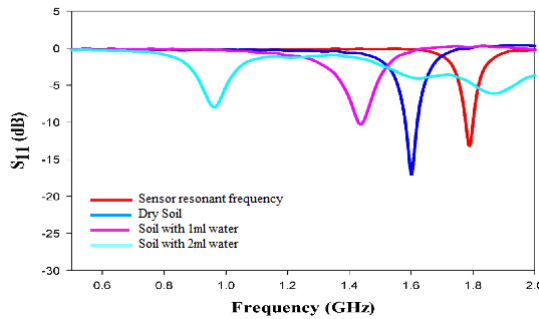


Figure 5.4: Reflection characteristics of **L-band** sensor antenna in soil (pH=4.7 sample a); Sensor Antenna Method

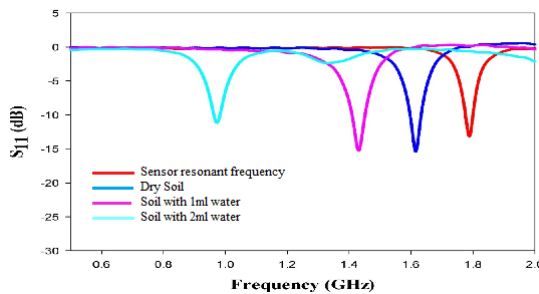


Figure 5.5: Reflection characteristics of **L-band** sensor antenna in soil (pH=6.3 sample a); Sensor Antenna Method

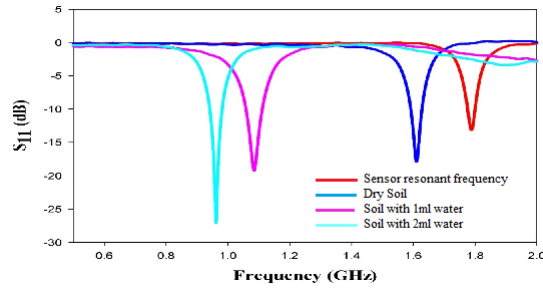


Figure 5.6: Reflection characteristics of **L-band** sensor antenna in soil (pH=7.4 sample a); Sensor Antenna Method

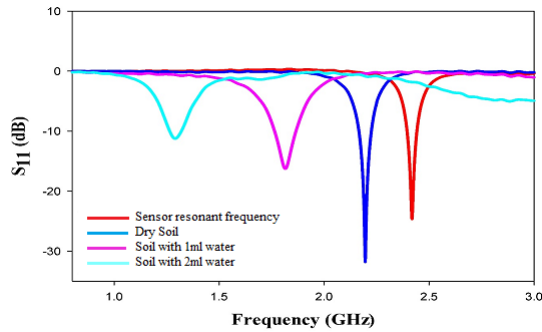


Figure 5.7: Reflection characteristics of **S-band** sensor antenna in soil (pH=4.7 sample a); Sensor Antenna Method

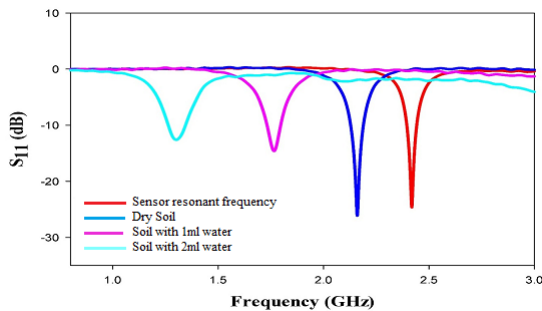


Figure 5.8: Reflection characteristics of **S-band** sensor antenna in soil (pH=6.3 sample a); Sensor Antenna Method

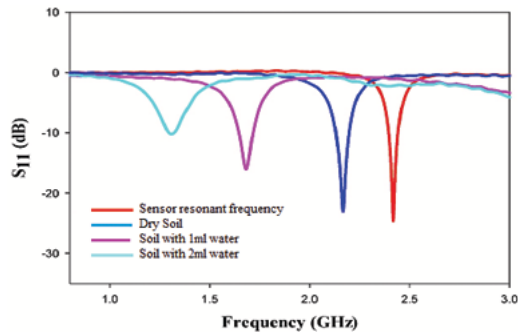


Figure 5.9: Reflection characteristics of **S-band** sensor antenna in soil (**pH=7.4 sample a**); Sensor Antenna Method

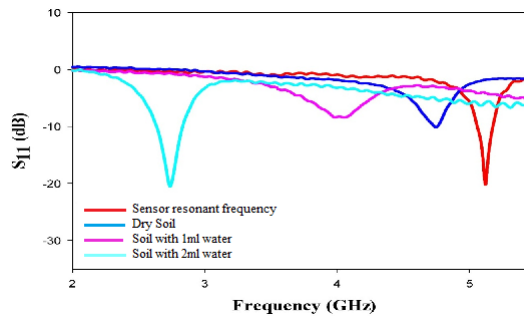


Figure 5.10: Reflection characteristics of **C-band** sensor antenna in soil (**pH=4.7 sample a**); Sensor Antenna Method

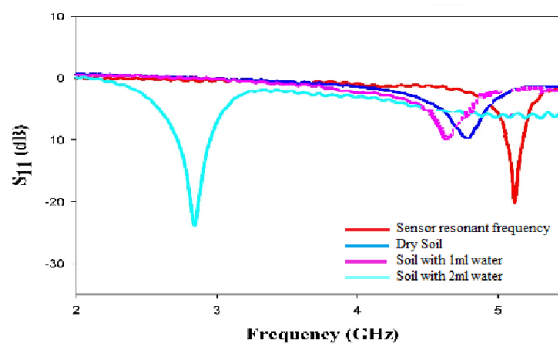


Figure 5.11: Reflection characteristics of **C-band** sensor antenna in soil (**pH=6.3 sample a**); Sensor Antenna Method

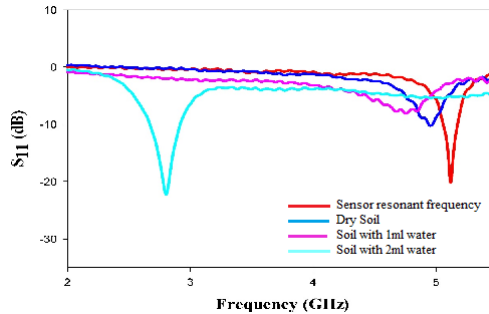


Figure 5.12: Reflection characteristics of **C-band** sensor antenna in soil (**pH=7.4 sample a**); Sensor Antenna Method

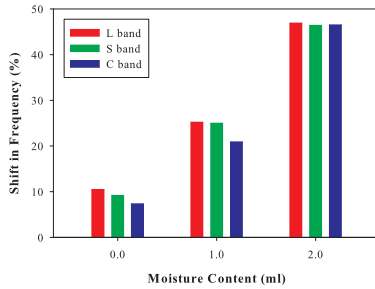
Figs. 5.13(a) to 5.13(c) compare the percentage shift in frequency of sensor antenna in each band with respect to variation in moisture content (MC) for the three soil samples. The plots clearly indicate that the frequency shift increases with MC. The increase in frequency shift of the sensor is due to the presence of moisture. This in turn implies that the sensor is sensitive to the dielectric constant of soil, and moisture in soil increases its dielectric constant. Or in other words, soil (along with its constituents such as moisture, fertilizers etc.) can be characterized with suitable microwave sensors.

To test the efficacy of the sensor antenna, a comparison with a commercially available sensor module is done and the results obtained are shown in Appendix A.

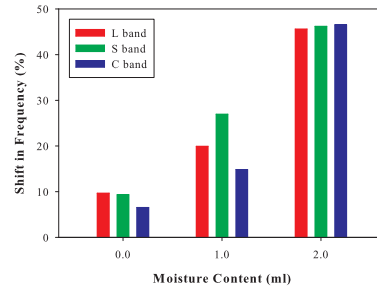
Case 2: Combination of Fertilizer and Moisture

This section discusses the characterization of various soil samples mixed with different types and concentration of fertilizers and moisture content using a sensor antenna resonating in the C-band.

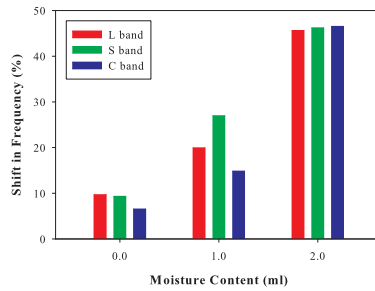
Also, two models based on ANN and regression analysis are developed for characterizing soil with varying fertilizer and moisture contents. An ANN model is trained based on the shift in resonant frequency of the sensor. Regression analysis is carried out to establish a relationship between moisture content and shift in frequency.



(a) Soil pH=4.7, sample a



(b) Soil pH=6.3, sample a



(c) Soil pH=7.4, sample a

Figure 5.13: Comparison of percentage shift in frequency of sensor antenna under varying moisture content for three different soil samples in the L, S & C bands; Sensor Antenna Method

Experimental Setup and Methodology

The structure of the sensor used for carrying out the experiment is given in Fig. 5.2(e). Four fertilizers are added to 5 ml of soil, in three different mixture-ratios of 16.67 %, 28.57 % and 37.5 % (Section 5.3). The shift in resonant frequency of the sensor when it is inserted in dry soil and soil with the three fertilizer mixture-ratios is measured using the experimental setup shown in Fig.5.3.

The experiment is continued by adding different quantities of water to soil-fertilizer mixture. Shifts in resonant frequency of the sensor antenna for different quantities of water added to soil-fertilizer mixture are measured. The procedure is repeated for all fertilizers and

corresponding readings are taken. This work thus presents a methodology wherein the combined effect of fertilizer and moisture in soil is analyzed.

Shifts in resonant frequency of the sensor for different conditions are shown in Tables 5.7 and 5.8 for a 5 ml soil (pH= 4.7, sample a). Figs. 5.14, 5.15 and 5.16 illustrate the shift in frequency (Δf) with respect to variation in percentage concentration of the different fertilizers in dry and moist soil (pH=4.7, sample a).

Table 5.7: Shift in frequency for fertilizer mixed with soil (pH=4.7, sample a); C-band ($f_r=5.2$ GHz); Fertilizers : PBA, NPK; Sensor Antenna Method

Fertilizer concentration, FC (%)	Shift in Frequency, Δf (GHz)					
	PBA			NPK		
	MC=0ml	MC=1ml	MC=2ml	MC=0ml	MC=1ml	MC=2ml
16.67	0.34	0.68	2.51	0.29	0.62	2.46
28.57	0.38	0.93	2.62	0.32	0.84	2.56
37.50	0.42	1.34	2.90	0.38	1.30	2.87

Table 5.8: Shift in frequency for fertilizer mixed with soil (pH=4.7, sample a); C-band ($f_r=5.2$ GHz); Fertilizers : Potash, Urea; Sensor Antenna Method

Fertilizer concentration, FC (%)	Shift in Frequency, Δf (GHz)					
	Potash			Urea		
	MC=0ml	MC=1ml	MC=2ml	MC=0ml	MC=1ml	MC=2ml
16.67	0.30	0.64	2.48	0.28	0.61	2.45
28.57	0.34	0.85	2.59	0.31	0.83	2.55
37.50	0.39	1.32	2.89	0.37	1.29	2.84

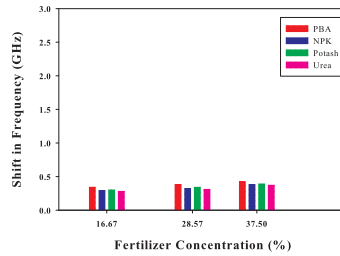


Figure 5.14: Shift in frequency vs. fertilizer concentration for soil (pH=4.7, sample a); all fertilizers; MC=0ml; C-band; Sensor Antenna Method

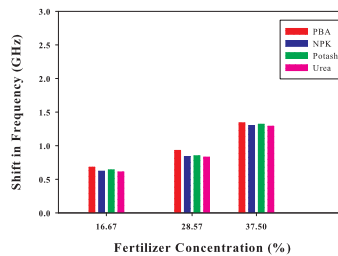


Figure 5.15: Shift in frequency vs. fertilizer concentration for soil (pH=4.7, sample a); all fertilizers; MC=1ml; C-band; Sensor Antenna Method

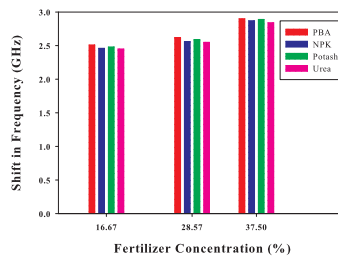


Figure 5.16: Shift in frequency vs. fertilizer concentration for soil (pH=4.7, sample a); all fertilizers; MC=2ml; C-band; Sensor Antenna Method

The experiment is repeated for all dry and moist soil samples with pH=4.9, 5.0, 5.1, 5.2, 5.3, 5.4, 5.7, 5.8, 5.9, 6.1, 6.2, 6.3, 6.4, 7.0, 7.1, 7.2, 7.3, 7.4 & 7.5. The corresponding results are plotted in Figs. 5.17 to 5.35. The list of soil samples thus includes the entire set of twenty distinct soil samples (fourteen acidic and six alkaline types), as presented in Section 4.1.

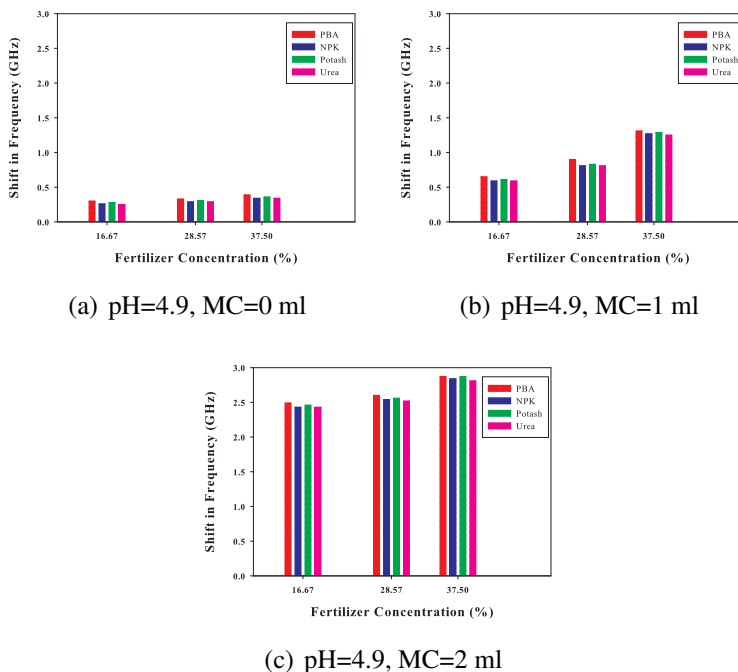
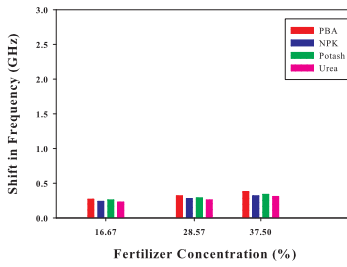
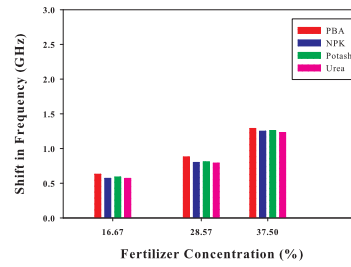


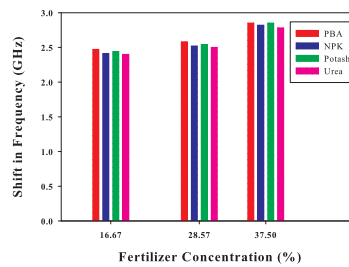
Figure 5.17: Shift in frequency vs. fertilizer concentration for soil (pH=4.9, sample a) mixed with 0 ml, 1 ml & 2 ml MC; all fertilizers; C-band; Sensor Antenna Method



(a) pH=5.0, MC=0 ml



(b) pH=5.0, MC=1 ml



(c) pH=5.0, MC=2 ml

Figure 5.18: Shift in frequency vs. fertilizer concentration for soil (pH=5.0, sample a) mixed with 0 ml, 1 ml & 2 ml MC; all fertilizers; C-band; Sensor Antenna Method

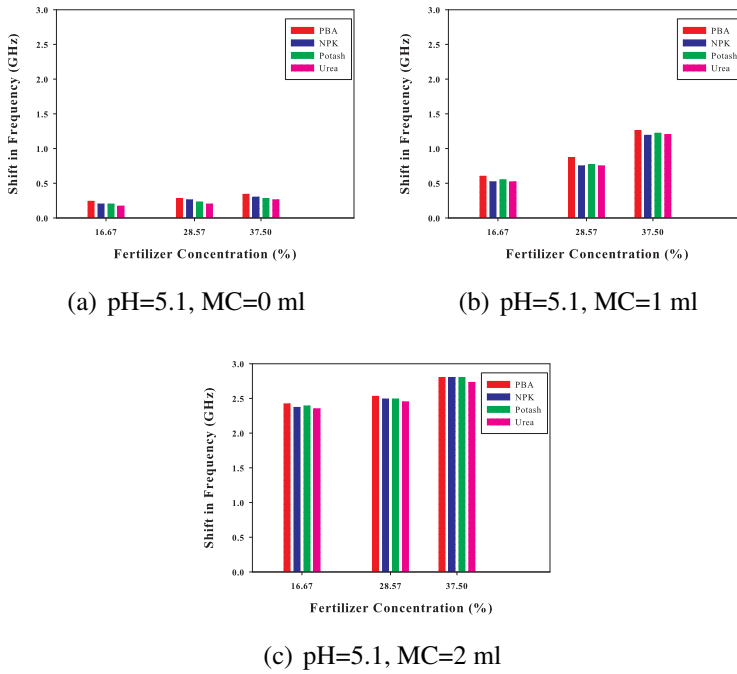
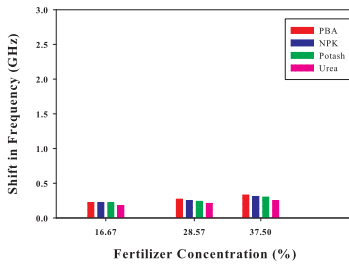
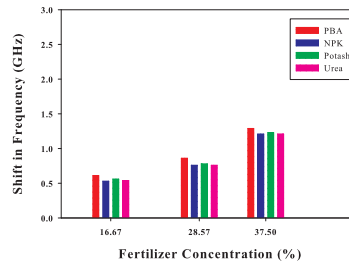


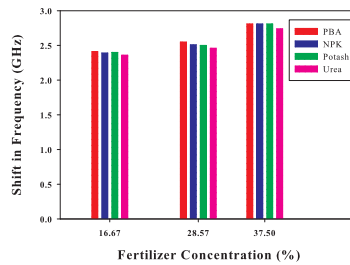
Figure 5.19: Shift in frequency vs. fertilizer concentration for soil (pH=5.1) mixed with 0 ml, 1 ml & 2 ml MC; all fertilizers; C-band; Sensor Antenna Method



(a) pH=5.2, MC=0 ml



(b) pH=5.2, MC=1 ml



(c) pH=5.2, MC=2 ml

Figure 5.20: Shift in frequency vs. fertilizer concentration for soil (pH=5.2) mixed with 0 ml, 1 ml & 2 ml MC; all fertilizers; C-band; Sensor Antenna Method

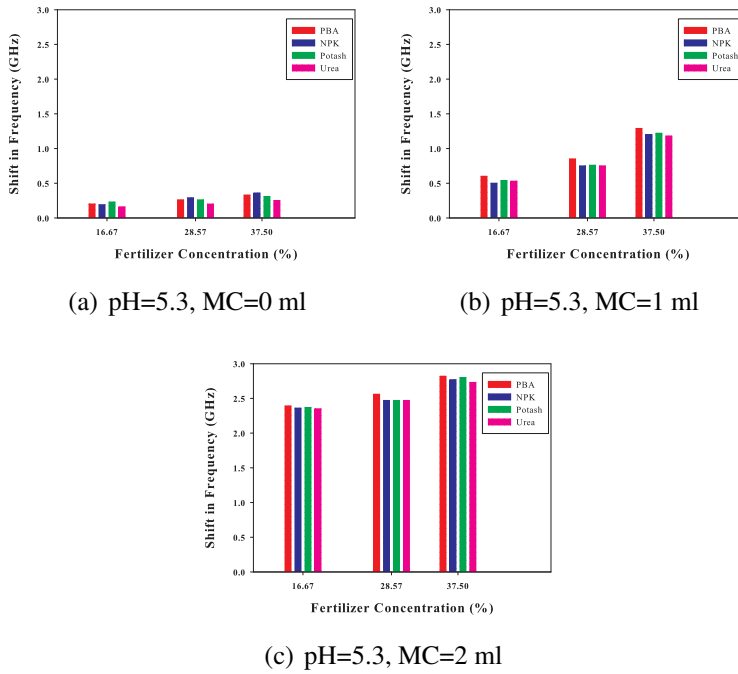
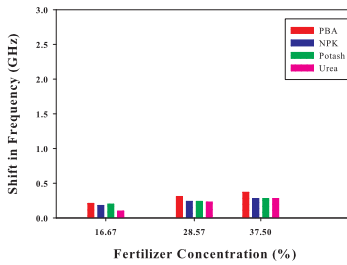
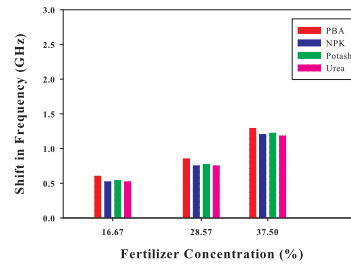


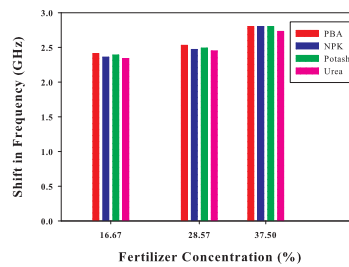
Figure 5.21: Shift in frequency vs. fertilizer concentration for soil (pH=5.3, sample a) mixed with 0 ml, 1 ml & 2 ml MC; all fertilizers; C-band; Sensor Antenna Method



(a) pH=5.4, MC=0 ml



(b) pH=5.4, MC=1 ml



(c) pH=5.4, MC=2 ml

Figure 5.22: Shift in frequency vs. fertilizer concentration for soil (pH=5.4) mixed with 0 ml, 1 ml & 2 ml MC; all fertilizers; C-band; Sensor Antenna Method

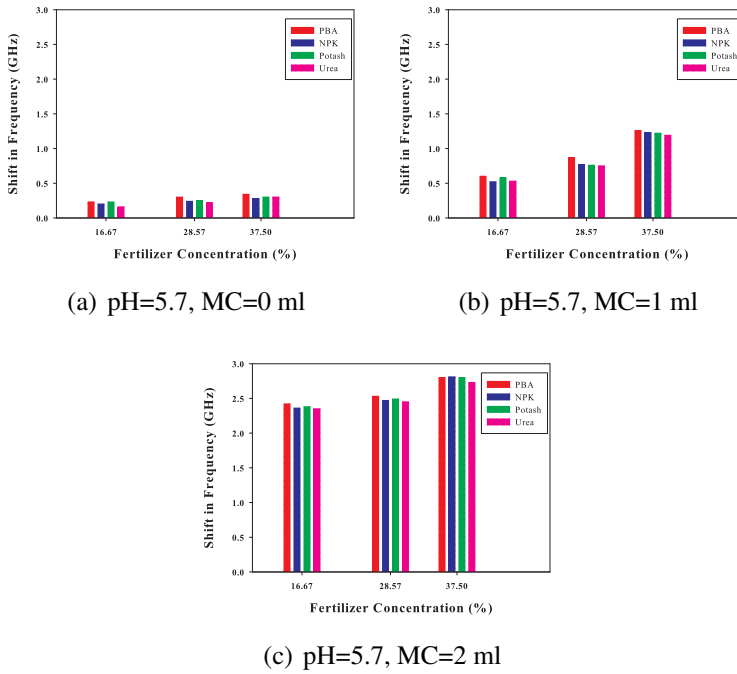
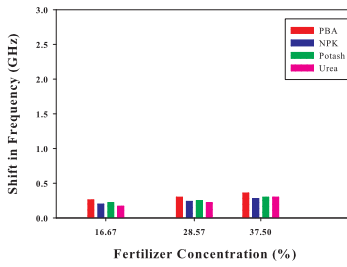
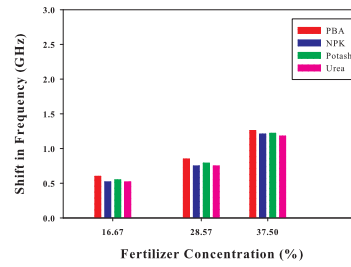


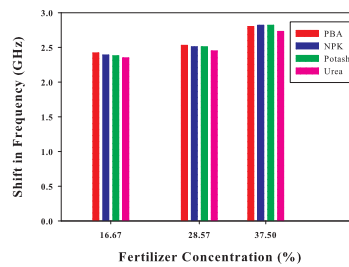
Figure 5.23: Shift in frequency vs. fertilizer concentration for soil (pH=5.7) mixed with 0 ml, 1 ml & 2 ml MC; all fertilizers; C-band; Sensor Antenna Method



(a) pH=5.8, MC=0 ml



(b) pH=5.8, MC=1 ml



(c) pH=5.8, MC=2 ml

Figure 5.24: Shift in frequency vs. fertilizer concentration for soil (pH=5.8, sample a) mixed with 0 ml, 1 ml & 2 ml MC; all fertilizers; C-band; Sensor Antenna Method

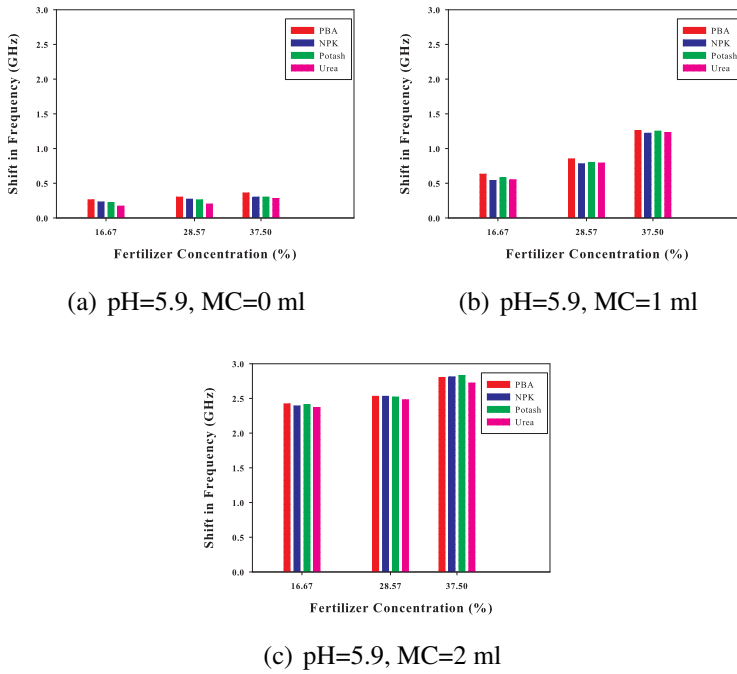
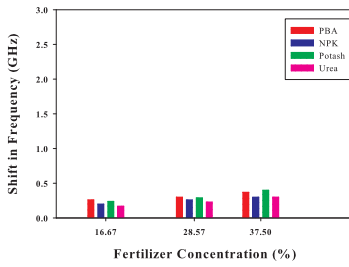
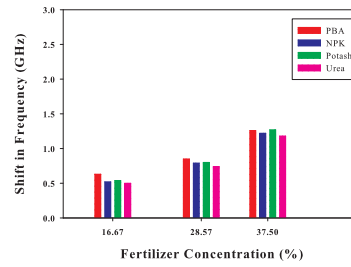


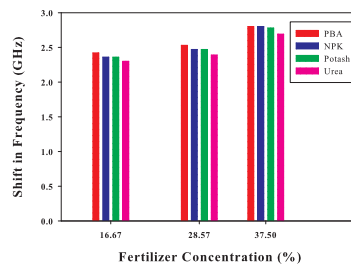
Figure 5.25: Shift in frequency vs. fertilizer concentration for soil (pH=5.9) mixed with 0 ml, 1 ml & 2 ml MC; all fertilizers; C-band; Sensor Antenna Method



(a) pH=6.1, MC=0 ml



(b) pH=6.1, MC=1 ml



(c) pH=6.1, MC=2 ml

Figure 5.26: Shift in frequency vs. fertilizer concentration for soil (pH=6.1) mixed with 0 ml, 1 ml & 2 ml MC; all fertilizers; C-band; Sensor Antenna Method

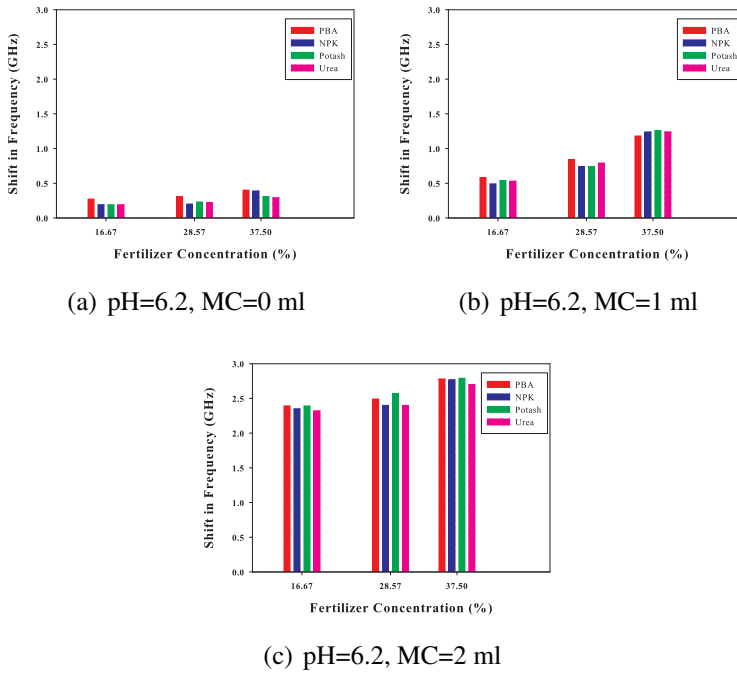
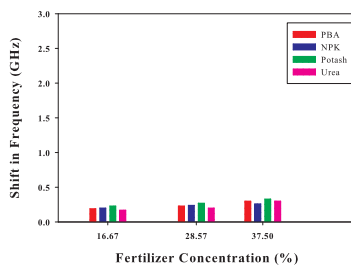
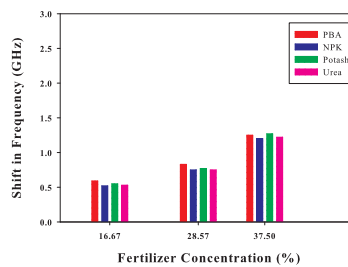


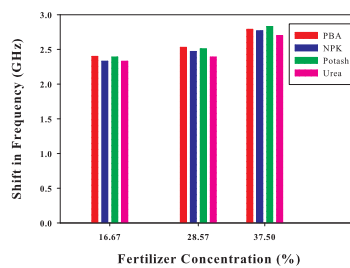
Figure 5.27: Shift in frequency vs. fertilizer concentration for soil (pH=6.2, sample a) mixed with 0 ml, 1 ml & 2 ml MC; all fertilizers; C-band; Sensor Antenna Method



(a) pH=6.3, MC=0 ml

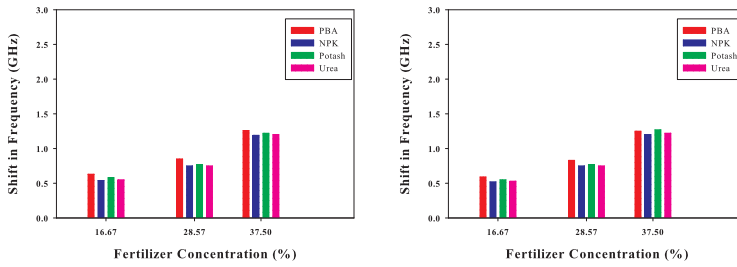


(b) pH=6.3, MC=1 ml



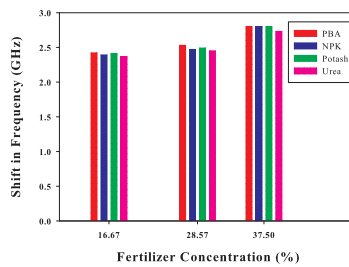
(c) pH=6.3, MC=2 ml

Figure 5.28: Shift in frequency vs. fertilizer concentration for soil (pH=6.3, sample a) mixed with 0 ml, 1 ml & 2 ml MC; all fertilizers; C-band; Sensor Antenna Method



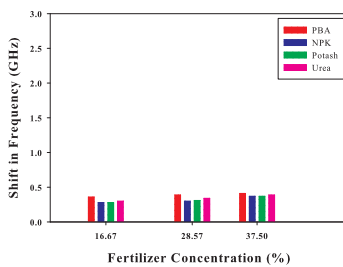
(a) pH=6.4, MC=0 ml

(b) pH=6.4, MC=1 ml

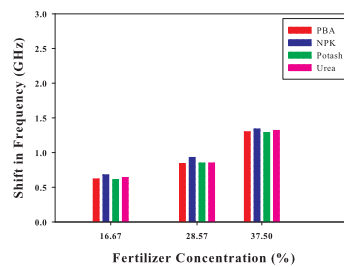


(c) pH=6.4, MC=2 ml

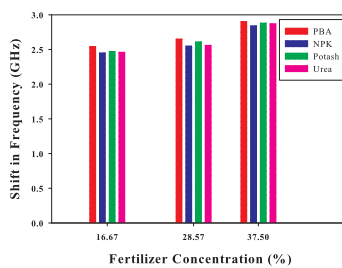
Figure 5.29: Shift in frequency vs. fertilizer concentration for soil (pH=6.4, sample a) mixed with 0 ml, 1 ml & 2 ml MC; all fertilizers; C-band; Sensor Antenna Method



(a) pH=7.0, MC=0 ml

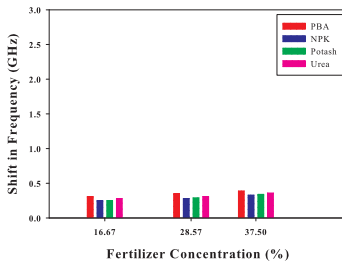


(b) pH=7.0, MC=1 ml

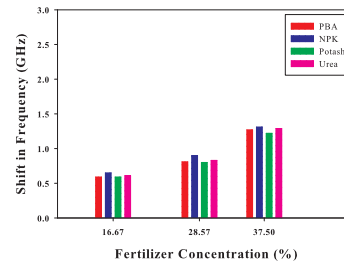


(c) pH=7.0, MC=2 ml

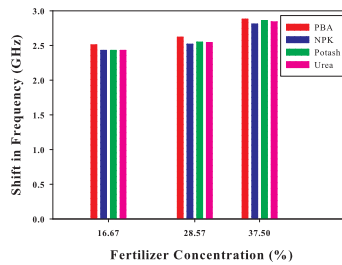
Figure 5.30: Shift in frequency vs. fertilizer concentration for soil (pH=7.0, sample a) mixed with 0 ml, 1 ml & 2 ml MC; all fertilizers; C-band; Sensor Antenna Method



(a) pH=7.1, MC=0 ml

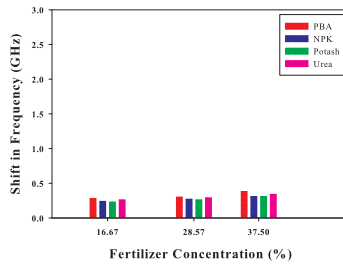


(b) pH=7.1, MC=1 ml

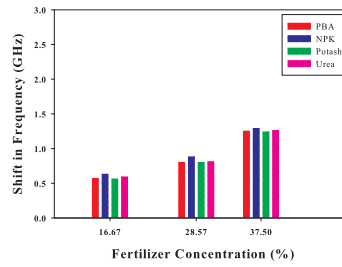


(c) pH=7.1, MC=2 ml

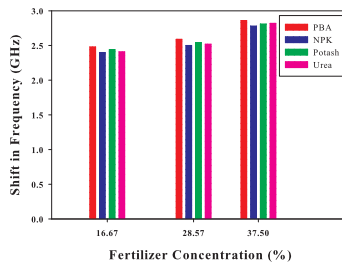
Figure 5.31: Shift in frequency vs. fertilizer concentration for soil (pH=7.1, sample a) mixed with 0 ml, 1 ml & 2 ml MC; all fertilizers; C-band; Sensor Antenna Method



(a) pH=7.2, MC=0 ml

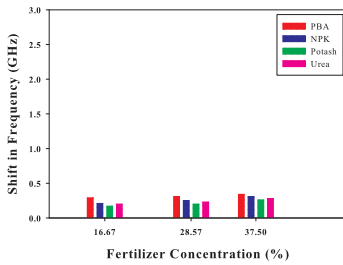


(b) pH=7.2, MC=1 ml

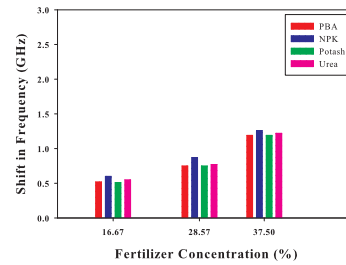


(c) pH=7.2, MC=2 ml

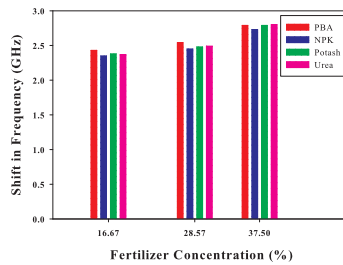
Figure 5.32: Shift in frequency vs. fertilizer concentration for soil (pH=7.2, sample a) mixed with 0 ml, 1 ml & 2 ml MC; all fertilizers; C-band; Sensor Antenna Method



(a) pH=7.3, MC=0 ml

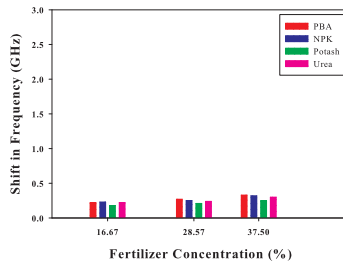


(b) pH=7.3, MC=1 ml

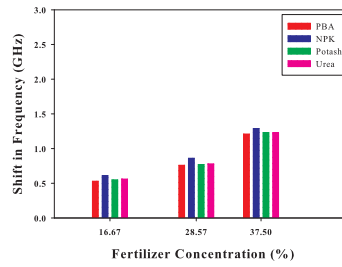


(c) pH=7.3, MC=2 ml

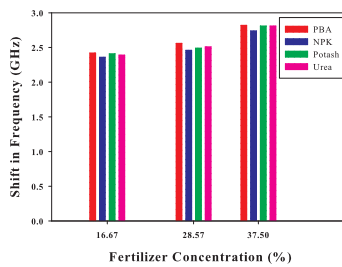
Figure 5.33: Shift in frequency vs. fertilizer concentration for soil (pH=7.3, sample a) mixed with 0 ml, 1 ml & 2 ml MC; all fertilizers; C-band; Sensor Antenna Method



(a) pH=7.4, MC=0 ml



(b) pH=7.4, MC=1 ml



(c) pH=7.4, MC=2 ml

Figure 5.34: Shift in frequency vs. fertilizer concentration for soil (pH=7.4, sample a) mixed with 0 ml, 1 ml & 2 ml MC; all fertilizers; C-band; Sensor Antenna Method

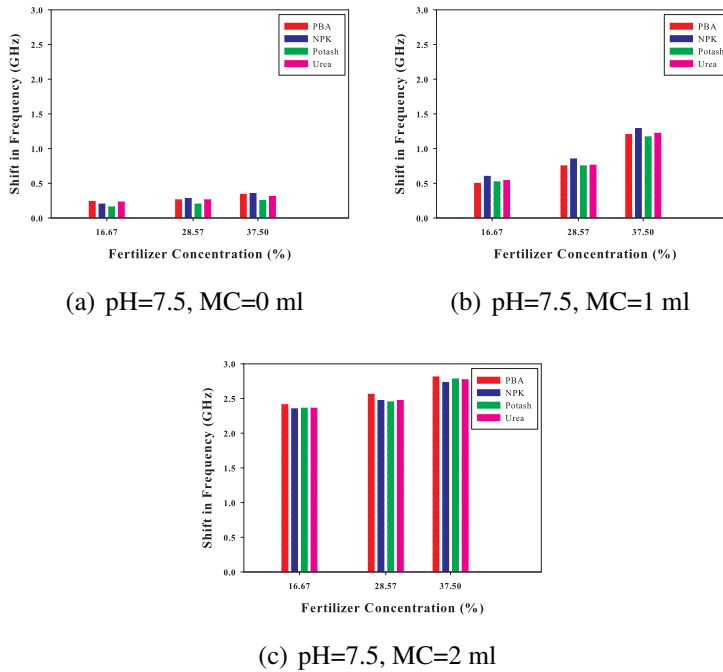


Figure 5.35: Shift in frequency vs. fertilizer concentration for soil (pH=7.5, sample a) mixed with 0 ml, 1 ml & 2 ml MC; all fertilizers; C-band; Sensor Antenna Method

In Chapter 4, wherein free-space transmission method was used to characterize soil, it was observed that as the moisture content (MC) in soil increases, dielectric constant of soil-moisture mixtures also increases (Tables 4.4 to 4.6). The same dependence of dielectric constant of soil-fertilizer mixtures was evident as per Tables 4.29 to 4.31. Thus microwave parameters of soil (such as its dielectric constant) and soil-constituents (moisture and fertilizers) were found to have a relationship with the characteristics of the transmitting/receiving antennas. The results obtained in this chapter reveal that there is a larger shift in resonant frequency of the sensor antenna as concentration of fertilizers and MC in soil increase. Since this change is identical to the one observed for the variation of dielectric constant of soil-moisture

and soil-fertilizer mixtures, a relationship between frequency-shift of the sensor antenna and soil parameters can be established.

Frequency-shift is also seen to depend on the type of fertilizer used. The largest frequency shift is noted for PBA, which has the highest dielectric constant among the four fertilizers used, as given in Table 4.32. The experimental observations also imply that an increase in the fertilizer concentration (FC) improves the moisture-retention capacity and increase in moisture content (MC) increases the fertilizer-absorption capability of soil.

5.4 Analytical Models

With a view to analyzing the results obtained in the previous section, two models are developed using the values of frequency shifts (Δf). The first model uses an ANN structure; the second is based on regression analysis. The two models are described below.

5.4.1 ANN Model

Here, a multilayered ANN based on the Levenberg-Marquardt algorithm, as explained in Section 4.2.5, is used. The structure of the ANN model is shown in Fig. 5.36.



Figure 5.36: Structure of the feed-forward neural network

It is a single feed-forward model, with 2 hidden layers having 20 and 10 neurons respectively. Shift in frequency corresponding to the entire set of 20 distinct soil samples mixed with all the four fertilizers

for varying fertilizer-moisture content forms the training data-set. The training, validation and testing ratios are fixed as 90, 7 and 3 %. The shift in frequency corresponding to the three fertilizer concentrations forms the input data. The output consists of the corresponding moisture content (MC). Training and testing of data are carried out using MATLAB[®]. Tables 5.9 to 5.20 list the MC values - actual & evaluated using the ANN model - and the corresponding error for 6 soil types (pH=4.7, 5.3, 6.4, 7.0, 7.2 & 7.5, all sample a).

A Graphical User Interface (GUI), developed using MATLAB[®] to make the program user-friendly is shown in Fig. 5.37.

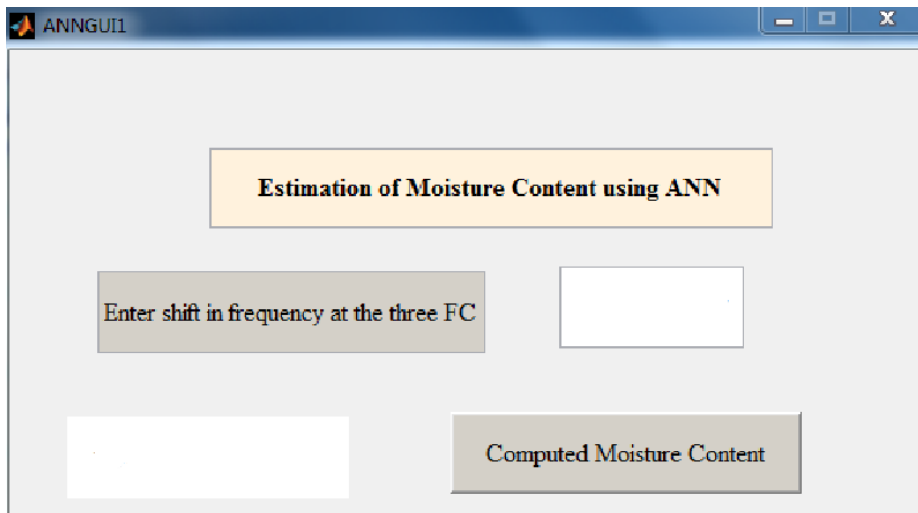


Figure 5.37: GUI used for Moisture Content estimation; ANN Model; Sensor Antenna Method

Table 5.9: Error in the actual and evaluated values of MC for soil [pH=4.7 (sample a)] mixed with **PBA & NPK**; C-band; Sensor Antenna Method

FC (%)	PBA				NPK			
	Δf	MC (ml)		Error	Δf	MC (ml)		Error
		Actual	ANN			Actual	ANN	
16.67	0.34	0	0.0016	0.0016	0.29	0	0.0005	0.0005
28.57	0.38	0	0.0012	0.0012	0.32	0	0.0007	0.0007
37.50	0.42	0	0.0089	0.0089	0.38	0	0.0012	0.0012
16.67	0.68	1	0.9979	0.0021	0.62	1	1.0009	0.0009
28.57	0.93	1	1.0002	0.0002	0.84	1	1.0000	0.0000
37.50	1.34	1	1.0090	0.0090	1.30	1	0.9997	0.0003
16.67	2.51	2	2.0000	0.0000	2.46	2	2.0000	0.0000
28.57	2.62	2	2.0000	0.0000	2.56	2	2.0001	0.0001
37.50	2.90	2	2.0010	0.0010	2.87	2	1.9992	0.0008

Table 5.10: Error in the actual and evaluated values of MC for soil [pH=4.7 (sample a)] mixed with **Potash & Urea**; C-band; Sensor Antenna Method

FC (%)	Potash				Urea			
	Δf	MC (ml)		Error	Δf	MC (ml)		Error
		Actual	ANN			Actual	ANN	
16.67	0.30	0	0.0004	0.0004	0.28	0	0.0002	0.0002
28.57	0.34	0	0.0016	0.0016	0.31	0	0.0001	0.0001
37.50	0.39	0	0.0030	0.0030	0.37	0	0.0002	0.0002
16.67	0.64	1	1.0006	0.0006	0.61	1	1.0009	0.0009
28.57	0.85	1	1.0004	0.0004	0.83	1	0.9995	0.0005
37.50	1.32	1	0.9996	0.0004	1.29	1	0.9999	0.0001
16.67	2.48	2	1.9996	0.0004	2.45	2	2.0004	0.0004
28.57	2.59	2	1.9994	0.0006	2.55	2	2.0003	0.0003
37.50	2.89	2	2.0001	0.0001	2.84	2	1.9993	0.0007

Table 5.11: Error in the actual and evaluated values of MC for soil [pH=5.3 (sample a)] mixed with **PBA & NPK**; C-band; Sensor Antenna Method

FC (%)	PBA				NPK			
	Δf	MC (ml)		Error	Δf	MC (ml)		Error
		Actual	ANN			Actual	ANN	
16.67	0.20	0	0.0002	0.0002	0.19	0	0.0000	0.0000
28.57	0.26	0	0.0005	0.0005	0.29	0	0.0005	0.0005
37.50	0.33	0	0.0013	0.0013	0.36	0	0.0012	0.0012
16.67	0.60	1	1.0007	0.0007	0.50	1	1.0050	0.0050
28.57	0.85	1	1.0004	0.0004	0.75	1	1.0000	0.0000
37.50	1.29	1	0.9999	0.0001	1.20	1	0.9998	0.0002
16.67	2.39	2	1.9995	0.0005	2.36	2	2.0000	0.0000
28.57	2.56	2	2.0001	0.0001	2.47	2	1.9997	0.0003
37.50	2.82	2	1.9997	0.0003	2.77	2	2.0005	0.0005

Table 5.12: Error in the actual and evaluated values of MC for soil [pH=5.3 (sample a)] mixed with **Potash & Urea**; C-band; Sensor Antenna Method

FC (%)	Potash				Urea			
	Δf	MC (ml)		Error	Δf	MC (ml)		Error
		Actual	ANN			Actual	ANN	
16.67	0.23	0	0.0003	0.0003	0.16	0	0.0009	0.0009
28.57	0.26	0	0.0005	0.0005	0.20	0	0.0002	0.0002
37.50	0.31	0	0.0001	0.0001	0.25	0	0.0004	0.0004
16.67	0.54	1	0.9984	0.0016	0.53	1	0.9991	0.0009
28.57	0.76	1	1.0006	0.0006	0.75	1	1.0000	0.0000
37.50	1.22	1	1.0001	0.0001	1.18	1	1.0002	0.0002
16.67	2.37	2	1.9996	0.0004	2.35	2	2.0005	0.0005
28.57	2.47	2	1.9997	0.0003	2.47	2	1.9997	0.0003
37.50	2.80	2	2.0002	0.0002	2.73	2	1.9994	0.0006

Table 5.13: Error in the actual and evaluated values of MC for soil [pH=6.4 (sample a)] mixed with **PBA & NPK**; C-band; Sensor Antenna Method

FC (%)	PBA				NPK			
	Δf	MC (ml)		Error	Δf	MC (ml)		Error
		Actual	ANN			Actual	ANN	
16.67	0.26	0	0.0005	0.0005	0.23	0	0.0003	0.0003
28.57	0.31	0	0.0001	0.0001	0.24	0	0.0000	0.0000
37.50	0.34	0	0.0016	0.0016	0.30	0	0.0004	0.0004
16.67	0.63	1	1.0008	0.0008	0.54	1	0.9984	0.0016
28.57	0.85	1	1.0004	0.0004	0.75	1	1.0000	0.0000
37.50	1.26	1	1.0000	0.0000	1.19	1	0.9998	0.0002
16.67	2.42	2	2.0005	0.0005	2.39	2	1.9995	0.0005
28.57	2.53	2	2.0003	0.0003	2.47	2	1.9997	0.0003
37.50	2.80	2	2.0002	0.0002	2.80	2	2.0002	0.0002

Table 5.14: Error in the actual and evaluated values of MC for soil [pH=6.4 (sample a)] mixed with **Potash & Urea**; C-band; Sensor Antenna Method

FC (%)	Potash				Urea			
	Δf	MC (ml)		Error	Δf	MC (ml)		Error
		Actual	ANN			Actual	ANN	
16.67	0.22	0	0.0004	0.0004	0.17	0	0.0005	0.0005
28.57	0.24	0	0.0000	0.0000	0.23	0	0.0003	0.0003
37.50	0.28	0	0.0002	0.0002	0.26	0	0.0005	0.0005
16.67	0.58	1	1.0001	0.0001	0.55	1	0.9986	0.0014
28.57	0.77	1	1.0007	0.0007	0.75	1	1.0000	0.0000
37.50	1.22	1	1.0001	0.0001	1.20	1	0.9998	0.0002
16.67	2.41	2	2.0001	0.0001	2.37	2	1.9996	0.0004
28.57	2.49	2	1.9997	0.0003	2.45	2	2.0004	0.0004
37.50	2.80	2	2.0002	0.0002	2.73	2	1.9994	0.0006

Table 5.15: Error in the actual and evaluated values of MC for soil [pH=7.0 (sample a)] mixed with **PBA & NPK**; C-band; Sensor Antenna Method

FC (%)	PBA				NPK			
	Δf	MC (ml)		Error	Δf	MC (ml)		Error
		Actual	ANN			Actual	ANN	
16.67	0.26	0	0.0005	0.0005	0.24	0	0.0002	0.0002
28.57	0.39	0	0.0004	0.0004	0.31	0	0.0005	0.0005
37.50	0.41	0	0.0002	0.0002	0.37	0	0.0004	0.0004
16.67	0.62	1	1.0008	0.0008	0.59	1	1.0013	0.0013
28.57	0.84	1	1.0004	0.0004	0.80	1	1.0000	0.0000
37.50	1.30	1	1.0000	0.0000	1.28	1	1.0001	0.0001
16.67	2.42	2	2.0005	0.0005	2.36	2	2.0000	0.0000
28.57	2.65	2	2.0003	0.0003	2.55	2	1.9997	0.0003
37.50	2.90	2	2.0002	0.0002	2.80	2	2.0002	0.0002

Table 5.16: Error in the actual and evaluated values of MC for soil [pH=7.0 (sample a)] mixed with **Potash & Urea**; C-band; Sensor Antenna Method

FC (%)	Potash				Urea			
	Δf	MC (ml)		Error	Δf	MC (ml)		Error
		Actual	ANN			Actual	ANN	
16.67	0.34	0	0.0000	0.0000	0.29	0	0.0005	0.0005
28.57	0.37	0	0.0005	0.0005	0.34	0	0.0003	0.0003
37.50	0.40	0	0.0044	0.0044	0.37	0	0.0004	0.0004
16.67	0.67	1	0.9984	0.0016	0.64	1	1.0050	0.0050
28.57	0.79	1	0.9995	0.0005	0.72	1	0.9990	0.0010
37.50	1.18	1	1.0000	0.0000	1.01	1	1.0002	0.0002
16.67	2.41	2	2.0000	0.0000	2.36	2	1.9976	0.0024
28.57	2.57	2	1.9997	0.0003	2.49	2	1.9995	0.0005
37.50	2.83	2	2.0006	0.0006	2.74	2	2.0011	0.0011

Table 5.17: Error in the actual and evaluated values of MC for soil [pH=7.2 (sample a)] mixed with **PBA & NPK**; C-band; Sensor Antenna Method

FC (%)	PBA				NPK			
	Δf	MC (ml)		Error	Δf	MC (ml)		Error
		Actual	ANN			Actual	ANN	
16.67	0.27	0	0.0003	0.0003	0.24	0	0.0000	0.0000
28.57	0.32	0	0.0001	0.0001	0.28	0	0.0002	0.0002
37.50	0.38	0	0.0044	0.0044	0.32	0	0.0030	0.0030
16.67	0.63	1	1.0001	0.0001	0.57	1	0.9906	0.0094
28.57	0.88	1	1.0000	0.0000	0.80	1	0.9990	0.0010
37.50	1.29	1	1.0002	0.0002	1.25	1	1.0001	0.0001
16.67	2.47	2	1.9995	0.0005	2.41	2	2.0005	0.0005
28.57	2.58	2	1.9997	0.0003	2.52	2	1.9998	0.0002
37.50	2.85	2	2.0006	0.0004	2.82	2	2.0005	0.0005

Table 5.18: Error in the actual and evaluated values of MC for soil [pH=7.2 (sample a)] mixed with **Potash & Urea**; C-band; Sensor Antenna Method

FC (%)	Potash				Urea			
	Δf	MC (ml)		Error	Δf	MC (ml)		Error
		Actual	ANN			Actual	ANN	
16.67	0.26	0	0.0000	0.0000	0.23	0	0.0000	0.0000
28.57	0.29	0	0.0003	0.0003	0.26	0	0.0004	0.0004
37.50	0.34	0	0.0001	0.0001	0.31	0	0.0005	0.0005
16.67	0.59	1	0.9984	0.0016	0.57	1	0.9991	0.0009
28.57	0.81	1	0.9990	0.0010	0.79	1	1.0001	0.0001
37.50	1.26	1	1.0000	0.0000	1.23	1	1.0001	0.0001
16.67	2.44	2	1.9995	0.0005	2.40	2	2.0012	0.0012
28.57	2.54	2	1.9999	0.0001	2.50	2	1.9998	0.0002
37.50	2.85	2	2.0005	0.0005	2.78	2	2.0007	0.0007

Table 5.19: Error in the actual and evaluated values of MC for soil [pH=7.5 (sample a)] mixed with **PBA & NPK**; C-band; Sensor Antenna Method

FC (%)	PBA				NPK			
	Δf	MC (ml)		Error	Δf	MC (ml)		Error
		Actual	ANN			Actual	ANN	
16.67	0.19	0	0.0000	0.0000	0.16	0	0.0002	0.0002
28.57	0.29	0	0.0003	0.0003	0.26	0	0.0000	0.0000
37.50	0.34	0	0.0004	0.0004	0.30	0	0.0005	0.0005
16.67	0.59	1	1.0005	0.0005	0.54	1	1.0013	0.0013
28.57	0.84	1	0.9995	0.0005	0.71	1	1.0000	0.0000
37.50	1.36	1	1.0001	0.0001	1.29	1	0.9998	0.0002
16.67	2.40	2	1.9998	0.0002	2.29	2	2.0014	0.0014
28.57	2.56	2	2.0003	0.0003	2.47	2	1.9997	0.0003
37.50	2.73	2	2.0005	0.0005	2.73	2	2.0005	0.0005

Table 5.20: Error in the actual and evaluated values of MC for soil [pH=7.5 (sample a)] mixed with **Potash & Urea**; C-band; Sensor Antenna Method

FC (%)	Potash				Urea			
	Δf	MC (ml)		Error	Δf	MC (ml)		Error
		Actual	ANN			Actual	ANN	
16.67	0.24	0	0.0003	0.0003	0.19	0	0.0005	0.0005
28.57	0.37	0	0.0003	0.0003	0.26	0	0.0002	0.0002
37.50	0.38	0	0.0013	0.0013	0.31	0	0.0004	0.0004
16.67	0.52	1	0.9986	0.0014	0.45	1	0.9991	0.0009
28.57	0.75	1	1.0007	0.0007	0.54	1	1.0000	0.0000
37.50	1.17	1	1.0000	0.0000	1.03	1	1.0001	0.0001
16.67	2.36	2	1.9995	0.0005	2.28	2	2.0014	0.0014
28.57	2.45	2	2.0000	0.0000	2.32	2	1.9995	0.0005
37.50	2.78	2	1.9994	0.0006	2.54	2	2.0007	0.0007

A screen-shot of MC values returned by the model for soil (pH=5.3, sample a) mixed with 37.5 % of PBA (Table 5.11) is shown in Fig. 5.38.

```
>> test_Fs_MC

Moisture_Content =

      1.9997      0.9999      0.0013
```

Figure 5.38: Screen-shot of MC for soil (**pH=5.3, sample a**) mixed with **PBA**; C-band; ANN Model; Sensor Antenna Method

The ANN model has been developed to analyze the effect of soil-fertilizer mixtures under varying moisture content (MC) on the sensor antenna. The model returns an MC value and compares it with the actual one. From the results, it is found that the model is able to predict the MC with a maximum error of 0.94 % irrespective of the fertilizer type and concentration. The largest shift in frequency is obtained as 2.90 GHz (Table 5.15). Any value exceeding this can be considered as arising out of a water-logged soil sample. It is presumed that there will not be a shift beyond this value using any commercial fertilizer or normal moisture content in soils of the regions, as enumerated in Table 4.1.

5.4.2 Regression Model

This chapter discussed how the characterization of soil mixed with fertilizers and moisture is carried out using the variation in resonant behaviour of a sensor antenna. The Moisture Content (MC) can be evaluated based on the shift in frequency (Δf) of the sensor. Regression Analysis, as a statistical tool to establish a relationship between two variables, was presented in 2.3.2. In this section, the two variables of interest are Δf & MC.

Regression Analysis is carried out on the entire set of 20 distinct soil samples mixed with the four fertilizers under three different concentrations of moisture and fertilizers. The dependence of MC upto

a cubic polynomial regression-fit of shift in frequency is obtained. An empirical relation between MC present in any of the soil samples and shift in frequency of the sensor is derived as given in Eqn. 5.2.

$$MC = 0.157977 \times \Delta f^3 - 0.96957 \times \Delta f^2 + 2.398608 \times \Delta f - 0.47837 \quad (5.2)$$

Table 5.21 shows the error (in %) of MC between the actual value and that computed using Eqn. 5.2 for soil samples (pH=5.1, 5.2, 5.4, 5.9 & 6.1) mixed with Potash and Urea.

Table 5.21: Error in the actual and empirically-obtained values of MC for soil [pH=5.1, 5.2, 5.4, 5.9 & 6.1] mixed with **Potash & Urea**; C-band; Sensor Antenna Method

Soil Sample	Fertilizer Type	Δf	MC		Error %
			Actual	Empirical	
5.1	Potash	2.63	2	1.997381	0.1
5.1	Urea	2.58	2	1.969213	1.5
5.2	Potash	2.81	2	2.111097	5.6
5.2	Urea	2.74	2	2.064389	3.2
5.4	Potash	2.49	2	1.921621	3.9
5.4	Urea	2.45	2	1.901605	4.9
5.9	Potash	2.36	2	1.858718	7.1
5.9	Urea	2.30	2	1.831509	8.4
6.1	Potash	2.39	2	1.872712	6.4
6.1	Urea	2.32	2	1.840472	8.0

The statistical measures for goodness-of-fit such as coefficient of determination (R-squared) and significance (P-value) between the parameters MC and Δf are noted (Buse, 1973). A high R-squared value of 93.66% and low P-values (of the order of 10^{-63} , 10^{-19} and 10^{-10} respectively on the linear, quadratic and cubic powers of Δf) obtained suggest that the proposed model has a highly valid goodness-of-fit.

Validation of the analytical models

The two analytical models developed have used the shift in resonant frequency (Δf) of the C-band sensor to compute the moisture content

(MC) in soil samples. The ANN model returns the MC value if the Δf corresponding to any soil sample is given as input. In the regression model, MC and Δf are related as given in Equation 5.2.

In Chapters 3, 4 & 5, dielectric constant (ϵ'_r) of soil samples - both dry and under different moisture content and fertilizer concentration - at the L, S and C bands in the regions under test was reported. Thus, since the ϵ'_r is known, the Volumetric Water Content (θ_v) of any sample can be computed using Topp's Equation, as given below.

$$\theta_v = 4.3 \times 10^{-6} \times \epsilon_r'^3 - 5.5 \times 10^{-4} \times \epsilon_r'^2 + 2.92 \times 10^{-2} \times \epsilon_r' - 5.3 \times 10^{-2} \quad (5.3)$$

θ_v corresponding to the MC obtained from the two models is computed. Validation of the results obtained using the two models is done by comparing the results with θ_v computed using Topp's Equation. Tables 5.22 to 5.25 show the comparison for a set of dry soil samples (MC=0 ml) for the C-band sensor antenna. Here, results already obtained for soil types (pH=4.7, 5.3, 6.4, 7.0, 7.2 & 7.5, all sample a) with fertilizer-soil mixture ratio of 16.67 % are considered.

θ_v for any moisture content in fertilizer-soil mixture is computed as in Eqn. 5.4.

$$\theta_v = \frac{MC_R}{\text{Volume of fertilizer} + \text{Volume of moisture} + \text{Volume of soil}} \quad (5.4)$$

where MC_R is the moisture content obtained using regression analysis.

Thus, θ_v for MC=0ml (inherent moisture content with no added moisture) is computed as in Eqn. 5.5.

$$\theta_v[MC = 0ml] = \frac{MC_R}{6} \quad (5.5)$$

where the factor 6 indicates that the fertilizer-soil mixture ratio of 16.67 % corresponds to 1 ml fertilizer in 5 ml dry soil.

Table 5.22: Comparison of θ_v values for **PBA-mixed** dry soil samples (MC=0 ml)

pH of soil sample	ϵ'_r	Δf	θ_v computed using		
			Topp's Equation	ANN Model	Regression Model
4.7	3.84	0.34	0.0513	0.00027	0.03855
5.3	3.60	0.20	0.0452	0.00003	0.00603
6.4	3.68	0.26	0.0472	0.00008	0.01375
7.0	3.32	0.26	0.0380	0.00008	0.01375
7.2	3.74	0.27	0.0487	0.00005	0.01695
7.5	3.28	0.19	0.0370	0.00000	0.00943

Table 5.23: Comparison of θ_v values for **NPK-mixed** dry soil samples (MC=0 ml)

pH of soil sample	ϵ'_r	Δf	θ_v computed using		
			Topp's Equation	ANN Model	Regression Model
4.7	3.84	0.29	0.0513	0.00008	0.02326
5.3	3.60	0.19	0.0452	0.00000	0.00943
6.4	3.68	0.23	0.0472	0.00005	0.00399
7.0	3.32	0.20	0.0380	0.00003	0.00603
7.2	3.74	0.19	0.0487	0.00000	0.00943
7.5	3.28	0.20	0.0370	0.00003	0.00603

13

Table 5.24: Comparison of θ_v values for **Potash-mixed** dry soil samples (MC=0 ml)

pH of soil sample	ϵ'_r	Δf	θ_v computed using		
			Topp's Equation	ANN Model	Regression Model
4.7	3.84	0.30	0.0513	0.00007	0.02637
5.3	3.60	0.23	0.0452	0.00005	0.00399
6.4	3.68	0.22	0.0472	0.00007	0.00068
7.0	3.32	0.24	0.0380	0.00000	0.00727
7.2	3.74	0.19	0.0487	0.00000	0.00943
7.5	3.28	0.23	0.0370	0.00005	0.00399

Table 5.25: Comparison of θ_v values for **Urea-mixed** dry soil samples (**MC=0ml**)

pH of soil sample	ϵ'_r	Δf	θ_v computed using		
			Topp's Equation	ANN Model	Regression Model
4.7	3.84	0.28	0.0513	0.00003	0.02012
5.3	3.60	0.16	0.0452	0.00015	0.01979
6.4	3.68	0.17	0.0472	0.00008	0.01631
7.0	3.32	0.17	0.0380	0.00008	0.01631
7.2	3.74	0.19	0.0487	0.00000	0.00943
7.5	3.28	0.17	0.0370	0.00008	0.01631

Similarly, Tables 5.26 to 5.29 show the comparison for a set of moist soil samples (MC=2 ml) for the same sensor, soil types and fertilizer-soil mixture ratio. Eqn. 5.6 gives the corresponding θ_v for MC=2 ml.

$$\theta_v[MC = 2ml] = \frac{MC_R}{8} \quad (5.6)$$

Here the fertilizer-soil mixture ratio of 16.67 % corresponds to 1 ml fertilizer in 5 ml soil mixed with 2 ml moisture, giving a factor of 8 in the denominator.

Table 5.26: Comparison of θ_v values for **PBA-mixed** moist soil samples (**MC=2 ml**)

pH of soil sample	ϵ'_r	Δf	θ_v computed using		
			Topp's Equation	ANN Model	Regression Model
4.7	13.37	2.51	0.2494	0.2500	0.2415
5.3	13.04	2.39	0.2438	0.2499	0.2341
6.4	13.19	2.42	0.2463	0.2501	0.2359
7.0	12.96	2.42	0.2424	0.2501	0.2359
7.2	13.32	2.39	0.2485	0.2499	0.2341
7.5	12.48	2.40	0.2341	0.2500	0.2347

Table 5.27: Comparison of θ_v values for **NPK-mixed** moist soil samples (**MC=2 ml**)

pH of soil sample	ϵ'_r	Δf	θ_v computed using		
			Topp's Equation	ANN Model	Regression Model
4.7	13.37	2.46	0.2494	0.3333	0.23832
5.3	13.04	2.36	0.2438	0.2500	0.23234
6.4	13.19	2.39	0.2463	0.2499	0.23409
7.0	12.96	2.36	0.2424	0.2500	0.23234
7.2	13.32	2.35	0.2485	0.2500	0.23176
7.5	12.48	2.33	0.2341	0.2501	0.23062

Table 5.28: Comparison of θ_v values for **Potash-mixed** moist soil samples (**MC=2 ml**)

pH of soil sample	ϵ'_r	Δf	θ_v computed using		
			Topp's Equation	ANN Model	Regression Model
4.7	13.37	2.48	0.2494	0.2499	0.23957
5.3	13.04	2.37	0.2438	0.2499	0.23292
6.4	13.19	2.41	0.2463	0.2500	0.23528
7.0	12.96	2.36	0.2424	0.2500	0.23234
7.2	13.32	2.39	0.2485	0.2499	0.23409
7.5	12.48	2.39	0.2341	0.2499	0.23409

Table 5.29: Comparison of θ_v values for **Urea-mixed** moist soil samples (**MC=2 ml**)

pH of soil sample	ϵ'_r	Δf	θ_v computed using		
			Topp's Equation	ANN Model	Regression Model
4.7	13.37	2.45	0.2494	0.2501	0.23770
5.3	13.04	2.35	0.2438	0.2501	0.23176
6.4	13.19	2.37	0.2463	0.2499	0.23292
7.0	12.96	2.30	0.2424	0.2497	0.22894
7.2	13.32	2.32	0.2485	0.2502	0.23006
7.5	12.48	2.33	0.2341	0.2502	0.23062

These results can be used to assess the condition of soil in terms of an MC-scale ranging from 0 to 2 (totally dry to water-logged). Soil having MC values close to zero can be considered as dry and those above 2, as water-logged. Closeness of MC values to 0 ml and 2 ml in Tables 5.25 and 5.29 respectively suggests that the models developed give results to decide whether to start irrigation or not. If the type of crop best-suited in these regions is known a priori, it will be beneficial for the farmers to not only provide irrigation of his land based on the moisture content, but to apply other nutrients or change his crop based on the evaluated fertilizer concentration as well.

5.5 Moisture detection using colour mapping

Microwave Imaging technique as a tool for colour-mapping of materials to detect embedded objects was discussed in Section 2.4. Detection of moisture in soil through the variation in S-parameter and consequent colour-mapping was explained in Section 4.2.6 using free-space transmission method. In this chapter, moisture detection in soil using the sensor antenna method is examined.

A rectangular soil sample holder of dimension $16.5 \text{ cm} \times 3.5 \text{ cm} \times 1.3 \text{ cm}$ is used and 50 ml soil is spread uniformly in it. In the experimental setup shown in Fig. 5.39, the sensor antenna connected to port 1 of the VNA is inserted into soil.

An array of 84 points in the form of 3 rows and 28 columns is considered along the holder. Water is added to locations (2,6) & (2,7) and (2,19) & (2,20) using a syringe. Water spreads into locations (2,5) & (2,8) and (2,18) & (2,21). The shift in resonant frequency of the sensor with respect to dry areas from locations (1,1) to (3,28) is noted.

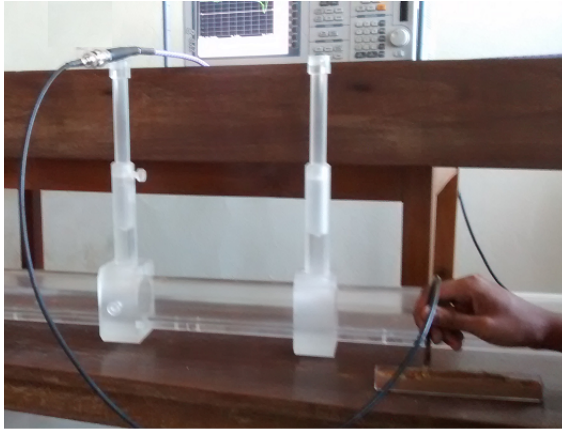


Figure 5.39: Experimental setup for moisture detection using colour-mapping; Sensor Antenna Method

Illustrative result of the colour-map due to the frequency-shifts, along with a camera shot of the holder with water added to soil is shown in Fig. 5.40. Plot shows that when more water is present, the shift in resonant frequency is more. The imaging method thus shows that the sensor is effective in detecting the presence of soil moisture.



Figure 5.40: Result for moisture detection using colour-mapping (a) Camera shot (b) Colour-map; Sensor Antenna Method

Integration of such sensors with communication modules will lead to remote characterization of soil as done in satellite-based sensing. For instance, the e-agriculture project in Kerala stresses on using Information Technology, through an Internet platform, in all stages of

agriculture crop-cycle by analyzing the current situation and making prediction for the future to support farmers (CIPS, 2006). A typical situation is illustrated in Fig. 5.41. This is also the essence of Precision Agriculture, as envisaged by the Ministry of Agriculture, Govt. of India (TechMah, 2016).

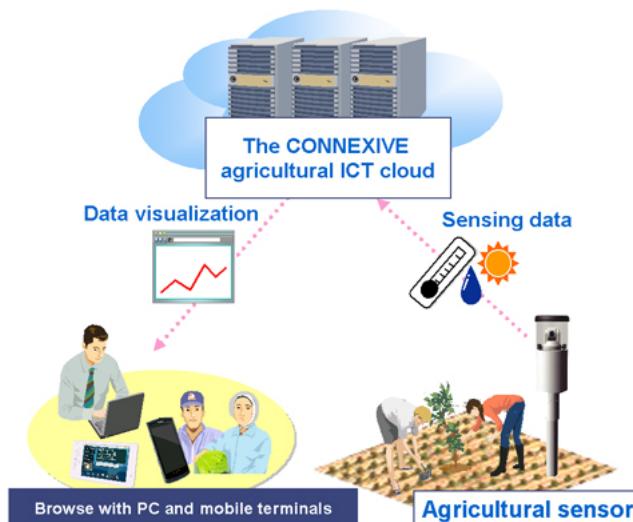


Figure 5.41: e-Agriculture Cycle (Courtesy : NEC Technologies India Pvt. Ltd.)

In such a scenario, a possible issue is the contamination of colour-mapped image with speckle-like noise. Hence despeckling of colour-mapped images has to be carried out. Appendix B discusses an algorithm to reduce speckle noise in images using a combined space-frequency domain approach.

5.6 Chapter Summary

This chapter presents the characterization of soil using sensor antenna method. The parameters monitored are the moisture content and fertilizer concentration using various soil samples available in

Ernakulam and Palakkad districts of Kerala. pH of soil samples under test varied from low-acidic (4.7) to moderate-alkaline (7.5). Commercially used fertilizers (PBA, NPK, Potash & Urea) are applied in varying concentrations. The effect of soil-fertilizer mixture and water in varying quantities on the resonant frequency of sensor antenna is evaluated. The need for an elaborate experimental setup involving two antennas and a sample-holder as in Free-space Transmission Method and issues in conventional methods such as Cavity Perturbation Method and Superstrate Method used for soil characterization are avoided in this approach. A preliminary simulation study is carried out using HFSS to ascertain the dependence of sensor antenna parameters on materials that come in its vicinity. Experiments are carried out with a setup using a sensor antenna embedded in soil and fertilizer/water mixture taken in a small plastic cup. Two models based on ANN and Regression are developed to analyze & compare the results obtained. The results given by the models are also validated by comparing them with θ_v from Topp's Equation. Microwave Imaging can be used as a potential tool for soil characterization. Shift in resonant frequency of the sensor antenna, plotted as a colour-map, is an indication of moist spots in soil.

These experiments revealed the following:

- Presence of moisture and its varying concentration in soil can be monitored using a sensor antenna.
- Presence of fertilizers and their varying concentration also can be monitored using a sensor antenna.
- An increase in the fertilizer concentration improves the moisture-retention capacity and increase in MC increases the fertilizer-absorption capability of soil.
- The sensor antenna method offers a minimally-invasive and compact scheme for soil characterization.

- One significant advantage with this method and the associated models developed is that there is no need to test the pH value of the soil sample. Hence all the associated pre-processing steps, such as drying, pulverizing etc. of soil samples under test, can be avoided.
- Microwave Imaging can be used as a potential tool for soil characterization. Shift in resonant frequency of the sensor antenna, plotted as a colour-map, is an indication of moist spots in soil.

The highlight of the chapter is the development of a regression equation relating the moisture content in soil with shift in resonant frequency of a C-band sensor antenna. This chapter also shows that sensors can be used to detect the presence of moisture using imaging. Hence remote characterization of soil can be done if sensors are integrated with communication modules. Thus these sensors can be used in real environment to find the dry or humid nature of soil for irrigation purpose. An array of such sensors embedded in a farmland can thus be used in precision agriculture without any human intervention.

Chapter 6

CONCLUSION

Contents

6.1 Thesis Highlights	205
6.2 Performance Comparison of the different methods for Soil Characterization	209
6.3 Suggestions for Future Work	210

6.1 Thesis Highlights

The thesis discusses methods for characterization of soil using microwaves. The importance of soil as a major life-supporting entity and the significance of soil moisture and fertilizer contents is also highlighted. The four main methods discussed for characterization are the Cavity Perturbation Method, Superstrate Method, Free-space Transmission Method and Sensor Antenna Method. Methods based on ANN model and Regression are adopted for analysis. Imaging technique for colour-mapping, used to characterize material for

detecting embedded matter, is extended to soil for detecting moist patches.

Highlights of the thesis are as follows.

- Confirmation of the use of microwaves in the characterization of soil
- Experimental validation of results for soil characterization using Cavity Perturbation Method, Superstrate Method, Free-space Transmission Method and Sensor Antenna Method
- Estimation of moisture and fertilizer content in soil from the outcome of the above experiments
- Experimental compilation of dielectric constant of soil samples in two major regions under test of Kerala, namely Ernakulam and Palakkad districts
 - Soil Testing Laboratory at Nettur in Ernakulam provided 20 varieties of 37 acidic soil samples with pH ranging from 3.4 to 6.4 [6 samples with pH=3.4 to 5.1 (Table 3.1) and 31 samples with pH=4.7 to 6.4 (Table 4.1)]
 - 6 varieties of 31 alkaline soil samples with pH ranging from 7.0 to 7.5 were supplied by the Soil Testing Laboratory at Pattambi in Palakkad [Table 4.1]
- Recognizing the fact that moisture and its varying concentration increase the dielectric constant of soil
- Realizing the fact that fertilizers and their varying concentration will increase/decrease the dielectric constant of soil
- Understanding the inverse relationship between dielectric constant of soil and microwave frequency, for any given moisture and fertilizer concentration

- Validation of experimental methods using Topp's Equation relating dielectric constant and volumetric water content
- Observing experimentally that the free-space transmission and sensor antenna methods offer simple and convenient schemes for soil characterization
- Figuring out that Microwave Imaging using simple colour-mapping technique can be used as a potential tool for soil characterization
- Development of ANN model for soil characterization in the L, S and C bands
 - to estimate Volumetric Water Content (θ_v) of soil samples, using Free-space Transmission Method
 - to estimate Fertilizer Concentration (FC) in soil, using Free-space Transmission Method
 - to estimate Moisture Content (MC) of varying soil fertilizer/moisture mixture, using Sensor Antenna Method
- Formulation of an empirical relation between the moisture content in soil and shift in resonant frequency of a C-band sensor antenna, using Regression Analysis
- Foreseeing that an array of microwave sensors embedded in a farmland can be used for precision agriculture without human intervention.

A major societal application of the thesis is the assistance and timely information that can be provided to farmers on when and how much to irrigate and supply nutrients. Also a knowledge about the dielectric constant, and in turn the moisture and fertilizer contents in soil, can help in deciding whether his land is cultivable or not and to take appropriate measures to improve productivity. Thus this work is expected to be beneficial to all those who are involved in agriculture.

An introduction to material characterization using microwaves was given in **Chapter 1**. Microwave properties of materials and soil were presented. A literature review on relevant topics connected with material characterization and microwave imaging for soil characterization was presented. The chapter ended by explaining the motivation and objectives of the work and presented the organization of the thesis.

Chapter 2 focussed on the methodologies adopted in this work. Different measurement and analytical methods for material characterization were explained in this chapter. Imaging method for colour-mapping was also explained.

Different methods for the determination of microwave properties of soil were explained in **Chapters 3 to 6**. **Chapter 3** discussed the characterization of soil using the two traditional methods, namely the Cavity Perturbation Method and the Superstrate Method. Simulation as well as experimental results were also presented and discussed in detail.

Chapter 4 discussed the characterization of soil using the Free-space Transmission Method. Computation of dielectric constant of soil samples was also carried out. Simulation as well as experimental results for the characterization of soil in the presence of moisture and fertilizers were presented. Colour-mapping as a tool to detect the presence of moisture in soil was illustrated. The chapter discussed an analytical method using an Artificial Neural Network (ANN) model for moisture content estimation and the results were validated.

Chapter 5 discussed the characterization of soil using the Sensor Antenna Method. Dielectric constant of soil samples with varying soil-fertilizer mixture-ratios and moisture content was computed. Simulation as well as experimental results for soil-characterization in the presence of moisture and fertilizers were explained. The chapter also discussed moisture detection in soil using sensor antenna and colour-mapping. ANN and Regression models for added moisture and fertilizer contents were presented. A regression equation relating the moisture content in soil with shift in resonant frequency of a sensor antenna was developed.

Chapter 6 summarizes the highlights of the research work. Performance comparison of the various methods and suggestions for future studies are also presented.

6.2 Performance Comparison of the different methods for Soil Characterization

Tables 6.1 & 6.2 compare the different methods outlined in the thesis for soil characterization.

Table 6.1: Performance Comparison for Soil Characterization; Measurement Methods

Description	Measurement Methods			
	Cavity Perturbation Method	Superstrate Method	Free-space Transmission Method	Sensor Antenna Method
Soils used	6 acidic	3 (Red, White and Black)	62 (31 acidic, 31 alkaline)	62 (31 acidic, 31 alkaline)
Source of soil samples	Soil Testing (ST) Lab at Nettur	Geotechnical Lab, CUSAT Soil Conservation Office, Ernakulam	ST Labs at Nettur & Pattambi	ST Labs at Nettur & Pattambi
Frequency band(s)	S band	L, S & C bands	L, S & C bands	L, S & C bands
Parameters monitored	Dielectric Constant (ϵ'_r)	Frequency, Normalized Impedance	Phase-variation ($\Delta\phi$) Dielectric Constant (ϵ'_r), Volumetric Water Content (θ_v), Fertilizer Concentration (FC)	Frequency-shift (Δf) Dielectric Constant (ϵ'_r), Moisture Content (MC) Fertilizer Concentration (FC)
Relevant results	Confirmation of Soil Characterization using Microwaves, Validation of material ϵ'_r , Compilation of soil ϵ'_r	Confirmation of Soil Characterization using Microwaves	Soil Characterization using Microwaves, Compilation of Soil ϵ'_r (plain and with varying MC & FC)	Soil Characterization using Microwaves, Compilation of Soil ϵ'_r (plain and with varying MC & FC)

Table 6.2: Performance Comparison for Soil Characterization; Analytical Methods

Description	Analytical Methods		
	ANN	Regression	Colour-mapping
Soils used	62 (31 acidic, 31 alkaline)	62 (31 acidic, 31 alkaline)	62 (31 acidic, 31 alkaline)
Frequency bands	L, S & C bands	L, S & C bands	L, S & C bands
Measurement method(s) supported	Free-space Transmission Method, Sensor Antenna Method	Sensor Antenna Method	Free-space Transmission Method, Sensor Antenna Method
Parameters monitored	Dielectric Constant (ϵ'_r), Volumetric Water Content (θ_v)	Frequency-shift (Δf), Moisture Content (MC)	Transmission coefficient (S_{21}), Moisture Content (MC)
	Dielectric Constant (ϵ'_r), Soil-fertilizer mixture ratio		Frequency-shift (Δf), Moisture Content (MC)
Relevant results	Validation of Measurement Methods	Validation of Sensor Antenna Method, Formulation of Equation relating MC & Δf	Validation of Measurement Methods, Detection of Embedded Objects & Moisture in Soil

6.3 Suggestions for Future Work

The work presented in this thesis is restricted to characterizing the surface moisture which is in the upper 10 cm of soil. Though this is sufficient for most of the geological and atmospheric studies, an improvement in sensitivity of the sensor antenna structures used can provide characterization of root-zone soil also. Two analytical tools based on ANN and Regression models are developed. The suitability of better sensitive antennas and more intelligent mathematical models to characterize soils in microwave bands can be explored. Employing a grid array of sensors and integrating them with communication modules will allow for remote characterization of soil as is practised in satellite-based sensing.

Appendices

Appendix A

SOIL MOISTURE CONTENT MEASUREMENT USING RESISTANCE-PROBES

A.1 Introduction

Soil moisture sensor (or hygrometer) is used to detect or monitor moisture content in soil. If used in conjunction with a microcontroller-based intelligent system, sensors can be used for smart agricultural purposes wherein the irrigation process is controlled based on data obtained from them. This serves a two-fold purpose: optimal use of water and prevent damage of crops. Also, variability in the supply of water can be done, as different crops require varying amounts of water for cultivation. A farmer can bury sensors at different depths along the root of a plant or in soil-bed. Doing so he can determine whether water has reached the lowest level of root or it has seeped much below the root level resulting in wastage or if stagnation has occurred at a certain level in soil. Similarly these sensors are used in urban planning, in researches to improve soil and crop-quality, local gardening in house plantations, horticulture, climatic studies, etc.

A.2 Experimental setup and Results

The sensor used is YL-69 Soil Moisture Sensor. It is shown in Fig. A.1 and can be interfaced with Arduino microcontroller board.

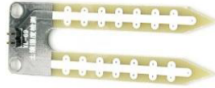


Figure A.1: YL-69 Soil Moisture Sensor

It uses two copper strips or probes embedded in a PCB and painted with epoch paint on both sides for better conductivity. Also, one of the probes of the sensor is made up of aluminium and the other one coated with polyaniline nanoparticles for better conductivity. The sensor is used for both dry and wet sensing. It senses the level of water in the soil into which it is inserted by measuring the soil resistance.

The sensor uses the two probes to pass current through the soil. More water makes the soil conduct electricity more easily giving less resistance, while dry soil conducts electricity poorly.

Overall dimension of the sensor is $6\text{ cm} \times 2\text{ cm} \times 5\text{ mm}$; its typical electrical specifications are:

- **Operating voltage:** DC 3.3 V to 5 V
- **Output voltage signal:** 0 V to 3.5 V - 4.2 V
- **Current:** 35 mA
- **LED:** Power indicator (Red) and Digital switching output indicator (Green)

The sensing unit has two parts: the basic sensor with the two strips, that detects the moisture content is at the left and the electronic board with potentiometer is at the right, as shown in Fig. A.2. The electronic board has sensitivity adjustment of the digital output (D0), a power LED and a digital output LED.



Figure A.2: Soil Moisture Sensing Unit with Electronic Board

ATmega328 microcontroller-based Arduino Uno circuit is used to interface with the sensing unit. The overall experimental setup with the sensing unit, electronic board and Arduino circuit is shown in Fig. A.3.

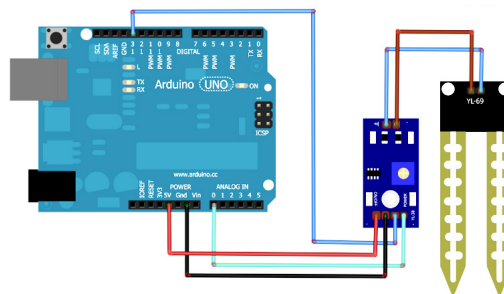


Figure A.3: Experimental setup for Sensing Soil Moisture using YL-69 Sensor and Arduino Uno Board

As mentioned in Section 5.3, the efficacy of the sensor antenna discussed there is compared with the YL-69 sensor module. For this, water is added to 20 ml of 10 different soil samples (5 acidic and 5 alkaline from the regions under test). Ten cases of water-mixing are considered, with moisture content ranging from 0 % (dry) to 31.03 % (water-logged). Resistance of the sensing unit changes in accordance with the water content in soil. As mentioned earlier, it is maximum when the soil is dry and reduces as water is added. The parameter returned by the experimental setup is denoted as R , which is related to the resistance offered by the soil under test. Results obtained using the

sensor antenna resonant at 4.48 GHz and YL-69 Sensor Module Probe (SMP), showing the shift in resonant frequency of the former and shift in R value of the latter for all the cases and soil samples are tabulated in Tables A.1 to A.5.

Table A.1: Comparison of results obtained for soil samples **pH=4.7 & 4.9** using Sensor Antenna and SMP for varying moisture content

MC (ml)	MC (%)	pH=4.7				pH=4.9			
		Sensor Antenna		SMP		Sensor Antenna		SMP	
		f (GHz)	Δf (GHz)	R	ΔR	f (GHz)	Δf (GHz)	R	ΔR
0	0	4.220	0.260	102	0	4.240	0.240	102	0
1	4.76	3.975	0.505	99	3	3.995	0.485	99	3
2	9.09	3.940	0.540	96	6	3.960	0.520	96	6
3	13.04	3.905	0.575	92	10	3.925	0.555	92	10
4	16.67	3.870	0.610	89	13	3.890	0.590	89	13
5	20.00	3.835	0.645	86	16	3.855	0.625	86	16
6	23.08	3.746	0.734	81	21	3.766	0.714	81	21
7	25.93	3.716	0.764	78	24	3.736	0.744	78	24
8	28.57	3.660	0.820	72	30	3.680	0.800	72	30
9	31.03	3.488	0.992	67	35	3.508	0.972	67	35

Table A.2: Comparison of results obtained for soil samples **pH=5.0 & 5.3** using Sensor Antenna and SMP for varying moisture content

MC (ml)	MC (%)	pH=5.0				pH=5.3			
		Sensor Antenna		SMP		Sensor Antenna		SMP	
		f (GHz)	Δf (GHz)	R	ΔR	f (GHz)	Δf (GHz)	R	ΔR
0	0	4.270	0.210	102	0	4.310	0.170	102	0
1	4.76	4.025	0.455	99	3	4.065	0.415	99	3
2	9.09	3.990	0.490	96	6	4.030	0.450	96	6
3	13.04	3.955	0.525	92	10	3.995	0.485	92	10
4	16.67	3.920	0.560	89	13	3.960	0.520	89	13
5	20.00	3.885	0.595	86	16	3.925	0.555	86	16
6	23.08	3.796	0.768	81	21	3.836	0.644	81	21
7	25.93	3.766	0.714	78	24	3.806	0.674	78	24
8	28.57	3.710	0.770	72	30	3.750	0.730	72	30
9	31.03	3.538	0.942	67	35	3.578	0.902	67	35

Table A.3: Comparison of results obtained for soil samples **pH=6.4 & 7.0** using Sensor Antenna and SMP for varying moisture content

MC (ml)	MC (%)	pH=6.4				pH=7.0			
		Sensor Antenna		SMP		Sensor Antenna		SMP	
		f (GHz)	Δf (GHz)	R	ΔR	f (GHz)	Δf (GHz)	R	ΔR
0	0	4.260	0.220	102	0	4.190	0.290	102	0
1	4.76	4.015	0.465	99	3	3.945	0.535	99	3
2	9.09	3.980	0.500	96	6	3.910	0.570	96	6
3	13.04	3.945	0.535	92	10	3.875	0.605	92	10
4	16.67	3.910	0.570	89	13	3.840	0.640	89	13
5	20.00	3.875	0.605	86	16	3.805	0.675	86	16
6	23.08	3.786	0.694	81	21	3.716	0.764	81	21
7	25.93	3.756	0.724	78	24	3.686	0.794	78	24
8	28.57	3.700	0.780	72	30	3.630	0.850	72	30
9	31.03	3.528	0.952	67	35	3.458	1.022	67	35

Table A.4: Comparison of results obtained for soil samples **pH=7.1 & 7.2** using Sensor Antenna and SMP for varying moisture content

MC (ml)	MC (%)	pH=7.1				pH=7.2			
		Sensor Antenna		SMP		Sensor Antenna		SMP	
		f (GHz)	Δf (GHz)	R	ΔR	f (GHz)	Δf (GHz)	R	ΔR
0	0	4.230	0.250	102	0	4.240	0.240	102	0
1	4.76	3.845	0.495	99	3	3.995	0.485	99	3
2	9.09	3.950	0.530	96	6	3.960	0.520	96	6
3	13.04	3.915	0.565	92	10	3.925	0.555	92	10
4	16.67	3.880	0.600	89	13	3.890	0.590	89	13
5	20.00	3.845	0.635	86	16	3.855	0.625	86	16
6	23.08	3.756	0.724	81	21	3.766	0.714	81	21
7	25.93	3.726	0.754	78	24	3.736	0.744	78	24
8	28.57	3.670	0.810	72	30	3.680	0.800	72	30
9	31.03	3.498	0.982	67	35	3.508	0.972	67	35

Table A.5: Comparison of results obtained for soil samples **pH=7.3 & 7.5** using Sensor Antenna and SMP for varying moisture content

MC (ml)	MC (%)	pH=7.3				pH=7.5			
		Sensor Antenna		SMP		Sensor Antenna		SMP	
		f (GHz)	Δf (GHz)	R	ΔR	f (GHz)	Δf (GHz)	R	ΔR
0	0	4.290	0.190	102	0	4.300	0.180	102	0
1	4.76	4.045	0.435	99	3	4.055	0.425	99	3
2	9.09	4.010	0.470	96	6	4.020	0.460	96	6
3	13.04	3.975	0.505	92	10	3.985	0.495	92	10
4	16.67	3.940	0.540	89	13	3.950	0.530	89	13
5	20.00	3.905	0.575	86	16	3.815	0.565	86	16
6	23.08	3.816	0.664	81	21	3.826	0.654	81	21
7	25.93	3.786	0.694	78	24	3.800	0.684	78	24
8	28.57	3.730	0.750	72	30	3.740	0.740	72	30
9	31.03	3.558	0.922	67	35	3.568	0.912	67	35

From the tables, the following points are observed:

- For both sensor antenna and SMP, increase in MC for different soil samples leads to increase in corresponding shift parameter, Δf and ΔR .
- In the case of sensor antenna, variation in Δf is observed for all soil samples with varying MC as well as pH.
- In the case of SMP, ΔR remains constant with varying pH for any MC in soil. For example, when MC=20%, $\Delta R=16$ for all soil samples.

A.3 Inference

The aim of this work is to test the efficacy of the sensor antenna discussed in Section 5.3 and make a comparison with a readily available sensor module. Sensor antenna method provides variation with respect to MC and pH, whereas the SMP setup shows variation with MC only, thereby failing to differentiate soil samples on the basis of pH.

Appendix B

SPECKLE NOISE REDUCTION IN IMAGES USING A COMBINED SPACE-FREQUENCY DOMAIN APPROACH

B.1 Introduction

Speckle noise is found when images are generated using coherent illumination such as acoustic imagery, laser imaging, Synthetic Aperture Radar (SAR) data etc. It is produced because of the variation in backscatter from inhomogeneous cells. Constructive and destructive interference of multiple echoes from pixels in the image causes the received signal to vary randomly and the appearance of the image gets corrupted by such granular patterns.

The granular nature of speckled images makes them hard to interpret, both for the human eye and automated segmentation and classification algorithms (Jenicka and Suruliandi, 2015). So, it is important to carry out despeckling as a pre-processing step (El-Zaart, 2009; Shanthy and Valarmathi, 2015) for further feature extraction, analysis and recognition stages of image processing tasks.

Significant achievements are made using SAR data in microwave

imaging applications such as remote sensing. SAR images are generally satellite images of large areas with high resolution and corrupted by speckle noise. Early methods of despeckling were developed in the spatial domain and were obtained by making assumptions on the statistical properties of reflectivity and speckle. A good technique improves the signal-to-noise ratio and at the same time preserves the edges and other details in an image. Initial techniques were based on speckle filters such as Box filter (Li et al., 1983), Median filter (Pratt, 1978), Lee filter (Lee, 1980) Enhanced Lee filter (Lee, 1983), Frost filter (Frost et al., 1982), Wiener filter, Kaun filter (Kuan et al., 1985), Geometric filter (Crimmins, 1985) and so on. Most of them used a defined filter window to estimate the local noise variance of speckle image and performed individual unique filtering process. Dewaele, in (Dewaele et al., 1990), has compared speckle reduction techniques using Lee's statistical filter, sigma filter and Crimmin's geometric filter. These filters were able to remove moderate speckle in the images; however edges got blurred.

Apart from Meer's filter (Meer et al., 1994) and the filter based on Laplacian pyramid (Aiazzi et al., 1998), most transform domain methods of despeckling exploit the multiresolution concepts of Discrete Wavelet Transform (DWT) (Ruchira et al., 2015). Homomorphic filtering in the wavelet domain has been used extensively in the past. Classical hard and soft thresholding methods were applied to wavelet transform coefficients. A novel speckle reduction method based on thresholding the wavelet coefficients of the logarithmically transformed image was proposed by Guo (Guo et al., 1994). An improved speckle reduction algorithm that combines adaptive wavelet soft-thresholding operation with partial difference equations is proposed by Liu (Liu et al., 2014). Here, SAR image is divided into sub-blocks and the most homogeneous sub-block is selected to calculate the threshold.

A simple algorithm, based on Wiener filtering and adaptive soft thresholding of wavelet transform coefficients, is suggested. The threshold at each subband is calculated automatically from the variance

of the subband. Two level decomposition of the wavelet transform is considered and thresholding is applied only to detail coefficients.

B.2 Wavelet based Image Denoising Technique

B.2.1 Speckle Noise Model

Speckle appears as spatially correlated, multiplicative noise that is statistically independent of the image intensity. It can be modelled as a multiplicative random noise in spatial domain as

$$g = Df.s \quad (\text{B.1})$$

where g , f and s represent the noisy image, original image and the multiplicative speckle noise respectively. The matrix D is a linear degradation process and operator “.” means element by element multiplication. The image despeckling problem is to obtain an estimate of f from the known g and D .

In order to convert the multiplicative model to additive, logarithmic transform is applied prior to the denoising technique. At the end, output is exponentially transformed to obtain the despeckled image.

B.2.2 Wiener Filter

Wiener filter, known as least mean square filter, minimizes the overall mean square error in the process of inverse filtering and noise smoothing. It works best for the suppression of additive as well as multiplicative noise.

B.2.3 Wavelet Thresholding

Multiscale transforms are found to be suitable for image denoising because they are very much useful for isolating discontinuities present in the image. Speckle noise usually occupies medium and high frequency components in the transform domain.

Application of 2-D DWT to an image decomposes an image into four subbands LL, LH, HL, HH and these subbands are created from low pass filter, L and high pass filter, H each down sampled by 2. The approximation coefficients at level j , LL_j is decomposed into four components that are the approximation coefficients at level $j + 1$ ie. LL_{j+1} and the three detail coefficients LH_{j+1} , HL_{j+1} and HH_{j+1} as shown in Figure B.1. So, wavelet decomposition done at multiple levels helps to separate the noise components from image details.

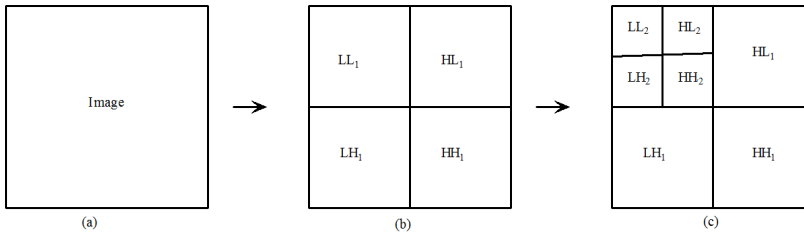


Figure B.1: Image, first and second level Wavelet Transform decomposition

Wavelet thresholding has proved to be successful in removing speckle noise. Using wavelet transform, image is decomposed into low frequency (approximation) and high frequency (detail) subbands. The speckle noise contribution usually reflects in the detail coefficients and their values will be small. So soft thresholding helps in separating useful information from unwanted noise. Soft thresholding can be defined as

$$\tilde{W}_j(x, y) = \begin{cases} \text{sign}(W_j(x, y))(|W_j(x, y)| - T_j), & |W_j| > T_j \\ 0, & \text{otherwise} \end{cases} \quad (\text{B.2})$$

where W_j is the detail subband of the j^{th} level decomposition, \tilde{W}_j is subband after thresholding and T_j is the corresponding threshold.

Selection of appropriate threshold is very important because noise cannot be completely removed by setting the threshold value low and significant image information will be lost if threshold is set very high. Also, depending upon image type and the amount of noise variance, the threshold level may vary.

B.2.4 Threshold Computation

Threshold value, T_j at the j^{th} decomposition level, which is adaptive to various subbands of the wavelet decomposition is given below. The only parameter used for threshold calculation is the standard deviation, σ_j , of the detail subbands.

$$T_j = \frac{\sigma_j}{\sqrt{2\log(N_j)}} \quad (\text{B.3})$$

where N_j is the size of the subband.

Thresholding is applied to LH_j , HL_j and HH_j subbands of wavelet decomposition at the j^{th} level. Thresholding is not done on the LL_j subband of the wavelet decomposition since it carries approximation coefficients.

B.2.5 Despeckling Algorithm

The algorithm for despeckling is summarized below.

1. Wiener filtering is applied to the speckled image.
2. Multiplicative noise model is transformed to an additive one by taking logarithm of the resultant image.
3. Discrete Wavelet Transform is applied on the image and decomposition is performed with the help of Meyer wavelet upto level 2.

4. Thresholds are computed for each subband except the lowest level LL band using Eq. B.3.
5. Soft thresholding is done for all LH, HL and HH subbands.
6. Inverse Wavelet transform is computed on the approximation and thresholded detail coefficients.
7. The exponent is taken to get the despeckled image.

B.2.6 Quantitative Evaluation

The image quality, after the application of despeckling algorithm, can be assessed using metrics like Peak Signal-to-Noise Ratio (PSNR) and Structural SIMilarity (SSIM) index.

A simple and widely used full-reference fidelity measure is the Peak Signal-to-Noise Ratio (PSNR). The corresponding distortion metric is the Mean-Squared Error (MSE) (Girod, 1993). They are expressed as

$$MSE = \frac{1}{MN} \sum_{i=0}^{M-1} \sum_{j=0}^{N-1} (g(i, j) - f(i, j))^2 \quad (\text{B.4})$$

$$PSNR = 10 \log_{10} \left(\frac{(L-1)^2}{MSE} \right) dB \quad (\text{B.5})$$

where f and g denote the original and de-noised images respectively, MN is the size of the image and L is dynamic range of pixel values (256 for 8-bit gray scale images). These methods directly measure the pixel-by-pixel differences between the images.

Another metric based on Human Visual System (HVS) for measuring the similarity between two images, SSIM (Wang et al., 2004), is given by

$$SSIM = \frac{(2\mu_g\mu_f + c_1)(2\sigma_{gf} + c_2)}{(\mu_g^2 + \mu_f^2 + c_1)(\sigma_g^2 + \sigma_f^2 + c_2)} \quad (\text{B.6})$$

where μ , σ is the average, standard deviation of corresponding images, σ_{gf} is the covariance of g and f , $c_1 = (k_1L)^2$, $c_2 = (k_2L)^2$, $k_1=0.01$, $k_2=0.03$ by default.

B.3 Simulation Results

The speckle reduction algorithm is implemented in the MATLAB environment and is applied to general and SAR images. To estimate the performance of the algorithm, original speckle-free images are taken and they are synthetically speckled by adding speckle noise. This method is compared and quantitatively assessed using performance measures such as PSNR and SSIM with the speckle reduction algorithm (Liu et al., 2014).

B.3.1 General Images

The algorithm is tested on a set of standard benchmark monochrome images such as *lena*, *pentagon*, *zelda*, *cameraman*, *egypt*, *monarch*, *house* etc. Images are mixed with speckle noise of different variance. Figure B.2 shows original images, images mixed with speckle noise of variance 0.01, despeckled images using Liu's method and despeckled images using proposed algorithm.

Table B.1 shows the values of PSNR, SSIM and computation time in seconds for the two despeckling algorithms. Various general images are considered for a noise variance of 0.01.

Figure B.3 (a) and (b) compare the corresponding plots of PSNR and SSIM values obtained for the two algorithms. Table and figures show that the proposed algorithm works better.



Figure B.2: (a) General images(*lena*, *cameraman*, *egypt*, *monarch*, *house*) (b) images mixed with speckle noise variance of 0.01 (c) despeckled images by (Liu et al., 2014) (d) despeckled images using proposed algorithm

Table B.1: Comparison of PSNR in dB, SSIM and computation time in seconds for various general images

Images	Algorithm by Liu (Liu et al., 2014)			Proposed algorithm		
	PSNR	SSIM	Time(Sec)	PSNR	SSIM	Time(Sec)
<i>lena</i>	27.02	0.76	1.25	29.97	0.83	0.84
<i>pentagon</i>	24.69	0.66	0.75	26.98	0.77	0.69
<i>zelda</i>	30.81	0.88	1.35	33.22	0.92	0.80
<i>cameraman</i>	26.48	0.76	0.98	29.31	0.82	0.79
<i>egypt</i>	26.61	0.75	1.15	29.50	0.84	1.06
<i>monarch</i>	25.71	0.81	1.13	29.67	0.89	0.89
<i>house</i>	29.38	0.77	0.95	31.30	0.80	0.81

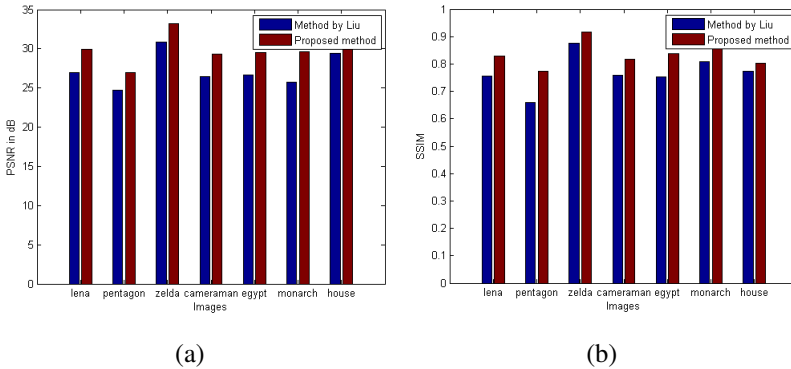


Figure B.3: Plots to compare (a) PSNR (b) SSIM values of reconstructed general images for the two methods

B.3.2 SAR Images

Radar Satellite-1 (RISAT-1) is a state-of-the-art microwave remote sensing satellite carrying an SAR payload operating in the C-band (5.35 GHz), which enables imaging of the surface features during both day and night under all weather conditions. Fig. B.4 shows RISAT-1 image acquired on 13th September 2012 showing Changanacheri town in Kerala, India, image mixed with speckle noise of variance 0.01,

despeckled image using Liu's method and despeckled image using the proposed algorithm.

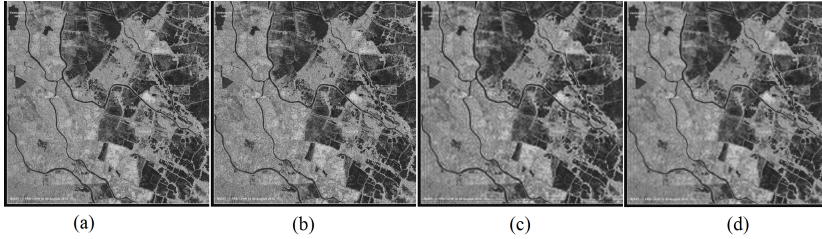


Figure B.4: (a) Original RISAT-1 image (b) mixed with speckle noise of variance 0.01 (c) despeckled image by Liu (d) despeckled image using the proposed algorithm

Table B.2 shows the values of PSNR and SSIM for different variances of the RISAT image and the corresponding plot is shown in Figure B.5. On comparison of these values for the two algorithms, the proposed method is found to be better.

Table B.2: Comparison of PSNR in dB and SSIM values of RISAT image for different variances

Variance	Algorithm by Liu (Liu et al., 2014)		Proposed algorithm	
	PSNR	SSIM	PSNR	SSIM
0.01	23.10	0.57	25.09	0.66
0.02	22.47	0.53	24.76	0.65
0.04	21.60	0.49	24.11	0.64
0.06	21.22	0.47	23.43	0.62
0.08	20.91	0.45	22.81	0.60
0.10	20.52	0.44	22.32	0.58
0.15	19.68	0.41	21.16	0.53
0.20	18.79	0.38	20.30	0.49

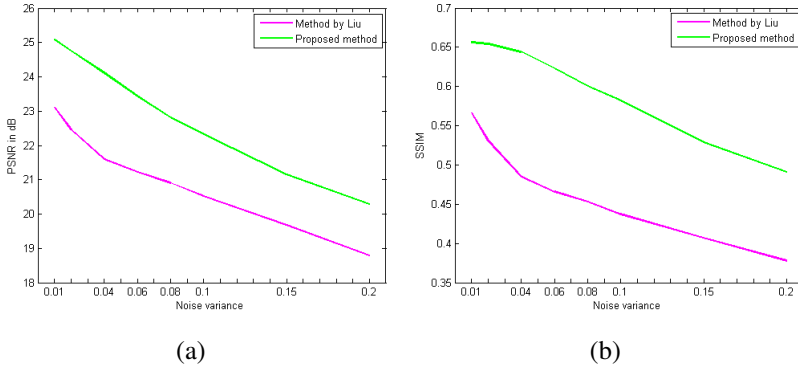


Figure B.5: Plots to compare (a) PSNR (b) SSIM values of despeckled RISAT images for different variances

B.4 Inference

SAR is a coherent active microwave imaging method used to reliably map Earth's surface and usually corrupted by speckle noise. Primary goal of despeckling is to reduce the speckle noise without sacrificing the information content. A combination of spatial and frequency domain techniques is successfully adopted. Wiener filtering is performed in the spatial domain and an adaptive thresholding of wavelet transform coefficients is done for speckle reduction. Threshold values corresponding to each detail subband of the wavelet transform are computed from the standard deviation of that subband. The proposed method can significantly reduce the speckle noise compared to Liu's method and finds applications in remote sensing.

REFERENCES

- [1] **Afsar M. N, Birch J. R, Clarke R. N and Chantry G. W** (1986) The measurement of the properties of materials. *IEEE Transactions of Instrumentation and Measurement*, 74 (1):183–199, 1986
- [2] **Agilent, 5965-7708E** (2000) *Exploring the Architectures of Network Analyzers*. Agilent Application Note 1287-2, 2000.
- [3] **Aiazzi B, Alparone L and Baronti S** (2016) Multiresolution local-statistics speckle filtering based on a ratio Laplacian pyramid. *IEEE Trans. Geoscience & Remote Sensing*, 36 (5):1466–1476, Sept. 1998.
- [4] **Al Ghamdi A. A, Omar A. Al-Hartomy, Falleh R. Al-Solamy, Dishovsky N, Zaimova D, Shtarkova R and Iliev V** (2016) Some factors influencing the dielectric properties of natural rubber composites containing different carbon nanostructures. *Materials sciences and applications*, 7(2):108–118, Jan. 2016.
- [5] **Alex Z. C and Behari J** (1996) Complex dielectric permittivity of soils as function of frequency, moisture and texture. *Indian Journal of Pure and Applied Physics*, 34: 319–323, 1996.
- [6] **Alsmadi M. K. S, Omar K. B and Noah S. A** (2009) Back propagation algorithm: The best algorithm among the multi-layer perceptron algorithm. *International Journal of Computer Science and Network Security*, 9(4):378–383, 2009.
- [7] **Altschuller H. M** (1963) Dielectric constant, In: M. Sucher and J.Fox, Eds., *Handbook of Microwave Measurements*. Brooklyn, Polytechnic Press, NewYork, Vol. II, 1963.
- [8] **Anju P** (2015) *Investigations on Metamaterial Based Spiral Inductors for Compact Microwave Devices*. Ph.D thesis, Cochin University of

Science and Technology, 2015.

- [9] **Balanis C. A (2005)** *Antenna Theory: Analysis and Design*. John Wiley & Sons, Inc., 2005.
- [10] **Bengtsson N. E and Risman P. O (1971)** Dielectric properties of foods at 3GHz as determined by a cavity perturbation technique. *Journal of Microwave Power, Taylor and Francis*, 6(2):107–123, 1971.
- [11] **Bernard P. A and Gautray J. M (1991)** Measurement of dielectric constant using a microstrip ring resonator. *IEEE Transactions on Microwave Theory and Techniques*, 39(3):592 - 595, March 1991.
- [12] **Bethe H. A and Schwinger J (1943)** *Perturbation Theory for Cavities*. Cornell University, 1943.
- [13] **Bindlish R, Jackson T, Sun R, Cosh M. H, Yueh S and Dinardo S (2009)** Combined passive and active microwave observations of soil moisture during CLASIC. *IEEE Geoscience and Remote Sensing Letters*, 6(4):644–648, Oct. 2009.
- [14] **Blackham D. V and Pollard R. D (1997)** An improved technique for permittivity measurements using a coaxial probe. *IEEE Trans. on Instr. Meas.*, 46(5):1093–1099, Oct. 1997.
- [15] **Brady N. C (1972)** *Advances in agronomy*. Academic Press, 1972.
- [16] **Brodie G (2012)** *Applications of Microwave Heating in Agricultural and Forestry Related Industries*. InTech, 2012.
- [17] **Buse A (1973)** Goodness of fit in generalized least squares estimation. *The American Statistician*, 27(3):106–108, June 1973.
- [18] **Calla O. P. N (1990)** Applications of microwaves in remote sensing. *Indian Journal of Radio and Space Physics*, 19:343–358, Dec. 1990.
- [19] **CSA Canadian Space Agency (2015)** Radarsat, 2015. URL <http://www.asc-csa.gc.ca/eng/satellites/radarsat> 2015.

REFERENCES

- [20] **Charman P and Murphy B** (1991). *Soils, their properties and management*. Sydney University Press, 1991.
- [21] **Chen L. F, Ong C. K, Neo C. P, Varadan V. V and Vijay K. Varadan** (2004) *Microwave Electronics: Measurement and Materials Characterization*. John Wiley & Sons, 2004.
- [22] **Chen P, Yunmin Chen, Wei Xu, Zhigang Liang and Wei Feng** (2008) A new equation for dielectric permittivity of saturated soils based on polarization mechanic. *Journal of Zhejiang University-SCIENCEA*, 9(9):293–302, March 2008.
- [23] **Centre for Innovations in Public Systems** (2006) CIPS. *E-KRISHI Kerala-ICT in Agriculture*. Govt. of Kerala, 2006.
- [24] **Clipper Controls** (2015) Dielectric constants, 2015. URL www.clippercontrols.com 2015.
- [25] **Corcoran P. T, Nelson S. O, Stetson L. E and Schlaphoff C. W** (1970) Determining dielectric properties of grain and seed in the audio frequency range. *Transactions of the ASAE*, 13(3):348–351, 1970.
- [26] **Costanzo S** (2012) *Microwave Material Characterization*. InTech Publishers, 2012.
- [27] **Crimmins T. R.** (1985) Geometric filter for speckle reduction. *Applications of Optics*, 24(10):1438 - 1443, May 1985.
- [28] **De Loor G. P and Meijboom F. W** (1966) The dielectric constant of foods and other materials with high water contents at microwave frequencies. *Journal of Food Technology*, 1:313–322, Dec. 1966.
- [29] **Deshours F, G. Alqui, H. Kokabi, Rachedi K, Tlili M, Hardinata S and Koskas F** (2018) Improved microwave biosensor for non-invasive dielectric characterization of biological tissues. *Microelectronics Journal*, Feb. 2018.

REFERENCES

- [30] **Dewaele P, Patrick Wambacq, Oosterlinck A and Marchand J. L** (1990) Comparison of some speckle reduction techniques for SAR images. In *10th Annual International Symposium on Geoscience and Remote Sensing*, pages 2417–2422, May 1990.
- [31] **Dobson M. C and Ulaby F. T** (1986) Active microwave soil moisture research. *IEEE Transactions on Geoscience and Remote Sensing*, Ge-24(1):23–36, Jan. 1986.
- [32] **Ekmekci E and Turhan-Sayan G** (2011) Metamaterial sensor applications based on broadside-coupled SRR and V-shaped resonator structures. In *Proc. Int. Symp. Antennas and Propagation*, pages 1170–1172, Jeju, South Korea, 2011.
- [33] **El-Zaart A** (2009) Contrast enhancement of bimodal SAR images using a new desired histogram method with gamma distribution. *Int. J. of Internet Technology and Secured Transactions*, 1(3/4):215–227, Jan. 2009.
- [34] **Eleftheriades G. V and Selvanayagam M** (2012) Transforming electromagnetics using metamaterials. *IEEE Microwave Magazine*, 13(2):26–38, April 2012.
- [35] **Engelder S. E and Buffler C. R** (1991) Measuring dielectric properties of food products at microwave frequencies. *Microwave World*, 12(2):6–15, 1991.
- [36] **Engman E. T** (1990) Progress in microwave remote sensing of soil moisture. *Canadian Journal of Remote Sensing*, 16(3):6–14, 1990.
- [37] **Fallahpour M** (2013) *Synthetic aperture radar-based techniques and reconfigurable antenna design for microwave imaging of layered structures*. Doctoral Dissertations, 2013.
- [38] **Fallahpour M, Joseph T. Case, Mohammad Ghasr T and Zoughi R**

- (2014) Piecewise and Wiener filter-based SAR techniques for monostatic microwave imaging of layered structures. *IEEE Transactions on Antennas and Propagation*, 62(1), 2014.
- [39] **Hippel von A** (1954) *Lumped circuits and dielectric measuring techniques*. In *Dielectric Materials and Applications*. 12-22 New York, NY: John Wiley & Sons, 1954.
- [40] **Friedman S** (2011) Overview of electromagnetic methods for evaluation of soil water content and salinity. In *AGRI-SENSING 2011: International Symposium on Sensing in Agriculture in Memory of Dahlia Greidinger*, Technion, Haifa, Israel, Feb. 2011.
- [41] **Frost V. S, Stiles J, Shanmugan K and Holtzman J** (1982) A model for radar images and its application to adaptive digital filtering of multiplicative noise. *IEEE Trans. on pattern analysis and machine intelligence*, PAMI-4(2):157–165, 1982.
- [42] **Ghannouchi F. M and Bosisio R. G** (1989) Measurement of microwave permittivity using a six-port reflectometer with an open-ended coaxial line. *IEEE Transactions on Instrumentation and Measurement*, 38(2):505–508, 1989.
- [43] **Ghosh A, Behari J and Pyne S** (1998) Dielectric parameters of dry and wet soils at 14.89 GHz. *Indian Journal of Radio and Space Physics*, 27, 1998.
- [44] **Girod B** (1993) *What's wrong with mean-squared error ?*, In *Digital Images and Human Vision*. Ed. Cambridge, MA: MIT Press, 1993.
- [45] **Grant J. P, Clarke R. N, Symm G. T and Spyrou N. M** (1989) A critical study of the open-ended coaxial line sensor technique for RF and microwave complex permittivity measurements. *Journal of Physics: Electronics and Scientific Instrument*, 22(9):757 - 770, 1989.

REFERENCES

- [46] **Guo H, Odegard J. E, Lang M, Gopinath R. A, Selesnick I. W and Burrus C. S** (1994) *Wavelet based speckle reduction with application to SAR based ATD/R*. Department of Electrical and Computer Engineering, Rice University, Houston, 1994.
- [47] **HakimBoughrie A, Legrand C and Chapoton A** (1997) Non-iterative stable transmission/reflection method for low-loss material complex permittivity determination. *IEEE Transaction on microwave theory and methods*, 45(1): 52–57, Jan. 1997.
- [48] **Hanson B. R and Peters D. W** (2000) *Soil types affect accuracy of dielectric moisture sensors*. California Agriculture, 54(3):43–47, 2000.
- [49] **Haykin S** (2005) *Neural Networks-A Comprehensive Foundation*. Pearson Prentice Hall, 2005.
- [50] **Hazelton P and Murphy B. W** (2007) *Interpreting soil test results: what do all the numbers mean?* CSIRO Publishing, Australia, 2007.
- [51] **Hippel A. R** (1954) *Dielectric Materials and Applications*. Artech House, 1954.
- [52] **Honeywell** (2011) URL www.honeywellprocess.com/library/marketing/techspecsDielectricConstantTable.pdf, 2011.
- [53] **Horsfield B, Ball J. A. R, Holdem J. R, Keam R. B, Holmes W. S and Green A** (1996) Cheese curd permittivity and moisture measurement using a microwave reflectometer. *In Proceedings of IEEE Asia-Pacific Microwave Conference*, pages 128–132, 1996.
- [54] **James R. B** (1990) *Transmission/Reflection and short-circuit line permittivity measurement methods*. Technical Note, NIST, 1341, July 1990.
- [55] **Jenicka S and Suruliandi A** (2015) Texture-based classification of remotely sensed images. *International Journal of Signal and Imaging*

Systems Engineering (IJSISE), 8:260 - 272, July 2015.

- [56] **Jha A. K and Akhtar M. A** (2015) An improved rectangular cavity approach for measurement of complex permeability of materials. *IEEE Transactions on Instrumentation and Measurement*, 64:995–1003, 2015.
- [57] **Jin M, Zheng X, Jiang T, Xiaofeng Li, Xiaojie Li and Zhao K** (2017) Evaluation and improvement of SMOS and SMAP soil moisture products for soils with high organic matter over a forested area in Northeast China. *Remote Sensing*, 9(387):1–17, April 2017.
- [58] **Jingchu H and Geyi W** (2013) A new method for measuring the properties of dielectric materials. *IEEE Antennas and Wireless Propagation Letters*, 12:425–428, 2013.
- [59] **Joshi K. K, Pollard R. D and Postoyalko V** (1994) Microstrip with dielectric overlay: variational analysis and validation. *IEE Proceedings -Microwaves, Antennas and Propagation*, 141(2):138–140, April 1994.
- [60] **Kashid P. B, Kulkarni D. C, Surve V. G and Puri V** (2013) Microwave permittivity and Permeability of $Mg_xMn_{(0.9-x)}Al_0.1Zn_{0.8}Fe_{1.2}O_4$ thick films using superstrate method. *Microelectronics International*, 30(1):40–46, 2013.
- [61] **Keam R. B and Holmes W. S** (1995) Uncertainty analysis of measurement of complex dielectric permittivity using microstrip transmission line. In Proceedings of 1995 SBMO/IEEE *MTT-S International Microwave and Optoelectronics Conference*, pages 137–142, Rio de Janeiro, Brazil, 24-27 July 1995.
- [62] **F. Kelleners, Deshours, D. A. Robinson, P. J. Shouse, J. E. Ayars, and T. H. Skaggs**. Frequency dependence of the complex permittivity and its impact on dielectric sensor calibration in soils. *Soil Science*

Society of America Journal, 69:67–76, Feb. 2005.

- [63] **Kent M and Kress-Rogers E** (1986) Microwave moisture and density measurements in particulate solids. *Transactions of the Institute of Measurement and Control*, 8(3): 167–168, 1986.
- [64] **Kim Y. R, Morgan M. T, Okos M. R and Stroshine R. L** (1998) Measurement and prediction of dielectric properties of biscuit dough at 27 MHz. *Journal of Microwave Power*, 33(3):184–194, 1998.
- [65] **Kitic G, Vasa Radoni and Vesna Crnojevi-Bengin** (2012) Soil moisture sensors based on metamaterials. *Songklanakarin Journal of Science and Technology*, 34:689–693, Dec. 2012.
- [66] **Kraszewski A** (1996) *Microwave aquametry: electromagnetic wave interaction with water- containing materials*. IEEE Press, New York, 1996.
- [67] **Kraszewski A** (1991) Microwave aquametry-needs and perspectives. *Microwave Theory and Techniques*, 39(5):828–835, 1991.
- [68] **Kuan D, Alexander A. Sawchuk, Timothy C. Strand and Pierre H. Chavel.** (1985) Adaptive noise smoothing filter for images with signal-dependent noise. *IEEE Trans. Pattern Anal. Mach. Intell.*,PAMI-7(2):165–177, Feb. 1985.
- [69] **Lawrence K. C, Nelson S. O and Bartley P.G Jr.** (1998) Coaxial dielectric sensor for cereal grains. In MTC/98 Conference Proceedings. *IEEE Instrumentation and Measurement Technology Conference. Where Instrumentation is Going* (Cat. No.98CH36222), St. Paul, MN, USA, 18-21May 1998.
- [70] **Lee J** (1983) *Digital image smoothing and the sigma filter*. Computer vision, graphic and image processing, 24:255–269, 1983.
- [71] **Lee J. S** (1980) Digital image enhancement and noise filtering by use of

- local statistics. *IEEE Trans. Pattern Anal. Mach. Intell.*,PAMI-2(2):165–168, Feb. 1980.
- [72] **Li F. K, Cheryl Croft and Daniel N. Held** (1983) Comparison of several techniques to obtain multiple-look SAR imagery. *IEEE Trans. on Geoscience and Remote sensing*, GE-21:370–375, Aug. 1983.
- [73] **Lianlin L, Wenji Zhang and Fang Li** (2010) Derivation and discussion of the SAR migration algorithm within inverse scattering problem: Theoretical analysis. *IEEE Transactions on Geoscience and Remote Sensing*, 48(1):415–422, Jan. 2010.
- [74] **Liao X, Raghavan V. G, Meda V and Yaylayan V. A** (2001) Dielectric properties of supersaturated alpha-D-glucose aqueous solutions at 2450 MHz. *Journal of Microwave Power and Electromagnetic Energy*, 36(3):131–138, 2001.
- [75] **Liu J, Ding Z, Zhao L, Dong F and Liu D** (2014) An adaptive SAR image speckle reduction algorithm based on wavelet transform and partial differential equations. In *Proceedings of 10th European Conference on Synthetic Aperture Radar (EUSAR)*, pages 1–4, June 2014.
- [76] **Lu H, Toshio Koike, Tetsu Ohta, David Ndegwa Kuria, Kun Yang Hideyuki Fujii, Hiroyuki Tsutsui and Katsunori Tamagawa** (2009) *Monitoring Soil Moisture from Spaceborne Passive Microwave Radiometers*. InTech, Rijeka, 2009.
- [77] **Madelung O** (1996) *Semiconductors -Basic Data*. Springer Verlag, 1996.
- [78] **Manab C** (2010) Overview of SAR applications-lecture notes on radar remote sensing and applications. In *Fourth RISAT-UP Training Programmes*, SAC-ISRO, Ahmedabad, Feb. 2010.

- [79] **Maryott A. A and Smith E. R** (1951) *Table of Dielectric Constants of Pure Liquids*. National Bureau of Standards Circular 514, 1951.
- [80] **Mathew K. T and Raveendranath U** (1993) Waveguide cavity perturbation method for measuring complex permittivity of water. *Microwave and Optical Technology Letters*, 6(2):104–106, Feb. 1993.
- [81] **Mathew K. T and Raveendranath U** (2000) *Cavity Perturbation Techniques for Measuring Dielectric Parameters of Water and Other Allied Liquids*. *Sensors Update*, Wiley-VCH, 2000.
- [82] **Meda V** (1996) *Cavity perturbation technique for measurement of dielectric properties of some agrifood materials*, 1996.
- [83] **Meer P, Park R. H and Cho K. J** (1994) Multiresolution adaptive image smoothing. *Graph. Models Image Process.*, 56(2):140–148, March 1994.
- [84] **Metaxas A. C and Meredith R. J** (1983) *Industrial Microwave Heating*. Peter Peregrinus, 1983.
- [85] **Mironov V, Kerr Y, Jean-Pierre Wigneron and Demontoux F** (2013) Temperature- and texture-dependent dielectric model for moist soils at 1.4GHz. *IEEE Geoscience and Remote Sensing Letters*, 10(3):419–423, May 2013.
- [86] **Mittermayer J, Alberga V, Buckreuss S and Riegger S** (2002) TerraSAR-X-predicted performance. *In Proc. SPIE2002*, Agia Pelagia, Crete, Greece, Sept. 2002.
- [87] **Moore D. M and Reynolds R. C Jr.** (1999) *X-Ray Diffraction and the Identification and Analysis of Clay Minerals*. Oxford University Press, 1999.
- [88] **Nelson S. O.** (1983) Density dependence of the dielectric properties of particulate materials pulverized coal, flour, wheat samples.

REFERENCES

Transactions of the ASAE, 26(6):1823–1825, 1983.

- [89] **Nelson S. O** (1991) Dielectric properties of agricultural products - measurements and applications. *IEEE Transactions on Electrical Insulation*, 26(5):845–869, 1991.
- [90] **Nelson S. O** (1998) *Dielectric properties measuring techniques and applications*. ASAE Paper No. 983067. St. Joseph, MI: ASAE, 1998.
- [91] **Nelson S. O and Bartley P. G** (2002) Measuring frequency- and temperature-dependent permittivities of food materials. *IEEE Transactions on Instrumentation and Measurement*, 51(4):589–592, Aug. 2002.
- [92] **Nelson S. O and Kraszewski A. W** (1990) Grain moisture content determination by microwave measurements. *Transactions of the ASAE*, 33(4):1303–1305, July 1990.
- [93] **Nikolova N. K** (2017) *Introduction to Microwave Imaging*. Cambridge University Press, 2017.
- [94] **Oliveira P. W. S, Pires Junior G. F. M, Sales A. J. M, Rodrigues H. O and Sombra A. S. B** (2017) Experimental and numerical investigation of the microwave dielectric properties of the MgTiO₃ ceramic matrix added with CaCu₃Ti₄O₁₂. *J. Microwave Optoelectron. Electromagn. Appl.*, 16(2):403–418, June 2017.
- [95] **Onimisi M. Y, Ikyumbur J. T, Abdu S. G and Hembra E. C** (2016) Frequency and temperature effect on dielectric properties of Acetone and Dimethyl formamide. *Physical Science International Journal*, 11(4):1–8, 2016.
- [96] **Online** (2016) URL <http://www.keralaagriculture.gov.in/html/crops/fertiliserrec.html>, 2016.
- [97] **O’Toole M. D, Marsh L, Davidson J. L, Tan Y. M, Armitage D and**

- Peyton A. J** (2015) Rapid non-contact relative permittivity measurement of fruits and vegetables using magnetic induction spectroscopy. In *IEEE Sensors Applications Symposium*, Croatia, April 2015.
- [98] **Owe M and Van de Gried A** (1998) Comparison of soil moisture penetration depths for several bare soils at two microwave frequencies and implications for remote sensing, *Water resources research*, 34(9):2319–2327, Sept. 1998.
- [99] **Pastorino M** (2010) Microwave Imaging. Wiley online library, 2010
- [100] **Paz A. M, Trabelsi S, Nelson S. O and Thorin E** (2011) Measurement of the dielectric properties of sawdust between 0.5 and 15 GHz. *IEEE Transactions on Instrumentation and Measurements*, 60(10):3384–3390, Oct. 2011.
- [101] **Persson M, Zeng X and Fhager A** (2011) Microwave imaging for medical applications. In Proceedings of the 5th *European Conference on Antennas and Propagation, EUCAP 2011*, pages 3070–3072, Rome, April 2011.
- [102] **Pooja M and Dharmendra S** (2013) Transmission line theory based two layer model for determining soil moisture. *ISPRS -International Archives of the Photogrammetry, Remote Sensing and Spatial Information Sciences*, XL-1/W1:21–24, May 2013.
- [103] **Pratt W. K** (1978) *Digital Image Processing*. Wiley, New York, 1978.
- [104] **Premachandran P. N** (2007) *Bench Mark Soils of Kerala*. Soil Survey Organization, Department of Agriculture (SC Unit), Government of Kerala, 2007.
- [105] **Puranik S, A. Kumbharkhane and Mehrotra S** (1991) Dielectric properties of honey-water mixtures between 10 MHz to 10 GHz using

- time domain technique. *Journal of Microwave Power and Electromagnetic Energy*, 26(4):196–201, 1991.
- [106] **Raj A, Kumar A, Hussain A, Panda S and Akhtar M. J** (2016) Metamaterial-inspired microwave sensor for measurement of complex permittivity of materials. *Microwave and Optical Technology Letters*, 58(11):2577–2581, Nov. 2016.
- [107] **Raveendranath U, Jacob J and Mathew K. T** (1996) Complex permittivity measurement of liquids with coaxial cavity resonators using a perturbation technique. *Electronics Letters*, 32(11):998–990, 1996.
- [108] **Raveendranath U, Bijukumar S and Mathew K. T** (2000) Broadband coaxial cavity resonator for complex permittivity measurements of liquids. *IEEE Transactions on Instrumentation and Measurement*, 49(6):1305–1312, 2000.
- [109] **Remenyi D, George Onofrei and Joseph English** (2009) *An Introduction to Statistics using Microsoft Excel*. Academic Publishing Ltd., 2009.
- [110] **RFcafe** (2015) Dielectric constants, URL www.rfcafe.com/references/electrical/dielectric-constants-strengths.htm, 2015.
- [111] **Roberts S and Hippel A. V** (1946) A new method for measuring dielectric constant and loss in the range of centimetre waves. *Journal of Applied Physics*, 17, 610-616 1946.
- [112] **Robinson M. C and Hollis Hallet A. C** (1966) The static dielectric constant of NaCl, KCl and KBr at temperatures between 4.2K and 300K. *Canadian Journal of Physics*, 44 (10):2211–2230, 1966.
- [113] **RogersCorp** (2008) www.rogerscorp.com/documents/3269/acs/AD1000-Data-Sheet.pdf, 2008.

REFERENCES

- [114] **Roja R** (1996) *The Back-propagation Algorithm, Chapter 7: Neural Networks*. Springer- Verlag, Berlin, 1996.
- [115] **Rosenqvist A, Masanobu Shimada and Manabu Watanabe** (2004) ALOS PALSAR: Technical outline and mission concepts. *In 4th International Symposium on Retrieval of Bio-and Geophysical Parameters from SAR Data for Land Applications*, Innsbruck, Austria, Nov. 2004.
- [116] **Ruchira G, Lalit Jain and Rajesh Rai** (2015) Speckle reduction of Synthetic Aperture Radar Images using Median Filter and Savitzky-Golay Filter. *International Journal of Computer Applications*, 113:38–43, March 2015.
- [117] **Santamaria J. C and Fam M** (1997) Dielectric permittivity of soils mixed with organic and inorganic fluids (0.02GHz to 1.30GHz). *Journal of Environmental and Engineering Geophysics*, 2(1):37–51, March 1997.
- [118] **SIC Satellite Imaging Corporation** (2014) IKONOS Satellite Sensor URL <http://www.satimagingcorp.com/satellite-sensors/ikonos>, 2014.
- [119] **Schueler M, Mandel C, Puentes M and Jakoby R** (2012) Metamaterial inspired microwave sensors. *IEEE microwave magazine*, 13(2):57–68, April 2012.
- [120] **Sears F. W and Zemansky M. W** (1955) *University Physics*. Addison-Wesley Pub. Co., 1955.
- [121] **Shanthi I and Valarmathi M. L** (2015) Contourlet transform with modified particle swarm optimization for despeckling and feature enhancement of SAR images. *International Journal of Computer Applications in Technology*, 51(1):31–42, April 2015.
- [122] **Sharma G.P and Prasad S** (2002) Dielectric properties of garlic at

- 2450 MHz as function of temperature and moisture content. *Journal of Food Engineering*, 52(4):343–348, 2002.
- [123] **Sheen N. I and Woodhead I. M** (1999) An open-ended coaxial probe for broadband permittivity measurement of agricultural products. *Journal of Agricultural Engineering*, 74:193–202, 1999.
- [124] **P. Skocik and Neumann P** Measurement of complex permittivity in free space. In *Procedia Engineering*, pages 100–104, 2015.
- [125] **Soontornpipit P, Furse C, Chung Y and Bryan M. Lin** (2006) Optimization of a buried microstrip antenna for simultaneous communication and sensing of soil moisture. *IEEE [Transactions on Antennas and Propagation]*, 54(3):797–800, March 2006.
- [126] **Spazio S.** (2011) ENVISAT and ERS Missions, 2011.
- [127] **Stuchly M. A and Stuchly S. S** (1980) Dielectric properties of biological substances tabulated. *Journal of Microwave Power*, 15(1):19–26, 1980.
- [128] **TechMah** (2016) Precision agriculture and potential market in India, URL www.techmahindra.com, 2016.
- [129] **Then Y. L, Kok Yeow You and Mohamad Ngasri Dimon** (2014) Soil moisture dielectric measurement using microwave sensor system. *International Symposium on Antennas and Propagation Conference Proceedings*, 2014.
- [130] **Topp G. C, Davis J. L and Annan A. P** (1980) Electromagnetic determination of soil water content and electrical conductivity measurement using time domain reflectometry. *Water Resources Research*, 16:574–582, 1980.
- [131] **Trabelsi S, Kraszewski A. W and Nelson S. O** (1997) A new density-independent function for microwave moisture content determination in

- particulate materials. In *IEEE Instrumentation and Measurement Technology Conference Sensing, Processing, Networking*. IMTC Proceedings, pages 648–652, Ottawa, Canada, 19-21 May 1997.
- [132] **Venkatesh M. S.** (2002) *Development of integrated dual frequency permittivity analyzer using cavity perturbation concept*. Ph.D. Thesis. Montreal, QC: Department of Agricultural and Biosystems Engineering, McGill University., 2002.
- [133] **Venkatesh M. S and Raghavan G. S. V** (2005) An overview of dielectric properties measuring techniques. *Canadian Biosystems Engineering*, 47:7.15–7.30, 2005.
- [134] **Venkatesh M. S, Raghavan G. S. V and Sotocinal S. A** (1998) Development of a permittivity analyzer to operate at 915 and 2450 MHz using cavity perturbation technique. In *CSAE Paper No. 98-315*, Winnipeg, MB: CSAE/SCGR, 1998.
- [135] **Vivek Y, AnilKumar, Sharan S, Sinha A. K, Yadav M, Gupta V. K and Jangid R. A.** (2009) Measurement of dielectric behaviour of fertilized soil at microwave frequency. *Journal of Agricultural Science*, 1(2):42–49, Dec. 2009.
- [136] **Von Hippel.** (1954) *Dielectrics and Waves*. Wiley, 1954.
- [137] **Wagner N, Katja Emmerich and Klaus Kupfer** (2011) Experimental investigations on the frequency-and temperature-dependent dielectric material properties of soil. *IEEE Transactions on Geoscience and Remote Sensing*, 49(7):2518–2530, July 2011.
- [138] **Wang L and Qu J. J** (2009) Satellite remote sensing applications for surface soil moisture monitoring : Areview. *Frontiers of Earth Science in China*, 3(2):237–247, June 2009.
- [139] **Wang S. S, Tang J, Johnson J. A, Mitcham E, Hansen J. D,**

- Hallman G, Drake S. R and Wang Y** (2003) Dielectric properties of fruits and insect pests as related to radio frequency and microwave treatments. *Biosystems Engineering*, 85(2):201–212, June 2003.
- [140] **Wang Z, Bovik A. C, Sheikh H. R and Simoncelli E. P** (2004) Image quality assessment: From error visibility to structural similarity. *IEEE Trans. Image Process*, 13:600–612, 2004.
- [141] **Wobschall D** (1977) A theory of the complex dielectric permittivity of soil containing water: The semidisperse model. *IEEE Trans. on Geoscience Electronics*, 15(1):49–58, 1977.
- [142] **You K. Y, Salleh J, Abbas Z and Liling You** (2010) A rectangular patch antenna technique for the determination of moisture content in soil. *PIERS Online*, pages 850–854, Jan. 2010.
- [143] **Youn H, Loon Yip Lee and Magdy F. Iskander** (2010) In-situ broadband soil measurements : Dielectric and magnetic properties. In Geoscience and Remote Sensing Symposium (IGARSS), 2010 *IEEE International*, Honolulu, HI, USA, 25-30 July 2010.
- [144] **Zaeytijd J De, Franchois A, Christelle Eyraud and Jean-Michel Geffrin.** (2007) Full-wave three-dimensional microwave imaging with a regularized Gauss Newton method, theory & experiment. *IEEE Transactions on Antennas & Propagation*, 55(11):3279–92, Nov. 2007.
- [145] **Zhu Z and Guo W** (2017) Frequency, moisture content and temperature dependent dielectric properties of potato starch related to drying with radio-frequency microwave energy. *Scientific Reports*, 7:1–11, Aug. 2017.
- [146] **Zivkovic I and Murk A** (2012) Free-Space Transmission Method for the Characterization of Dielectric & Magnetic Materials at Microwave Frequencies. *InTech*, 2012.

REFERENCES

LIST OF PAPERS SUBMITTED ON THE BASIS OF THIS THESIS

I. REFEREED JOURNALS

1. **Rajesh Mohan R**, S Mridula and P Mohanan, “Study and Analysis of Dielectric Behavior of Fertilized Soil at Microwave Frequency”, European Journal of Advances in Engineering and Technology, Vol.2, Issue 2, pp. 73-79, 2015.
2. **Raman Rajesh Mohan**, Shanta Mridula and Pezhohil Mohanan, “Artificial Neural Network Model for Soil Moisture Estimation at Microwave Frequency” Progress In Electromagnetics Research M, Vol. 43, 175181, 2015.

II. PRESENTATIONS IN CONFERENCES

1. **R Rajesh Mohan**, Binu Paul, S Mridula and P Mohanan, “ANN Model for Material Characterization”, 2nd International Conference on Advanced Functional Materials (ICAFM 2014), Thiruvananthapuram, India, pp. 112-113, February 19-21, 2014.
2. **Rajesh Mohan R**, Binu Paul, Mridula S and Mohanan P, “Measurement of Soil Moisture Content at Microwave Frequencies”, Procedia Computer Science (ICICT 2014), Vol. 46, pp. 1238-1245, 3-5 Dec. 2014.

3. A S Pathma Priyaa, Adil Mohammed, Ambili C, Anusree N S, Anne Varghese Thekekara, **Rajesh Mohan R** and S. Mridula, “Microwave Sensor Antenna for Soil Moisture Measurement”, 2015 Fifth International Conference on Advances in Computing & Communications (ICACC), RSET, Kakkand, Kochi, Sep. 2-4, 2015.
4. **R Rajesh Mohan**, Anju Pradeep, S Mridula and P Mohanan, “Microwave Imaging for Soil Moisture Content Estimation”, 2016 IEEE International Symposium on Antennas and Propagation (APSURSI), Fajardo, Puerto Rico, 26 June-1 July, 2016.
5. **Rajesh Mohan R**, S Mridula and P Mohanan, “Speckle Noise Reduction in Images using Wiener Filtering and Adaptive Wavelet Thresholding”, 2016 IEEE Region 10 Conference (TENCON), Singapore, 22-25 Nov. 2016.
6. Lakshmi Priya R, Midhu S Valsan, Mohammed Anas M, Neethu Mohan, Nidhiya Shaji, **Rajesh Mohan R** and S Mridula, “Microwave Sensing of Properties”, Proc. 4th National Technological Congress, Kerala (NATCON-2014), Government Engineering College, Wayanad, pp.168-173, February 20-21, 2014.

CURRICULUM VITAE

Rajesh Mohan R
Associate Professor (Electronics)
Govt. Model Engineering College, Thrikkakara
Ernakulam, Kerala - 682 021



Education

Course	Year	Institution	University/Board	Class
S.S.L.C	1984	St. Joseph's Boys' High School, Thalassery	Board of Public Examinations, Kerala	First Class with Distinction
P.D.C	1986	Govt. Brennen College, Thalassery	University of Calicut	First Class with Distinction
B.Tech	1990	College of Engineering, Thiruvananthapuram	University of Kerala	First Class with Distinction
M.Tech	2001	Regional Engineering College, Kozhikode	University of Calicut	First Class
Ph.D	Registered on 25/11/2011	Division of Electronics, School of Engineering	Cochin University of Science and Technology	

Personal Information

Date of Birth : 18/11/1968
Gender : Male
Address :

Present

Flat No. 3D, Vinayaka Daffodils Apartments,
Erroor, Ernakulam - 682 306.

Permanent

Vyjayanthi, North of Sree Rama Swamy
Temple, Tiruvangad, Thalassery - 670 103.

Fields of Interest : Microwave Imaging, Digital Communications
Research Publications : International Journals : 2
International Conferences : 5
National Conferences : 1

Contact Details : Email : rmm1968@yahoo.co.in
Phone No.: +91 98461 38648

Index

- Acidic, 7, 75, 87, 96, 166, 206, 215
AgRISTARS, 27
Alkaline, 7, 87, 166, 206, 215
Artificial Neural Network, 33, 61,
86, 116, 140, 141, 150,
185, 208
Asymmetric Coplanar Strip, 59

Cavity Perturbation Method, 14,
39, 74
Colour-mapping, 32, 85, 86, 125,
150, 199, 205, 208
Complex Relative Permittivity, 4

Dielectric Constant, 4, 40–42, 51,
52, 57, 58, 77, 111, 128,
152, 185, 195, 206

Fertilizer Concentration, 128, 155
Fertilizer Content, 8
Free-space Transmission Method,
23, 56, 125, 140, 205

Gravimetric Water Content, 8

Loss-factor, 4
Loss-tangent, 4,40

Material Characterization, 3, 38,
59, 61, 74, 87, 154
Material Under Test, 13, 38, 47, 69
Metamaterial, 14, 150
Microstrip Patch Antenna, 47, 87
Microwave Imaging, 4, 68
Moisture Content, 6, 87, 154, 213

NPK, 10, 129, 133, 155

Open-ended Probe Technique, 20

PBA, 129, 133, 155
Permeability, 3, 37, 151
Permittivity, 3, 37, 56, 151
pH, 6, 75, 76, 86, 87, 155, 159,
206, 218
Potash, 129, 133, 155

Regression, 33, 67, 193, 208
Remote Sensing, 220, 228

Sensor Antenna, 24, 59, 150, 215,
218
Sensor Antenna Method, 58
Sensor Module Probe, 216
Soil, 5, 51, 75, 77, 81, 82, 86, 87,
89, 91, 92, 96, 97, 101,
107, 150, 154, 157, 159,
166, 186, 193, 195,
197–199, 210

- Soil Testing Laboratory, 32, 87
- Speckle Noise, 228, 229
- Speckle Noise Reduction, 33
- Superstrate Method, 33, 47, 65, 77,
208
- Synthetic Aperture Radar, 27, 219

- Time-domain Reflectometry, 19
- Topp's Equation, 9, 110, 117, 195
- Total Soluble Salt, 75
- Transmission/reflection Method,
18

- Urea, 28, 129, 133, 155

- Vector Network Analyzer, 13
- Volumetric Water Content, 9, 86,
116, 195